The NADPH oxidase-induced phagosomal environment of neutrophils and other phagocytes

Juliet Rachel Foote

Submitted to
University College London
for the degree of Doctor of Philosophy

2018

Centre for Molecular Medicine
Division of Medicine

Supervisors:
Prof. A.W. Segal
Dr. A. Zdebik

Declaration

I, Juliet Foote, confirm that the work presented in this thesis is my own. Where information has been derived from other sources or generated from collaboration with other researchers, I confirm that this has been indicated in the thesis.

Abstract

The central focus of this thesis is to understand some of the fundamental physiology of the neutrophil phagosome in relation to the effects of the NADPH oxidase. The NADPH oxidase, when activated and assembled at the phagosomal membrane, translocates electrons into the phagosome which create superoxide anions and initiates a cascade of reactive oxygen species. This negative charge across the membrane must be compensated to allow further oxidase activity. We know that the proton channel, HVCN1, plays a major role in neutrophil charge compensation, but other ion channels must be involved as *Hvcn1*$^{-/-}$ mice still have some oxidase activity. One way to measure ionic flow and potentially identify ion channels involved is recording phagosomal pH, using the ratiometric indicator SNARF-1. The first results chapter describes using knockout mouse models lacking different ion channels, and the use of ion channel inhibitors to measure any effects on phagosomal pH or area and oxidase activity in neutrophils. While the effects of some broad-spectrum channel inhibitors suggested involvement of chloride and potassium conductances in the neutrophil phagosome, they and the mouse models failed to convincingly identify a specific channel.
The second results chapter aimed to characterise a mouse neutrophil cell line as an alternative tool to investigate the neutrophil phagosome. The Hoxb8 cell line is made up of conditionally immortalised mouse myeloid progenitor cells that can be differentiated into neutrophils. The wildtype C57BL/6 and *Hvcn1*$^{-/-}$ Hoxb8 lines were studied and compared to primary bone marrow neutrophils to validate their use as a neutrophil model.
Finally, other human primary phagocytes were investigated and compared to neutrophils. This aimed to provide insight into the function and effect of the NADPH oxidase in these cells by measuring pH with and without the oxidase inhibitor DPI and measuring oxidase activity.

Impact Statement

The main beneficiary of the work carried out within this thesis will be the international academic research field, particularly immunology and cell biology, although there is potential translation to scientific industry. Probably the most important is the immortalised Hoxb8 myeloid cell system. The Hoxb8 neutrophils can be generated in much greater numbers than primary cells isolated from a single mouse, and they can easily be genetically modified in the progenitor form. This has profound implications in both academic and industrial research. It could drastically reduce the number of mice used in research, Hoxb8 neutrophils could even replace live mice in some cases, which would be cost-effective and limit animal suffering. A genetically altered Hoxb8 neutrophil line would be engineered in a much shorter time than making a live mouse model, which would save the researcher time in the magnitude of months and years. Once academic research has established that Hoxb8 neutrophils are a reliable and convenient model for murine neutrophils, it may also be employed by industry perhaps in the areas of drug discovery or toxicology, as a cheaper and effective alternative to primary mouse neutrophils for basic research. This thesis aims to add to the foundational academic research.

The overarching theme of this thesis has been to investigate the phagosomal environment of neutrophils. Neutrophils are critical for innate host defence but have also been implicated in autoimmune disease states such systemic lupus erythematosus and rheumatoid arthritis, so it is of importance to study their biology. The same methods have also been applied to other innate immune cells which will provide further information about the function of the phagolysosome in innate host defence. Some of the work generated within this Ph.D. has already been published in academic journals and most of them are open-access.

Acknowledgements

The following people I would like to thank for their involvement in my Ph.D.:

First, my primary supervisor, Tony Segal, for the Ph.D. opportunity; for his guidance, focus, and encouragement throughout my studies, and the Irwin Joffe Memorial Trust and Susan Harbour Foundation for the financial support of my studies.

My secondary supervisors, Anselm Zdebik and David Sattelle, for their support and thoughtful input.

Andrew Smith, for his help and advice throughout, especially his technical expertise with cell culture that aided the expansion of this project.

All the members of the Segal and Smith labs, past and present, for making the Rayne a great place to work: Sabrina Pacheco, for great technical instruction and guidance in my first year; Sophia Joyce, for her kindness and support; Julio Martinez-Torres; for his amazing technical support and patience; Andre Ribeiro; for technical support; Adam Levine, Nikolas Pontikos, and Matthew Frampton for their superb bioinformatics and statistical assistance with endless patience; and Mathena Vinayaga-Pavan, Erni Marlina, Aziz Ghannam, Tomoko Kumagai, and Francesca Semplici for all-round support.

Simon Yona, for collaboration and advice, and Amit Patel and Jamie Evans for flow cytometry help. Sam Ranasinghe and Michael Duchen for excellent microscopy assistance.

All the patients and volunteers who very generously donated their blood for numerous experiments, and the UCL KLB animal facility staff.

Finally, my friends and family, for their unending love and support without which this thesis would not be possible.

Table of contents

Declaration **2**

Abstract **3**

Impact statement **4**

Acknowledgements **5**

Table of contents **6**

List of abbreviations **12**

List of figures **13**

List of tables **15**

Chapter 1 *Introduction* **16**

1.1 General overview 16

1.2 Haematopoiesis 17

1.3 Neutrophils 21

Microbial sensing 21

Phagocytosis 22

Granulopoiesis and degranulation 26

The NADPH oxidase 29

Charge compensation 33

pH 37

Oxidative killing 39

Non-oxidative killing 41

1.4 Intracellular environments of other professional phagocytes 45

1.5 Cell models of innate immune cells 49

1.6 Methodology for investigations of the phagosomal environment 53

pH

NADPH oxidase activity 56

1.7 Outline of thesis 59

Chapter 2 *Materials and Methods* **60**

2.1 Healthy control and patient ethics

2.2 Knockout mouse models

Source of mice

Mouse husbandry

2.3 Materials 61

General buffers

Duchen buffer

pH buffers for SNARF-1 calibration

Western blot buffers

Candida albicans stock and culture broth 62

Confocal microscopy dyes and equipment

Reagents for respiratory burst assays

Ion channel inhibitors

Buffers and antibodies for flow cytometry 63

Solutions and antibodies for western blots 64

Cell isolation materials and culture media

Hoxb8 generation reagents 65

2.4 Primary cell isolation and culture 66

Neutrophil isolation

Human neutrophil isolation

Mouse neutrophil isolation

Human monocyte isolation kit 67

Fluorescence Assisted Cell Sorting (FACS) of human blood mononuclear cells

Monocyte-derived macrophages (MDMs) 68

Monocyte-derived dendritic cells (MoDCs)

2.5 The Hoxb8 immortalised mouse myeloid progenitor cell line 69

Culture of SCF-producing CHO cell line

Retroviral infection of mouse bone marrow progenitor cells

Transformation of competent E. coli cells 70

Retroviral generation using GP-293 HEK cells 71

Preparation of bone marrow progenitor cells

Spin infection of progenitor cells 72

Culture of Hoxb8 immortalised myeloid progenitor cells

Differentiation of Hoxb8 progenitors into neutrophils 73

GFP-LC3 adenoviral transfection of Hoxb8 neutrophils

Generation of adenovirus

Adenoviral transfection of Hoxb8 neutrophils

2.6 *C. albicans* generation 74

Broth culture and stock preparation

Mouse serum production

2.7 SNARF-1 phagosomal pH confocal microscopy 75

Labelling of C.albicans with SNARF-1

SNARF-labelled *Candida* (SNARF-Ca) opsonisation

Microscopy plate preparation

Cell cytoplasmic staining 76

Confocal microscopy setup

Phagocytosis snapshot and time course

Standard curve generation 77

Data analysis 78

Snapshot experiments

Time course experiments

Phagocytosis uptake 79

Efferocytosis of apoptotic neutrophils by MDMs

Generation of apoptotic neutrophils (AN)

Staining of AN

Staining of MDMs 80

Imaging of efferocytosis

2.8 Amplex UltraRed respiratory burst assay

2.9 Seahorse oxygen consumption assay 81

2.10 Flow cytometry 82

2.11 Western blots

Sample preparation

Gel preparation 83

Gel electrophoresis

Gel to membrane transfer 84

Antibody staining and film development

2.12 Cell staining for brightfield microscopy

2.13 Compiling gene expression datasets of human neutrophils 85

2.14 Statistics 87

Chapter 3 *Investigating ion channels in the neutrophil phagosome* 88

3.1 Background and aims

3.2 Dissecting the relationship between NADPH oxidase activity and phagosomal pH with DPI 89

3.3 A study of ion channels present in neutrophil mRNA expression data 92

3.4 Investigating the effect of chloride channel inhibitors on phagosomal pH and area 93

3.5 Investigating the effect of potassium channel inhibitors on phagosomal pH and area 97

3.6 The effect of ion channel inhibitors on the respiratory burst 99

Chloride channel inhibitors decrease the respiratory burst only when applied with zinc chloride

Potassium channel inhibitors only significantly decrease the respiratory burst when applied with zinc chloride 100

3.7 Mice lacking candidate chloride and potassium ion channels have broadly normal phagosomal environments 101

3.8 Other knockout mouse models have varying phagosomal pH and area 105

3.9 Respiratory burst activity in knockout mouse neutrophils 106

3.10 Phagosomal environments of mice with non-functional *Lrrc8a* 107

3.11 Neutrophil phagosomal pH and area from cystic fibrosis patients appear normal 110

3.12 Discussion 111

Chapter 4 *Characterising the Hoxb8 immortalised myeloid cell line* 120

4.1 Background and aims

4.2 Generation of a conditionally Hoxb8 immortalised cell line 122

4.3 Optimisation of Hoxb8 cell viability and proliferation after estradiol removal 125

4.4 Time course of cell surface differentiation markers 126

4.5 Changes in Hoxb8 cell morphology following estradiol removal 130

4.6 Western blotting of the Hoxb8 protein and NADPH oxidase subunits in Hoxb8 neutrophils and primary BM neutrophils 132

4.7 The respiratory burst in Hoxb8 neutrophils 134

4.8 Comparison of respiratory burst activity in primary BM neutrophils with day 4 Hoxb8 neutrophils 137

4.9 Comparison of phagosomal pH in primary BM neutrophils with day 4 Hoxb8 neutrophils 138

4.10 Preliminary localisation experiments of GFP-tagged LC3 in Hoxb8 neutrophils 141

4.11 Discussion 148

Chapter 5 *Variations in the phagosomal environments of human neutrophils and mononuclear phagocytes* **151**

5.1 Background and aims

5.2 Phagosomal pH and NADPH oxidase activity in neutrophils and monocytes 153

5.3 Phagosomal pH and NADPH oxidase activity in monocyte subsets 157

5.4 Comparison of phagosomal environments between two dendritic cell subsets 161

5.5 The effect of LPS stimulation on MoDC phagosomal environment 165

5.6 The effect of macrophage polarisation on phagosomal pH 169

5.7 Preliminary investigations of pH within the efferosomes of polarised monocyte-derived macrophages 172

5.8 Discussion 178

Chapter 6 General discussion **183**

6.1 Summary of findings

6.2 Overall discussion of findings and future directions 185

Appendix **193**

List of publications

References **194**

List of Abbreviations

AML	Acute Myeloid Leukemia
APC	Allophycocyanin
BM	Bone marrow
BSA	Bovine serum albumin
CGD	Chronic granulomatous disease
CML	Chronic Myeloid Leukemia
ER	Estrogen receptor
FACS	Fluorescence Activated Cell Sorting
FCS	Fetal calf serum
FITC	Fluorescein isothiocyanate
G-CSF	Granulocyte Colony Stimulating Factor
GFP	Green Fluorescent Protein
GM-CSF	Granulocyte Macrophage – Colony Stimulating Factor
HOCl	Hypochlorous acid
HRP	Horseradish peroxidase
H_2O_2	Hydrogen peroxide
HSC	Haematopoietic Stem Cell
IFN-γ	Interferon gamma
IL	Interleukin
Ig	Immunoglobin
LPS	Lipopolysaccaride
M-CSF	Macrophage – Colony Stimulating Factor
MPO	Myeloperoxidase
NADPH	Nicotinamide adenine diphosphate
PE	Phycoerythrin
PMA	Phorbol myristate acetate
ROS	Reactive oxygen species
RPMI	Roswell Park Memorian Institute
SNARF-1	Seminaphthorhodafluor-1
WT	Wildtype

List of Figures

1.2	The hierarchical nature of haematopoiesis	18
1.3.1	General mechanism of phagocytosis	23
1.3.2	Types of PRRs in neutrophils which are involved in ROS production	24
1.3.3	Granulopoiesis and associated expression changes in transcription factors	26
1.3.4	Mechanisms of NADPH oxidase activation	30
1.3.5	Proposed NADPH oxidase-induced ion fluxes in the neutrophil phagosome	35
1.4	Phagocytosis in macrophages and DCs	47
2.7	Relationship of SNARF fluorescence ratio to pH	77
3.2	Both NOX2 activity and phagosomal pH are inhibited by DPI, but phagosomal pH is more sensitive to its effects	91
3.4	Chloride channel inhibitors cause significant phagosomal acidification and increase phagosomal swelling	95
3.5	Potassium channel inhibitors cause varying phagosomal effects	97
3.6	The effect of ion channel inhibitors on human neutrophil oxygen consumption during phagocytosis of opsonised Candida	100
3.7.1	Phagosomal pH and area measured in the single knockout *Clic1*$^{-/-}$ mice, and in the double knockout *Hvcn1*$^{-/-}$/*Clic1*$^{-/-}$ mice	102
3.7.2	Phagosomal pH and area measured in the single knockout *Clc3*$^{-/-}$ mice, and in the double knockout *Hvcn1*$^{-/-}$/*Clc3*$^{-/-}$ mice	
3.7.3	Phagosomal pH and area measured in the single knockout Kc*c3*$^{-/-}$ mice, and in the double knockout *Hvcn1*$^{-/-}$/*Kcc3*$^{-/-}$ mice	103
3.8	Phagosomal pH and area measured in Kcnj*15*$^{-/-}$ and *Trpm2*$^{-/-}$ mice models	105
3.9	Measuring oxygen consumption in *Clc3*, *Kcc3* and *Hvcn1* with *Hvcn1*/*Clic1* deficient mice peritoneal neutrophils induced by PMA and serum-opsonised *Candida*	107
3.10	The *ebo/ebo* mice have similar phagosomal environments to WT mice	109
3.11	Phagosomal pH and area from two patients with cystic fibrosis (CF) with and without 100 μM zinc	110
4.2.1	Schematic depicting immortalisation of bone marrow progenitors using ER-Hoxb8	123

4.2.2	Confirmation of new conditionally immortalised Hoxb8 progenitor cells compared to stock Hoxb8 cells	124
4.3	Cell viability and expansion of Hoxb8 cells after removal of estrogen and addition of G-CSF	126
4.4	Cell marker surface expression in Hoxb8 cells compared to primary neutrophils	128
4.5	Time course of changes in cell morphology of Hoxb8 neutrophils compared with primary neutrophils	131
4.6	Representative western blot demonstrating Hoxb8 neutrophil development in WT and *Hvcn1*$^{-/-}$ cells	134
4.7	Time course of respiratory burst activity in Hoxb8 neutrophils	136
4.8	Comparison of the respiratory burst in Hoxb8 neutrophils with primary neutrophils	137
4.9	Analysis of phagosomal ion fluxes in the Hoxb8 neutrophil model compared to primary neutrophils	140
4.10.1	Schematic of the link between phagocytosis and different classes of autophagy in neutrophils	142
4.10.2	Qualitative analysis of adenoviral GFP-tagged LC3 in WT day 4 Hoxb8 neutrophils	145
4.10.3	Qualitative analysis of GFP-LC3 formation in z stacks of phagocytosing WT day 4 neutrophils	146
4.10.4	Qualitative analysis of GFP-LC3 formation in z stacks of phagocytosing Hvcn1-/- day 4 neutrophils	147
5.2	Comparison of phagosomal pH and NOX2 activity between neutrophils and monocytes	154
5.3	The phagosomal environments of monocytes differ between subsets	158
5.4	cDC2s and MoDCs have acidic phagosomes with low oxidase activity	163
5.5	LPS treatment increased the respiratory burst activity and phagosomal pH of MoDCs	166
5.6	Phagosomal pH varies between different monocyte-derived macrophage subsets	171
5.7	AnnexinV-Propidium iodide assay for apoptotic neutrophils	174
5.7.2	Confocal images of live polarised macrophages efferocytosing	175
5.7.3	apoptotic neutrophils	176

5.8 A summary of chapter five's main results 179
6 A schematic summary 190

List of tables

1.3 Granule subsets and their components 43
2.13 Source of online study datasets for neutrophil composite mRNA expression 86
3.3 A compilation of the averaged results of nine online datasets of mRNA expression in neutrophils 92
3.4 Phagosomal pH and area experimental measurements and statistics for chloride channel inhibitors 96
3.5 Phagosomal pH and area experimental measurements and statistics for potassium channel inhibitors 98
3.7 Statistics of phagosomal pH and area for the knockout mouse models 104
3.12.1 Summary of the effects of specified compounds with their reported sites of activity, and the general effect on phagosomal pH and area in human neutrophils 113
3.12.2 Summary of the KO mouse and patient neutrophil data with reported chemical inhibition or activation 115

Chapter One: Introduction

1.1 General overview

The immune system is an interconnected family of specialised cells and chemical mediators that aim to maintain the host's equilibrium against pathogenic invasion by microbial threat and misdirected attack by host effector cells or tumours. It can be split into two general arms: the innate side, the cells which respond first to inflammation, and the adaptive side, which takes time to mount a highly specific attack.

In the situation of infection, neutrophils are usually the first cells on the scene as they can extravasate quickly from blood vessels into tissue. They are recruited to the damaged area by chemical mediators released by resident phagocytes, such as resident macrophages or dendritic cells (DCs), or by patrolling non-classical monocytes (Auffray *et al.*, 2007). Neutrophils engulf pathogens quickly and release cytokines to attract other innate cells. These include inflammatory monocytes, which mostly arrive 48-72 hours after the primary neutrophil infiltration (Patel *et al.*, 2017). These assist in phagocytosis of pathogenic material, release other mediators, and can differentiate into macrophages and dendritic cells depending on the tissue environment.

The monocyte-derived macrophages and DCs, along with tissue resident macrophages, aid in the clear-up of tired and pathogen-laden apoptotic neutrophils and monocytes through efferocytosis (Norling & Perretti, 2013). This works to resolve the inflammatory response and to reduce the dissemination of harmful antimicrobial agents which may escape apoptotic immune cells (Gordon & Plüddemann, 2018). Phagocytosing macrophages and DCs can activate the adaptive immune system by presenting antigen to T and B cells. This thesis focuses primarily on how the

intracellular environment of neutrophils is regulated to contain and kill engulfed pathogens, with later investigations into other professional phagocytes.

1.2 Haematopoiesis

The production of the heterogeneous variety of blood cells is defined as haematopoiesis. It is a very complex and controlled process, beginning as primitive haematopoiesis in the yolk sac of the embryo containing the initial haemangioblast, transitioning to the fetal liver, before the establishment of definitive haematopoiesis which takes place in adult life in the bone marrow (Jagannathan-Bogdan & Zon, 2013). All types of blood cells originate from one type of precursor in the bone marrow, the haematopoietic stem cell (HSC), which has the ability of self-renewal and differentiation into daughter cells (Kondo *et al.*, 2003). With increasing differentiation in response to environmental growth factors and molecules, the variety of cell fates and ability to self-replicate decreases. The process is hierarchical up to a point of multipotent precursors, which have limited cell differentiation. Thereafter, the cells are committed to lineage-specific paths in becoming terminally differentiated cells (Seita and Weissman, 2010).

HSCs have the ability of self-renewal to maintain their population, either as long-term or short-term HSCs, and can differentiate into multipotent progenitors (MPPs). MPPs have lost the capacity for self-renewal, with differentiation they become oligopotent progenitors with decreased cell fate capacity. These include the megakaryocyte-erythrocyte progenitor (MEP), the common myeloid progenitor (CMP), and the common lymphoid progenitor (CLP). Mast cells are thought to arise directly from the CMP through related precursor cells. The CMP can also give rise to the granulocyte-monocyte precursor (GMP) and the MEP. These progenitors next differentiate into

lineage-specific progenitors, which overall are restricted to differentiate into certain terminally differentiated cells. The MEP differentiates into the megakaryocyte

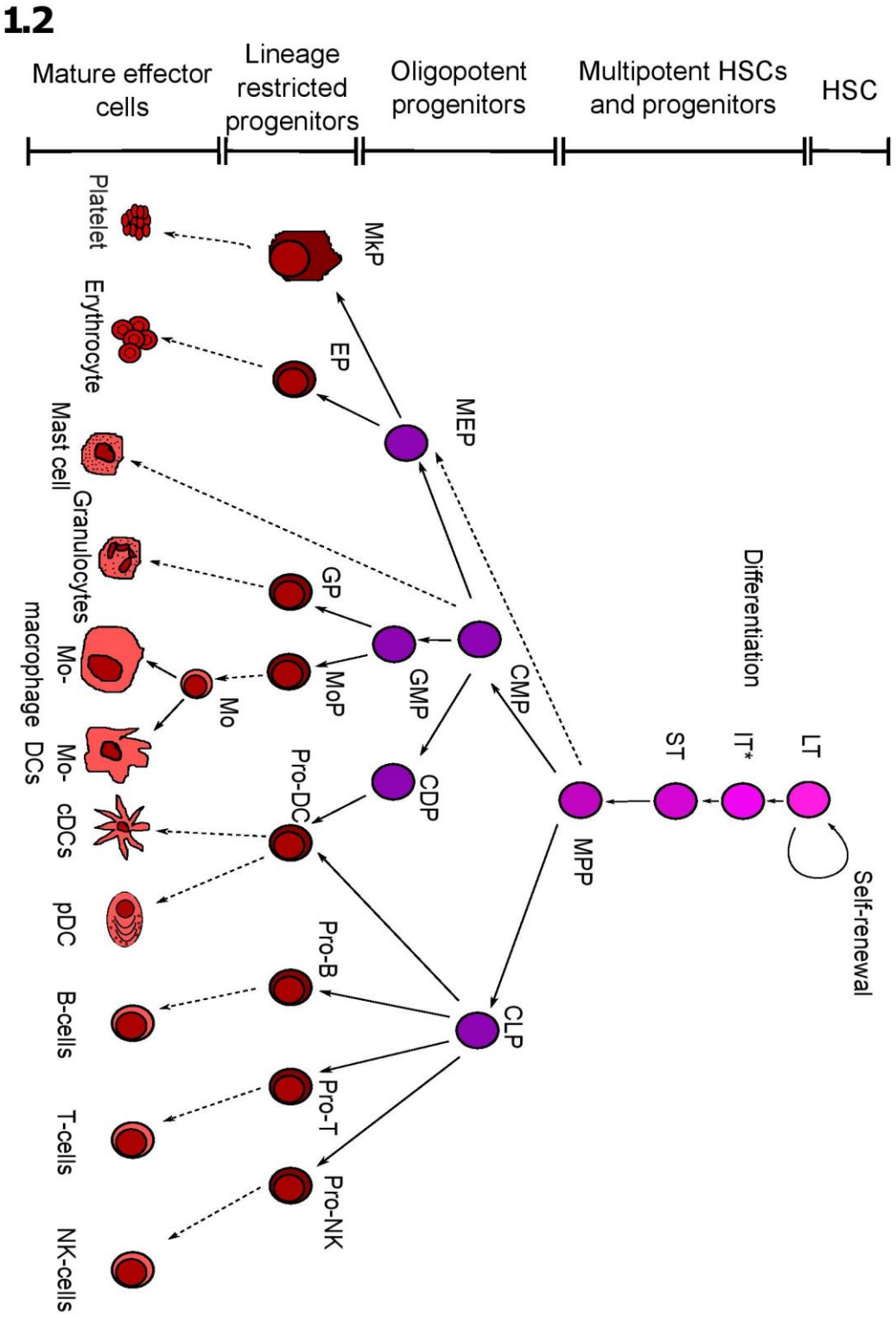

Figure 1.2 | The hierarchical nature of haematopoiesis. *LT; long-term, IT; intermediate-term (*currently shown only in mice, not humans), ST; short-term, MPP; multipotent progenitor, CMP; common myeloid progenitor, CLP; common lymphoid*

progenitor, MEP; megakaryocyte-erythroid progenitor, GMP; granulocyte/monocyte progenitor, CDP; common dendritic cell progenitor, MkP; megakaryocyte precursor, EP; erythrocyte precursor, GP; granulocyte precursor, MoP; monocyte precursor, Pro-DC; DC precursor, Mo; monocyte, cDCs; conventional DC classes, pDC; plasmacytoid DC. Adapted from (Seita and Weissman, 2010).

precursor and erythrocyte precursor, finally becoming platelets and erythrocytes respectively. The GMP gives rise to the granulocyte progenitor which terminally differentiates into neutrophils, eosinophils and basophils (the granulocytes). The GMP also differentiates into the monocyte precursor (MoP), which differentiates into monocytes, which can further differentiate into monocyte-derived macrophages in certain circumstances. It is now known that most tissue-resident macrophages originate from precursor cells from the yolk sac and not from definitive haematopoiesis (Ginhoux & Guilliams, 2016). The origin of DCs is not fully understood, but it is thought that the blood dendritic cells (conventional and plasmacytoid classes) can arise from a separate progenitor, the common dendritic cell progenitor (CDP) (Lee *et al.*, 2015), as well as from the CLP. Monocytes can also differentiate into monocyte-derived DCs. The CLP differentiates into precursor cells of B, T and NK cells, which terminally differentiate into B, T and NK cells respectively. Cells at different stages of haematopoiesis are defined by specific cell markers which change over time. **Figure 1.2** describes the outline of haematopoiesis in mouse and human.

Activation of transcription factors by growth factors and associated proteins is essential for the maintenance and movement of correct haematopoiesis. For example, the *c-kit* ligand or stem-cell factor (SCF) is well characterised as an essential factor for HSCs, which is secreted by structural stromal cells in the bone marrow. It binds to the receptor tyrosine kinase, *c-kit*, which is a classical marker of murine HSCs (Ogawa *et al.*, 1991), which in turn activates transcription factors like RUNX1 (also known as AML-1) (Growney *et al.*, 2005; Ichikawa *et al.*, 2004) and

CCAAT/enhancer binding protein alpha (C/EBPα) (Zhang *et al.*, 2004). Mutations in RUNX-1 can result in acute myeloid leukaemia (AML) (Ganly, Walker & Morris, 2004). IL-3, IL-6, IL-11 and fms-like tyrosine kinase (Flt-3) ligand have all been reported as cytokines important for HSC biology (Seita and Weissman, 2010), but there are redundancies in their necessary expression (Nandurkar *et al.*, 1997). Additionally, upregulation of Flt-3 receptor on HSCs has been associated with lack of self-renewal capacity (Adolfsson *et al.*, 2001). PU.1 is expressed by HSC but is continually expressed for the correct development of mononuclear cells (myelopoiesis) (Dakic *et al.*, 2005; Nutt *et al.*, 2005). IRF8 is not expressed in HSC, but later in CMP and GMP (Wang *et al.*, 2014) and is also a crucial transcription factor (Tamura, Kurotaki & Koizumi, 2015). IRF8 blocks C/EBPα to permit myelopoiesis (Kurotaki *et al.*, 2014), but C/EBPα expression is required for generation of GMP (D'Alo' *et al.*, 2003).

There are four glycoprotein cytokines that are master regulators of HSC differentiation into assorted cell types: Granulocyte-macrophage colony stimulating factor (GM-CSF), macrophage-colony stimulating factor (M-CSF), granulocyte-colony stimulating factor (G-CSF) and IL-3 (originally known as multipotential colony-stimulating factor) (Metcalf, 2013). They were first discovered when they were found to be essential for neutrophil and macrophage colony formation from mouse bone marrow progenitors *in vitro* through binding to cell surface receptors to initiate downstream signalling events (Ichikawa, Pluznik & Sachs, 1966; Burgess, Camakaris & Metcalf, 1977; Ihle *et al.*, 1982; Nicola *et al.*, 1983). They are involved in the haematopoiesis specifically of myeloid cells by involvement in lineage-commitment choices (Rieger *et al.*, 2009), for stimulation of cell-division (Lord *et al.*, 1991), and viability of progenitor cells by inhibiting apoptosis (Williams *et al.*, 1990). IL-3 has the capacity to produce many different cell types: megakaryocytes, mast cells, eosinophils, basophils, erythrocytes, neutrophils and macrophages (Schrader, 1998). The other CSFs are more limited; G-CSF stimulates production and affects neutrophils (Semerad *et al.*, 2002; Rapoport,

Abboud & DiPersio, 1992), M-CSF for macrophages (Stanley *et al.*, 1997), while GM-CSF is linked to macrophage, neutrophil, eosinophil and DC formation (Sheridan, Metcalf & Stanley, 1974; Rapoport, Abboud & DiPersio, 1992). CSFs also govern actions of terminally differentiated for specific effector functions such as G-CSF for phagocytosis and NADPH oxidase stimulation in neutrophils (Yamaguchi, Yamaguchi & Hayakawa, 1998). Neutrophils are the primary focus of this thesis, therefore, their biology will subsequently be discussed in further detail.

1.3 Neutrophils

Neutrophils are the most abundant white blood cell in the body and play key roles in host response to infection (Nathan, 2006) but are implicated in many disease states. They are terminally differentiated cells with limited protein production. This agrees with most researchers' view of their short life-span of approximately 24 hours *in vitro* (McCracken & Allen, 2014; Lee, Herant & Heinrich, 2011), but there is other evidence to suggest they can last up to 5-6 days *in vivo* (Pillay *et al.*, 2010; Yamashiro *et al.*, 2001). This section will describe in more detail their response to a bacterial infection, focusing on the intracellular processes related to the killing and degradation of the engulfed bacteria, and then the natural clearance of neutrophils after they have carried out their microbicidal function.

Microbial sensing

Neutrophils represent only a fraction of total cells in the body, but they must be able to move quickly and cover great distances across them to reach the sources of pathogenic stimuli. Neutrophils can respond to molecules sourced directly from microbes, such as cell wall components or released toxins, or from chemical signals released from other host cells. There is an increasing chemical concentration that

guides the neutrophil, known as a chemotactic gradient, towards the stimuli. There are overlapping gradients supplied by other mediators along the way to the primary stimulus which helps to maintain the right path for the neutrophil (Foxman, Campbell & Butcher, 1997). Once the neutrophil reaches the origin of the stimulus, if it can locate the bacterium it will attempt to engulf it in a process termed phagocytosis. In the event that the neutrophil cannot appropriately physically neutralise the pathogen, it will release its toxic granular contents into its immediate surroundings, in the hope that they will affect nearby extracellular bacteria (Nathan, 1987). The extruded components include enzymes which break down the extracellular matrix. This aids neutrophils in reaching the bacteria which can become trapped in the deconstructed tissue, but it must be tightly controlled and resolved to prevent unnecessary damage to the host, which can lead to certain diseases of chronic inflammation.

Phagocytosis

Phagocytosis is defined as the receptor-mediated engulfment of particles greater than 0.5 μm in diameter into a membrane-lined intracellular compartment named the phagosome or phagocytic vacuole (Swanson, 2008; Flannagan, Jaumouillé & Grinstein, 2011). The first step of phagocytosis is the connection of phagocyte to the particle. Internalisation can occur via opsonic or non-opsonic receptors (**Fig. 1.3.1**). Opsonins are host serum factors that attach to the microbe surface to make them detectable by phagocytic cells; the word derives from Greek meaning “to prepare a meal” (Swanson, 2008). The most studied opsonins are immunoglobin (Ig) proteins and members of the complement system.

Ig antibodies are produced by B cells and are comprised of 5 different isotypes, but the most abundant and relevant isotype in the context of phagocytosis is IgG. It is further made up of four subclasses, each with slightly varying functions such as

affinity for a type of foreign antigen and half-life (Vidarsson, Dekkers & Rispens, 2014). The fragment crystallizable (Fc) structural part of an Ig molecule is the specific antigen for Fcγ-receptors present on leukocytes (Jefferis & Lund, 2002). There are also different FcγRs classified based on cell distribution and specific function, but most are involved with phagocytosis (Kapur, Einarsdottir & Vidarsson, 2014). The isoforms present on neutrophils involved in phagocytosis best described are the low-affinity FcγRIIA (CD32) and FcγRIIIB (CD16) (Urbaczek *et al.*, 2014; Swanson & Hoppe, 2004) on resting neutrophils, but when activated they upregulate expression of high-affinity FcγRI.

1.3.1

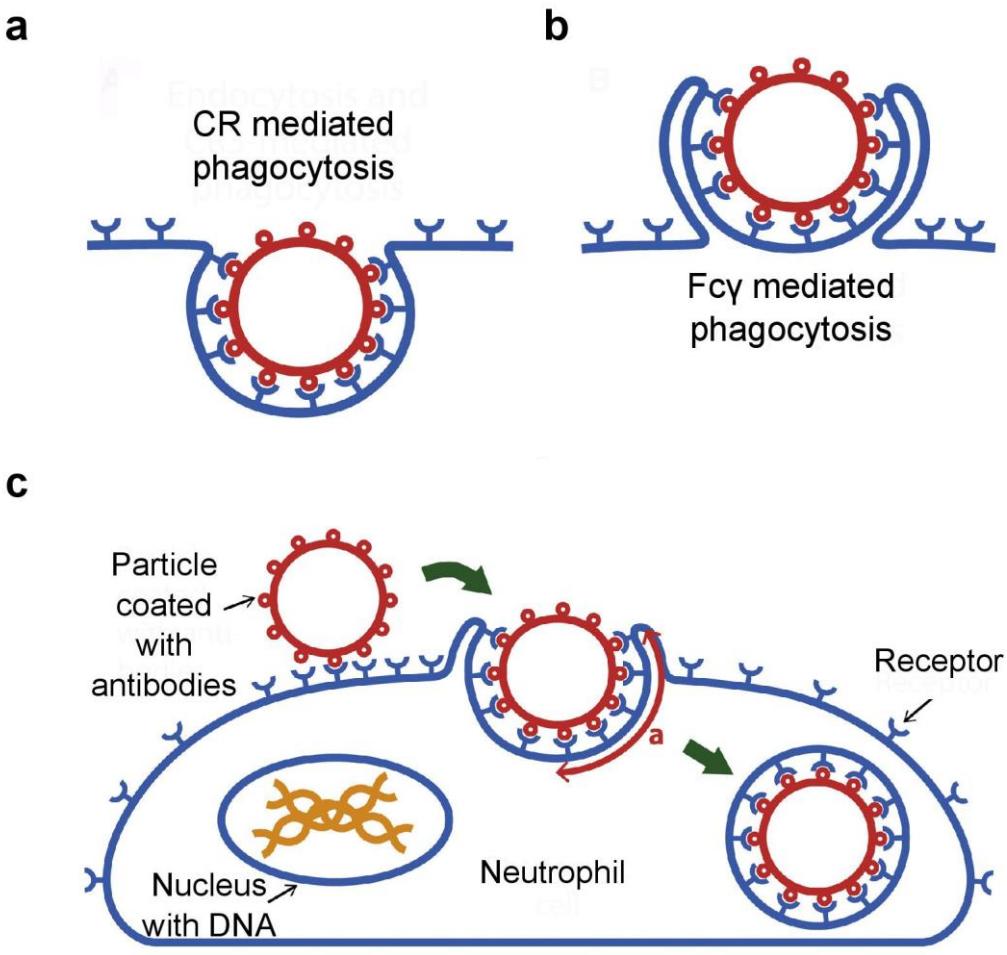

Figure 1.3.1 | General mechanism of phagocytosis (a-c). (**a**) *A particle coated with opsonins sinks into the cell by CR mediated phagocytosis, whereas in* (**b**) *the neutrophil extends pseudopodia around a particle coated with Ig to engulf it via Fcγ*

mediated phagocytosis. (**c**) *A general overview of cell attachment to the antibody-coated particle, the arc length (a) of phagosomal membrane increases to accommodate the particle into the cell. Adapted from (Richards & Endres, 2014).*

The complement system is composed of three arms, the classical, alternative, and lectin pathway (Merle *et al.*, 2015), which despite having varied intermediary processes, all lead to the cleavage of C3 into C3a and C3b. C3b is a fundamental opsonin which can be further cleaved into iC3b that still acts as an opsonin but loses the ability to activate other complement pathways (Morgan & McGeer, 1995). Complement opsonins are ligands for complement receptors (CRs), which are abundant on myeloid and lymphoid cell surfaces. While there is a variety of different CRs based on protein structure, only certain ones are specialised for phagocytosis of opsonised pathogens such as CR1, CR3 and CR4. CR1, otherwise known as CD35, is a member of the short consensus repeat superfamily (Dustin, 2016), while CR3 (Mac-1/CD11b) and CR4 (CD11c/CD18) are members of the β2 integrin family (Springer & Dustin, 2012).

1.3.2

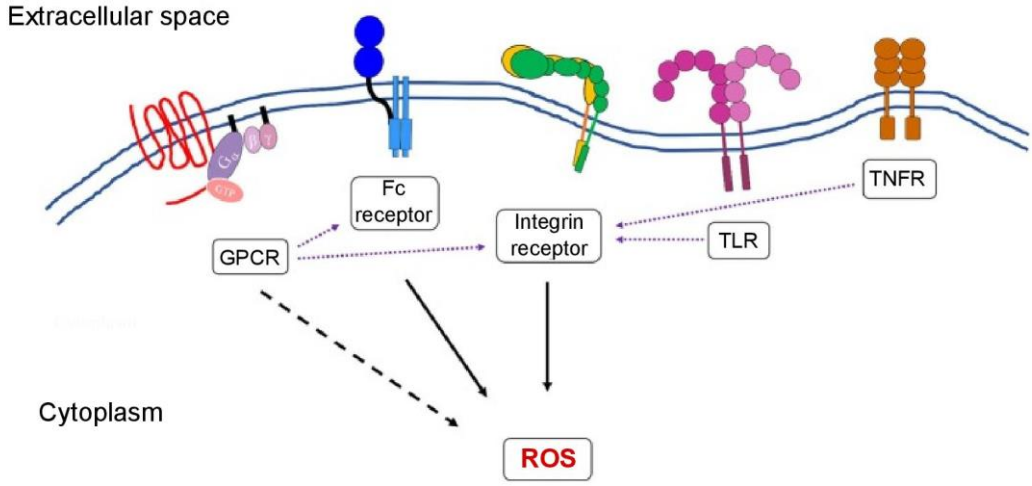

Figure 1.3.2 | Types of PRRs in neutrophils which are involved in ROS production. *GPCR; g-protein coupled receptors, TNFR; tumour necrosis factor receptors. Taken from (Nguyen, Green & Mecsas, 2017)*

Professional phagocytes can also associate directly with microbes through pathogen associated molecular pattern molecules (PAMPs) without the need for opsonins. These are proteins specific to microbes that include β1,3-glucan on fungal cell walls, lipopolysaccharide (LPS) which is a Gram-negative bacterial cell wall component, and CpG (unmethylated cytosine guanine bacterial DNA motifs). PAMPs interact with phagocytes via pattern recognition receptors (PRRs), which are varied and have specificity for different microbial proteins (**Fig. 1.3.2**). These include Toll-like (TLRs), nucleotide-binding and oligomerisation domain (NOD)-like (NLRs), RIG-I-like and C-type lectin receptors (Kumar, Kawai & Akira, 2011). TLRs themselves are not phagocytic receptors but help to prime the phagocytic response by activating integrin receptors (Parker *et al.*, 2005).

Once the opsonins or microbial products have bound to their respective receptors on the neutrophil cell membrane, they activate a series of complex downstream signalling that results in engulfment of the attached particle. For IgG-FcγR mediated phagocytosis, this has been well characterised as the “zipper” model, as there is tight interaction of host and pathogen cell surface molecules on host pseudopodia that encapsulates the microbe (Michl *et al.*, 1979). The iC3b-CR specific phagocytosis varies in that there is more space between host and microbe in the host phagocytic cup. Numerous molecules are recruited to the so-called “phagocytic synapse” to aid in internalisation by actin cytoskeleton rearrangement including phospholipases, Rho-family GTPases and adaptor proteins (Goodridge *et al.*, 2011). In neutrophils, the newly-engulfed membrane-bound compartment then immediately progresses with fusion of small cytoplasmic vesicles called granules.

Granulopoiesis and degranulation

Neutrophils, eosinophils and basophils are all named due to their cytoplasmic granule composition – granulocytes. Granules store a wide selection of antimicrobial enzymes, peptides, receptors, that are emptied into the phagosome or extracellular space upon fusion with the activated membrane. This degranulation occurs within a matter of seconds in neutrophils (Segal, Dorling & Coade, 1980). There are distinct subsets of granules which are defined by their specific contents, and they are generated at different stages in neutrophil differentiation in the bone marrow (granulopoiesis). Work from the Bainton and Borregaard labs has been central to our understanding of neutrophil granule biology.

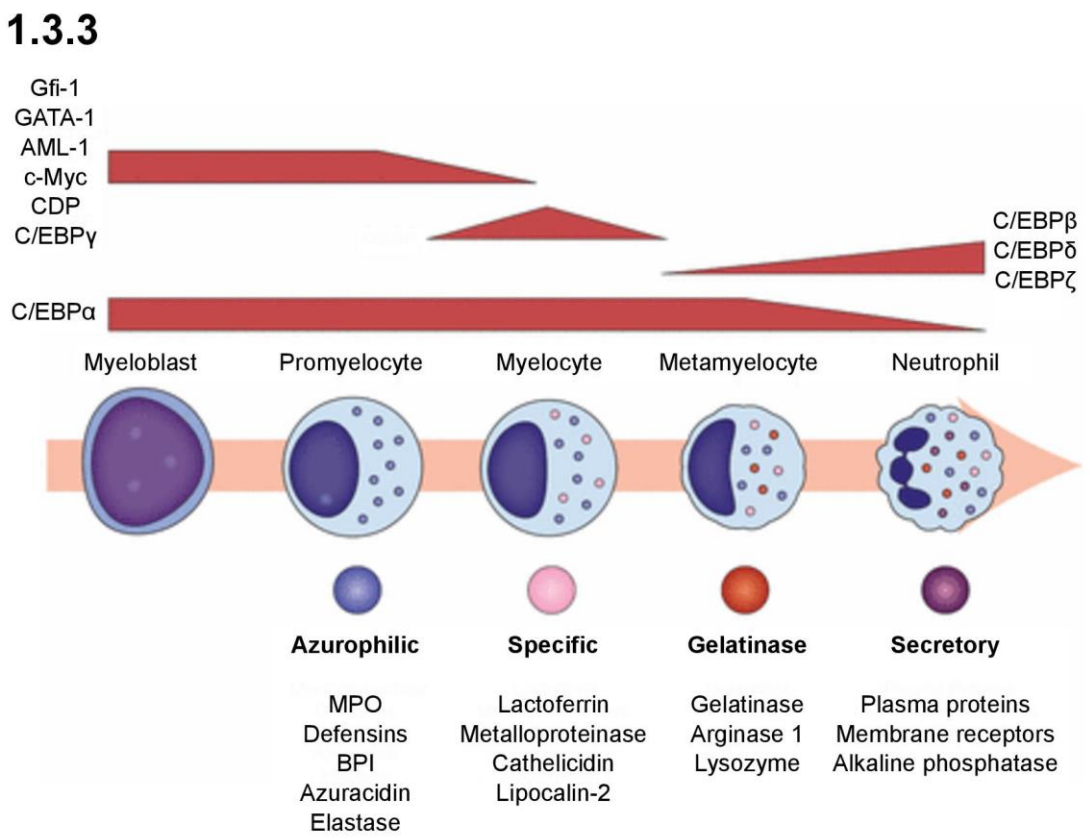

Figure 1.3.3 | Granulopoiesis and associated expression changes in transcription factors. *Taken from (Lawrence, Corriden & Nizet, 2018).*

The expression of C/EBPε is localised to the myelocyte stages, as the cell differentiates into the terminal stages of band cell and polymorphonuclear neutrophil, there is increased expression of C/EBPβ, C/EBPδ and C/EBPζ (Bjerregaard *et al.*,

2003). The granules produced in this stage are known as tertiary or gelatinase granules. They are similar to specific granules in that they also contain gelatinase and cytochromeb_{558}, however, gelatinase granules are much smaller and contain fewer proteins; for example, they lack lactoferrin (Kjeldsen *et al.*, 1994).

The promyelocyte is the next differentiation step after the GP or myeloblast, and where the generation of granules begins (**Fig. 1.3.3**). The first made are primary or azurophil granules, which contain mainly proteinases such as myeloperoxidase (MPO), elastase and defensins but few surface receptors. They are heterogeneous in sizes and vesicular content depending on the time they were formed; defensins are acquired in the later stages (Egesten *et al.*, 1994). As the cell divides and progresses into the myelocyte/meta-myelocyte stages, production of specific or secondary granules commences. The transcription factors, AML-1 and c-Myc, that stimulate expression of azurophilic granule proteins begin to decline, while those for specific granule protein expression rise. The main transcription factor for specific granules is CCAAT/enhancer binding protein-ε (C/EBPε), that is demonstrated in patients with neutrophil-specific granule deficiency who have a mutation in this gene (Gombart *et al.*, 2001). Specific granules noticeably lack peroxidases such as MPO but contain a large arsenal of other potent agents. These include lactoferrin, gelatinase, lysozyme and collagenase. There is increased synthesis of membrane-bound receptors and proteins compared to the azurophil granules, such as CD11b, CD66 and the NADPH oxidase subunits gp91phox and p22phox (cytochromeb_{558}).

There is another intracellular vesicle similar to granules that was discovered later than the first three, called secretory vesicles. They contain more cell surface receptors than the other granule subsets, such as the phagocytic receptors CD11b, FcγRIII and CR1. Their main difference from the classical granules is that they are thought to be formed by endocytosis, as they contain proteins which are normally present in the plasma and not made by neutrophils (Borregaard *et al.*, 1995). However, this

hypothesis may need closer examination as proteomic studies of secretory vesicles have found the presence of neutrophil plasma membrane proteins, but there are a few caveats related to purity of sample preparation (Uriarte *et al.*, 2008; Jethwaney *et al.*, 2007).

Timing is a big factor in granule biology. The composition of granules depends on the progression of proteins emitted from the Golgi apparatus which changes over time (Le Cabec, Calafat & Borregaard, 1997). The fusion of granules with the phagocytic or activated cell surface membrane is not random but synchronised. Secretory vesicles are the first to degranulate, with minimal stimulation from soluble factors such as fMLP of bacterial origin, and host chemokines, leukotriene B4 (LTB4), tumour necrosis factor (TNF), IL-8 and GM-CSF (Borregaard *et al.*, 1994). They quickly fuse with the plasma membrane and release their contents by exocytosis. The enclosed receptors join the outer cell membrane in case they are needed for phagocytosis, and for efficient binding to endothelium for chemotaxis (Rorvig *et al.*, 2013). The secretory vesicles also contain superoxide dismutase (SOD) which is not of neutrophil origin, but endocytosed from the extracellular matrix and stored in the vesicles until the neutrophil is activated (Iversen *et al.*, 2016). SOD scavenges superoxide radicals and converts them into molecular oxygen or hydrogen peroxide, slightly less reactive oxygen forms. It is hypothesised that the neutrophils could be tempering its oxidative effects on the extracellular matrix (Yao *et al.*, 2010).

Degranulation continues in reverse order of granulopoiesis with gelatinase granules following secretory vesicles, then specific and finally azurophilic granules (Sengelov *et al.*, 1995). The order of release correlates with increasing threshold stimulation for exocytosis and granular content potency, ideally to limit extracellular exposure of degradative granule components. Consequently, the movement and fusion of granules are tightly regulated by various vesicular trafficking mechanisms. A major protein family involved are members of the Rab GTPases, part of the superfamily of

Ras-like monomeric GTPases (Pereira-Leal & Seabra, 2000). Various Rab GTPases and their effector proteins have been implicated in neutrophils for distinct functions. For example, Rab27a and b regulate azurophilic granule exocytosis (Johnson *et al.*, 2010), while another group has shown Rab27a to regulate secondary and tertiary granule release (Herrero-Turrión *et al.*, 2008). Rab5a has been implicated in fusion of granules to phagosomes containing *Mycobacterium tuberculosis* and *Staphylococcus aureus* (Perskvist *et al.*, 2002) and therefore a regulator of phagosomal maturation.

The NADPH oxidase

With phagocytosis of captured bacteria or fungi, one of the first biochemical observations made in neutrophils was a large burst of respiration or respiratory burst (Baldridge & Gerard, 1933; Sbarra & Karnovsky, 1959); that is, transient intake of oxygen. This fuelled many decades of intensive research to work out the causative enzyme involved in the non-mitochondrial oxygen consumption, increased activity of the hexose monophosphate shunt (Sbarra & Karnovsky, 1959), and increased production of hydrogen peroxide (H_2O_2) (Iyer, Islam & Quastel, 1961).

A multicomponent enzyme complex was eventually discovered present in the phagosomal membrane that transfers electrons to oxygen to form superoxide radicals, called the NADPH oxidase. In the neutrophil isoform NOX2, it is composed of two membrane-bound subunits which reside in the granules in non-activated neutrophils: the alpha subunit, $p22^{phox}$, and beta subunit, $gp91^{phox}$, which together make up the heterodimer (flavo)cytochromeb_{558} (Segal & Jones, 1978), the “phox” standing for phagocyte oxidase. The electrons are passed from the defining nicotinamide adenine dinucleotide phosphate (NADPH) which binds to a position on the cytosolic c-terminal end of the complex, to an associated flavin adenine

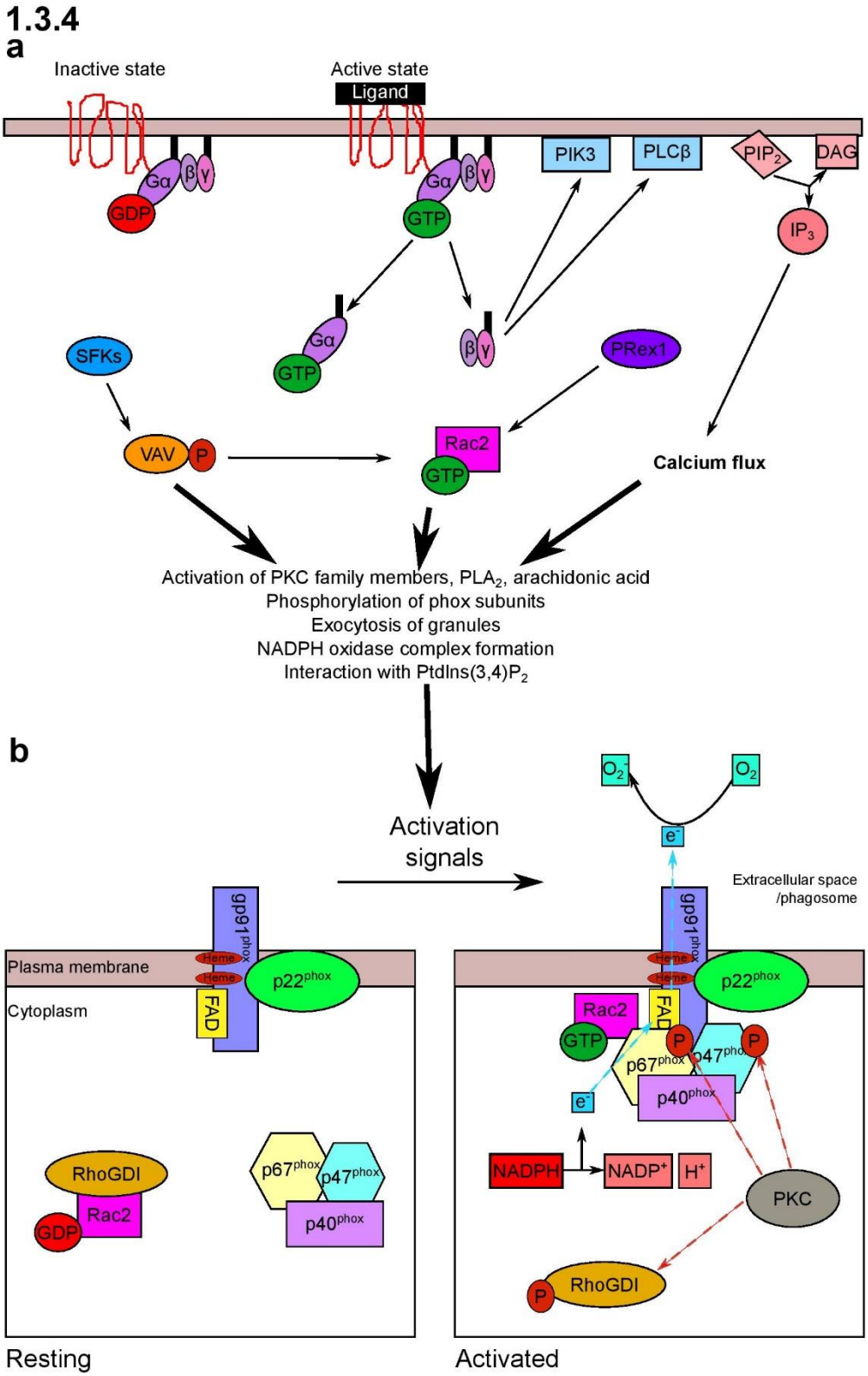

Figure 1.3.4 | Mechanisms of NADPH oxidase activation (a-b). (**a**) *Activation of the formyl receptor (a GPCR) that initiates NOX2. (***b***) The changes resulting from activation signals such as formyl receptor activation* (**a**) *on NADPH oxidase assembly and activation. Adapted from (Nguyen, Green & Mecsas, 2017) and (George et al., 2010)*

dinucleotide (FAD), then to the two heme (iron-containing) groups positioned in the membrane, and finally to oxygen across the membrane in the phagocytic vacuole (Sumimoto *et al.*, 1992). These redox centres are all positioned on the gp91^{phox} with p22^{phox} binding tightly to it.

It has been hypothesised that the main function of p22^{phox} is to act as high-affinity binding sites for the cytosolic components of the oxidase (Cross & Segal, 2004). These include p67^{phox}, p47^{phox}, p40^{phox} and Rac-2, a small G-protein. The *phox* subunits were numbered by their band sizes on Western blots. The binding of these cytosolic subunits is essential for correct electron transport of the oxidase, and their localisation and activation at the membrane happen almost instantaneously.

The exact mechanisms of NOX2 activation are still being investigated but involve many protein-protein interactions and phosphorylation. The most common trigger for NADPH oxidase activation is ligand-binding to cell surface receptors, such as fMLP to its specific formyl-peptide receptor or IgG binding on opsonised bacteria to an FcR. They have different initial downstream effects: the formyl-peptide receptor uses G-proteins to transmit the activation signal via exchange of bound guanosine diphosphate (GDP) to guanine triphosphate (GTP), which then activates phospholipases and protein tyrosine kinases (Belambri *et al.*, 2018) (**Fig. 1.3.4a**). Whereas the FcR activates SRC kinases which phosphorylate ITAMs, leading to recruitment of SYK kinases (Tohyama & Yamamura, 2009), activating other complexes such as phosphoinositide 3-kinase (PI3K). This generates phosphatidylinositol-3,4,5-trisphosphate (PtdIns(3,4,5)P3) (Nimmerjahn & Ravetch, 2008), which activates phospholipases. These include phospholipase C (PLC) which catalytically cleaves phosphatidylinositol 4,5-bisphosphate (PIP2) into diacylglycerol (DAG) and inositol-triphosphate (IP3). DAG activates the family of protein kinase C (PKC) which ultimately phosphorylate p47^{phox}, p40^{phox} (Bouin *et al.*, 1998), p67^{phox} (Benna *et al.*, 1997) and gp91^{phox} (Raad *et al.*, 2009). There is evidence of it

phosphorylating $p22^{phox}$ but other enzymes including phospholipase D play a role (Regier *et al.*, 2000). There are other pathways for phosphorylation, including PI3K activation of MAPK (ERK1/2 and p38MAPK) pathways which mainly phosphorylate $p47^{phox}$ (Yamamori *et al.*, 2000), $p67^{phox}$ and $p40^{phox}$ (McLaughlin *et al.*, 2008). The commonly used *in vitro* oxidase stimulator phorbol 13-myristate 13-acetate (PMA) diffuses across the plasma membrane to directly activate PKC (Karlsson, Nixon & McPhail, 2000).

In the inactive state, Rac2 is bound to GDP by its inhibitor Rho-GDI (a guanine nucleotide dissociation inhibitor) and is activated with the exchange of GDP for GTP by guanine nucleotide exchange factors (GEF) (Hodge & Ridley, 2016), which in turn are stimulated by the downstream products of membrane stimulation. For example, phospholipase D2 is known to act as a GEF (Mahankali *et al.*, 2011).

Once the cytosolic subunits are phosphorylated and Rac2 is activated, they translocate to the membrane to interact with the cytochrome *b* to form complete assembly of the oxidase complex (**Fig. 1.3.4b**). $p47^{phox}$ and $p67^{phox}$ bind directly to cytochrome *b* at two different sites but interact to stabilise each other, as $p47^{phox}$ acts as an adaptor between $p22^{phox}$ and $p67^{phox}$ (DeLeo & Quinn, 1996). The translocation of $p40^{phox}$ to the membrane is thought to be dependent on $p47^{phox}$ with input from $p67^{phox}$ (Dusi, Donini & Rossi, 1996), where it interacts with $p47^{phox}$ and $p67^{phox}$ (Wientjes *et al.*, 1996). Rac2 translocates independently of the other cytosolic phox subunits and first binds to $gp91^{phox}$ before finally associating with $p67^{phox}$ (Bedard & Krause, 2007). After complete assembly of all subunits, cytochrome *b* undergoes a conformational change to allow electron transport.

Researchers have utilised different methods for understanding the very complex assembly and activation of the NADPH oxidase, which can complement each other or alternatively demonstrate that the oxidase has certain redundancies. For instance, the cell-free assays, comprising only the isolated granular and cytosolic fractions of

the cell in a test-tube, provided essential roles for $p47^{phox}$, $p67^{phox}$ and Rac2 for efficient oxidase activity through their interactions with cytochrome *b*. However, it appeared that $p40^{phox}$ had a participating role but was dispensable (Cross, 2000). These conclusions were corroborated in genetic and biochemical studies of neutrophils from patients with chronic granulomatous disease (CGD), who have recurrent, life-threatening infections due to malfunctioning of the NADPH oxidase through reduced or ablated superoxide production. There were reported mutations in $gp91^{phox}$, $p22^{phox}$, $p67^{phox}$, $p47^{phox}$ first reported from the 1930s, but none in $p40^{phox}$ (Holland, 2010). The mutations in Rac2 resulted in partial CGD phenotypes (Ambruso *et al.*, 2000). That was until 2009 when a new population of CGD patients was described with $p40^{phox}$ mutations (Matute *et al.*, 2009). It transpired that $p40^{phox}$ was not essential for oxidase activity on the plasma membrane or in cell-free assays, but was important for intracellular phagosomal ROS production (Ellson *et al.*, 2006). Similarly, Rac2's involvement in oxidase activity was found to be dependent on certain signalling pathways (Kim & Dinauer, 2001), which were elucidated using knockout mouse models (Roberts *et al.*, 1999).

Charge compensation

The result of NADPH oxidase activity is the transfer of electrons from NADPH to molecular oxygen. Electrons are negatively charged, so their continued movement would depolarise the plasma or phagosomal membrane leading to inhibition of the oxidase. Indeed, seminal observations of plasma membrane potential in neutrophils and eosinophils using dyes or patch-clamping show that treatment with PMA causes a membrane depolarisation that is linked to ROS production but is quickly reversed 1 minute after stimulation (Henderson, Chappell & Jones, 1987; DeCoursey, Morgan & Cherny, 2003a; Schrenzel *et al.*, 1998). However, the ROS production is sustained despite a plateau in membrane voltage. The negative charge entering the phagosome

or extracellular space must be neutralised or compensated by positive charge moving in the same direction, or negative charge moving in the opposite.

The patch-clamp experiments, the technique of measuring ionic currents on the activated plasma membrane, measured a large proton conductance that was coupled to the NADPH-oxidase current and both were sensitive to zinc inhibition (DeCoursey, Morgan & Cherny, 2003b; Schrenzel *et al.*, 1998). It was therefore hypothesised that a voltage-gated proton channel was compensating for the majority of the charge generated by the NADPH oxidase.

It was first considered if the NADPH oxidase itself acted as a compensatory proton channel since the two conductances were tightly coupled (Henderson & Meech, 1999; Maturana *et al.*, 2001). But this theory was overtaken when the hydrogen voltage-gated channel 1 (Hv1, gene name HVCN1) was cloned in 2006 through bioinformatic searches based on relevant cation channels (Ramsey *et al.*, 2006; Sasaki, Takagi & Okamura, 2006) and a knockout mouse model created. The channel was highly expressed in granulocytes, activated by membrane depolarisation, sensitive to pH, inhibited by zinc, and in the deficient mouse model had greatly reduced NADPH oxidase activity which made them more susceptible to certain bacterial infections (Ramsey *et al.*, 2009; Morgan *et al.*, 2009; El Chemaly *et al.*, 2014; Okochi *et al.*, 2009). The NADPH oxidase activity in *Hvcn1*$^{-/-}$ mouse neutrophils ranged from 30-70% of normal, which leads to the conclusion that Hvcn1 is not the sole charge compensating channel.

There have been many investigations into phagosomal ionic flux in neutrophils but unfortunately little consensus. A particular challenge is the measurement of an intracellular compartment that is also very reactive. Whole-cell patch-clamping electrophysiology was one of the first methods to provide insight into neutrophil ionic flux, by measuring ion conductances on the plasma membranes of resting and activated neutrophils and the closely related eosinophils who also have similar

NADPH oxidase activity when their plasma membranes are stimulated with PMA. The proton conductance, now known to be through Hv1, was the largest outward current recorded, but there were also reports of smaller conductances of calcium (Ca^{2+})-activated potassium (K^+) and chloride (Cl^-) channels (Schumann & Raffins, 1994; Krause & Welsh, 1990) and volume-regulated Cl^- currents (Stoddard, Steinbach & Simchowitz, 1993) in neutrophils. In activated eosinophils, there were very small K^+ and Cl^- recorded currents (Schwingshackl, Moqbel & Duszyk, 2000), including Ca^{2+}-activated K^+ channels (Saito *et al.*, 1997). Unfortunately, it appeared impossible to patch the phagosomal membrane itself to obtain a direct reading.

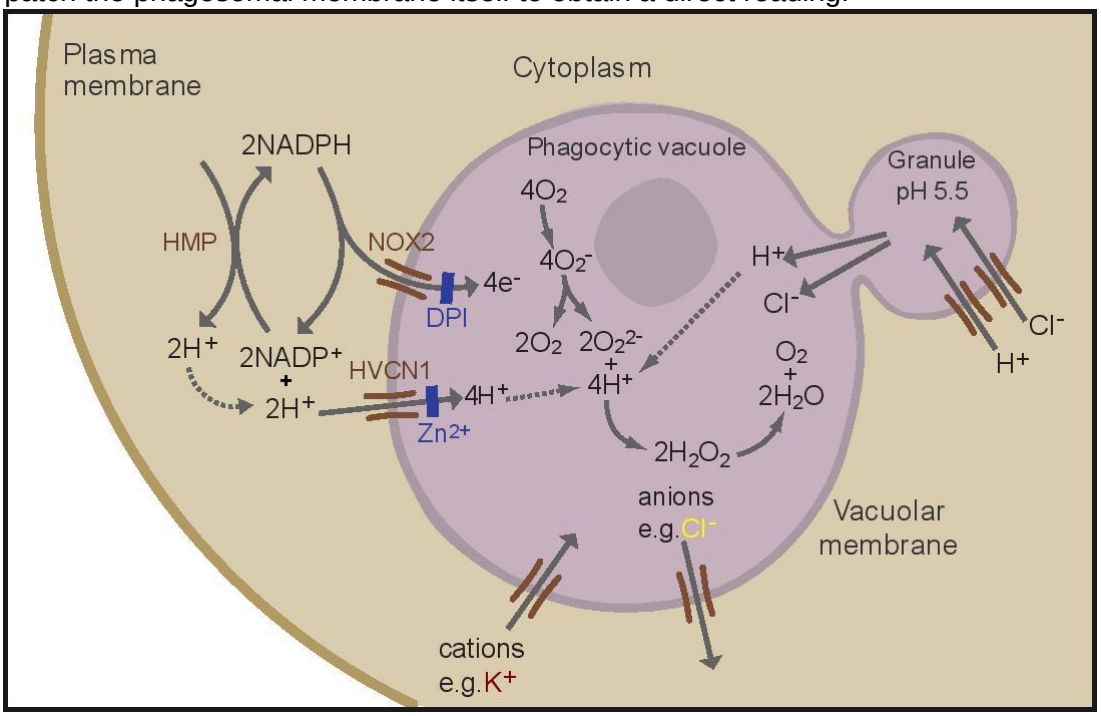

Figure 1.3.5 | Proposed NADPH oxidase-induced ion fluxes in the neutrophil phagosome. *The hexose monophosphate shunt (HMP) supplies NADPH in the cytosol for the oxidase (NOX2) which transfers electrons into the phagocytic vacuole for downstream oxidative reactions. It is inhibited by DPI, while the charge compensating HVCN1 is inhibited by zinc.*

These initial findings of K^+ and Cl^- channels on the granulocyte plasma membrane lead to the reasoning that these ions were compensating some of the NADPH oxidase-induced charge. The ions are both present in significant concentrations in the extracellular space and in the neutrophil cytoplasm (Simchowitz & De Weer, 1986; Simchowitz, Spilberg & De Weer, 1982), providing relevance for their participation. A

study in eosinophils found that depletion of K^+ from the extracellular medium decreased superoxide production (Schwingshackl, Moqbel & Duszyk, 2000). Biochemical studies then followed to demonstrate K^+ and Cl^- flux in neutrophils using radiolabelled isotopes of K^+ and Cl^-. Busetto and colleagues used $^{36}Cl^-$ to demonstrate an efflux of Cl^- from the neutrophil into the extracellular medium with phagocytosis of opsonised *Candida albicans* and *S. aureus* (Busetto *et al.*, 2007), while Reeves and co-workers described a K^+ flux into the phagocytic vacuoles of neutrophils phagocytosing *S. aureus* using the K^+ ionophore $^{86}Rb^+$, and an outward flux into the extracellular medium when the oxidase was stimulated at the plasma membrane (Reeves *et al.*, 2002). K+ efflux of activated neutrophils was also demonstrated by another group (Rada *et al.*, 2004).

A problem for some researchers is that efflux of Cl^- from the phagosome would deplete the substrate for MPO to make HOCl needed for pathogen killing activity, so Cl^- will be moving from the relatively high concentration in the cytosol into the phagosome. This would be in the same direction as the oxidase associated electron movement and therefore be electrochemically unfavourable. A possible solution is the suggestion that the granules are a source of Cl^- for charge compensation and enzyme substrate (Segal, 2005) or transport of Cl^- occurs into the phagosome from the cytosol via electroneutral channels to then be pumped out by electrogenic ones (Wang & Nauseef, 2015).

There is evidence for calcium flux in neutrophils, as it is needed for proper granule release and subsequent oxidase activity (von Tscharner *et al.*, 1986; Simchowitz, Foy & Cragoe, 1990; Borregaard *et al.*, 1992), and has been shown to leave neutrophil phagosomes rapidly after phagocytosis into the cytosol (Lundqvist-Gustafsson, Gustafsson & Dahlgren, 2000; Nunes *et al.*, 2012). However, the positively charged ion would be moving in the opposite direction to compensate for the inward movement of electrons.

In regards to sodium flux, in resting neutrophils there is an inward flux from the extracellular medium into the cytosol (Simchowitz, Spilberg & De Weer, 1982) and many sodium channels have been described in neutrophils which range from voltage-gated Na^+ (Krautwurst *et al.*, 1992) to transient receptor potential (TRP) channels (Heiner, Eisfeld & Lückhoff, 2003). These comprise several families of cation channels that vary in their specificity to Na^+, Ca^{2+} and K^+ (Gees *et al.*, 2012). Despite the identification of numerous potential Na^+ channels in neutrophils, there are few reports of it carrying out phagosomal charge compensation. The focus has been on Cl^- and K^+ conductance and postulated to account for 5-10% of the charge not compensated by the Hv1 proton channel. A limiting factor for K^+ involvement has been its osmotic function – if it were to account for a larger part of compensation it would cause enormous swelling of the phagocytic vacuole.

pH

Charge compensation in the neutrophil phagosome is inextricably linked to pH when the majority of the charge is compensated by protons and Hv1 is known to play a significant role in ROS production. Therefore, measuring phagosomal pH has become an alternative way to measure phagosomal ionic fluxes. The first reports of neutrophil phagosomal pH were acidic in the range of pH 5-6, but it was found later to have a biphasic profile: alkaline to pH 7.5-8 immediately after phagocytosis then to slowly become acidic to pH 6/6.5 (Segal *et al.*, 1981; Cech & Lehrer, 1984; Jankowski, Scott & Grinstein, 2002). This conclusion was further revised with the use of another different pH indicator that found the phagosomal alkalinisation is maintained at pH 8.5 for 30 minutes after phagocytosis (Levine *et al.*, 2015). Importantly, the alkalinisation was found to be a direct consequence of NADPH oxidase activity as the phagosomes from CGD patients and healthy cells treated with diphenylene iodonium (DPI), an oxidase inhibitor, acidified to pH 5.5/6 immediately after phagocytosis

(Segal *et al.*, 1981; Jankowski, Scott & Grinstein, 2002; Levine *et al.*, 2015). The rise in pH is hypothesised to result from the consumption of protons in the reaction with superoxide produced by the oxidase to form water or H_2O_2.

As might be expected in *Hvcn1*$^{-/-}$ mouse neutrophils, they do not exhibit acidic but surprisingly very alkaline phagosomes due to the lack of proton influx (Levine *et al.*, 2015). They also have very large, swollen phagosomes. This observation suggests there is an osmotically active ion moving into the phagosome to account for charge compensation, and the aforementioned evidence points to K^+ movement.

It is also important to consider the pH of the cytosol when the oxidase is activated, as its ionic composition will provide the electrochemical gradient for channel activity. Many studies now agree that the cytosol is initially acidic, caused by the generation of protons when NADPH is reduced by the oxidase, then the cytosol becomes more alkaline in most cases (Morgan *et al.*, 2009; Levine *et al.*, 2015). The Hv1 channel is thought to remove the excess protons into the phagosome, as cytosolic pH is very acidic in the knockout mouse model compared to wildtype neutrophils (Morgan *et al.*, 2009; Levine *et al.*, 2015). But other channels have been implicated in regulating neutrophil cytosolic pH, such as the Na^+/H^+ exchanger (Grinstein, Furuya & Biggar, 1986), Cl^-/HCO_3^- antiport (Giambelluca & Gende, 2011), and the V-ATPase (Nanda *et al.*, 1996; Gilman-Sachs *et al.*, 2015).

It is obvious that the regulation of phagosomal ionic flux is a complex process that has not yet been fully characterised or fundamental aspects agreed upon by the research community. More details of the specific ion channels involved in charge compensation and pH of the neutrophil phagosomes are found in chapter three of this thesis, which attempts to address the gaps in our understanding.

Oxidative killing

It is important for us to understand how the activity of the NADPH oxidase is regulated because its correct functioning is essential for the killing of certain pathogens, as demonstrated in CGD patients. Oxidative killing describes the microbicidal actions directly inflicted by the biochemical products of the NADPH oxidase, i.e. the reactive oxygen species and subsequent reactions. Superoxide radicals (O_2^-) are the primary oxidase product formed by the reduction of molecular oxygen with electrons and are generated in vast quantities (Segal & Coade, 1978). H_2O_2 is then immediately formed through spontaneous dismutation of O_2^- and H^+ or by catalysis of superoxide dismutase. Although superoxide is produced in high quantities by the oxidase, and originally perceived to be microbicidal (Babior, Kipnes & Curnutte, 1973), it is now thought that it is not a particularly reactive molecule despite its radical (one electron) nature as it has limited destructive effect on bacterial structures (Imlay, 2003; Sawyer & Valentine, 1981; Reeves *et al.*, 2003). H_2O_2 is even less reactive than superoxide, and can actually diffuse out of the phagosome unlike superoxide (Winterbourn & Kettle, 2012). Their actual roles may be to act as substrates for subsequent reactions, including iron-based Fenton reactions, involvement with nitric oxide, and the MPO system.

The activity of MPO has been a paradigm for neutrophil microbicidal activity for decades. It is a peroxidase with several enzymatic activities (Klebanoff *et al.*, 2013), is highly expressed in the azurophil granules of neutrophils (Faurschou & Borregaard, 2003), and is what gives pus its characteristic green colour (Klebanoff, 2005). Its main studied reaction is the formation of hypochlorous acid (HOCl) from H_2O_2 and Cl^-, which is thought to be one of the most toxic phagosomal products utilised for the cell's killing activity (Klebanoff *et al.*, 2013), although MPO can generate other toxic chlorinated products such as chloramines (Green *et al.*, 2017). HOCl has been detected in phagocytosing neutrophils using various methods such as GFP-

expressing bacteria, which lost fluorescence with HOCl contact as it causes photobleaching (Schwartz *et al.*, 2009; Palazzolo *et al.*, 2005). Although in these studies, bacterial viability decreased at a faster rate than GFP fluorescence, and not all phagosomes lost fluorescence. Other probes for HOCl with postulated specificity have been generated (Xu *et al.*, 2013; Kenmoku *et al.*, 2007).

An alternative view of MPO has been proposed due to certain inconsistencies. The primary reason being that MPO deficiency in humans does not cause fatal infection, with only a few microbial species providing problems such as *C. albicans* (Levine & Segal, 2016), although it does seem to be more life-threatening in mouse models possibly because they contain fewer antimicrobial peptides (Hurst, 2012; Aratani *et al.*, 2002). The second reason is that, as discussed earlier, the phagosomal pH of neutrophils is alkaline immediately after phagocytosis which is maintained for at least 30 minutes, but MPO has optimum activity at pH 6 (Levine *et al.*, 2015). Therefore, initial MPO activity could be lower than currently thought, but due to its presence in massive quantities in the granules and consequently phagosomes, there is still detectable production of HOCl. Furthermore, the recorded optimal pH was for catalytic production of HOCl, but the alkaline pH may allow different MPO catalytic processes such as reactions with superoxide (Winterbourn & Kettle, 2012). Additionally, it has been shown that the phagosomal pH drops later, and as H_2O_2 is long-lasting (Imlay, 2003), the MPO-induced HOCl production may occur later to degrade the engulfed pathogen. Indeed, some experiments using HOCl probes show greater activity with time around 120 minutes after phagocytosis when the pH would be acidic (Schwartz *et al.*, 2009).

MPO deficiency but lack of serious infection could result from adaptation and increased involvement of the other oxidative killing mechanisms. For example, superoxide reacts with nitric oxide (NO) to form peroxynitrite which is extremely toxic to bacteria (Brunelli, Crow & Beckman, 1995). Enzymes for NO production, NO

synthases, are reportedly increased in activated compared to resting neutrophils and linked to bacterial killing (Jyoti *et al.*, 2014; Wheeler *et al.*, 1997). Superoxide and H_2O_2 will be in much greater concentrations in the phagosome without consumption by MPO-dependent reactions and could possibly inflict greater damage than normal. There have also been mechanistic studies demonstrating how initial exposure of bacteria with $O2^-$ can damage iron-containing dehydratases, releasing iron which binds to bacterial DNA (Keyer & Imlay, 1996). There is then the possibility of Fenton reactions which involve H_2O_2 to cause double-strand cleavage, and subsequent bacterial killing (Park, You & Imlay, 2005; Jang & Imlay, 2007). Moreover, there is evidence of NO production in CGD neutrophils (Tsuji *et al.*, 2002, 2012)

Non-oxidative killing

Non-oxidative killing has historically referred to the microbicidal effects of the granule proteins or killing mechanisms that do not involve ROS. The azurophilic granules contain the most potent microbicidal agents, and their release into the phagosomes are the most carefully controlled of the subsets (Sengelov *et al.*, 1995). These antimicrobial peptides are aimed to directly lyse microbial structures or to sequester nutrients to inhibit microbial function when trapped in the phagosome (**Table 1.3**).

Within azurophil granules are three serine proteases, or serprocidins, with proteolytic activity that have been extensively studied: elastase, cathepsin G, and proteinase 3 (PR3) (Korkmaz, Moreau & Gauthier, 2008). Elastase and PR3 have substrate specificity towards small hydrophobic residues (Lestienne & Bieth, 1980; Rao *et al.*, 1991), while cathepsin G is targeted towards aromatic or positively charged residues (Blow & Barrett, 1977). All three enzymes can cleave extracellular matrix and plasma proteins at inflammatory sites, inflammatory mediators and some receptors (Korkmaz, Moreau & Gauthier, 2008), and have bactericidal activity although through

different mechanisms. Elastase targets mainly Gram-negative bacteria by cleaving their virulence factors and outer membrane proteins (Belaaouaj *et al.*, 1998; Belaaouaj, 2002; Lebargy *et al.*, 2017), whereas the cationic nature of the cathepsin G peptide interferes directly with the structure of Gram-positive bacteria such as *S. aureus* (Shafer *et al.*, 2002). PR3 can also generate LL-37, another potent antibacterial peptide, through the processing of cathelicidin hCAP-18 (Sørensen *et al.*, 2001), which is present in specific granules (Bülow *et al.*, 2002). Although elastase, cathepsin G, and PR3 have different activities, they have all been described to have alkaline pH optima: elastase from pH 8-9, cathepsin G pH 7.5-9, and PR3 pH 8.5 (Korkmaz, Moreau & Gauthier, 2008; Levine *et al.*, 2015).

Azurocidin is also a serprocidin with high homology to the three other serprocidins, but due to a mutation in a substrate binding site does not exhibit enzymatic activity (Gabay *et al.*, 1989). Instead, its cationic (positively charged) membrane charge binds to anionic (negatively charged) bacteria in a similar fashion to the other cationic peptides. Azurocidin has specific potent action against Gram-negative bacteria, and also activity, albeit less, towards Gram-positive bacteria and fungi (Campanelli *et al.*, 1990; Gabay *et al.*, 1989). Interestingly, azurocidin activity increases in acidic conditions, unlike the neutral serine proteases (Campanelli *et al.*, 1990). Despite their apparent different pH optima, azurocidin has been shown to “synergize” or increase elastase and cathepsin G enzymatic activity (Miyasaki & Bodeau, 1992).

Four types of α-defensin have been identified in human azurophil granules, making up a significant portion of total cellular content at 5-18% (Gabay & Almeida, 1993; Rice *et al.*, 1987). They are characterised by a triple-stranded β-hairpin structure, six conserved disulphide-linked cysteine residues and a net positive charge, although they have a mixture of charged and hydrophobic residues (Hill *et al.*, 1991). They demonstrate wide-ranging destructive action towards both Gram-negative and positive bacteria, fungi, and viruses (Lehrer & Lu, 2012). Defensins exert microbicidal

effects through their different structural areas. Again, like the other antimicrobial peptides, the positively-charge residues of defensins mediates binding to anionic Gram-negative bacteria to mediate cell wall damage. However, their hydrophobic residues may contribute to Gram-positive bacterial damage (Wei *et al.*, 2010) and anti-viral activity (Demirkhanyan *et al.*, 2012). The residues containing disulphide bonds act as crucial stabilising structures rather than directly exerting antimicrobial effects (Zhao & Lu, 2014).

Table 1.3 Granule subsets and their contents (Borregaard *et al.*, 1995)

Azurophil/ primary	Specific/ secondary	Gelatinase/ tertiary	Secretory vesicles
Membrane			
CD63 CD68	CD15 antigens, CD66, CD67, FMLP-R, Cytochrome-b_{558} Fibronectin-R, G-protein α-subunit, Laminin-R, Mac-1 (CD11b), NB 1 antigen, Rapi, Rap2 Thrombospondin-R, TNF-Receptor, Vitronectin-R	Cytochrome-b_{558}, Diacylglycerol-deacylating enzyme, FMLP-R, Mac-1	Alkaline phosphatase, CR1 (CD35), Cytochrome-b_{558}, FMLP-R, Mac-1, Uroplasminogen activator-R, CD1O, CD13, CD45 PcIRIII (CD16), Clq-receptor, DAF
Matrix			
Acid β-glycerophosphatase, Acid mucopolysaccharide, α_1-antitrypsin, α -mannosidase, Azurocidin/CAP37/ Heparin binding protein, BPI, β-glycerophosphatase, β-glucuronidase, Cathepsins, Defensins, Elastase, Lysozyme, Myeloperoxidase, N-Acetyl-11- β-glucosaminidase, Proteinase-3, Sialidase	β2-microglobulin, Collagenase, Gelatinase, Histaminase, Heparanase, Lactoferrin, Lysozyme, NGAL, Plasminogen activator, Sialidase, Vit. B_{12}-binding protein	Acetyltransferase β2-microglobulin, Gelatinase, Lysozyme	Plasma proteins (incl. tetranectin)

Bactericidal/permeability-increasing protein (BPI) is another azurophil granule constituent. It is also cationic, exhibiting powerful endotoxin-neutralising activity (such as LPS and lipooligosaccharides) and high-affinity binding to the lipid A moiety of LPS

(Gazzano-Santoro *et al.*, 1992). It seems to be selective towards Gram-negative bacteria (Weiss *et al.*, 1978). The initial electrostatic connection with the lipid A moiety occurs through the N-terminal end of BPI (Ooi *et al.*, 1991), then BPI creates a stronger binding to the bacterial outer membrane which results in increased permeability of the membrane (Gazzano-Santoro *et al.*, 1995). BPI also causes hydrolysis of bacterial wall phospholipids by bacterial phospholipases and host phospholipases A_2 (Zhao & Kinnunen, 2003; Forst *et al.*, 1987) and synergizes with other neutrophil granule proteins to cause irreversible bacterial membrane lesions (Zarember *et al.*, 1997).

Another function of granular proteins is to inhibit microbial growth. Lactoferrin is a prominent example, an iron-binding glycoprotein stored in specific granules which removed iron that is necessary for microbial growth (Bullen, Rogers & Leigh, 1972). It does, however, seem to be multifunctional, with activity against various Gram-negative and positive bacteria, viruses, and fungi not only through iron sequestering but also direct protein-protein interactions due to its cationic surface (Jenssen & Hancock, 2009).

While it has been mentioned that the serine proteases work best at alkaline pH, there have been other suggested interacting processes that activate granule proteins. The granules consist of a peptidoglycan matrix to which the proteins bind. It was posited by Reeves and the Segal lab that the influx of K^+ observed with NADPH oxidase activation is needed to mobilise granule proteins from the matrix so they can carry out their antimicrobial functions. MPO instead protects the proteolytic enzymes from ROS-induced damage through SOD and catalase activity (Reeves *et al.*, 2002), as HOCl is damaging to their activity (Schiller *et al.*, 2000). But contrary to this, MPO was also found to inactivate elastase via oxidation (Hirche *et al.*, 2005), and that elastase can activate MPO-related killing mechanisms (Odeberg & Olsson, 1976).

Clearly, further investigations are required for a more detailed understanding of the interactions between oxidative and non-oxidative mechanisms.

Although there is cooperation between the two systems in fulfilling their antimicrobial defence, there is also specific relevance for each system in the killing of certain microbial species. For example, serine protease activity is needed for *S. pneumoniae* killing (Hahn *et al.*, 2011; Standish & Weiser, 2009). Both elastase and cathepsin G are required for killing of *Aspergillus fumigatus* (Tkalcevic *et al.*, 2000), and cathepsin G for *Capnocytophaga* (Gram-negative) killing (Miyasaki & Bodeau, 1991). The importance of granule protein activity is further demonstrated in MPO-deficient neutrophils that still have candidacidal activity under certain conditions (Lehrer, Ladra & Hake, 1975). Equally, CGD neutrophils can kill certain bacteria through granule protein-mediated mechanisms (Odell & Segal, 1991), without K^+ mobilisation or MPO activation.

Synergism is an important factor to consider in the phagosome as a whole, interconnected environment. Redundancies may exist to support failings but to protect the host there will be many overlapping and cooperative antimicrobial systems. Therefore, studying different aspects individually, such as purified components *in vitro* or computer models of certain enzyme kinetics, can lead to inaccurate conclusions.

1.4 Intracellular environments of other professional phagocytes

Neutrophils are not the only innate immune cell capable of phagocytosis; the mononuclear cells monocytes, macrophages and dendritic cells also have important phagosomal functions. All the professional phagocytes have NADPH oxidase expression and activity but to varying degrees.

Macrophages are predominantly known for their phagocytic and microbicidal activity which is similar to neutrophils, but they have crucial differences that set them apart. Macrophages are much larger, adherent cells which phagocytose at a slower rate than neutrophils but can take up more particles. The development of a mature, antimicrobial compartment in neutrophils is very quick as they contain pre-formed granules which fuse almost instantaneously to the phagosome. In macrophages, the generation of the phagolysosome occurs over a longer duration, with gradual fusion of endosomes and lysosomes to the phagocytic vacuole that evolves it into a more precise killing and degradative compartment (Flannagan, Cosío & Grinstein, 2009; Desjardins *et al.*, 1994). The phagosomal pH is also different between the two cell types. Neutrophils generate an alkalinised phagosome, while in the majority of macrophage subsets reported, they have very acidic compartments (Ohkuma & Poole, 1978; Yates, Hermetter & Russell, 2005; Flannagan, Heit & Heinrichs, 2016). Macrophages also have lower NADPH oxidase activity than neutrophils (Nathan & Shiloh, 2000; Dale *et al.*, 2008). Accordingly, their phagosomal antimicrobial components are different. Macrophages have several acid hydrolases, such as cathepsins B and L, which prefer acidic environments for their degradative activity (Turk *et al.*, 2012).

Macrophages also have the important job of clearing away apoptotic neutrophils after their initial microbicidal attack. Efferocytosis is the process where dead or apoptotic cells are removed by phagocytosing cells; the word means literally “to carry to the grave” (deCathelineau & Henson, 2003). Although efferocytosis is very similar to phagocytosis and shares some of the same machinery, they both have fundamental differences. After recognition and engulfment of apoptotic cells, by specific surface expression of so-called “find me” and “eat me” signals for the professional phagocytes (Lauber *et al.*, 2003), the degrading intracellular compartment named as the efferosome goes through maturation steps. According to one study, the early

maturation stages resemble closely to phagocytosis (Yin *et al.*, 2016), but diverge in the later stages.

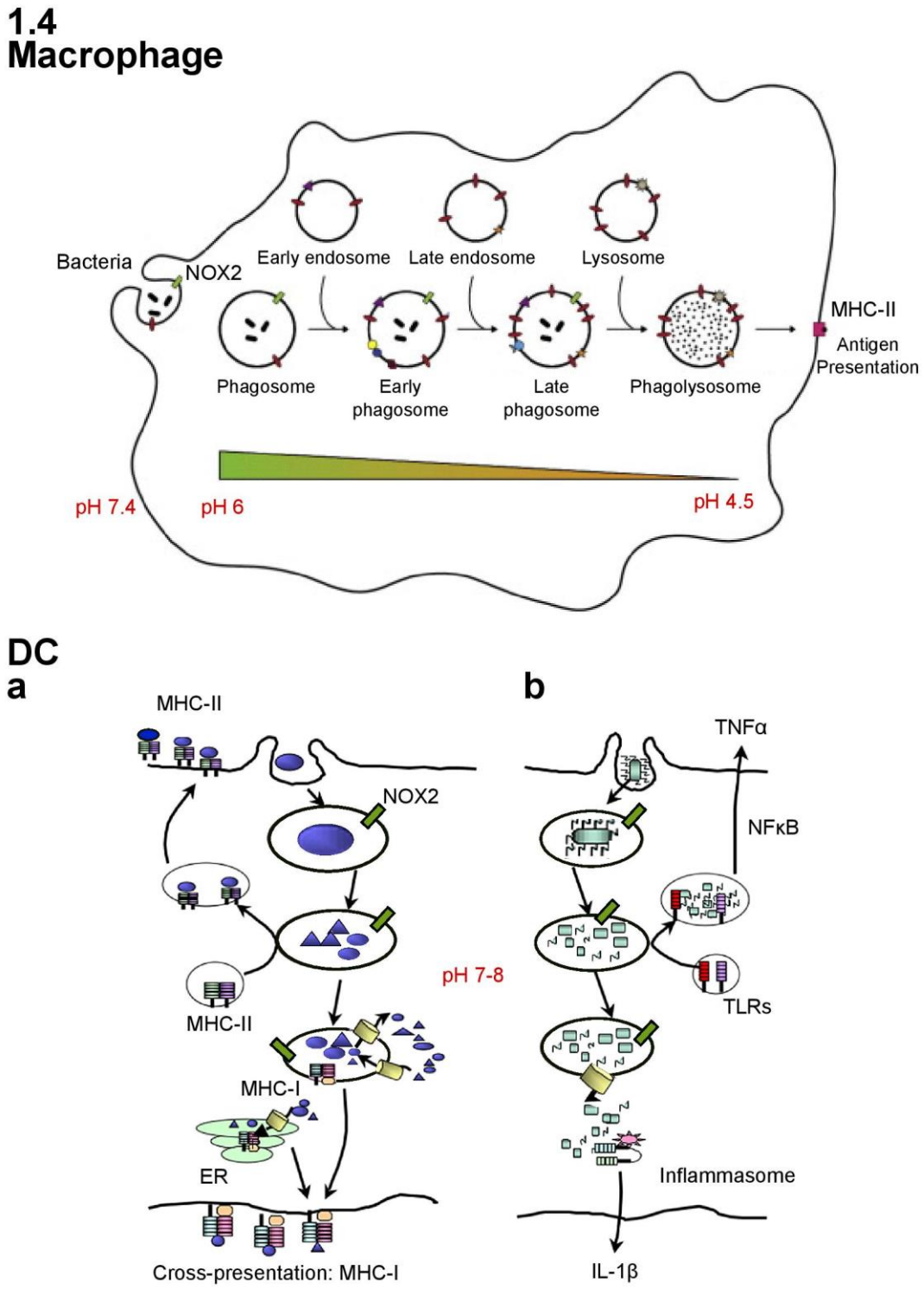

Figure 1.4 | Phagocytosis in macrophages and DCs. *Both macrophages and DCs have endosomal fusion events with the developing phagolysosome with NOX2 activity. In macrophages, the pH becomes more acidic over time. In DCs, the*

*phagosomal environment is different in (**a**) cross-presentation of exogenous antigen and (**b**) phagocytosis of bacteria, with recorded phagosomal alkaline pH in both pathways. Adapted from (Poirier & Av-Gay, 2012) and (Stuart & Ezekowitz, 2005).*

Efferocytosis also occurs in DCs, but their main function is antigen presentation rather than microbial destruction (Savina & Amigorena, 2007). DCs act as sentinels in various locations of the body such as peripheral tissue and secondary lymphoid organs and use phagocytosis to acquire foreign antigens. This phagocytosis stimulates a signalling cascade which limits further uptake in the presence of certain accompanying signals when the DCs evolve from immature to mature cells (Nagl *et al.*, 2002; Alloatti *et al.*, 2015). Phagosomal maturation seems to occur in endosomal fusion events similar to macrophages, although they can differ for direct or cross-presentation pathways (Embgenbroich & Burgdorf, 2018; Nair-Gupta *et al.*, 2014) (**Figure 1.4**). The antigens of phagocytosed particles are thought to be conserved in an alkaline environment, to inhibit their degradation by acid hydrolases before they are presented on the cell surface (Mantegazza *et al.*, 2008; Savina *et al.*, 2006). DCs contain much fewer of these proteolytic enzymes (e.g. various cathepsins) compared with macrophages (Delamarre *et al.*, 2005; Dinter *et al.*, 2014). It has also been proposed that it is not the pH regulating the enzymatic activity, but a reductive environment (Rybicka *et al.*, 2012). While these are two opposing theories, both are reportedly caused by NADPH oxidase activity, even though ROS production is very low in comparison with neutrophils (Elsen *et al.*, 2004).

The phagosomal environments of monocytes are poorly researched in comparison to the other professional phagocytes. The emphasis on related research has historically been their roles as precursors to specific subsets of macrophages and DCs. There is increasing evidence that they are effector cells in their own right, especially when they are essential for clearance of certain bacterial infections in murine models such as *Listeria monocytogenes* (Rosen, Gordon & North, 1989), *Mycobacterium tuberculosis* (Peters *et al.*, 2001), *Toxoplasma gondii* (Robben *et al.*, 2005), and *Cryptococcus*

neoformans (Traynor *et al.*, 2000). They share similarities with neutrophils, including response to inflammatory stimuli (Serbina & Pamer, 2006), production of reactive nitrogen intermediates and ROS (Zawada *et al.*, 2011), and activity of phagosomal proteolytic enzymes (Levy, Kolski & Douglas, 1989) which all contribute to pathogen killing. Monocytes contain granules and granule proteins similar to neutrophils, but elastase, for example, is lost with differentiation to monocyte-derived macrophages (Campbell, Silverman & Campbell, 1989). However, there are three subsets of monocytes categorised by their cell surface expression of CD14 and CD16 molecules which exhibit genetic and phenotypic differences; the classical subset ($CD14^{+}CD16^{-}$), intermediate ($CD14^{+}CD16^{+}$), and non-classical ($CD14^{lo}CD16^{+}$) (Wong *et al.*, 2012; Cros *et al.*, 2010; Ziegler-Heitbrock *et al.*, 2010).

The phagosomal environments of human neutrophils, monocytes, dendritic cells and macrophages are directly compared in chapter five, where they are discussed in more detail.

1.5 Cell models of myeloid cells

To efficiently study cellular mechanisms requires a large number of cells that can be easily obtained. Only a limited quantity of cells can be isolated from humans and mice, so from the 1950s researchers have exploited the capacity of certain cancer cells to divide *in vitro* with the appropriate nutrients so that they may be cultured indefinitely. HeLa cells were the first of the immortalised cell lines, derived from a patient, Henrietta Lacks, with cervical cancer (Scherer, Syverton & Gey, 1953). The ethical and scientific breakthroughs surrounding this discovery are excellently told by Rebecca Skloot (Skloot, 2010). In the case of myeloid cells, these usually arise from haematopoietic malignancies such as types of myeloid leukaemia, which have mutations affecting the progenitor cells, so they are still able to proliferate. Leukaemia

is defined as the abnormal and uncontrolled growth of haematopoietic cells (De Kouchkovsky & Abdul-Hay, 2016). However, with appropriate stimuli such as cytokines and growth factors, the haematopoietic cancer cells can differentiate into terminally-differentiated cells resembling primary cells. This is an especially important tool for neutrophil compared to macrophage research because neutrophils are short-lived, terminally differentiated cells which are difficult to genetically manipulate and keep in culture for any length of time.

The most commonly used cell lines to generate human neutrophil-like cells are HL60 and NB4, that were both initially derived from the peripheral blood and bone marrow, respectively, of patients with acute promyelocytic leukaemia (APL) (Collins, Gallo & Gallagher, 1977; Lanotte *et al.*, 1991), but with subsequent appraisal of HL60 cells the correct diagnosis should have been acute myeloid leukaemia (AML) (Dalton *et al.*, 1988). The cells in suspension culture exhibit a promyeloblast phenotype; large, rounded cells with large nuclei and dark-staining cytoplasm (Birnie, 1988). With addition of dimethyl sulphoxide (DMSO) or all trans retinoic acid (ATRA) or in combination, a proportion of the myeloblasts develop into mature, differentiated cells resembling neutrophils (Gupta *et al.*, 2014; Barber, Belov & Christopherson, 2008; Jacob *et al.*, 2002; Khanna-Gupta *et al.*, 1994). With stimulation by chemicals including PMA and 1,25-dihydroxyvitamin D_3 can induce differentiation to monocyte/macrophage-like cells (Xu *et al.*, 2010; Song & Norman, 1998).

The neutrophils generated from the two models have been thoroughly investigated and found to exhibit some hallmark neutrophil characteristics: NADPH oxidase expression and activity (Teufelhofer *et al.*, 2003; N'Diaye *et al.*, 1997), MPO expression (Parker *et al.*, 2011; Pullen & Hosking, 1985; Khanna-Gupta *et al.*, 1994), degranulation (Korchak, Rossi & Kilpatrick, 1998; Lanotte *et al.*, 1991), microbial killing (Bonvillain *et al.*, 2010; Gazendam *et al.*, 2016), amongst others. Yet they also have significant deficiencies which limit their utilisation in some areas of neutrophil

research, such as the lack of specific granules (Le Cabec, Calafat & Borregaard, 1997; Grégoire *et al.*, 1998; Khanna-Gupta *et al.*, 1994).

Myeloid leukaemia can arise through spontaneous mutations or those caused by viral infection. This genetic engineering mechanism has been adopted by researchers to generate immortalised murine cell lines. The target genes of interest come from previous research into haematopoietic malignancies, which enhance our understanding of haematopoietic processes. For example, the retinoic acid receptor (RAR), which ATRA binds to in the HL60/NB4 models to induce differentiation, is a master transcription factor of growth and differentiation in many cell types. In the human NB4 cell line, and in AML, it is a mutation in this receptor which abrogates correct myeloid differentiation (Lawson & Berliner, 1999). In a mouse model, a retroviral construct was developed to transfect a dominant-negative RAR into bone marrow progenitor cells. When the transfected cells were cultured in medium containing GM-CSF and a selecting antibiotic (geneticin), a proportion of the cells remained in a myeloblast state. The new cell line was named MPRO, after mouse promyelocyte (Tsai & Collins, 1993). The MPRO cells were found to have low responsiveness to RA, which kept them in their undifferentiated state, but with high concentrations of RA they terminally differentiated into mature neutrophils after three days (Lian *et al.*, 2001). A similar model with a slightly different mutation in the same RAR gene which had multipotency was also generated. Maintenance of the myeloblast EML (erythroid myeloid lymphoid) cells was dependent on the presence of stem-cell factor (SCF) in the culture medium. If erythropoietin was added, some of the cells terminally differentiated into erythrocytes. If the EML cells were co-cultured with bone stromal cells and IL-7, they differentiated into B-cell progenitors. To generate mature neutrophils, EML cells were first incubated with IL-3 and RA with continued SCF supplementation to generate early promyelocytic cell line (EPRO), then terminally differentiated with RA and GM-CSF, taking 12 days in total for mature

neutrophil generation (Tsai *et al.*, 1994; Gupta *et al.*, 2014). Neutrophils derived from MPRO and EPRO cell lines exhibited classical primary neutrophil features, including correct granule expression (Lawson, Krause & Berliner, 1998; Lian *et al.*, 2002).

Other murine immortalised cell lines have been developed that employ different genes involved in myeloid haematopoiesis. The homeobox (Hox) genes are a family of transcription factors that have an essential role in embryonic development and haematopoiesis (Argiropoulos & Humphries, 2007). They are evolutionary conserved, and through studies with knockout mouse models or ectopic expression of certain members have been directly implicated in haematopoietic cell self-renewal (Abramovich & Humphries, 2005). Furthermore, mutations in these genes are causative for types of myeloid leukaemia, such as Hox2.4 (alternatively known as Hoxb8) in the murine myelomonocytic leukaemia WEHI-3B (Perkins *et al.*, 1990) and other Hox genes in AML (Rice & Licht, 2007; Roche *et al.*, 2004).

The WEHI-3B cell line was generated from a mouse model which developed myelomonocytic leukaemia after mineral oil injections (Warner & Moore, 1969). Subsequent studies found that mutations in the Hoxb8 and IL-3 genes which lead to their dual constitutive expression caused the malignancy, which was confirmed in healthy wildtype bone marrow progenitors that were transfected with a retroviral vector causing ectopic expression of Hoxb8 cultured in medium containing IL-3. The transfected cells maintained a promyelocytic phenotype with long-life in culture (Perkins & Cory, 1993).

This information was pursued further to use the Hoxb8 transfected bone marrow progenitor cells as a source of terminally differentiated myeloid cells. Wang and colleagues constructed a retroviral plasmid with the Hoxb8 gene fused to the estrogen receptor so that the presence of estrogen would activate expression of Hoxb8 (Wang *et al.*, 2006) – this was a modified receptor that would not be activated by the low levels of estrogen found in fetal calf serum. Like the WEHI-3B leukaemia line, the

conditionally immortalised Hoxb8 progenitors have an unlimited capacity for self-renewal in the myeloblast form, while estrogen and SCF are present in the culture medium. But when estrogen is removed and replaced with granulocyte colony stimulating factor (G-CSF), the progenitors differentiate into mature neutrophils. With GM-CSF, the progenitors can become macrophage-like cells. They can be generated not only from bone marrow progenitors but also from fetal liver progenitors (Wang *et al.*, 2006), which may be extremely useful for the immortalisation of some embryonic lethal knockout models. Moreover, stimulation with Flt3 ligand and IL-3 can induce them towards a lymphoid phenotype (Redecke *et al.*, 2013). The Hoxb8 progenitor cell line is discussed in more detail in chapter four where it is compared to primary bone marrow neutrophils.

Cell lines have inherent mutations which lead to disadvantages of their use as a perfect tool of primary cells, but they have a place in fundamental research of cell differentiation and function, and to reduce the cost and animal suffering.

1.6 Methodology for investigations of the phagosomal environment

Detection of biochemical events happening within the phagosome is difficult in the neutrophil because of the reactive nature of the compartment. Probes which rely on fluorescence or chemical reactions are especially susceptible to distortion by the harsh environment. Some of the most commonly used methods are described below.

pH

There a vast number of pH-sensitive dyes available, but they must be used in accordance with their unique chemistries which may add certain limitations based on the situations they are used in. A robust pH indicator should ideally be only selective

to proton concentration and be resistant to oxidation. It must be restricted to the phagosome, either by conjugation with phagocytosable particles or be membrane impermeable. Photobleaching is a common problem with fluorescent dyes. It is the photo-based degradation of the fluorophore by the lamp source, which can result in the release of damaging by-products and decrease in fluorophore concentration, but can be minimised by exciting the dye at a low intensity (Bright *et al.*, 1989). A popular type of pH indicator includes those that change their emission or excitation spectral properties in response to changes in pH. It is most convenient when the dye has a dual emission or excitation response so a ratiometric measurement can be calculated. This is the case for the commonly used pH indicators SNARF-1 and fluorescein isothiocyanate (FITC).

In acidic conditions, the SNARF molecule is protonated and produces an emission signal between 560 and 600 nm when excited at 488 nm or above. When the molecule is deprotonated in more alkaline conditions, the emission wavelength is over 600 nm (Buckler & Vaughan-Jones, 1990). A ratio of the fluorescence intensities at these two wavelengths indicates the emission shift, which is more reliable than single fluorescence measurements, as it is unaffected by fluorophore concentration and cell structure. FITC has dual excitation spectra: when it is excited at 450 nm, the emission is not sensitive to pH, but when it is excited at 490 nm, the intensity of emission increases with increasing pH (Ohkuma & Poole, 1978).

The two molecules also have different pKa values; the pH at which the protonated and deprotonated forms are equal in concentration, which is a measure of its buffering capacity. SNARF has a pKa of 7.5, while for FITC it is 6.5 (Tsien, 1989), which makes SNARF suited for measuring more alkaline environments than FITC.

Neutrophil phagosomal pH was originally measured using FITC, but it was later found to be oxidised and photobleached by MPO (Hurst *et al.*, 1984), which is expressed in great quantities in neutrophils. MPO inhibitors such as sodium azide were then

employed to reduce this effect, but it was found that sodium azide also affects the observed fluorescence (Levine *et al.*, 2015); it may be showing the phagosome as more acidic than it really is. Therefore, FITC should not be the dye of choice to measure pH in neutrophils. However, SNARF-1 is not without its limitations. Its spectral properties are sensitive to changes in temperature, where the fluorescence intensity decreases slightly with increasing temperature (Bond & Varley, 2005).

BCECF is also commonly used for intracellular pH measurements because it has a neutral pKa, can easily be loaded and trapped inside cells and like FITC has a dual excitation profile. To make it suitable for phagosomal pH, it has been conjugated to dextran which the cell phagocytoses (Bright *et al.*, 1989), or by staining of bacteria (Loike *et al.*, 2013). However, like FITC, it is also susceptible to photobleaching. Many dyes have an acetoxymethyl (AM) ester group that allows it easily to pass through the membrane into the cytoplasm, where it is then cleaved by cytoplasmic esterases that makes it membrane impermeable (Han & Burgess, 2010).

Single excitation/emission spectrum dyes may be made more robust when used in conjunction with a pH-insensitive probe. For example, pHrodo, a pH-sensitive dye, can be attached to zymosan particles with Alexa-488-succinimidyl ester, a pH-insensitive dye (Nunes-Hasler *et al.*, 2017). Succinimidyl ester (SE) groups on dyes allow covalent binding to particles or bacteria that contain amine groups (Lim *et al.*, 2014). This is important for detecting pH with pHrodo, as it decreases in fluorescence with increasing pH. The constant fluorescence of the conjugated Alexa-488 ensures the decrease in fluorescence is not due to a decrease in dye concentration or improper focusing if using microscopy.

NADPH oxidase activity

NADPH oxidase activity can be measured either by consumption of oxygen or by the production of reactive oxygen species (ROS) that can be detected extracellularly or inside the phagosome. The original measure of NOX2 activity was using an adapted Clark electrode, which consists of a chamber attached with a platinum electrode that can detect oxygen tension (Clark *et al.*, 1953). Cell suspensions and opsonised particles are added to the chamber, which is heated to 37 ˚C and mixed with a magnetic stirrer, and the decrease in oxygen concentration is recorded (Segal & Allison, 1979; Nagasawa *et al.*, 1982). The same principle was applied in newer versions involving plate readers that contain oxygen electrodes, such as the Seahorse apparatus (Chacko *et al.*, 2013; Gerencser *et al.*, 2009), which were primarily designed for mitochondrial respiration (Dranka *et al.*, 2011). The addition of wells allows more conditions to be tested simultaneously than the individual chamber. While the main and substantial advantage of this method is the lack of chemical interference with the cell environment, its limitations include the use of a large number of cells for reliable analysis, phagocytosis is asynchronous, and the measurement is of the cell population not on the individual cell phagosomal level. There is also no differentiation between NADPH oxidase-induced and mitochondrial respiration.

Consequently, other assays have been developed to measure ROS production, many of which use chemical reactions or fluorescent probes. In contrast to pH-sensitive probes, these may depend on oxidation for their signal (redox-sensitive) but should be resistant to pH changes. Ideally, the probe should be specific for only one type of ROS and be able to measure production kinetically.

Chemiluminescence methods use dyes that release light energy when excited by ROS. Commonly used substrates include lucigenin (bis-N-methyl acridinium nitrate), luminol (5-amino-2,3-dihydro-1,4-phthalazinedione), and isoluminol (6-amino-2,3-dihydro-1,4-phthalazinedione). Lucigenin and luminol are cell permeable while

isoluminol is not, measuring total cell ROS and extracellular ROS respectively. Luminol can be conjugated to opsonised latex particles for specific detection of phagosomal ROS (Savina *et al.*, 2006). Although they are widely used, they do not seem to be specific for one NADPH oxidase product and may be sensitive to other reactive species in the phagosome (Faulkner & Fridovich, 1993; Vilim & Wilhelm, 1989). Despite these caveats, they require much fewer cells for analysis than the oxygen electrode-based experiments but commonly use a plate reader which is still an assessment of population kinetics. Alternatively, the luminol-bound latex particles can be visualised by microscopy.

Other dyes are available that utilise peroxidase-catalysed reactions of H_2O_2. One of the more sensitive and specific dyes is the Amplex UltraRed reaction, in which a fluorescent product is formed, Resorufin, when the reagent reacts with H_2O_2 in the presence of horseradish peroxidase (HRP) (Summers *et al.*, 2013). The fluorescence intensity is measured using a plate reader. Although it is generally specific for H_2O_2, the dye is impermeable so can only measure extracellular H_2O_2 which is produced by plasma membrane stimulation of the oxidase by PMA.

For intracellular ROS detection, popular dyes include OxyBURST, dihydrorhodamine (DHR) and hydroethidine (HE). There are two commercially available forms of Oxyburst, the dichlorodihydrofluorescein ($DCFH_2$) and dihydro-2',4,5,6,7,7'-hexafluorofluorescein (H2HFF). They are both derivatives of fluorescein and are both oxidised by H_2O_2 in the presence of a catalyst such as peroxidases (MPO) in the phagosome, more than superoxide or H_2O_2 alone (Wardman, 2007; VanderVen, Yates & Russell, 2009), but DCFH2 can also be oxidised by reactive nitrogen species (RNS) (Crow, 1997). H2HFF is relatively insensitive to pH (VanderVen, Yates & Russell, 2009; Chen, 2002) while $DCFH_2$ is not (Van Acker *et al.*, 2016), so H2HFF should be preferred for measuring neutrophil phagosomal pH. But both dyes can be

conjugated to phagocytosable beads to directly measure phagosomal ROS generation.

DHR is membrane permeable and lipid soluble, when it enters the phagosome it is oxidised by H_2O_2 to form red fluorescent rhodamine 123 in the presence of peroxidase (Henderson & Chappell, 1993). The dye and its product also tend to accumulate in the mitochondria (Jankowski & Grinstein, 1999), so when measuring fluorescence with a plate reader or flow cytometry, the oxidation cannot be distinguished between phagosomal and mitochondrial. It also has reported sensitivity to RNS (Crow, 1997) and decreases in fluorescence above pH 8.5 (Kooy *et al.*, 1994).

In contrast to the other dyes, HE seems to be preferentially oxidised by superoxide rather than H_2O_2 (Walrand *et al.*, 2003; Rothe & Valet, 1990), but can be oxidised by H_2O_2 in the presence of peroxidases (Rothe & Valet, 1990). When it is oxidised by superoxide, the fluorescent metabolite 2-hydroxyethidium (Zhao *et al.*, 2003) is formed that can be detected by fluorescence microscopy or flow cytometry. Unfortunately, this metabolite was found to be pH-sensitive between pH 6 to 10 (Zielonka, Vasquez-Vivar & Kalyanaraman, 2008) so it is not appropriate for ROS detection in neutrophils because of their alkaline phagosomes.

It is apparent that probes to detect pH and NADPH oxidase activity should be chosen with care and an awareness of their limitations. The chosen instrumentation to record detection also comes with advantages and disadvantages. Fluorescence microscopy allows measurement of individual cells enabling detection of small changes, but it is very time-consuming to run and analyse the experiments and requires a high-level of technical expertise. Yet there are increasing advancements in automated software for efficiently analysing microscopy data. Flow cytometry is quick and straightforward to run experiments and provides a vast amount of data, but it cannot give detail on the singular cell level. It is not possible to synchronise phagocytosis and it is not possible to distinguish particles that may not be completely internalised. This,

however, may be improved with the ImageStream (Ploppa *et al.*, 2011), which combines microscopy with flow cytometry to distinguish individual cellular events. But flow cytometry lasers are kept at 4 ˚C which is not a physiological temperature for phagocytosis.

1.7 Outline of thesis

This thesis primarily describes the measurement of phagosomal pH and NADPH oxidase activity to address the following research topics:

- The ion channels and conductances regulating the phagosomal environment in neutrophils
- The utilisation of the immortalised Hoxb8 myeloid cell line as a model for mouse neutrophils
- The variations in phagosomal environment of other human professional phagocytes compared with neutrophils

Chapter Two: Materials and methods

2.1 Ethics approval

The study of patients with channelopathies was carried out in accordance with the recommendations of the Joint UCL/UCLH Committees on the Ethics of Human Research with written informed consent from all subjects (Project numbers 02/0324 and 10/H0806/115). All healthy controls gave written informed consent in accordance with the Declaration of Helsinki.

The study of mouse models was carried out in accordance with the recommendations of the United Kingdom Home Office (Project licence 70/8452).

2.2 Knockout mouse models

Sources of mice

Wildtype C57BL/6 (The Jackson Laboratory)*, Hvnc1* (Capasso et al., 2010), *Clic1* (Samuel Breit (Qiu et al., 2010)), *Clc3* (Thomas Jentsch (Stobrawa et al., 2001)), *Kcc3* (Frederique Scamps (Lucas et al., 2012)), *Kcnj15* (Okamoto et al., 2012), *Trpm2* (Yasuo Mori (Yamamoto et al., 2008)), Ébouriffé (*Lrrc8a deficient* (Platt et al., 2017)). Refer to chapter 3 table 3.3 further gene information.

Mouse husbandry

Mice were bred in individually ventilated cages (IVCs) in a pathogen-free environment in the Biological Services Unit at UCL. Mice were fed with Harlan 2018 Teklad Global 18% protein rodent diet and breeders were fed with 19% protein rodent diet. Sabrina Pacheco and Francesca Semplici kindly carried out mouse genotyping for confirmation of double knockout offspring.

2.3 Materials

General buffers

Duchen buffer

156 mM NaCl, 3 mM KCl, 1.25 mM KH_2PO_4, 2 mM $MgSO_4$, 2 mM $CaCl_2$, 10 mM glucose and 10 mM Hepes in water. After mixing with a magnetic stirrer, the solution was adjusted to pH 7.4 using NaOH then filtered with 0.2 µm PES filter.

pH buffers for SNARF-1 calibration

15 ml final volume: 5 ml of 0.15 M buffer solution + 10 ml 0.15 M NaCl solution

0.15 M NaCl solution: 8.77 g in 1 L ddH_20.

pH 3 and pH 10: 0.15 M glycine solution: 1.265 g in 100 mL ddH_20, 2 solutions.

pH 4, 5 and 6: 0.15 M sodium acetate solution: 2.04 g in 100 mL ddH_20.

pH 7, 8 and 9: 0.15 M Tris HCl solution: 2.36 g in 100 mL ddH_20.

pH 11, 12 and 13: 0.15 M sodium carbonate solution: 2.38 g in 100 mL ddH_20.

Either HCl or NaOH were used to adjust solutions to the correct pH.

Western blot buffers

Running buffer (10x stock): 30.3 g Tris base, 144 g glycine, 10 g SDS, dissolved in ddH_2O.

Transfer buffer (10x stock): 144 g glycine, 3.74 g SDS, 30.25 g Tris base. 1L of 1x solution was made by mixing 100 ml of 10x stock, 200 ml 100% methanol and 700 ml ddH_20.

Tris-buffered saline (TBS, 10x stock): 24 g Tris base, 88 g NaCl, dissolved in ddH_2O, adjusted to pH to 7.6.

TBS-Tween 0.1%: 100 ml 10x TBS, 900 ml ddH_20 and 1 ml Tween-20.

NuPage MOPS SDS running buffer x20 for precast gels.

Candida albicans stock and culture broth

Candida albicans ATCC 10231 Vitroids 80 CFU (Sigma RQC14003-10EA); one added directly to a YPD agar plate according to the manufacturer's instructions. YPD broth: 50 g YPD broth (Sigma) with 1 L ddH_20. YPD agar: 50 g YPD broth (Sigma), 15 g/L agar, 1 L ddH_20. 10% normal mouse serum (VWR)

Confocal microscopy dyes and equipment

SNARF-1 Carboxylic Acid, Acetate, Succinimidyl Ester - Special Packaging (for *C. albicans* labelling, Thermofisher), 5-(and-6)-Carboxy SNARF-1, Acetoxymethyl Ester, Acetate (for cell cytoplasm staining, Thermofisher), Calcein acetoxymethyl ester (Thermofisher), Laser scanning confocal microscope (Zeiss LSM 700). Ibidi µ slide 8 well ibiTreat and 15 well angiogenesis slide (Ibidi).

Reagents for respiratory burst assays

Horseradish peroxidase (50 IU/ml, Sigma), Amplex Ultrared reagent 10 mM stock in DMSO (Thermofisher), Phorbol 12-myristate 13-acetate (PMA) 1 mg/mL stock in DMSO (Sigma). 96 well fluorescence plate reader (FluoStar Omega), 96 well plates (Corning).

Ion channel inhibitors

Diphenylene iodonium (DPI, Sigma), zinc chloride (Sigma), 4-[(2-Butyl-6,7-dichloro-2-cyclopentyl-2,3-dihydro-1-oxo-1H-inden-5-yl)oxy]butanoic acid (DCPIB, Tocris), flufenamic acid (FFA, Sigma), anandamide (Tocris), quinidine (Sigma).

Buffers and antibodies for flow cytometry

Flow cytometry (FC) buffer: stock made of 500 ml PBS, 10 ml fetal calf serum (FCS 5%, Sigma), 50 mg sodium azide (Sigma).

For neutrophil and monocyte isolation purity analysis: (from BioLegend unless otherwise stated) CD3 (FITC, HIT3a); CD19 (FITC, HIB19); CD20 (FITC, 2H7); CD56 (FITC, MEM-188); CD66b (AF700, G10F5); HLA-DR (V500, G46-6, BD Biosciences); CD14 (PE, M5E2); CD16 (APC-Cy7, 3G8).

For FACS monocyte subset isolation: (from BioLegend unless otherwise stated) CD1c (PE-Cy7, L161); CD3 (FITC, HIT3a); CD11c (V450, B-ly6, BD Biosciences); CD14 (PE, M5E2); CD16 ((APC-Cy7, 3G8); CD19 (FITC, HIB19); CD20 (FITC, 2H7); CD56 (FITC, MEM-188); CD66b (AF700, G10F5); CD123 (PerCP-Cy5.5, 7G3); HLA-DR (V500, G46-6 BD Biosciences).

For monocyte-derived dendritic cell (MoDC) differentiation analysis: CD1a (BV510, BD Biosciences); CD1c (BV421, BD Biosciences); CD11c (PE-Cy7, BioLegend); CD14 (BV711, BioLegend); CD16 (PE, BD Biosciences); CD64 (FITC, BD Biosciences); CD141 (APC, Miltenyi Biotec).

For monocyte-derived macrophage differentiation analysis: CD80 (APC, clone 2D10); APC isotype control; CD200 receptor (PE, clone OX-108); PE isotype control; CD1a (FITC); FITC isotype control. All from BioLegend.

For mouse cell staining: CD11b (BV510 M1/70, BD Biosciences), CD45 (PerCP-Cy 5.5 38-F12), CD68 (BV421 F1-11, BioLegend), CD117 (BB515 2B8, BD Biosciences), F4/80 (FITC BM8, eBiosciences), Ly6C (APC AL-21, BD Biosciences), Ly6G (BV711 1A8, BioLegend), I-A/I-E (AF700 M5/114.15.2, eBiosciences).

Solutions and antibodies for western blots

Complete RIPA buffer: 10 ml RIPA buffer (Sigma) with one x cOmplete ULTRA protease inhibitor tablets (Roche) and one x PhosSTOP phosphatase inhibitor tablet (Sigma) was mixed on a roller for 20 min, then divided into 1 ml aliquots and stored at -20 °C. Housekeeping gene: vinculin mouse monoclonal (7F9, Merck) primary concentration 1:1000, secondary concentration 1:15,000. Hoxb8 mouse monoclonal antibody (4F8, Santa Cruz) 1° 1:1000, 2° 1:5,000, NADPH oxidase subunits: gp91phox mouse monoclonal (53, BD Biosciences) 1° 1:1000, 2° 1:10,000, generated in-house previously in rabbit; p67phox (1° 1:2000, 2° 1:10,000) and p47phox (1° 1:500, 2° 1:5000) (Abo et al., 1992). Secondary antibodies: Polyclonal Goat Anti-Mouse Immunoglobins/HRP and Polyclonal Goat Anti-Rabbit Immunoglobins/HRP, both from Dako.

Cell isolation materials and culture media

10% Dextran: made in 1x saline solution, Lymphoprep (Alere Ltd).

Sodium thioglycollate 3% solution: made by adding 1.5 g sodium thioglycollate (Sigma) to 50 ml 1x saline.

Mouse dissection medium: phosphate buffered saline (PBS, Gibco), 2% bovine serum albumin (Sigma), 1 mM EDTA (Sigma).

EasySep isolation medium: PBS, 2% fetal calf serum (Sigma), 1 mM EDTA.

Primary human cell culture medium: Roswell Park Memoriam Institute 1640 medium (RPMI, ThermoFisher), 10% fetal calf serum (FCS, Sigma), 5% pencillin/streptomycin (10,000 U/mL stock, ThermoFisher), 10 mM Hepes (Sigma). All growth factors were purchased from Peprotech unless otherwise stated. Granulocyte-macrophage colony stimulating factor (GM-CSF), macrophage colony stimulating factor (M-CSF),

lipopolysaccharide (LPS, from *Salmonella abortus equi* S-form (TLRgrade™), Enzo life sciences), interferon gamma (IFN-γ), interleukin 4 (IL-4).

CHO cell medium: RPMI, 10% FCS, 30 µM beta-mercaptoethanol (ThermoFisher), 5% penicillin/streptomycin.

HEK GP293 medium: DMEM high glucose (Gibco), 10% FCS, 5% penicillin/streptomycin, 1 mM sodium pyruvate (ThermoFisher).

Hoxb8 progenitor culture medium: RPMI, 10% FCS, 30 µM beta-mercaptoethanol, 5% penicillin/streptomycin, 4% CHO cell SCF supernatant, 10 µM beta-estradiol (Sigma).

Hoxb8 neutrophil differentiation medium: RPMI, RPMI, 10% FCS, 30 µM beta-mercaptoethanol, 5% penicillin/streptomycin, 4% CHO cell SCF supernatant, 20 ng/ml G-CSF.

Medium for apoptotic neutrophils: RPMI without phenol red (Gibco), 5% penicillin/streptomycin, 0.05% human serum albumin (Sigma).

Hoxb8 generation reagents

LB broth and agar with 100 ng/mL ampicillin (Sigma), HiSpeed Plasmid Maxi prep kit (Qiagen), collagen type I (from rat tail, Merck), Retro-X Tet-One Inducible Expression transfection reagent kit which includes an Eco envelope plasmid for murine virus production (Clontech), polybrene 1 mg/ml (Sigma), neomycin 1 mg/ml (Sigma), Stellar Competent cells (*E. coli* HST08 strain, Clontech), GP2-293 (HEK) retroviral packaging cell line (Clontech), GFP-LC3 adenovirus, gifted by Tom Wileman, UEA, originally from (Ni et al., 2011).

2.4 Primary cell isolation and culture

Neutrophil isolation

Human neutrophil isolation

All human blood was collected in syringes coated with heparin sodium unless otherwise stated. Per 10 ml of blood collected, 60 µl of heparin (1000 IU/ml) was first added. Then 1 ml of 10% dextran was added per 10 ml of blood, the syringe inverted gently 3 times, then left to sediment for 30-45 min. The top buffy coat layer was then layered on top of the density gradient medium Lymphoprep (ratio roughly 5 ml buffy coat to 2 ml Lymphoprep) and centrifuged at 1000 *g* for 10 min with the brakes on low (for example, deceleration 7 using the ThermoScientific Heraeus Multifuge X1R centrifuge). The supernatant was then discarded leaving a pellet. The erythrocytes were removed by hypotonic lysis; first a volume of distilled water used to resuspend the pellet by mixing for no more than 20 seconds, then an equal volume of 2x saline solution to restore isotonicity. The solution was centrifuged at 300 *g* for 5 min, then the pure population of resulting neutrophils was resuspended in the experimental buffer.

Mouse neutrophil isolation

Mice were sacrificed by carbon dioxide asphyxiation then cervical dislocation. The hind leg bones (tibia and femur) were removed while being careful to not break open the bones. The epiphyses of the bone were cut off, then using a 19-gauge needle with 1 ml syringe containing cell dissociation buffer, the red marrow was flushed out into a sterile petri dish. When all the bones for each mouse were treated in this way, a 21-gauge needle with syringe was used to break up the marrow into a consistent solution. To remove clumps of tissue and bone, the cell suspension was passed through a 70 µm cell-strainer (Greiner Bio-One). The cell solution was layered over

the Lymphoprep density gradient medium and neutrophils isolated as detailed in human neutrophil isolation.

For a purer population of neutrophils, instead of layering the cell solution over Lymphoprep, the mouse neutrophil enrichment isolation kit (Easy Sep) was used according to the manufacturer's instructions.

For the Seahorse oxygen consumption experiments in chapter three, murine neutrophils were isolated from the peritoneal cavity. Mice were injected by interperitoneal (i.p.) route with 3% thioglycollate solution (usually late afternoon). The next morning, the mice were given a fatal dose of pentobarbital, then the thioglycolate-elicited neutrophils were removed from the peritoneal cavity.

Human monocyte isolation kit

Peripheral blood from healthy controls was collected in syringes containing 60 µl of heparin sodium (1000 IU/ml) per 10 ml, and a final concentration of 1 mM EDTA. 50 ml of blood was diluted 1:2 with PBS, then the blood solution was layered over Lymphoprep 25:15 ml. These were centrifuged at 900 *g* for 30 min with acceleration and deceleration both at 7. The interphase layer containing peripheral blood monocytes (PBMCs) were carefully pipetted off and washed twice with PBS, then resuspended at 5 x 10^7/ml in the isolation buffer. The whole monocyte population (all three subsets) were further isolated according to the manufacturer's instructions using the EasySep Human Monocyte Enrichment Kit without CD16 depletion by magnetic bead-associated negative selection.

Fluorescence Assisted Cell Sorting (FACS) of human blood mononuclear cells

This technique was designed and performed by Amit Patel (Patel et al., 2017). In brief: the PBMCs were isolated at detailed in step 4.2. A cocktail of antibodies was

added to isolate different cell types: (from BioLegend unless otherwise stated) CD1c (PE-Cy7, L161); CD3 (FITC, HIT3a); CD11c (V450, B-ly6, BD Biosciences); CD14 (PE, M5E2); CD16 ((APC-Cy7, 3G8); CD19 (FITC, HIB19); CD20 (FITC, 2H7); CD56 (FITC, MEM-188); CD66b (AF700, G10F5); CD123 (PerCP-Cy5.5, 7G3); HLA-DR (V500, G46-6 BD Biosciences).

Monocyte-derived macrophages (MDMs)

PBMCs were isolated as set out in step 4.2, but without further enrichment of $CD14^+$ monocytes. Instead, PBMCs were resuspended in RPMI with 5% penicillin/streptomycin (Sigma) and 10 mM Hepes (Sigma) at 4 x 10^5 cells/well of Ibidi 8 well dish, or approximately 5 x 10^6 in 10 ml in a Nunclon™ Delta 10 cm tissue culture dish. After 1.5-2 hr incubation at 37 °C to allow cell adherence, the medium was replaced with the same solution as before, but now also containing 10% FCS. To generate M1 macrophages, the cell medium also contained 100 ng/ml GM-CSF for 5 days, then replaced with cell medium containing 75 ng/ml IFN-γ and 500 ng/ml LPS for an additional 2 days. For M2 macrophages, the medium contained 100 ng/ml M-CSF for 5 days, then 75 ng/ml IL-4 for the final 2 days. The medium was changed on the third day. Undifferentiated macrophages were cultured in medium only containing FCS, with medium changes on day 3 and 5. Cells were harvested by first washing the plate twice with cold PBS containing 10 mM EDTA, then gentle scraping.

Monocyte-derived dendritic cells (MoDCs)

$CD14^+$ monocytes were isolated via step 4.2, then resuspended in 10 ml of the medium used for macrophages, but instead with 150 ng/ml GM-CSF and 75 ng/ml IL-4. They were cultured in a 10 cm Nunc treated dish for 6 days, with an additional 10 ml of complete medium added on top on day 3. The resulting MoDCs remained in

suspension, therefore to harvest they were pipetted off and the plate washed twice with PBS.

2.5 The Hoxb8 immortalised mouse myeloid progenitor cell line

Culture of SCF-producing CHO cell line

The CHO cells were a kind gift from Annette Zehrer, who in turn had been gifted them by Hans Hacker. They had been genetically modified to constitutively express and secrete Stem Cell Factor (SCF) into their supernatant, which is necessary for progenitor cell survival. Cells were seeded at 3-4 million in 100 ml of CHO cell medium in a T175 flask. The cells were cultured for 2/3 days until the medium turned orange and confluency was approximately 80%. The supernatant was collected, centrifuged at 500 *g* for 5 min to remove cells, and stored at -80 °C. Fresh medium was replaced, then the supernatant was collected and stored in the same way the next day. The cells were detached by rinsing the flask with 10 ml PBS, then adding 10 ml of trypsin/EDTA solution (Sigma) and placing in the incubator for 2 min. 20 ml of medium was added to the flask to inactivate the trypsin, and the detached cells were centrifuged at 500 *g* for 5 min. The cells were resuspended in a fresh flask. This process was repeated until about 500 ml of supernatant was collected. The samples were then defrosted, pooled, and passed through a 0.2 µm filtering unit, and stored in 20 ml aliquots at -80 °C.

Retroviral infection of mouse bone marrow progenitor cells

The C57BL/6 wildtype and *Hvcn1*$^{-/-}$ Hoxb8 progenitor line were generously generated by Annette Zehrer, by immortalising cells present in the hind limbs of each mouse model sent over to her lab at Ludwig-Maximillians-University, Munich, Germany. However, when I carried out the retroviral infection myself, I followed the protocol set

out by Wang (Wang et al., 2006) with a few alterations. The retroviral plasmid containing the Hoxb8-estrogen receptor fusion domain was kindly provided by Hans Hacker, the same as used in (Wang et al., 2006). This is an MSCV structure with a neomycin cassette.

Transformation of competent E. coli cells

The Hoxb8 plasmid was delivered infused on blotting paper. This was resuspended in 50 µl sterile nuclease free H_2O for 1 hr under a laminar flow tissue culture hood. The DNA concentration of the suspension was measured by Nanodrop which had 6.9 ng/ µl DNA. Approximately 70 ng of plasmid DNA was mixed with 50 µl Stellar competent *E. coli* cells (1 x 10^9/mL) in a 1.5 mL Eppendorf tube by gently flicking the bottom of the tube a few times. The mixture was incubated on ice for 20 min, then heat shocked in a heat block set to 42 °C for 45 sec. The tube was incubated on ice for a further 2 min, then 250 µl LB medium without antibiotic was added, and the tube was incubated at 37 °C for 1 hour in a shaking incubator. 50 µl of the cell suspension was plated onto one LB agar plate with ampicillin, while the remaining suspension plated onto a separate agar plate. The plates were incubated overnight at 37 °C, then assessed for colony formation.

Starter growth cultures were created by picking one colony and adding to 20 mL of LB broth with ampicillin and incubating in a 37 °C incubator for 5 hr. This culture was then added to 180 mL of fresh broth, and incubated overnight. The next day, the growth suspension was centrifuged at 3000 *g* for 20 min. The supernatant was poured off, and the pellet dried out and stored at -20 °C until used for the maxi prep step. 50 mL of the growth suspension was used to create a glycerol stock of transformed bacteria, by resuspending in 2 mL of LB medium and 200 µl 100% glycerol. 4 aliquots were stored at -80 °C.

The maxi-prep was carried out exactly to the manufacturer's instructions. The final step was elution in 0.5 mL of TE buffer, which resulted in 494 ng/mL plasmid DNA.

Retroviral generation using GP-293 HEK cells

The following steps were carried out in a separate suite for viral cell culture. HEK cells were cultured in T175 flasks (Corning) in complete DMEM medium that had been pre-treated with collagen I solution to aid adherence, made by adding 10 mg collagen I to 50 mL ddH_2O. They were grown to ~80% confluency, then detached with trypsin/EDTA solution (Sigma), centrifuged at 500 *g* for 5 min, then resuspended at approximately 4 x 10^5/mL in complete medium. 10 mL of cell suspension was each added to 3 petri dishes (pre-treated with collagen I as before). The cells were left to adhere overnight in a 37 °C, 5% CO_2 incubator.

For transfection, 15 µg Hoxb8 plasmid DNA with 15 µg Eco viral envelope was added to a 1.5 mL Eppendorf tube with 600 µl Xfect reaction buffer, for the negative control the same reagents were added without the Hoxb8 plasmid DNA in a separate tube. The tubes were vortexed well for 5 min. 9 µl of Xfect polymer (after a thorough vortex) was added to each tube then vortexed at high speed for 10 seconds. The tube contents were left to incubate for only 10 min at room temperature. Each tube was then added dropwise to a plate of prepared HEK cells while it was rocked gently back and forth, then incubated overnight in the 37 °C, 5% CO_2 incubator.

The next day, the transfection medium was replaced with 10 mL of fresh complete cell medium, then returned to the incubator. 48 hr later, the supernatant containing retrovirus was harvested by filtering through a 0.2 µm PES filter. 1 mL aliquots were stored in 1.5 mL tubes at -80 °C.

Preparation of bone marrow progenitor cells

Mouse bone marrow was harvested in the same way as outlined in 4.1, but after passing the cell suspension through the cell-strainer, it was centrifuged at 500 *g* for 5 min. The pellet was resuspended in 4 ml of bone marrow outgrowth medium in one well of a 6 well tissue culture plate. This is composed of the same ingredients as the

Hoxb8 progenitor medium, except it contains no estradiol, and is supplemented with 10 ng/ml IL-3, 20 ng/ml IL-6 and 8% of the CHO-supernatant (generated as described in section 5.1). The cells were incubated in this medium for 2 days at 37 °C, 5% CO_2. Two repeats (two C57BL/6 mice) were prepared for retroviral infection, one for a negative control, no infection.

Spin infection of progenitor cells

The contents of each well were transferred to a separate sterile FACS tube, and centrifuged at 500 *g* for 5 min at 4 °C. The supernatant was removed, and the cells resuspended in 1 ml of the Hoxb8 retroviral supernatant with 8 µg/ml polybrene. The cells were spin-infected in a centrifuge pre-heated to 30 °C for 90 min at 300 *g*. Then the pellet was resuspended and transferred to a 6 well plate supplemented with 3 ml of complete Hoxb8 progenitor outgrowth medium (with 10 µM estradiol and 8% SCF, no IL-3 or IL-6). Two days later, 1 µg/ml neomycin was added to the cells to start the selection of successfully transfected progenitor cells. Neomycin was retained in the medium for approximately 3 weeks. The cells were split every 3-4 days. After 4 weeks, clusters of transfected cells began to form while non-transfected cells died off. The negative control had no viable cells. The conditionally immortalised Hoxb8 progenitor cells were transferred to T25 flasks (Corning).

Culture of Hoxb8 immortalised myeloid progenitor cells

Cells were maintained in the Hoxb8 culture medium at a density between 1 x 10^5 – 1 x 10^6/ml in T25 flasks. Cell viability averaged over 90% as assessed by trypan blue exclusion using the Biorad TC20 cell counter. The cells were passaged every 2/3 days, the flask was changed every week. Cell stocks were prepared in 90% FCS:10% DMSO and stored in liquid nitrogen.

Differentiation of Hoxb8 progenitors into neutrophils

Approximately 2.5 x 10^5 progenitors were washed once in 50 ml PBS, then resuspended in 13 ml of differentiation medium and added to a 10 cm Nunc treated petri dish. They were cultured at 37˚C 5% CO_2 for 4/5 days or as described.

GFP-LC3 adenoviral transfection of Hoxb8 neutrophils

Generation of adenovirus

The GFP-LC3 was gifted by Tom Wileman of UEA as 1 ml aliquots of cell medium supernatants containing adenovirus. To generate more aliquots, GP-293 HEK cells were grown in the same way as detailed for retroviral transfection of mouse bone marrow progenitor cells, in DMEM medium in a T175 flask until ~80% confluent. The medium was replaced with 16 ml fresh medium and 1 ml adenoviral GFP-LC3 supernatant was added. The supernatant was harvested once ~60% of HEK cells had detached, usually after 2-3 days. The cells were resuspended by knocking the flask, and pelleted in 100 µl medium. To release virus from the cell cytoplasm, cells were lysed by freeze/thawing by leaving pellet in -80 °C freezer for 10 min then 37 °C water bath for 5 min, repeating 4 times. After the last cycle, the cells were centrifuged at 500 *g* for 5 min, the supernatant was collected and added to the flask supernatant. Total supernatant passed through 0.2 µm PES filters and stored in 1 ml aliquots in the -80 °C freezer.

Adenoviral transfection of Hoxb8 neutrophils

Hoxb8 neutrophils were differentiated for three days as described above in 10 cm petri dishes. Then they were gently scraped and resuspended in their original 13 ml differentiation medium, 2 ml of cell suspension was added per well of a 12 well TC plate as required. 0.5 ml thawed GFP-LC3 adenoviral supernatant was added to each well containing Hoxb8 neutrophils. Wells without virus were kept as negative controls.

Cells were incubated with the virus for 18-24 hr before gently scraping to harvest cells, washing twice in PBS and imaging.

2.6 *C. albicans* generation

Broth culture and stock preparation

One *Candida* vitroid disc (Sigma) was grown on a YPD agar plate overnight at 37˚C in a non-CO_2 incubator. One colony was picked and cultured in 15 ml YPD broth in a heated shaking incubator until the broth turned cloudy. The solution was washed twice in PBS by centrifuging at 3000 *g* for 10 min. The yeast particles were resuspended in 50 ml PBS, and heat-killed by completely submerging the whole tube in a pre-warmed 60 ˚C water bath for one hour. Confirmation of killing was achieved by streaking a sample on a fresh YPD agar plate and culturing overnight. Heat-killed *Candida* was stored in 5 x 10^8/ml samples at -20 ˚C.

Mouse serum production

100 µl of 1 x 10^8/ml heat-killed *Candida* suspension was subcutaneously injected into the scruff of 15 BALB/c wildtype mice three times with 2-week intervals. To harvest the serum, each mouse was administered a fatal dose of pentobarbital then blood was taken by cardiac puncture. Cervical dislocation was used as secondary confirmation of death. The blood was left to clot overnight at 4 ˚C, then centrifuged at 1000 *g* for 10 min. The resulting top serum layer was removed, aliquoted at 50 µl in small Eppendorf tubes, and stored at -80 ˚C.

2.7 SNARF-1 phagosomal pH confocal microscopy

Labelling of *C. albicans* with SNARF-1

100 µl of DMSO was added to one tube of 50 µg carboxy-SNARF-1 succinimidyl ester and vortexed to mix. 1 x 10^8 heat-killed *Candida* was prepared in 1 ml of 0.1 M sodium bicarbonate pH 8.3 in a 15 ml tube wrapped in aluminium foil. The carboxy-SNARF-1 was added dropwise to the *Candida* solution with constant vortexing, then left on at roller at room temperature for 1 hr. The SNARF labelled *Candida* were washed three times by centrifugation at 3000 *g* for 10 min in the labelling buffer, resuspended in 1 ml of labelling buffer, and stored in 100 µl at -20 ˚C.

SNARF-labelled *Candida* (SNARF-Ca) opsonisation

100 µl of human pooled IgG serum (Vivaglobin), or 50 µl each of normal mouse serum (VWR) and *Candida* serum, was added to one 100 µl aliquot of SNARF-Ca and incubated for 1.5 hr in a heated tube shaker at 1100 rpm. The suspension was washed three times by centrifuging in a microcentrifuge at max speed (14,000 g) for 1 min, then resuspended in the experimental buffer.

Microscopy plate preparation

Ibidi 8-well µ slides were used to image cells. They were first pre-treated with poly-L-lysine (0.01% solution, Gibco) to allow cell adherence by adding 200 µl to each well and leaving for at least 30 min at room temperature, then washed off twice with distilled water. 200 µl of cell solution was added to each well and allowed to adhere for at least 30 min at room temperature, at approximate concentration of 2-4 million/ml.

Cell cytoplasmic staining

An aliquot of 5-(and-6)-carboxy SNARF-1 acetoxymethyl ester (SNARF-AM 50 µg, Invitrogen) is prepared by adding 100 µl of DMSO. A stock solution was made with a ratio of 10 µl SNARF-AM to 425 µl experimental buffer. 200 µl of the stock solution was added to each well and incubated for 30 min at room temperature. It was washed off twice with experimental buffer. If an inhibitor was used, a stock solution of it was made up in experimental buffer used to wash each desired well twice.

Confocal microscopy setup

The Zeiss 700 confocal microscope was used to image all SNARF pH assays. Laser excitation was set at 555nm, and two detecting channels collected emission: 560-600nm and over 600nm. Cells were viewed with a x 63 lens with oil. Laser intensity, gain, and fluorescence saturation were adjusted for optimal imaging.

Phagocytosis snapshot and time course

For phagocytosis snapshot images: 10 µl of opsonised SNARF-Ca was added to each well, then the plate was incubated for approximately 20 min at 37 ˚C. The cells were then placed on the confocal microscope, focused appropriately, then imaged in 9 square wells. At least 2 images in different locations were processed for each well.

For time course experiments: a heated stage set to 37 ˚C was inserted on the microscope, and the cell plate equilibrated on it for about 10 min. The microscope settings were adjusted to measure time course across 2 squares with 1 min intervals for 50 min to 1.5 hours. A basal reading was measured for 5 min before adding the Candida, and to adjust focus to an optimal cell density. Each run could measure 4 different positions or wells. Then 5-10 µl of opsonised SNARF-Ca was added to each well (based on cell density) and the experiment commenced. Focus was adjusted

manually throughout.40 µl of trypan blue (Sigma) was added to each well at the end of the experiment to quench fluorescence of extracellular *Candida*. Z stacks were taken at the end of time course experiments to measure percentage of cells phagocytosing by recording 8-9 slices throughout the cell monolayer.

Standard curve generation

Each of the pH buffers from step 3.1.2 were prepared and 200 µl added to each well of a microscopy plate. Then 5 µl of SNARF-Ca was added to each well, and a confocal snapshot image was taken as described in step 7.6. 3 images in different locations of the well were acquired for each buffer, for snapshot experiments which did not use a heated stage. To generate the standard curve for time courses, the plate was placed in the 37 ˚C heated stage for 10 min before image capture. The experiment was repeated three times and the average was used for SNARF fluorescence ratio to pH calibration, see **figure 2.7**. SNARF fluorescence has a slight pH dependence.

2.7

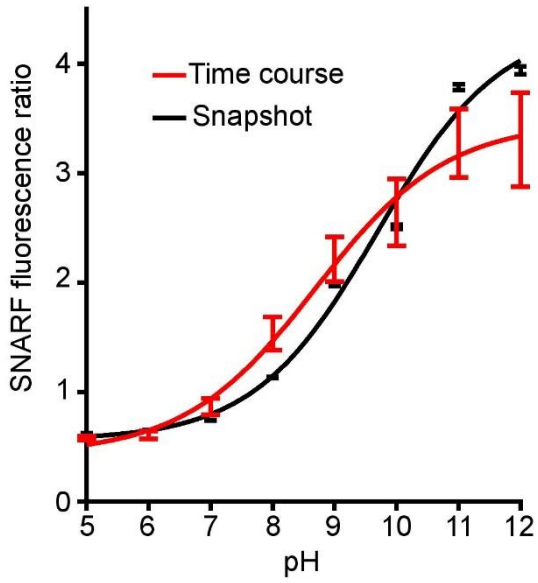

Figure 2.7 | Relationship of SNARF fluorescence ratio to pH. *The SNARF/pH calibration from experimental conditions for the snapshot experiments are plotted in black (approximately 25-27 ˚C), those for the time course experiments (37 ˚C) are in red. Mean is plotted ± SEM with non-linear regression curve from n=3.*

Data analysis

All analyses were carried out using the free software ImageJ (https://imagej.nih.gov/ij/).

Snapshot experiments

The custom-made macro was used to measure the ratio of the two emission channels for snapshot images. The pH of approximately 100 phagosomes was recorded for each image, or as many fully contained *Candida* particles could be identified. Where described, phagosomal area was measured by drawing free-hand around the periphery of single-particle phagosomes.

The human phagosomal pH snapshot data had a bimodal distribution profile of an alkaline population and an acidic population. A cluster analysis of the control phagosomal data was carried out to remove the acidic population, using the package 'Mclust' (Chris Fraley et al., 2012) in the programming software R (R Core Team, 2013). This fits data into Gaussian finite mixture models with an algorithm for model-based clustering, classification, and density estimation. The maximum measurement of the lower ratio acidic group was calculated, and points below this value were removed (see figure legends for exact number). *Hvcn1*$^{-/-}$ murine neutrophils also have a smaller subset of acidic phagosomes which were removed by the same method. This particular analysis was not necessary for wild type mouse neutrophil phagosomal pH as they tended to be more acidic and not readily separated into two clusters. The processed data was entered in the software program R to construct graphs. For both phagosomal pH and area, the measurements have been displayed as scatter plots with overlaying boxplots, which show the median and upper and lower quartiles.

Time course experiments

A custom-made macro was used to measure these experiments. First, all appropriate phagocytosis events were identified with squares added to the reference manager

and saved. These were particles that could be clearly tracked from the first minute of uptake for at least 30 min. All suitable events were recorded, or at least 30 events. All data was presented using GraphPad Prism version 7 (GraphPad software, La Jolla California, USA).

Phagocytosis uptake

Zen software (Zeiss) was used to analyse the z stacks recorded at the end of time courses; percentage of phagocytosing cells was calculated from the number of total cells and total cells with engulfed particles per square (2 squares per recording).

Efferocytosis of apoptotic neutrophils by MDMs

Generation of apoptotic neutrophils (AN)

Human neutrophils were isolated in the same way as described in section 2.4 and resuspended in AN medium at a concentration of 1 x 10^6/ml by adding 1 ml of cell suspension to each well of a 12 well non-coated tissue culture plate. Cells were incubated in a 37 °C, 5% CO_2 incubator for 24 or 48 hours. A sample of AN were compared against freshly isolated neutrophils using the AnnexinV-FITC and propidium iodide apoptosis kit (Biovision) according to the manufacturer's instructions.

Staining of AN

Cells were removed from the wells with gentle pipetting and transferred to a 50 ml Falcon tube where they were centrifuged at 300 *g* with low brakes for 3 min. They were resuspended in 1 ml of PBS in a dark 1.5 ml Eppendorf and centrifuged again at 300 *g* for 1 minute. The cells were resuspended to approximately 1 x 10^7 in 1 ml PBS. 10 µl of SNARF-1 carboxylic acid, succinimidyl ester (as prepared in section 2.7) was added to the AN dropwise, the mixture pipetted to mix gently, then left to incubate at room temperature for 1 hour. After incubation, the cells were washed twice

with PBS by centrifugation at 300 *g* for 1 minute. The cells were resuspended in 1 ml of PBS with 5 µl of 10% human serum albumin for 30 min at room temperature. Cells were washed once as before with PBS, then finally resuspended in 100 µl of PBS.

Staining of MDMs

"M1" and "M2" monocyte-derived macrophages were generated as described in section 4.4 by culturing human peripheral mononuclear cells in the central 4 wells of an 8 well µ-slide (Ibidi). For staining, the wells were first washed twice with Duchen buffer to remove non-adherent cells. 100 µl of DMSO was added to a tube containing 50 µg of calcein acetoxymethyl ester (Thermofisher) and vortexed to mix. A 1 µM calcien-AM in Duchen buffer was made by adding 1 ml of Duchen buffer and 1.19 µl of calcein-AM to a 1.5 ml Eppendorf and vortexing to mix, then 200 µl added to each macrophage well. Cells were incubated with the dye for 45 min in the dark before it was washed off twice with fresh Duchen buffer.

Imaging of efferocytosis

Time course experiments of ingestion of AN by macrophages was conducted in the same was as detailed in section 2.7, apart from an image was taken every 5 min for approximately 15 hours. To record calcein fluorescence, in addition to the laser settings for SNARF-1, the plate was excited at 488 nm and emission detected using the 488-560 nm long-pass filter.

2.8 Amplex UltraRed respiratory burst assay

Cells were resuspended at 2 x 10^6/ml in Duchen buffer. 20 µl of 1mg/ml PMA stock was added to 1 ml of buffer in a small bijou. The plate reader injector pump was first primed with the PMA solution. The assay was set up as follows: cells were excitated at 544 nm and emission measured at 590 nm every 30 sec for 50 min. The pump injected 20 µl of PMA solution on the fourth cycle. To prepare the cell suspension with

the assay reagents, 2.5 µl (final concentration 0.125 U/ml) of horseradish peroxidase and 5 µl (final concentration 50 µM) of Amplex UltraRed reagent were added per 1 ml of suspension. Here also an inhibitor or vehicle was added. 200 µl of complete cell suspension was transferred to each desired well of a 96 well plate, loaded into the plate reader and experiment commenced. The plate reader had an internal temperature of 37 ˚C.

2.9 Seahorse oxygen consumption assay

This assay measures oxygen consumption of neutrophils once they have ingested opsonised *C. albicans*, produced as detailed in step 2.6 and 2.7 (without SNARF labelling). A seahorse calibrant plate (Seahorse Biosciences) was prepared the day before the experiment by adding 1 ml of seahorse calibrant solution to each of the 24 wells. It was left overnight at 37 ˚C in a non-CO_2 incubator. The next day, the experimental plate was prepared by adding 50 µl of Cell-tak solution (Corning) to each well (14.5 µl in 1.2 ml 0.1M sodium bicarbonate solution). After 45 min at room temperature, the solution was removed and each well washed twice with distilled water. 2 x10^6 neutrophils in 100 µl phosphate-free Duchen buffer was added to each well, leaving 4 wells as blank with buffer alone. The cells were left to adhere for 45 min to 1 hour. Meanwhile, the experimental protocol on the Seahorse XFe24 Analyzer was set up that first involved calibration of the machine with the calibrant plate, then measuring oxygen consumption in the microplate every 3 min for 45 min at 37 ˚C. To increase cell adherence, the experimental plate was gently centrifuged at 450 *g* for 5 min with low brake. The 100 µl buffer in each well was gently pipetted off to remove non-adherent cells, and 600 µl fresh buffer very gently pipetted down the well wall to minimise cell monolayer disruption. The 2 x10^6 of opsonised *C. albicans* was added to each desired well, and the plate immediately inserted into the machine to start the

protocol. Data was analysed using the free accompanying software Wave Seahorse Biosciences.

2.10 Flow cytometry

Cells were resuspended at roughly 1 x 10^6/ml in FC buffer and 1 µl of FyRC block (Biolegend) added per 100 µl. Appropriate antibodies for each panel and cells were incubated in V-shaped plates at 4 ˚C in the dark for 30 min to 1 hour. Unstained control cells were run for each experiment. Compensation beads were run for each experiment after incubation with 1 µl of each antibody. After incubation, the plate was centrifuged at 500 *g* for 5 min at 4 ˚C, the supernatant removed, and cells and beads resuspended in 100 µl of FC buffer. This wash step was repeated three times. Then each well was resuspended in 150 µl of 1% paraformaldehyde in PBS, transferred to FACS tubes with a further 150 µl FC buffer added. The experiment was run immediately on a LSR Fortessa (BD Biosciences) or stored at 4 ˚C in the dark for no more than 4 hours.

2.11 Western blots

Sample preparation

Cells were harvested and washed once in PBS at 500 *g* for 5 min. 1 x 10^6 cells were lysed in 50 µl of complete RIPA buffer and left on ice for 30 min. Next, they were centrifuged at max speed (17,000 *g*) in a minicentrifuge (Thermofisher) for 15 min at 4 ˚C. Each sample was then sonicated three times in 10 second bursts at low settings. They were centrifuged again at the same settings. If they were being used on the same day, 7.15 µl beta-mercaptoethanol (Sigma) was added to each sample and incubated at room temperature for 30 min. Finally, 17.5 µl NuPage 4x LDS sampling buffer (Life Technologies) was added to each sample and heated for 15 min at 72 ˚C

(lower heating temperature for this reagent). For future experiments, the samples were stored at -20 ˚C without reducing agents.

Gel preparation

Optimisation experiments were carried out using home-made 10% acrylamide gels (two gels made at a time): 3.3 ml acrylamide, 2.5 ml 1.5M Tris pH 8.8, 4 ml water, 100 µl 10% sodium lauryl sulphate (SDS), 10% ammonium persulphate (APS), and 5 µl TEMED were mixed gently and quickly then added to glass 1 mm thickness gel casting cassettes. 200 µl ethanol was quickly added to remove bubbles. After waiting approximately 40 min for the gels to set, the ethanol was poured off and replaced with stacking solution comprised of 500 µl acrylamide, 380 µl 1M Tris pH 6.8, 2.1 ml water, 40 µl 10% SDS, 40 µl 10% APS, and 4 µl TEMED, and a 15 well comb divider. Gels were stored in water at 4 ˚C.

For optimised experiments, samples were run on NuPage 4-12% Bis-Tris precast polyacrylamide gels (ThermoFisher).

Gel electrophoresis

Home-made gels were used in the Mini-Protean gel system (Bio-Rad) with Tris-base running buffer, while the precast gels used the XCell4 Surelock™ Midi-cell (ThermoFisher) with the NuPage MOPS buffer. Optimised samples were loaded at 5 µl, 2 µl of Precision Plus Protein™ Dual Color Standards (Bio-Rad) was used as the protein ladder. Home-made gels were run at 120 volts for 1 hour, precast gels at the same voltage for 1.5 hr.

Gel to membrane transfer

Gels were transferred to polyvinylidene fluoride (Immobilon-FL PVDF, Merck) membranes using the Mini Blot Modules (Thermofisher). Membranes were first activated in 100 % methanol for 5 min, then incubated in transfer buffer for at least 5 min with the gel, 2 pieces of filter paper and 2 blotting sponge pads (Thermofisher). Starting from the cathode core of the blot modules the following was layered: sponge pad, filter paper, gel, membrane, filter paper, sponge pad, and finally the anode core. The modules were run for 1 hour at 20 V in the Bolt Mini Gel Tank (Thermofisher).

Antibody staining and film development

Membranes were blocked in 5% milk in TBS-T for 1 hour, then incubated on a roller overnight in primary antibody prepared in 5% milk/TBS-T. Membranes underwent 3 x 5 min washes in TBS-T before incubation in secondary antibodies for 2 hours at room temperature. The membranes were washed 3 x as before in TBS-T, then treated with 1 ml of Luminata Forte Western HRP Substrate (Merck) before development onto Amersham Hyperfilm (Thermofisher) for chemiluminescence using the Protec ECOMAX X-Ray film processer.

2.12 Cell staining for bright-field microscopy

Cells were resuspended to 5 x 10^5/ml in PBS with 10% FCS. 200 µl per slide was loaded into a cytospinner, set to 800 rpm for 8 min. After spinning, the slides were left to dry for 30 min, then fixed for 30 sec in 100 % methanol. Once the slides were dry, 1 ml of Wright-Giemsa stain (Sigma) was pipetted onto the slide and left for 1.5 minutes. Then 1 ml of distilled water was added to the stain, mixed by gently pipetting the solution, then incubated for 3 min. The solution was rinsed off with liberal amounts of distilled water for a few minutes, left to dry, then a coverslip mounted with DPX

mounting medium (Sigma). Slides were imaged with Zeiss Axio Vert A1 microscope on a x 63 lens with oil.

2.13 Compiling gene expression datasets of human neutrophils

Data was processed by Adam Levine. Gene expression data from resting human neutrophils from healthy individuals were isolated from nine individual publicly available studies on the Gene Expression Omnibus (Edgar et al., 2002) (**Table 2.13**). There were data from a total of 66 samples, a mean of seven (minimum three) per study. Data were analysed with R (R Core Team, 2013). For all but one dataset, raw data were processed using the Affy package (Gautier et al., 2004). For one dataset, pre-processed data were used. Raw data were imported using ReadAffy and normalised with Robust Multi-array Average. Detected probes were then identified per sample using pa.calls from the panp package (Warren, 2016). Probes that were detected in at least 50% of the individual samples within each data set were retained. Genes within a gene family (Gray et al., 2015) containing the terms channel or carrier or those with a GO term containing one of the following were retained: potassium, sodium, chloride, channel, or exchanger. Control genes that were known to be involved in neutrophil function or markers of possible contaminating cells were also retained. Within each dataset, the relative centile expression of the retained genes from all detected genes was determined. The summary statistics across the nine studies were combined by gene and the mean calculated. It is conceivable that a putative channel or exchanger involved in neutrophil charge compensation could have been inappropriately omitted by the requirement for either the gene family or GO term to be matched; however, this approach was utilised as a means of reducing the search space to contain a manageable number of the most likely candidates.

Table 2.13 | Source of online study datasets for neutrophil composite mRNA expression

Title of study	Source link	No. of samples per study
Transcription profiling of human neutrophil and PBMC gene expression data from Jobs Syndrome individuals	https://www.ebi.ac.uk/arrayexpress/experiments/E-GEOD-8507	11
Transcription profiling by array of human neutrophils after 30 minutes' exercise	https://www.ebi.ac.uk/arrayexpress/experiments/E-GEOD-8668	24
mRNA expression profiling of human immune cell subsets (HUG)	https://www.ebi.ac.uk/arrayexpress/experiments/E-GEOD-28491	5
Transcription profiling by array of human peripheral blood mononuclear cells after treatment with community-associated Staphylococcus aureus and incubation for different lengths of time	https://www.ebi.ac.uk/arrayexpress/experiments/E-GEOD-16837	4
Transcription profiling by array of human bone marrow CD34+ cells, promyelocytes and neutrophils, as well as PR-9 and NB-4 cell lines, to investigate acute myeloid leukaemia	https://www.ebi.ac.uk/arrayexpress/experiments/E-GEOD-12662	5
mRNA expression profiling of human immune cell subset (Roche)	https://www.ebi.ac.uk/arrayexpress/experiments/E-GEOD-28490	3
Transcription profiling by array of human neutrophils isolated via microfluidics after treatment with either lipopolysaccharide or granulocyte-macrophage colony-stimulating factor and interferon gamma	https://www.ebi.ac.uk/arrayexpress/experiments/E-GEOD-22103	4
Expression profiles from a variety of resting and activated human immune cells	https://www.ebi.ac.uk/arrayexpress/experiments/E-GEOD-22886	5
Transcription profiling of human neutrophils obtained after exposure endotoxin by bronchoscopic instillation reveals differential gene expression between air space and circulating neutrophils	https://www.ebi.ac.uk/arrayexpress/experiments/E-GEOD-2322	5

2.14 Statistics

For phagosomal pH and area snapshot data analysed in R, linear model analysis, using the lm function in the programming software R (R Core Team, 2013), was used to test the statistical significance of the comparison between the control condition and that in the presence of the inhibitor, or in cells with an altered genetic background. All other statistics were manipulated in GraphPad Prism version 7 (GraphPad software, La Jolla California, USA) using one-way ANOVA with Bonferroni post-tests for multiple comparisons. All experiments were conducted three times with technical replicates within each, unless otherwise stated. Statistics were calculated based on averages of each experiment.

Chapter Three: Investigating ion channels in the neutrophil phagosome

The majority of results discussed in this chapter were published in Frontiers in Pharmacology of Ion Channels and Channelopathies (Foote et al., 2017). Sabrina Pacheco and Janne Plugge carried out the mice husbandry and data acquisition for some of the mouse experiments. All the data was compiled and analysed by myself with bioinformatic assistance from Adam Levine, Nikolas Pontikos and Matthew Frampton.

3.1 Background and aims

As described in the introduction, neutrophils act as highly efficient first participators at the scene of infection by working quickly to engulf, kill and digest pathogenic particles. The phagosomal environment must be tightly regulated to ensure this effective removal. There is evidence to show that one way of regulation is through phagosomal pH, which in turn governs the phagosomal enzymes and antimicrobial components (Segal, 2005). The main driving factor of the phagosomal environment is through the activity of the NADPH oxidase. In its absence or malfunction, the result is chronic granulomatous disease (CGD), which comprises recurrent infection of bacteria and fungi and is life-threatening (Holland, 2010). The oxidase works mainly as an electron transport chain, passing electrons provided by NADPH in the cytosol across the phagosomal membrane to molecular oxygen, to form superoxide anions, and further downstream products which contribute to its microbicidal ability. However, this negative charge of electron movement must be neutralised to allow subsequent oxidase activity. We know that the predominant compensating movement is proton via HVCN1 (Petheo et al., 2010; Ramsey et al., 2009). But we also know that the neutrophil phagosome is not at first acidic, but alkaline (Levine et al., 2015; Segal et

al., 1981), demonstrating that there must be non-proton ions involved in charge compensation. To understand how the phagosomal pH is controlled will provide further insight into how the neutrophil successfully does its job.

This chapter sets out to investigate the biochemical ion fluxes induced by the neutrophil NADPH oxidase by aiming to:

- Understand the relationship between the respiratory burst and phagosomal pH
- Identify potential charge compensating channels through published human mRNA gene expression and published reports of studies
- Target potential channels with pharmacological inhibitors
- Study selected knockout mouse models and patients with a channelopathy

The results of the studies were measured as phagosomal pH and area using the pH-sensitive indicator, SNARF-1, labelled to opsonised heat-killed *Candida*, and NADPH oxidase activity either through oxygen consumption after phagocytosis of these particles or through the Amplex UltraRed assay which measures hydrogen peroxide generated by PMA stimulation at the plasma membrane.

3.2 Dissecting the relationship between NADPH oxidase activity and phagosomal pH with DPI

Diphenyleneiodonium (DPI) is a commonly used synthetic inhibitor of the oxidase (Cross and Jones, 1986). It exerts its effect by disrupting electron flow in the flavocytochrome component (O'Donnell et al., 1993). As aforementioned, neutrophils have alkaline phagosomes, but with the treatment of DPI they become very acidic (Levine et al., 2015). Here I used varying doses of DPI to observe the consequential changes in phagosomal pH and oxidase activity to understand if there is a direct linear relationship between them.

The phagosomal pH in human neutrophils is here presented as a snapshot at 30-40 minutes after addition of the opsonised *Candida* **(Fig 3.2a)**. This length of time allows sufficient phagocytosis by most cells but causes a broad spread of varying phagosomal pH, as the phagocytosis is not synchronised. However, the mean is approximately pH 8.5, which is consistent with previous measurements (Levine et al., 2015). At the lowest dose of DPI, 25 nM, the mean jumps significantly to pH 8.07. This effect contrasts with the effect of the same treatment on the respiratory burst, where there is a small but insignificant drop in activity. Although for both measurements, the biggest decline in activity comes at 250 nM, where the mean phagosomal pH falls below pH 7, and the maximum oxidase rate is under 50% of the control condition. For oxidation rate, between 250 nM to 5 µM there is a linear relationship, while for phagosomal pH it is between 0 to 100 nM, and nearly plateaus beyond this to 5 µM. This may be a limitation of the dye employed, SNARF-1, which shows no change in fluorescence lower than pH 5-5.5 **(Fig 2.1a)**, but 5 µM DPI has been recorded by others to cause the neutrophil phagosome to reach pH 5 (Jankowski et al., 2002).

An interpretation of phagosomal pH sensitivity to low concentrations of DPI is that an under 10% drop in oxidase activity will not have a major effect on the HVCN1 channel but may have on smaller compensating channels. These smaller channels may actually have a larger effect on the pH, through the virtue of the particular ions they are transporting across the phagosome.

Figure 3.2 | Both NOX2 activity and phagosomal pH are inhibited by DPI, but phagosomal pH is more sensitive to its effects (a-c). (**a**) *Quantification of phagosomal pH when treated with increasing doses of DPI. Each box represents an individual measurement; all measurements are shown from 3 separate experiments with at least 100 recordings for each condition. The median and interquartile range are overlaid as a boxplot*. (**b**) *Time course of the effect of DPI on the respiratory burst, recorded as hydrogen peroxide-induced relative fluorescence units (H_2O_2 RFU) for 30 minutes after stimulation with PMA. The mean with standard error*

(dashed lines) is plotted from 3 separate experiments. (**c**) *The maximum oxidation rate of (**b**), gathered from 3 separate experiments plotted as mean with SEM. Statistical significance is calculated against the vehicle control, *=p<0.05, ****=p<0.0001.*

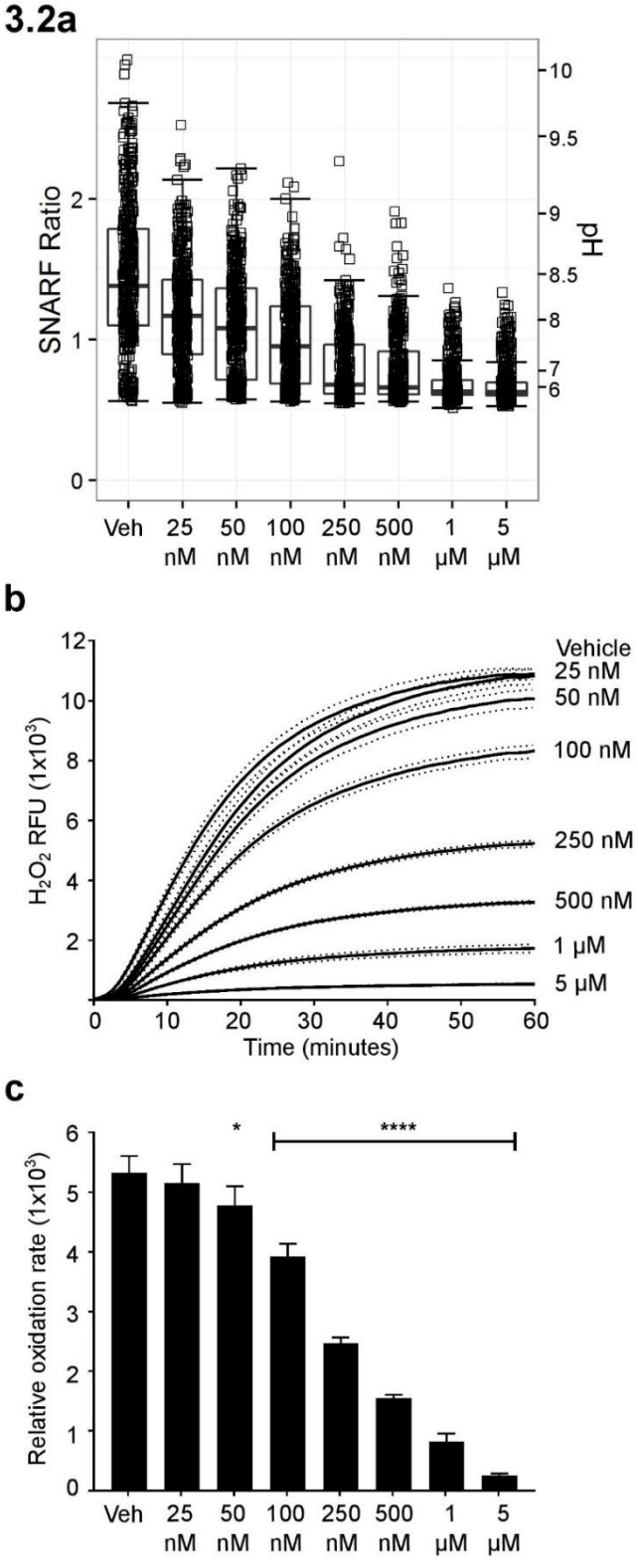

3.3 A study of ion channels present in the neutrophil mRNA expression data

Table 3.3 | A compilation of the averaged results of nine online datasets of mRNA expression in neutrophils

Gene symbol	Gene description	Relative expression (Human)	Cited in literature	
			Human	Mouse
Oxidase components				
NCF2	Neutrophil cytosolic factor 2	98.88		
CYBA	Cytochrome b-245, alpha polypeptide	97.24		
NCF4	Neutrophil cytosolic factor 4, 40kDa	94.80		
CYBB	Cytochrome b-245, beta polypeptide	62.99		
HVCN1	Hydrogen voltage-gated channel 1	83.62		
Chloride channels				
CLIC1	Chloride intracellular channel 1	95.92	(Averaimo et al., 2010)	
BEST1	Bestrophin 1	59.91	(Fischmeister and Hartzell, 2005)	
CIC7	Chloride channel, voltage-sensitive 7	41.53	(Graves et al., 2008)	
CIC3	Chloride channel, voltage-sensitive 3	35.36	(Moreland et al., 2006)	(Moreland et al., 2006)
Potassium channels				
KCNJ15	Potassium inwardly-rectifying channel, subfamily J, member 15	93.69		
KCNE3	Potassium voltage-gated channel, Isk-related family, member 3	77.44	(Barro-Soria et al., 2015)	
KCNJ2	Potassium inwardly-rectifying channel, subfamily J, member	80.66	(Vicente et al., 2003)	(Masia et al., 2015)
KCNQ1	Potassium voltage-gated channel, KQT-like subfamily, member 1	48.37		
KCNAB2	Potassium voltage-gated channel, shaker-related subfamily, beta	43.76		
KCNK7	Potassium channel, subfamily K, member 7	41.97		
KCNH7	Potassium voltage-gated channel, subfamily H (eag-related), member	32.57		
KCNH3	Potassium voltage-gated channel, subfamily H (eag-related), member	7.02		
Transient receptor potential channels				
TRPM6	Transient receptor potential cation channel, subfamily M, member 6	31.06		
MCOLN1	Mucolipin 1	31.60	(Bach et al., 1999)	
TRPV2	Transient receptor potential cation channel, subfamily V, member 2	17.94		(Link et al., 2010)
TRPV6	Transient receptor potential cation channel, subfamily V, member 6	11.15	(Heiner et al., 2003)	
Solute carriers/transporters				
SLC12A6 (KCC3)	Solute carrier family 12 member 6	92.47	(Sun et al., 2012)	(Sun et al., 2012)
SLC26A6	Solute carrier family 26, member 6	29.45		(Ishiguro et al., 2006)
SLC12A4 (KCC1)	Solute carrier family 12, member 4	14.34		

Genes were ranked on relative mean expression levels; a more detailed explanation for acquiring the data is described in the methods. Expression levels of components

of the neutrophil NOX2 oxidase system and HVCN1 are shown for comparison. The table has been edited to show channels linked to neutrophils, NOX systems or other immune cells in the literature. Sources of the online datasets are provided in chapter two materials and methods.

After hypothesising that there are smaller charge compensating channels involved in the NOX2-induced phagosomal arena, the next step was to look for potential candidate genes. Datasets of human mRNA expression from whole resting neutrophils in healthy individuals are readily available online, and they were used as a source of candidate genes. The data analysis was carried out by Adam Levine and is explained in full in the methods chapter. An important factor was which families of ion channels and transporters to target. **Table 3.3** summarises the genes found to have high expression in the data sets and accompanying literature which suggests their involvement in the biochemistry of innate immune cells. Based on these compiled data and to data collected from the literature, potassium and chloride channels were primarily considered.

3.4 Investigating the effect of chloride channel inhibitors on phagosomal pH and area

The human composite data provided several potential chloride channels, but first it was necessary to show that there is a chloride ion conductance involved in phagosomal dynamics. A large number and variety of pharmacological inhibitors were tested, but only two were found to have a reliable effect. These were 4-[(2-Butyl-6,7-dichloro-2-cyclopentyl-2,3-dihydro-1-oxo-1H-inden-5-yl)oxy]butanoic acid (DCPIB) and flufenamic acid (FFA). Both drugs are considered to be broad-spectrum chloride channel blockers, inhibiting a number of different channels, although DCPIB was first considered to be a selective inhibitor of the swell-activated chloride current ($I\text{Cl}_{\text{swell}}$) (Decher et al., 2001; Jin et al., 2003). An inhibitor of the proton channel HVCN1, zinc

chloride (Zn^{2+}), was used in conjunction with the chloride channel blockers to put further stress on the charge compensating system. This current is conducted through the volume-regulated anion channel (VRAC). Recently, the illusive putative pore-forming subunit of the channel was identified as leucine-rich repeat-containing 8A protein (LRRC8A), which was shown to be essential for osmotically controlled regulatory volume decrease (Qiu et al., 2014; Voss et al., 2014).

Both inhibitors caused phagosomal acidification, a recorded reduction in the pH from ~ 9.0 to 8.5 (**Fig. 3.4a, table 3.4** for detailed statistics) with the treatment of DCPIB, and to ~ pH 8.8 with FFA treatment. Zn^{2+} changed phagosomal pH in the opposite direction by increasing the phagosomal pH to ~ pH 9.2. The elevation in pH and phagosomal area induced by Zn^{2+} was still much less than that resulting from complete elimination of the channel in the mouse *Hvcn1*$^{-/-}$ cells (Levine et al., 2015; Ramsey et al., 2009), indicating that Zn^{2+} only caused a partial blockage. This was probably because it was used at 100 µM; 300 µM caused a more significant pH rise but was more toxic to the cells. Cells treated with the chloride channel blockers and Zn^{2+} did not have as alkaline phagosomes as Zn^{2+} alone, but were more alkaline than with DCPIB or FFA alone; ~ pH 8.8 and 9.0 respectively. These findings suggest that a Cl^- channel is likely to be involved in charge compensation.

There was a marginal effect of FFA on the phagosomal area (**Fig. 3.4b**), an increase of 13.4 μm^2 in non-treated cells to 13.9 μm^2. When Zn^{2+} and FFA were combined, the median phagosomal size was not significantly different from Zn^{2+} alone (which caused a slight increase of 0.4 μm^2). DCPIB did not affect the area when added to cells, but when it was combined with Zn^{2+} phagosomal size increased dramatically to 15.8 μm^2. The increased swelling induced by chloride channel blockers suggests that chloride is being retained within the phagosome and/or its export replaced, at least in part, by the influx of an osmotically active cation.

The experiments were conducted as snapshots of phagosomal pH and area approximately 30-50 minutes after addition of yeast particles, but phagocytosis was not synchronised. This meant that there tended to be two populations of phagosomes; those that were more alkaline and more acidic ones. The acidic phagosomes were fewer in number and may have been partially closed, and the focus of this investigation was to investigate the alkaline phagosomal regulation. Therefore, the acidic population was excluded using a statistical clustering feature in R but calculating a threshold SNARF fluorescence ratio (SFR). More information on this can be found in chapter two materials and methods.

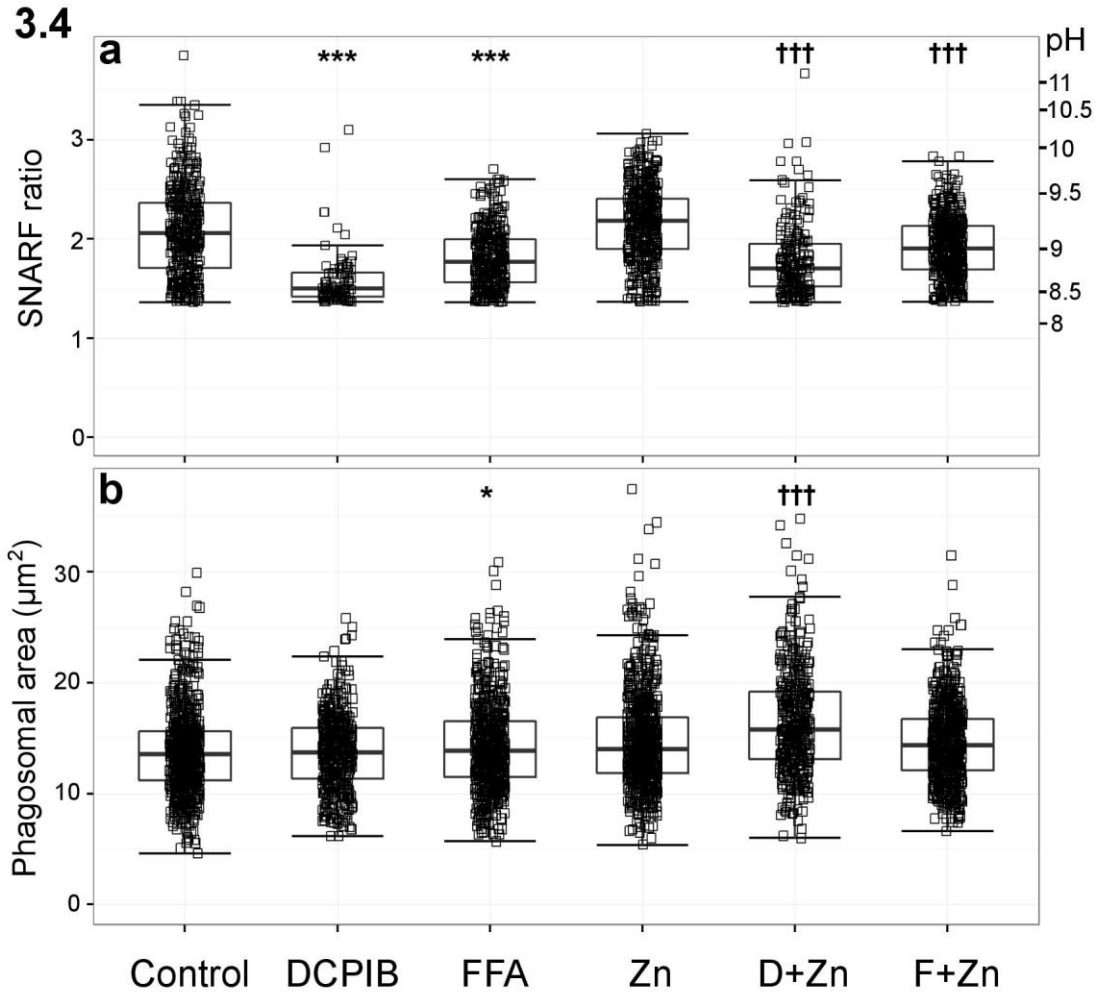

Figure 3.4 | Chloride channel inhibitors cause significant phagosomal acidification and increase phagosomal swelling (a-b). (**a**) *Quantification of phagosomal pH. The acidic phagosome population was removed as described in the*

methods section; the phagosomes excluded are those with an SFR below 1.36. (**b**) *Quantification of phagosomal area. DCPIB (20 mM), FFA (100 mM), Zn (Zn^{2+} 100 mM), D+Zn (DCPIB with Zn^{2+}), F+Zn (FFA with Zn^{2+}). Differences from control neutrophils: *p < 0.05, **p < 0.01, ***p < 0.001. Differences from neutrophils incubated with Zn^{2+}: †p < 0.05, ††p < 0.01, †††p < 0.001. For descriptive statistics see table 2.*

Table 3.4 | Phagosomal pH and area experimental measurements and statistics for chloride channel inhibitors

Phagosomal pH

N	Control	No. of points	Control median (SFR/pH)		Inhibitor	No. of points	Inhibitor median (SFR/pH)		*p*-value
11	Control	875	2.0	9.0	Zinc	1014	2.2	9.2	7.75×10^{-13}
3	Control	202	1.9	9.0	DCPIB	85	1.5	8.5	3.53×10^{-12}
4	Control	330	2.1	9.1	FFA	333	1.8	8.8	3.73×10^{-24}
3	Zinc	227	2.2	9.2	DCPIB + zinc	187	1.7	8.8	1.17×10^{-14}
4	Zinc	353	2.2	9.2	FFA + zinc	443	1.9	9.0	2.32×10^{-25}

Phagosomal area

N	Control	No. of points	Control median	Inhibitor	No. of points	Inhibitor median	*p*-value
11	Control	1537	13.2	Zinc	1574	13.9	1.25×10^{-8}
3	Control	454	13.4	DCPIB	429	13.7	0.145
4	Control	523	13.4	FFA	576	13.9	0.016
3	Zinc	380	13.6	DCPIB + zinc	406	15.8	2.52×10^{-7}
4	Zinc	560	13.8	FFA + zinc	581	14.3	0.093

N = number of experiments performed, no. of points describes the total number of individual measurements. The control and corresponding inhibitor medians are accompanied with the SFR and converted phagosomal pH.

3.5 Investigating the effect of potassium channel inhibitors on phagosomal pH and area

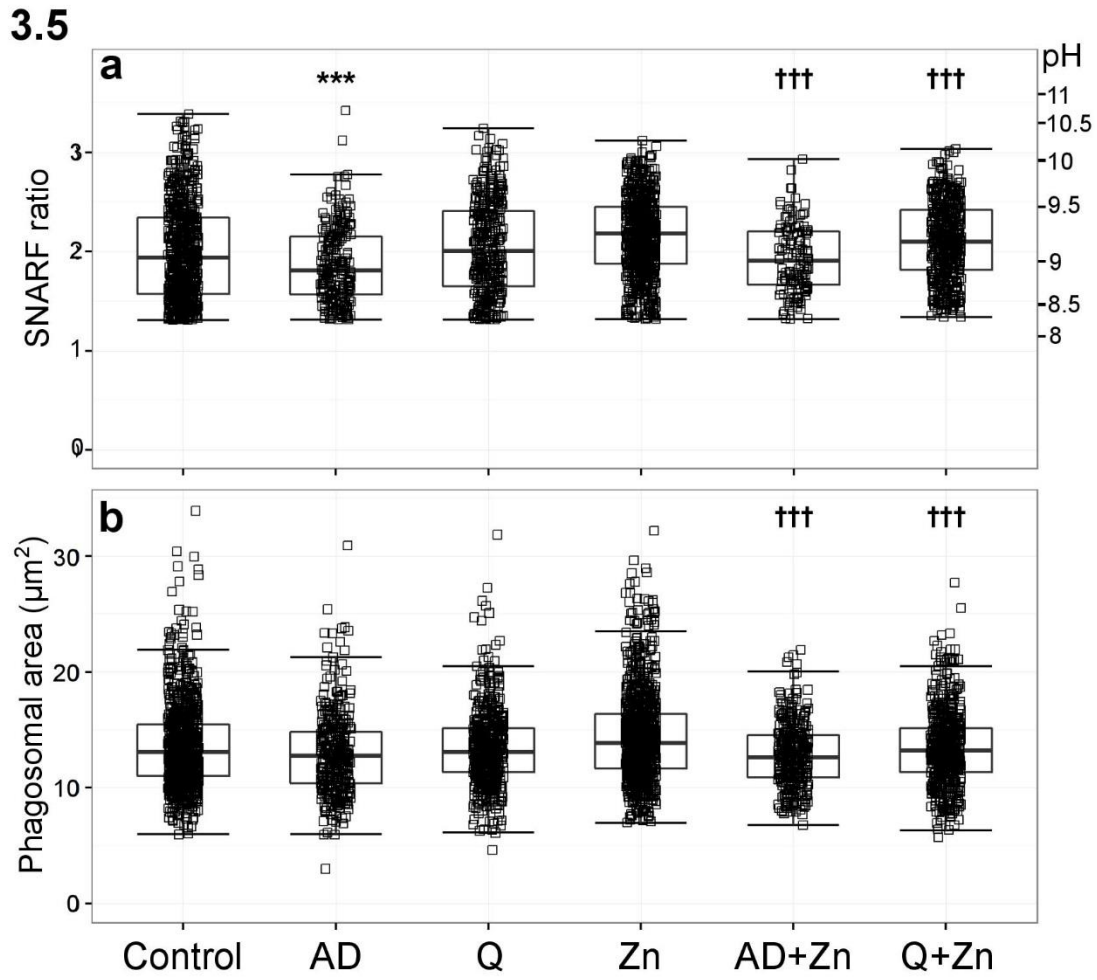

Figure 3.5 | Potassium channel inhibitors cause varying phagosomal effects (a-b). (**a**) *Quantification of phagosomal pH. The acidic phagosome population was removed with an SFR below 1.31*. (**b**) *Quantification of phagosomal area. Anandamide (20 mM), quinidine (100 mM), Zn (Zn^{2+} 100 mM), A+Zn (anandamide with Zn^{2+}), Q+Zn (quinidine with Zn^{2+}). Differences from control neutrophils: *p < 0.05, **p < 0.01, ***p < 0.001. Differences from neutrophils incubated with Zn^{2+}: †p < 0.05, ††p < 0.01, †††p < 0.001. For descriptive statistics see* ***table 3.5***.

Following the effects of the chloride channel inhibitors, and previous evidence of a K^+ conductance in the neutrophil phagosomes, I next looked at potassium channel blockers. Again, many selective inhibitors were tested, but it was two broad-spectrum inhibitors which produced the biggest changes in the system. These were anandamide and quinidine. Anandamide is an endocannabinoid, the amide of

arachidonic acid found in the brain (Maingret et al., 2001), but it is also a blocker of several potassium channels such as Shaker-related Kv1.2 K^+ channels (Poling et al., 1996), delayed activating K^+ channels (Oliver et al., 2004) and also calcium channels (Guo and Ikeda, 2004).

Table 3.5 | Phagosomal pH and area experimental measurements and statistics for potassium channel inhibitors

Phagosomal pH

N	Control	No. of points	Control median (SFR/pH)		Inhibitor	No. of points	Inhibitor median (SFR/pH)		*p*-value
3	Control	271	2.1	9.1	Anandamide	230	1.8	8.9	1.64×10^{-5}
4	Control	342	1.9	8.9	Quinidine	348	2.0	9.1	0.264
3	Zinc	308	2.2	9.2	Anandamide + zinc	128	1.9	9.0	1.12×10^{-6}
4	Zinc	372	2.2	9.2	Quinidine + zinc	461	2.1	9.1	3.88×10^{-6}

Phagosomal area

N	Control	No. of points	Control median	Inhibitor	No. of points	Inhibitor median	*p*-value
3	Control	336	12.8	Anandamide	346	12.8	0.085
4	Control	374	13.2	Quinidine	484	13.1	0.364
3	Zinc	392	14.2	Anandamide + zinc	324	12.6	6.11×10^{-14}
	Zinc	470	13.9	Quinidine + zinc	522	13.2	2.54×10^{-4}

N = number of experiments performed, no. of points describes the total number of individual measurements. The control and corresponding inhibitor medians are accompanied with the SFR and converted phagosomal pH.

Anandamide, similar to the chloride channel blockers, caused a slight reduction in phagosomal pH (**Fig. 3.5a**), from pH 9.1 to 8.9, and when combined with Zn^{2+}, from

pH 9.2 to 9.0 (see **table 3.5** for more descriptive statistics). Quinidine only significantly lowered pH with the treatment of Zn^{2+}. However, in contrast to the effect of the chloride channel blockers, anandamide and quinidine caused phagosomal shrinking - but only when applied with Zn^{2+} (**Fig. 3.5b**). Anandamide with Zn^{2+} was the most effective condition, causing a reduction in phagosomal area from 13.9 to 12.8 μm^2, while the median phagosomal area of quinidine with Zn^{2+} was 13.2 μm^2. This suggests that an osmotically active ion is being prevented from entering the phagosome.

3.6 The effect of ion channel inhibitors on the respiratory burst

Chloride channel inhibitors decrease the respiratory burst only when applied with zinc chloride

The respiratory burst was measured by recording oxygen tension in the extracellular medium of neutrophils phagocytosing opsonised heat-killed *Candida* (**Fig. 3.6**), to relate the changes in phagosomal pH and area to NADPH oxidase activity. It was not the inhibition of oxidase activity that lowered phagosomal pH, as neither drug had a statistically significant effect although the percentage mean oxygen consumed was slightly lower than control cells: DCPIB 91.8 ± 5.2% (SEM) of control activity, with FFA treatment 90.6 ± 1.5%. Treatment with Zn^{2+} lowered oxidase activity to 70.1 ± 4.2% (as previously reported (DeCoursey et al., 2003)), but the respiratory burst activity was considerably diminished when DCPIB and FFA were incubated with Zn^{2+}: DCPIB with Zn^{2+} induced a dramatic drop to 37.7 ± 7.9% (p = 0.01), while with FFA with Zn^{2+} only to 60.2 ± 5.1% (p = 0.038). These results suggest that blockage of HVCN1 and Cl^- channels together markedly impaired charge compensation.

Potassium channel inhibitors only significantly decrease the respiratory burst when applied with zinc chloride

With anandamide, again like the effect of DCPIB and FFA, phagocytosis-associated oxygen consumption was unaffected (it increased slightly to 111 ± 8.0%, p = ns, **Fig. 3.6**). Quinidine had a small but significant effect by lowering mean oxygen consumption to 80.3 ± 3.8% (p = 0.02). Zn^{2+} alone reduced respiration, and in combination with anandamide or quinidine it further decreased respiration, falling to 33.6 ± 6.4% ($p < 0.005$) and 42.9 ± 3.3% ($p < 0.01$) respectively. Anandamide and quinidine had different effects on phagosomal pH and area from the chloride channel inhibitors, but the effect on respiratory burst activity was similar, suggesting both chloride and potassium channels are involved in NADPH oxidase regulation.

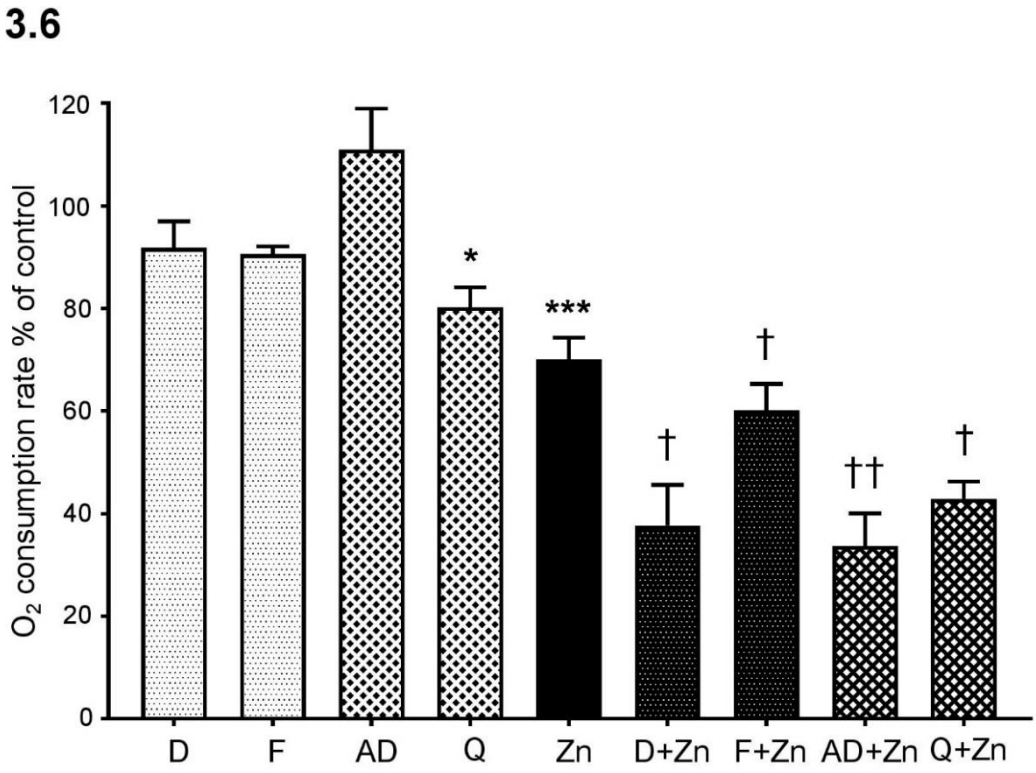

Figure 3.6 | The effect of ion channel inhibitors on human neutrophil oxygen consumption during phagocytosis of opsonised *Candida*. *Data are plotted as mean ± SEM, n=3, as a percentage of vehicle only oxygen consumption rate. Differences from control: *p < 0.05, ***p < 0.001. Differences from neutrophils incubated with Zn^{2+}: †p < 0.05, ††p < 0.01. D (DCPIB 20 μM), F (FFA 100 μM), AD (anandamide 100 μM), Q (quinidine 100 μM), and Zn (Zn^{2+} 100 μM).*

3.7 Mice lacking candidate chloride and potassium ion channels have broadly normal phagosomal environments

CLIC1 was very highly expressed in the human neutrophil composite mRNA datasets, scoring 95.92% relative expression, so the mouse model was tested. It has not been directly linked to neutrophil oxidase activity, but it is thought to be involved with lysosomal acidification in macrophages (Jiang et al., 2012) and dendritic cells (Salao et al., 2016). Single knockout *Clic1*$^{-/-}$ and double knockout *Hvcn1*$^{-/-}$/*Clic1*$^{-/-}$ neutrophils were compared to the wild-type (WT) or *Hvcn1*$^{-/-}$ controls (**Fig. 3.7.1**), but there was no significant difference in phagosomal pH. However, there was a noticeable decrease in phagosomal area in the *Hvcn1*$^{-/-}$/*Clic1*$^{-/-}$ neutrophils from a median area of 15.1 to 12.8 μm^2 (**Table 3.7**). The double knockout mice were used to put further pressure on the charge compensating system and are a much cleaner method than using zinc chloride.

KCC3, or solute carrier 12A6, was also significantly expressed in the neutrophil mRNA composite data (92.47%) and thought to be involved in neutrophil oxidase charge compensation as well as ClC3, which had a lower expression (35.36%). There were small variations in the phagosomal pH for *Hvcn1*$^{-/-}$/*Clc3*$^{-/-}$ but nothing grossly abnormal (**Fig. 3.7.2**). The phagosomal area was only slightly increased in the double knockout neutrophils by pH 11.1 to 11.2. No significant change in phagosomal pH or area was found for either *Kcc3*$^{-/-}$ or *Hvcn1*$^{-/-}$/*Kcc3*$^{-/-}$ (**Fig. 3.7.3**).

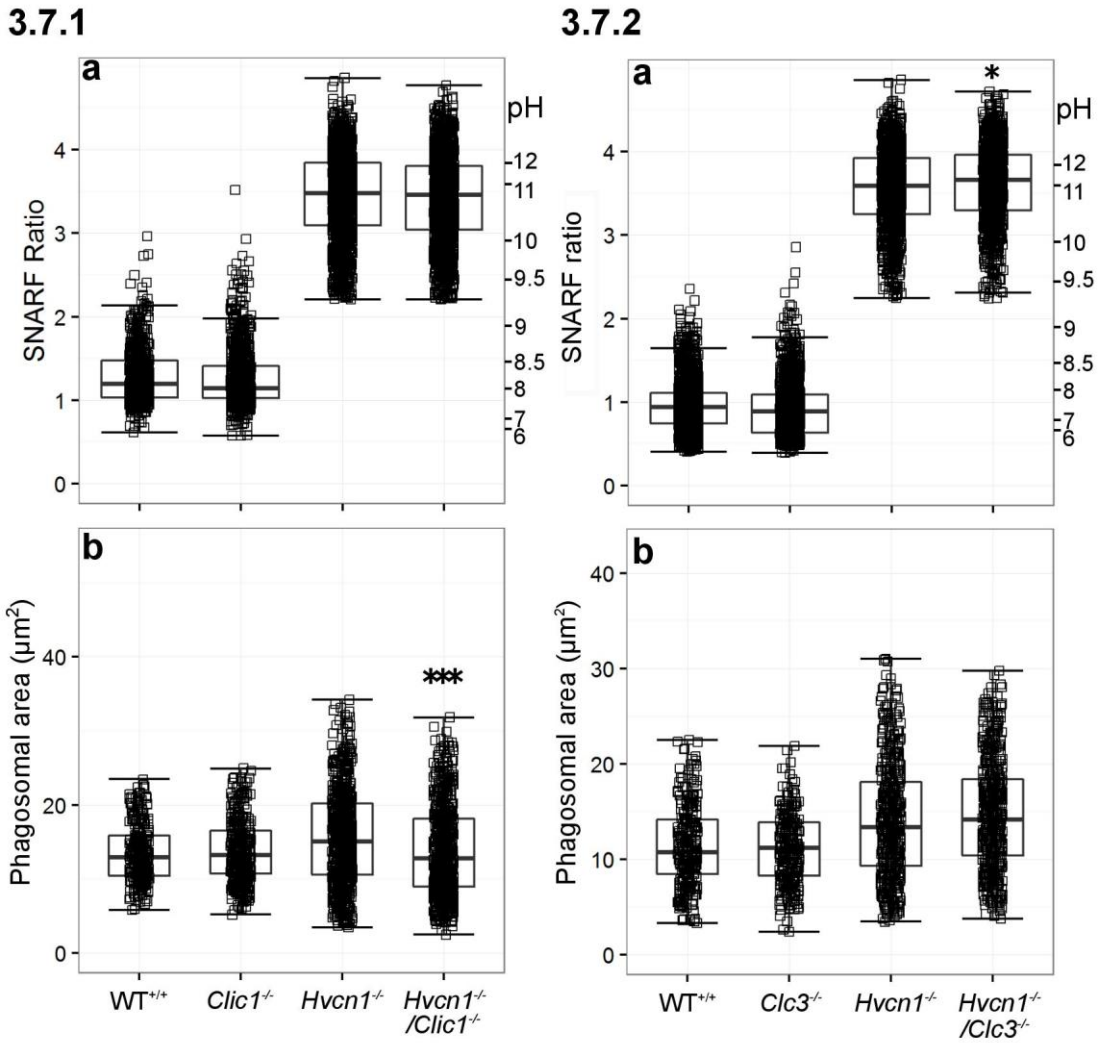

Figure 3.7.1 | Phagosomal pH and area measured in the single KO *Clic1*$^{-/-}$ nφ, and in the double KO *Hvcn1*$^{-/-}$/*Clic1*$^{-/-}$ nφ (a-b). (**a**) *Quantification of phagosomal pH. The acidic phagosome population was removed with SFR below 2.20 for the Hvcn1*$^{-/-}$ *and double KO nφ.* (**b**) *Quantification of phagosomal area. Individual points are plotted as small boxes with overlaying median and interquartile range. Detailed statistics are found in table 3.7, ***p < 0.001 for double KO compared with Hvcn1*$^{-/-}$ *nφ.*

Figure 3.7.2 | Phagosomal pH and area measured in the single KO *Clc3*$^{-/-}$ nφ, and in the double KO *Hvcn1*$^{-/-}$/*Clc3*$^{-/-}$ nφ (a-b). (**a**) *Quantification of phagosomal pH. The acidic phagosome population was removed with SFR below 2.23 for the Hvcn1*$^{-/-}$ *and double KO nφ.* (**b**) *Quantification of phagosomal area. Individual points are plotted as small boxes with overlaying median and interquartile range. Detailed statistics are found in table 3.7, *p < 0.05 for double KO compared with Hvcn1*$^{-/-}$ *nφ.*

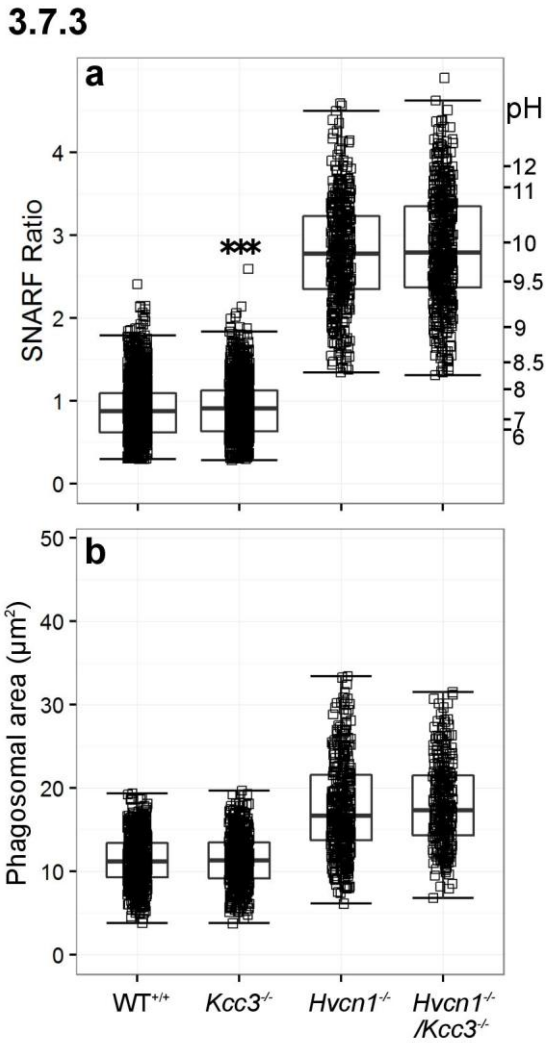

Figure 3.7.3 | Phagosomal pH and area measured in the single knockout *Kcc3*$^{-/-}$ nφ, and in the double knockout *Hvcn1*$^{-/-}$*lKcc3*$^{-/-}$ nφ (a-b). (**a**) *Quantification of phagosomal pH. The acidic phagosome population was removed with SFR below 1,31 for the Hvcn1*$^{-/-}$ *and double KO nφ.* (**b**) *Quantification of phagosomal area. Individual points are plotted as small boxes with overlaying median and interquartile range. Detailed statistics are found in table 3.7, ***p < 0.001 for Kcc3*$^{-/-}$ *compared with WT nφ.*

Table 3.7 | Statistics of phagosomal pH and area for the knockout mouse models

Phagosomal pH

N	Control	No. of points	Control median (SFR/pH)		Knockout (KO)	No. of points	KO median (SFR/pH)		*p*-value
3	WT	589	1.2	8.0	*Clic1*$^{-/-}$	780	1.2	8.0	0.598
3	*Hvcn1*$^{-/-}$	1594	3.5	10.8	*Hvcn1*$^{-/-}$ */Clic1*$^{-/-}$	1596	3.5	10.8	0.174
3	WT	1269	0.9	7.5	*Clc3*$^{-/-}$	1116	0.90	7.5	0.268
2	*Hvcn1*$^{-/-}$	1130	3.6	11.1	*Hvcn1*$^{-/-}$/ *Clc3*$^{-/-}$	1157	3.7	11.2	0.020
4	WT	1637	0.9	7.4	*Kcc3*$^{-/-}$	1340	0.9	7.5	2.0×10^{-4}
3	*Hvcn1*$^{-/-}$	383	2.8	9.8	*Hvcn1*$^{-/-}$ */Kcc3*$^{-/-}$	472	2.8	9.9	0.165
3	WT	898	1.0	7.8	*Kcnj15*$^{-/-}$	727	1.1	7.9	0.016
3	WT	371	1.0	7.8	*Trpm2*$^{-/-}$	399	1.0	7.8	0.087
1	*Hvcn1*$^{-/-}$	118	1.9	9.0	*Hvcn1*$^{-/-}$ */Trpm2*$^{-/-}$	82	1.8	8.9	0.120

Phagosomal area

N	Control	No. of points	Control median	Knockout (KO)	No. of points	KO median	*p*-value
3	WT	266	12.9	*Clic1*$^{-/-}$	346	13.2	0.167
3	*Hvcn1*$^{-/-}$	696	15.1	*Hvcn1*$^{-/-}$ */Clic1*$^{-/-}$	650	12.8	6.7×10^{-7}
3	WT	281	10.8	*Clc3*$^{-/-}$	273	11.2	0.650
2	*Hvcn1*$^{-/-}$	549	13.4	*Hvcn1*$^{-/-}$ */Clc3*$^{-/-}$	570	14.2	0.109
3	WT	445	11.2	*Kcc3*$^{-/-}$	458	11.3	0.469
3	*Hvcn1*$^{-/-}$	389	16.7	*Hvcn1*$^{-/-}$ */Kcc3*$^{-/-}$	287	17.3	0.554
3	WT	633	9.9	*Kcnj15*$^{-/-}$	387	10.4	0.003
3	WT	162	11.7	*Trpm2*$^{-/-}$	208	11.0	0.569
1	*Hvcn1*$^{-/-}$	78	17.1	*Hvcn1*$^{-/-}$/ *Trpm2*$^{-/-}$	39	18.7	0.830

N = number of experiments, no. of points describes the total number of individual experiments. *The control and corresponding knockout (KO) medians are accompanied with the SFR and converted phagosomal pH.*

3.8 Other knockout mouse models have varying phagosomal pH and area

The composite data motivated studying several different genes of interest. *Kcnj15* is a potassium channel that was highly expressed in table 3.3 at 93.69%. Only neutrophils from the single knockout mouse model was tested, but they did exhibit a small increase in phagosomal pH by 0.1 and in the phagosomal area – from 9.9 to 10.4 μm^2 (**Fig. 3.8**). *Trpm2* was not expressed in the data sets but was tested because of its link to phagocyte ROS regulation (Di et al., 2012, 2017). It did not seem to influence either phagosomal pH or area, even with the HVCN1 channel removed.

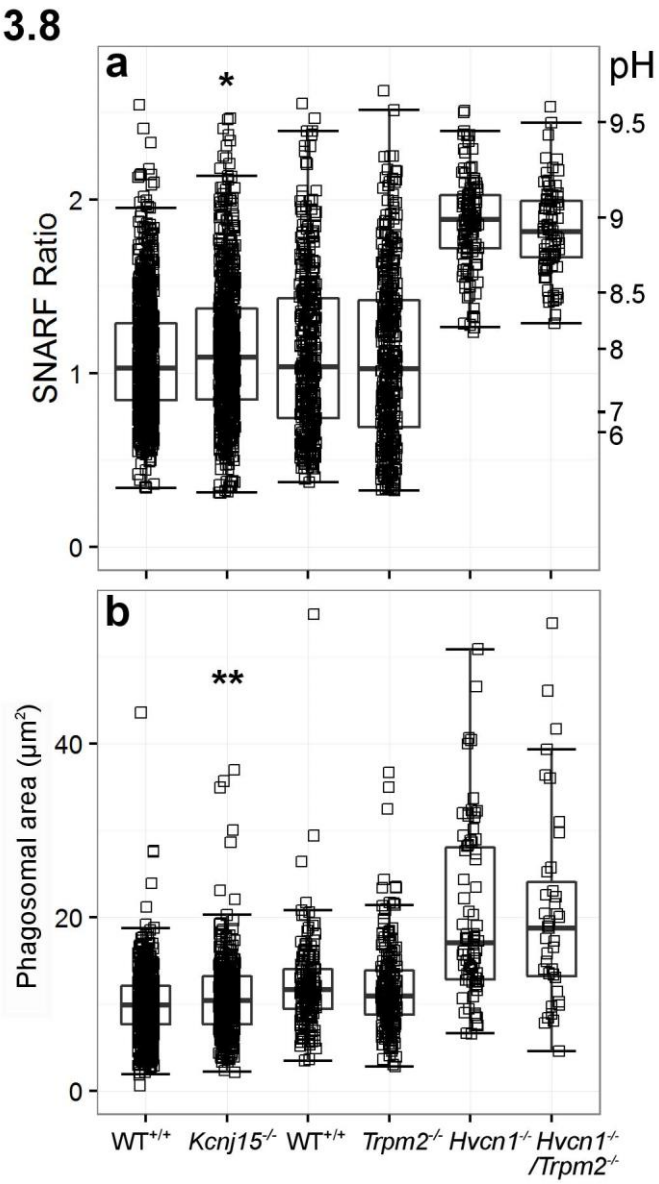

Figure 3.8 | Phagosomal pH and area measured in *Kcnj15*$^{-/-}$ and *Trpm2*$^{-/-}$ mice models (a-b).

(a) *Quantification of phagosomal pH. The acidic phagosome population was removed with SFR below 1.197 for the Hvcn1*$^{-/-}$ *and double KO nφ.* (**b**) *Quantification of phagosomal area. Individual points are plotted as small boxes with overlaying median and interquartile range. Detailed statistics are found in table 3.7, **p < 0.01, *p < 0.05 for Kcnj15*$^{-/-}$ *compared with WT nφ.*

3.9 Respiratory burst activity in KO mouse neutrophils

Due to low mice numbers, investigations into NADPH oxidase activity using the Seahorse apparatus was limited to a few mouse models. This involved adding neutrophils to 24 well plates and measuring the rate of oxygen concentration in the extracellular medium for 15 min after addition of opsonised heat-killed *Candida* or PMA. Oxygen tension is measured by oxygen-specific sensors without the use of any other chemical reagents. Neutrophils were elicited from the peritoneal cavity after injection with thioglycolate for collection of sufficient quantities of cells with the assistance of Sabrina Pacheco.

Moreland and colleagues have previously found that *Clc3*$^{-/-}$ neutrophils NADPH oxidase-induced respiration to be severely reduced with phagocytosis of opsonised zymosan and by stimulation with PMA (Moreland et al., 2006). This study was unable to reproduce those effects, as oxygen consumption induced by both PMA and the phagocytosis of heat-killed *Candida* in the knockout neutrophils was no different from WT neutrophils (*n*=3, **Fig. 3.9**).

However, there was confirmation that the *Kcc3*$^{-/-}$ neutrophils had abnormal oxidase activity, first described by Sun and co-workers (Sun et al., 2012). Oxygen consumption with phagocytosis dropped to roughly 63 ± 6.6% of WT levels (mean ± SEM, *n*=3), that was repeated with PMA (~53%) but was only carried out once.

NADPH oxidase activity in *Hvcn1*$^{-/-}$ neutrophils was approximately 53.6 ± 9.6% when stimulated with PMA, and 49.2 ± 4.7% with phagocytosis, repeating the findings of about 50% activity of WT neutrophils found by other researchers (Ramsey et al., 2009). Interestingly, the respiratory burst of *Hvcn1*$^{-/-}$/*Clic1*$^{-/-}$ neutrophils was greater than single knockout *Hvcn1*$^{-/-}$ neutrophils. It rose to 85.9 ± 14.1% with PMA stimulation, and 63.7 ± 3.8% after phagocytosis of *Candida*. This is in contrast to the

results published by Jiang (Jiang et al., 2012), who found that the respiratory burst initiated by serum-opsonised zymosan was about 25% lower in Clic1$^{-/-}$ macrophages.

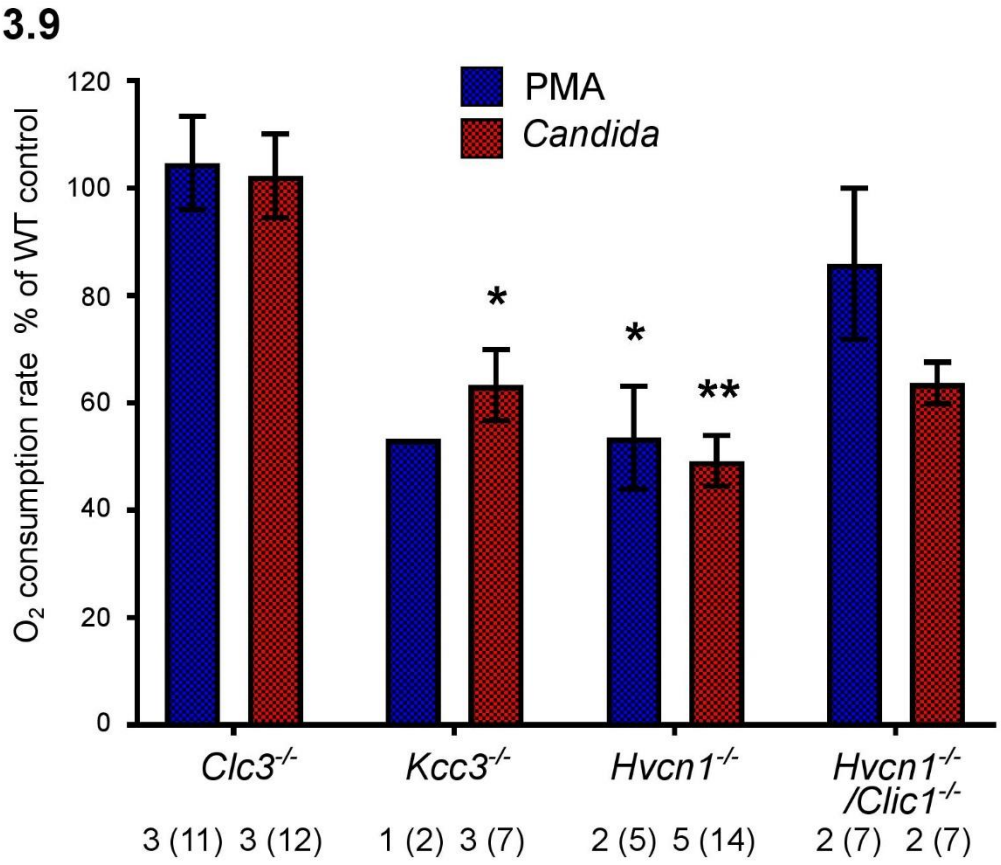

Figure 3.9 | Measuring oxygen consumption in *Clc3*, *Kcc3* and *Hvcn1* with *Hvcn1/Clic1* deficient mice peritoneal nφ induced by PMA and serum-opsonised *Candida*. *Oxygen consumption rate (OCR) is presented as a relative percentage of the wild-type control (mean ± SEM). The numbers below indicate the number of separate experiments with number of intra-experimental replicates in brackets. Differences from WT nφ within each experiment: *p<0.05, **p<0.01, ***p<0.001.*

3.10 Phagosomal environments of mice with non-functional LRRC8A

It was mentioned earlier that DCPIB is a purported inhibitor of the ICl_{swell} current, and it was recently identified after a lengthy investigation that LRRC8A is a fundamental subunit of the channel (VRAC) transmitting the current. A colleague in the group,

Philippe Behe, acquired a mouse model named *ébouriffé* (*ebo*), after their abnormally wavy hair, that has a truncated Lrrc8a protein that severely reduced VRAC activity (Platt et al., 2017). I was luckily able to use some of the *ebo*/*ebo* mice to study their phagosomal environments and oxidase activity.

Using the same methods as before, I found no significant differences in phagosomal pH or area between WT and *ebo*/*ebo* neutrophils (**Fig. 3.10a and b**). There also was no noticeable defect in phagocytosis. Because of their short lifespan and difficulty to breed due to poor fertility, it was not possible to gather enough cells for assessment of oxidase activity by Seahorse apparatus; oxygen consumption with phagocytosis of opsonised *Candida*. Instead, their respiratory burst was measured indirectly by hydrogen peroxide (H_2O_2) produced by stimulation with PMA, a potent oxidase agonist, which required much fewer cells. The *ebo/ebo* neutrophils were found to have an almost identical activity to WT neutrophils (**Fig. 3.10c and d**), both in amount and rate of H_2O_2-induced fluorescence.

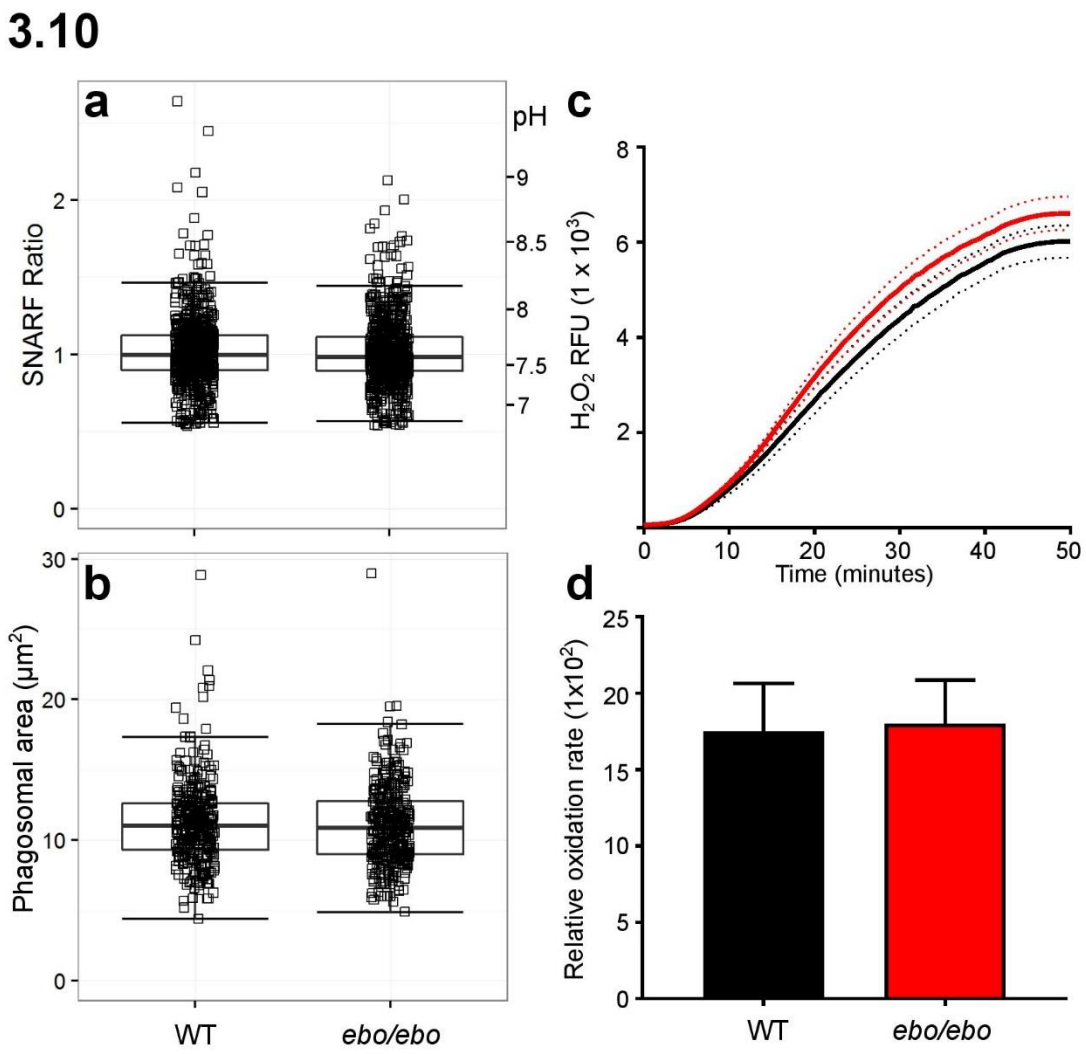

Figure 3.10 | The *ebo/ebo* mice have similar phagosomal environments to WT mice (a-d). (**a**) *Distribution of pH in phagosomes of heat-killed SNARF-labelled Candida by WT and ebo/ebo nφ (In total 733 and 735 particles measured respectively).* (**b**) *Distribution of phagosomal areas in nφ containing individual Candida in WT and ebo/ebo nφ (320 and 354 phagosomes measured respectively). Boxplots of the median and interquartile range are overlaid on small boxes describing individual measurements.* (**c**) *Time course of changes in NADPH oxidase activity after stimulation with PMA measured as H_2O_2-induced fluorescence (RFU), data are plotted as mean ± SEM (dashed lines) in WT (black) and ebo/ebo (red).* (**d**) *Relative oxidation rates of* (**c**). *For all experiments n=3.*

3.11 Neutrophil phagosomal pH and area from cystic fibrosis patients appear normal

The phagosomal environments of two cystic fibrosis (CF) patients with the ΔF580 mutation were compared with neutrophils from healthy controls. One study has reported abnormal neutrophil oxidase activity in CF patients (Brockbank et al., 2005). As shown in **figure 3.11**, the pH and areas in recorded CF neutrophils had no significant differences from control neutrophils, even when the proton channel was blocked with zinc treatment.

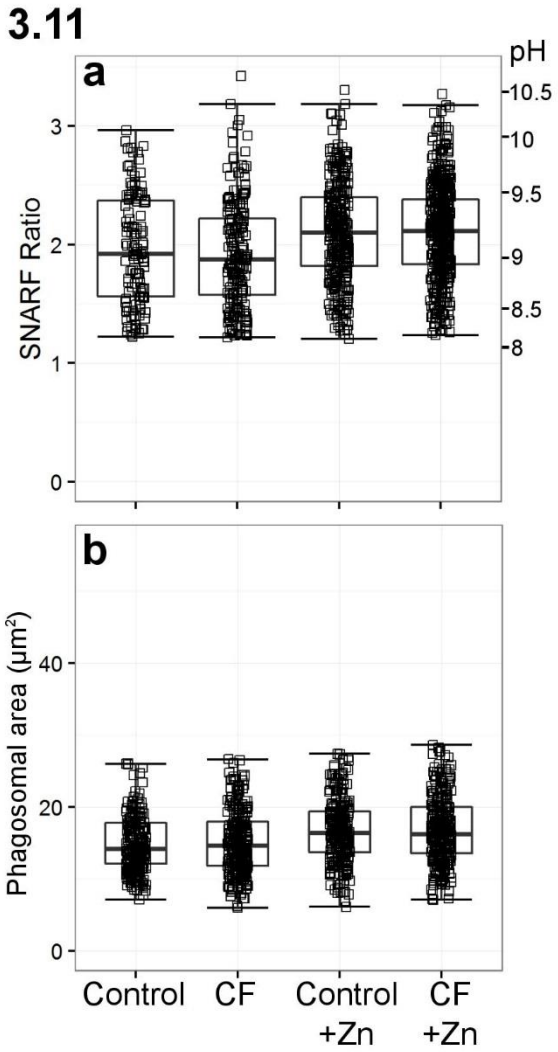

Figure 3.11 | Phagosomal pH and area from two patients with cystic fibrosis (CF) with and without 100 µM zinc. (**a**) *Quantitation of phagosomal pH, acidic phagosomes with an SFR value less than 1.2 were excluded. Between 120 and 440 phagosomes were counted for each condition.* (**b**) *Quantitation of phagosomal area, between 238 and 304 phagosomes were measured for each condition. No differences were observed between the healthy controls and the patients' phagosomal parameters. Both patients were tested only once.*

3.12 Discussion

This chapter documents a screening process to identify ion channels involved in neutrophil phagosomal regulation, predominantly through the recording of ionic flux, by phagosomal pH and area, and NADPH oxidase activity. Based on prior research, it is known that more than one ion channel compensates the negative charge generated by NADPH oxidase activity, because when the proton channel HVCN1 is knocked out or inhibited there is still about 50% residual oxidase activity. The removal of this channel also causes a change in phagosomal pH and area, demonstrating that they are both influenced by oxidase activity.

To further investigate the influence of the oxidase on phagosomal pH, I started with measuring human neutrophil phagosomal pH when treated with increasing doses of the oxidase inhibitor DPI. As has been found before, inhibition of NOX2 with DPI caused phagosomal acidification; with increasing concentration of DPI the phagosomal pH and hydrogen peroxide production were decreased. But it is crucial to note that at the smallest dose, 25 nM, the phagosomal pH was statistically different from that of the control condition, but the oxidase activity at that dose was not. This provides evidence of at least one minor channel that is involved in pH regulation, but the oxidase can generally function without it.

The method chosen to identify the ion channels contributing to charge compensation in neutrophils was to examine the effects of known channel inhibitors, and then the neutrophils of knockout mice and patients with channelopathies. First, an analysis of mRNA neutrophil data was undertaken to highlight potential channels of interest. The mRNA was of resting whole neutrophils, not of isolated phagosomes, so there may be ion channels identified that are not involved in phagosomal regulation. There are proteomic human neutrophil studies but they are few, and some do not detect expression of all the NADPH oxidase subunits which act as control proteins (Burlak,

2005). But in the currently available studies, there is expression of some ion channels or transporters in samples taken from phagosomes or neutrophil granules, including potassium channels KCNH7 and KCNAB1 in phagosomes (Burlak, 2005) and anion channels SLC4A1, VDAC-1,2 and -3 in granules (Lominadze et al., 2005). In another study, they found protein expression of potassium channels KCNA5, KCNB1, KCNG2. KCNJ11, KCNS1, and KTD17, SLC4A1 again, along with multiple other members of the solute carrier family found variously in the secretory vesicles and plasma membrane (Uriarte et al., 2008).

Most of the studies in neutrophils have looked at Cl^- flux partly because neutrophils have a relatively high cytoplasmic Cl^- concentration (~80 mEq (Simchowitz and De Weer, 1986)) compared to other innate cells. After stimulation by soluble agonists (Yasuaki et al., 1993) or phagocytosis (Busetto et al., 2007), they release large quantities of Cl^- into the extracellular medium (Menegazzi et al., 1999), which is thought to adjust for phagocytosis-induced cellular swelling (Stoddard et al., 1993).

Another widely held function of neutrophil Cl^- is to provide a substrate for the myeloperoxidase (MPO) for the generation of microbicidal hypochlorous acid (HOCl) (Klebanoff et al., 2013). For Cl^- to be used in the MPO system, it would need to be imported into the phagosome in the same direction as electrons from the NADPH oxidase, and hence against a robust electrochemical gradient. The potassium/chloride ion co-transporter *Kcc3* could potentially fill this role, but it would not be directly charge compensating as it would have no net change. Nevertheless, it has been implicated in neutrophil NADPH oxidase activity (Sun et al., 2012), which was also found in these respiratory burst experiments. Additionally, MPO has a pH optimum of 6, while the neutrophil phagosome is around pH 8.5-9. However, this is only in the first 30-40 minutes after phagocytosis; other researchers report more acidic phagosomes much later (Chiswick et al., 2015) which then may accommodate MPO activity.

It is important to consider chloride channels on neutrophil granule membranes, as their membrane will fuse with the phagosomal membrane when they degranulate. Neutrophil granules are maintained in highly acidic conditions through the action of the vacuolar ATPase proton channel (V-ATPase) (Gilman-Sachs et al., 2015). The movement of protons into the granules necessitates movement of negative charge in the same direction, thought to be accomplished by Cl^- movement. Macrophages also contain acidic endosomes where Clic1 has found to be essential for correct lysosomal and phagosomal pH (Jiang et al., 2012; Sakurai et al., 2012).

Table 3.12.1 | Summary of the effects of specified compounds with their reported sites of activity, and the general effect on phagosomal pH and area in human neutrophils

Compound	Sites of inhibition (specific channel/transporter or conductance)	Sites of activation	Effect on neutrophils compared to control	
				+ Zn^{2+} 100 µM
DCPIB	ICl_{swell} (Decher et al., 2001) ,Kir (Deng et al., 2016), KCC3 (Adragna et al., 2015a).	TREK-1,-2 (Minieri et al., 2013).	↓ pH	↓ pH ↑ area
FFA	ICl_{swell} (Jin et al., 2003), Ca^{2+} activated Cl^- (Liantonio et al., 2007; Oh et al., 2008), TRP (Guinamard et al., 2013).	TREK-1,-2 (Takahira et al., 2005)	↓ pH ↑ area	↓ pH
Anandamide	TASK-1, -3 (2P K channels) (Maingret et al., 2001), Kv channels (Poling et al., 1996).		↓ pH	↓ pH ↓ area
Quinidine	Na^+ channels (Hondeghem and Matsubara, 1988), KCa channels (Iwatsuki and Petersen, 1985), Kv channels (Yatani et al., 1993), 2P K channels (Patel et al., 2000), ICl_{swell} (Voets et al., 1996), KCNH1,-5 (Wulff and Zhorov, 2008)			↓ pH ↓ area

In line with the theory that Cl^- is involved in the neutrophil phagosomal dynamics, the classical broad-spectrum Cl^- channel blockers DCPIB and FFA both produced phagosomal acidification without inhibiting oxidase activity. This implies that they were preventing the efflux of Cl^- from the phagosome. Both these inhibitors induced phagosomal swelling when treated with zinc, a proton channel blocker, more so than zinc alone and despite diminished oxidase activity. It suggests that the additional swelling resulted from the influx of non-proton cations, K^+ and/or Na^+.

Although primarily thought of as blockers of Cl^- channels, DCPIB and FFA are rather non-specific – as detailed in **table 3.12.1**. As aforementioned, DCPIB was first described as an inhibitor of the swell-activated chloride current $I_{Cl,swell}$ (Decher et al., 2001). However, other DCPIB-sensitive ion channels have been reported. Sites of inhibition include inwardly rectifying K^+ channels (Deng et al., 2016), and the K^+/Cl^- co-transporter KCC3 (Adragna et al., 2015b), while it has been shown to activate the two-pore domain (2P) K^+ channels TREK-1 and TREK-2 (Minieri et al., 2013). There is evidence that it does not affect CFTR (Decher et al., 2001), another potential pathway for neutrophil Cl^- movement. FFA also blocks $I_{Cl,swell}$ (Jin et al., 2003), CFTR (McCarty et al., 1993) (used at a higher concentration than used in these studies), CLIC1 (Liantonio et al., 2007) (**Table 3.12.2**) and calcium-activated Cl^- channels (Oh et al., 2008), and some TRP channels (Guinamard et al., 2013). Both FFA and DCPIB apparently activate 2P K^+ channels TWIK-1 and TWIK-2 (Takahira et al., 2005). Owing to the vast array of non-specific sites affected by DCPIB and FFA, it was necessary to attempt to pinpoint their observed effects by removing individual channels.

While there was no observed impairment of phagosomal pH in *Clic1*$^{-/-}$ or *Hvcn1*$^{-/-}$/*Clic1*$^{-/-}$ bone marrow-derived neutrophils, there was a slight but significant decrease in phagosomal area in the double knockout neutrophils compared to the *Hvcn1*$^{-/-}$ controls. Surprisingly, oxidase activity was also raised in the double knockout

neutrophils, but it may need more experimental repeats to prove statistically significant. If Clic1 helps to compensate for V-ATPase activity by matching proton influx with chloride influx on granule and phagosomal membranes, then its deletion

Table 3.12.2 | Summary of the KO mouse and patient neutrophil data with reported chemical inhibition or activation

Gene	Effect on neutrophils compared to control	+ *Hvcn1*$^{-/-}$/Zn^{2+}	Classical Chemical inhibitors
Clic1	None	↓ area	FFA (Liantonio et al., 2007)
Clc3	None	↑ pH	DCPIB (Liang et al., 2014)
Hvcn1	↑ pH ↑ area ↓ NOX2 activity	-	Zinc chloride (Morgan et al., 2009)
Kcc3	↑ pH	↓ NOX2 activity	DCPIB (Adragna et al., 2015a)
Kcnj15	↑ pH ↑ area	-	?
Lrrc8a	None	-	DCPIB (Decher et al., 2001), FFA (Jin et al., 2003), quinidine (Voets et al., 1996)
Trpm2	None	None	?
CFTR	None	None	FFA (McCarty et al., 1993) (at higher concentrations)

might reduce water influx, and consequently phagosomal area. Despite finding an impairment of oxidase activity in *Kcc3*$^{-/-}$ neutrophils, there were no alterations in phagosomal pH or area. Perhaps the channel is directly involved with oxidase regulation separately from charge compensation.

It was fortunate to examine neutrophils from the recently generated *ebo/ebo* mice in which LRRC8A is not functional (Platt et al., 2017), as DCPIB, FFA, and quinidine have reported effects on its function (see **table 3.12.1 and 3.12.2**). This protein is an essential component of ICl_{swell} or the volume-regulated anion channel (VRAC) (Jentsch, 2016). Although it has been found to be important in T cell development (Kumar et al., 2014), mice deficient in the channel had normal neutrophil phagosomal pH and area and oxidase activity.

Two other channels have been proposed as conducting Cl^- into the phagosome, CFTR (Painter et al., 2010) and CLC3 (Nunes et al., 2013; Wang and Nauseef, 2015). Neutrophils are reportedly abnormal in patients with cystic fibrosis (CF), such as reduced phagocytosis (Morris et al., 2005) which contributes to the disease through improper clearance of opportunistic pathogens. *Pseudomonas aeruginosa* is a common CF infection and has been shown *in vitro* that neutrophils have impaired killing of the bacteria (Painter et al., 2008). However, the experiment was conducted in Cl^- free extracellular medium for the first 10 minutes, and the effect of such treatment on CF cells was not established. The results described in this chapter in CF patients with the common ΔF508 mutation were not tested in enough patients to reach a conclusive result, but they argue against an essential role for this channel in the charge compensation of the oxidase, as there were no abnormalities in phagosomal pH or area even when treated with zinc. There was also no evidence of significant levels of expression of CFTR in the archival neutrophil mRNA expression data, but there is evidence for its expression in neutrophils, albeit at very low levels (McKeon et al., 2010; Painter et al., 2006).

Moreland and co-workers have observed that *Clc3*$^{-/-}$ neutrophils displayed reduced NADPH oxidase activity in response to opsonised zymosan and after PMA stimulation (Moreland et al., 2006) and thus inferred participation of CLC3 in charge neutralisation. Experiments conducted within this chapter found oxidase activity in *Clc3*$^{-/-}$ neutrophils to be entirely normal after stimulation with both opsonised Candida and with PMA. However, there were slight but statistically significant abnormalities in phagosomal pH and area. The *Clc3*$^{-/-}$ neutrophils were more acidic than wild-type neutrophils by a minimal difference – in comparison to the large drop in pH elicited by DCPIB and FFA in human neutrophils. In contrast, *Hvcn1*$^{-/-}$/ *Clc3*$^{-/-}$ phagosomal pH was more alkaline than the *Hvcn1*$^{-/-}$ neutrophils, but again by a small margin. The phagosomal area was slightly higher in the double knockout cells. If we consider these results as relevant, it indicates that by removing this channel, more protons are entering the phagosome and thus lowering the pH. When both the proton and chloride channels are removed, the pH increases as other non-proton ions are compensating the oxidase-induced charge. This compensatory ion could be potassium, an osmotically active ion that draws in water, and so increases phagosomal area. There are chemical inhibitors of CLC3 such as 5-nitro-2-(3- phenylpropylamino) benzoic acid (NPPB) and phloretin (Gaurav et al., 2015), but they must be used with caution. NPPB acts as a protonophore (Lukacs et al., 1991), which would decrease phagosomal pH irrespective of the effect on channel activity, while phloretin is known to inhibit degranulation (Shefcyk et al., 1983).

The other potential charge compensating ion of interest potassium, as there is evidence that phagosomal K^+ influx is driven by activity of the oxidase (Reeves et al., 2002) and the enhanced swelling of the phagosome induced by DCPIB and FFA described above could reflect the augmented entry of this ion induced by these agents when Cl^- efflux is replaced by K^+ influx. The broad-spectrum cation blockers, anandamide and quinidine, did change phagosomal conditions. Anandamide caused

a decrease in both phagosomal pH and area, without inhibiting oxidase activity, suggesting that it was blocking the influx of non-proton cations. Their effects were exaggerated by the presence of zinc which led to a halving of oxygen consumption. In contrast, quinidine reduced phagosomal volume, but not pH, and reduced respiration by about 20%.

Anandamide and quinidine have some overlapping target channels (**table 3.12.1**). Anandamide is known to inhibit the 2P K^+ channels TASK-1 (KCNK3) (Maingret et al., 2001) and TASK-3 (KCNK9) (Andronic et al., 2013), and some voltage-dependent K+ channels (Moreno-Galindo et al., 2010; Poling et al., 1996). Of particular interest is the claim made that NOX4 modulates TASK-1 activity in oxygen-sensing cells (Lee et al., 2006). Perhaps it is similarly modulated by NOX2 in neutrophils. Quinidine is a relatively non-specific blocker of both Na^+ (Hondeghem and Matsubara, 1988) and K^+ channels (calcium-activated (Wrighton et al., 2015; Yatani et al., 1993)), voltage-gated (Attali et al., 1997; Tatsuta et al., 1994), and two-pore-domain (Andronic et al., 2013; Patel et al., 2000; Wulff and Zhorov, 2008), as well as the aforementioned swell activated chloride current (Voets et al., 1996). Unfortunately, the wide variety of target sites of inhibition or activation did not assist in identifying single charge compensating channels.

Once again, this led to knock-out mice lacking specific K^+ channels being examined. KCNJ15 was very highly expressed in the composite human neutrophil mRNA data (93.7%), but there is no reported evidence in neutrophil biology. Instead, they are known to act as a vasodilator and assist in water absorption in renal tubules (Huang et al., 2007). Further investigation is required to work out how this function correlates with the increased phagosomal pH and area found in *Kcnj15*$^{-/-}$ neutrophils. Transient receptor potential (TRP) channels are selective for cations, a few of which have been associated with neutrophil function, including TRPC1 (Lindemann et al., 2015) and TRPM2 (Heiner et al., 2005). TRPM2 has been described as a negative feedback

mechanism to prevent excess ROS produced by the NADPH oxidase in phagocytes by regulating phagosomal membrane depolarisation through Ca^{2+} and Na^{+} ionic movement (Di et al., 2012). There were, however, no observed changes in these experiments in the phagosomal pH and area compared to wildtype mice or in the double knockout neutrophils.

In summary, the broad-spectrum channel blockers, DCPIB and FFA, anandamide and quinidine, affected phagosomal physiology by altering pH and cross-sectional area in different ways. DCPIB and FFA are largely considered to block Cl^{-} channels and their effects were consistent with charge compensation by the efflux of this ion from the phagosome. In contrast, anandamide and quinidine are largely considered to be blockers of K^{+} channels and their effects were consistent with the oxidase induced flux of K^{+} into the phagosome. Even so, these inhibitors are not highly channel-specific. The studies into knockout mouse models require further investigations to confirm the mechanisms involved in phagosomal charge compensations. It is especially difficult to pin down individual channels, as the charge they are compensating for has been calculated to be 5% for both Cl^{-} and K^{+} flux (Murphy and DeCoursey, 2006), and there might be considerable redundancy in the system. For example, the loss of a channel might result in exaggerated membrane depolarisation to a level that would then open another voltage-gated channel that would not usually participate in physiological charge compensation. A method of detection more sensitive may be required to pick up on smaller changes, such as measuring phagosomal pH kinetically rather than as an unsynchronised endpoint. Further phagosomal proteomic experiments would help identification of ion channels present. However, the effects of the four stated ion channel blockers give reason to suggest that control of ion flux is essential for phagosomal pH and area regulation in neutrophil phagosomes. This provides an essential foundation for further, more informative experiments.

Chapter Four: Characterising the Hoxb8 immortalised myeloid cell line

4.1 Background and aims

For functional genetics studies in neutrophils, “knockout” or “knockin” mouse models have been the model of choice for many researchers. The advantages include relatively high gene homology with humans, and with the newer molecular techniques available the ability to manipulate the mouse genome has become relatively straightforward and affordable. There are accompanying frustrations with using primary mouse neutrophils which places major restrictions on the types of experiments that can be performed. The major problem results from the fact that neutrophils are terminally differentiated cells, which have a relatively short life *in vitro*, this means that they are very difficult genetically modify stably. It is also difficult to isolate large numbers of neutrophils from mice, so several mice are needed for each experiment, which leads to high costs for their housing and upkeep.

A way around these problems is the use of cell lines, such as the human HL60 line. These cells can be expanded indefinitely in culture and have been shown to have similar features to primary neutrophils (Teufelhofer *et al.*, 2003), although HL60 neutrophils cannot generate specific granules (Pullen & Hosking, 1985). Most cell lines origins are from cancers, which have inherent differences with primary cells and can be genetically unstable. Additionally, there are few cell lines to model neutrophil biology.

This chapter sets out to characterise a murine neutrophil model; the Hoxb8 immortalised myeloid cell system, that was first developed in 2006 by a team in Boston, USA (Wang *et al.*, 2006). Hoxb8 is a transcription factor that is specific for

myeloid cells with master control functions; when it is expressed, it maintains the cell in a self-renewing myeloid progenitor state. When it is switched off, the cell undergoes differentiation. By fusing an estrogen receptor promoter to Hoxb8, its expression can be controlled by the presence of estrogen in the cell medium. The immortalised progenitor cell lines are made by isolating bone marrow progenitors from mice and retrovirally transduced with the ER-Hoxb8 construct and maintained in medium containing estrogen and stem cell factor (SCF) which generates cells termed SCF estrogen-receptor (ER) Hoxb8 cells. They also found that if SCF was swapped for granulocyte-macrophage colony stimulating factor (GM-CSF), the majority of cells differentiated into macrophages after estrogen removal. Only SCF ER-Hoxb8 cells are used in all described experiments, so for conciseness, they will be referred to as simply Hoxb8 cells. The technique is gaining increasing popularity across many labs, although its use as a substitute for primary neutrophils is still being evaluated.

Here I will test the use of the Hoxb8 derived neutrophils in the model system described in the previous chapter - the *Hvcn1*$^{-/-}$ neutrophils – against wild-type (WT) cells with the following aims:

- Generate an immortalised wild-type Hoxb8 cell line using retroviral infections
- Optimise the days of differentiation for neutrophil maturation from progenitor cells
- Perform comparison experiments between Hoxb8 neutrophils and primary bone marrow-derived neutrophils of the two genotypes including:
    - Analysis of cell surface differentiation markers
    - Cell morphology
    - Respiratory burst functional assay
    - Phagosomal pH and area snapshots
    - Phagosomal pH time course
    - Western blotting of NADPH oxidase subunits

- Preliminary viral transduction experiments of GFP-tagged LC3 in Hoxb8 neutrophils

4.2 Generation of a conditionally Hoxb8 immortalised cell line

The WT and *Hvcn1*$^{-/-}$ Hoxb8 cells described in subsequent experiments of this chapter were very generously produced by Annette Zehrer at Ludwig-Maximilians-Universität, Germany or produced by myself at UCL. This was achieved through the retroviral transduction of the murine stem cell provirus (MSCV) expressing Hoxb8 fused to the estrogen-binding domain of the estrogen receptor into mouse bone marrow cells. This is the same vector described in the Wang paper, that was kindly gifted by Hans Hacker of St. Jude's Hospital, Boston, USA (Wang *et al.*, 2006). It contains a neomycin cassette that was used for antibiotic selection of successfully transduced cells.

In a deviation from published protocols, I did not use an isolation kit to enrich the bone marrow progenitor population but instead infected the entirety of bone marrow cells isolated from the hind legs of one C57BL/6 mouse. The Hoxb8-expressing retroviral supernatant was produced in GP-293 HEK cells with a murine-specific envelope vector (more details are provided in section **2.5**). 1 mL of viral supernatant was used for each mouse. For 2 weeks after infection, neomycin was added to the cell medium to allow cell outgrowth. After its removal, clusters or clones of cells began to emerge as non-transduced cells died and were removed by passaging. After approximately 8 weeks post-infection, cell viability was over 90% when measured with trypan blue exclusion. There were minimal levels of spontaneous differentiation into neutrophils in all Hoxb8 progenitor cultures determined by monitoring of cell size with the automated plate reader.

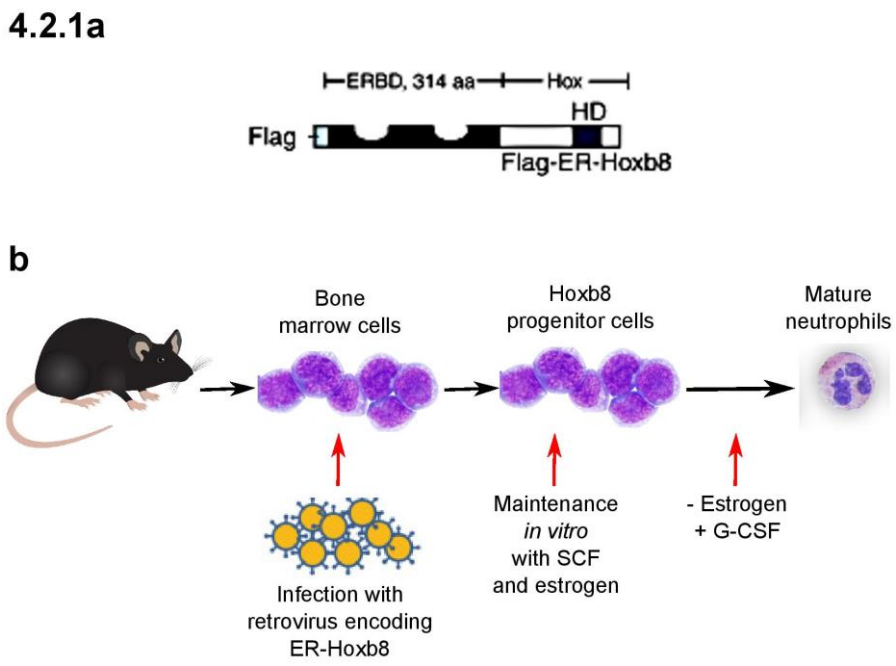

Figure 4.2.1 | A schematic depicting immortalisation of bone marrow progenitors using ER-Hoxb8 (a-b). (**a**) *A diagram of the estrogen receptor (ER) with the binding domain (BD) fused to the Hoxb8 gene which is transfected into bone marrow progenitors*. (**b**) *Flow plan of method: the cells are removed from the hind limbs of a mouse, infected with retrovirus encoding ER-Hoxb8 from* (**a**)*, maintained with suitable growth factors, then differentiated into neutrophil-like cells.*

The new WT Hoxb8 line was compared with the stock WT line for successful immortalisation by measuring cell marker surface expression with flow cytometry and Hoxb8 protein expression by Western blotting. **Figure 4.2.2a** shows that new WT Hoxb8 progenitors have similar CD117 expression to the stock cells, and no expression of the differentiated myeloid cell markers CD11b (Mac-1), CD68, Ly6C and Ly6G. The size and granularity as assessed by forward and side scatter also appear to be similar (**Fig. 4.2.2b**). **Figure 4.2.2c** provides evidence that all the progenitor cells are producing Hoxb8, which is rapidly lost upon differentiation. Also, freshly isolated bone marrow neutrophils which have undergone differentiation in vivo have lost the expression of Hoxb8.

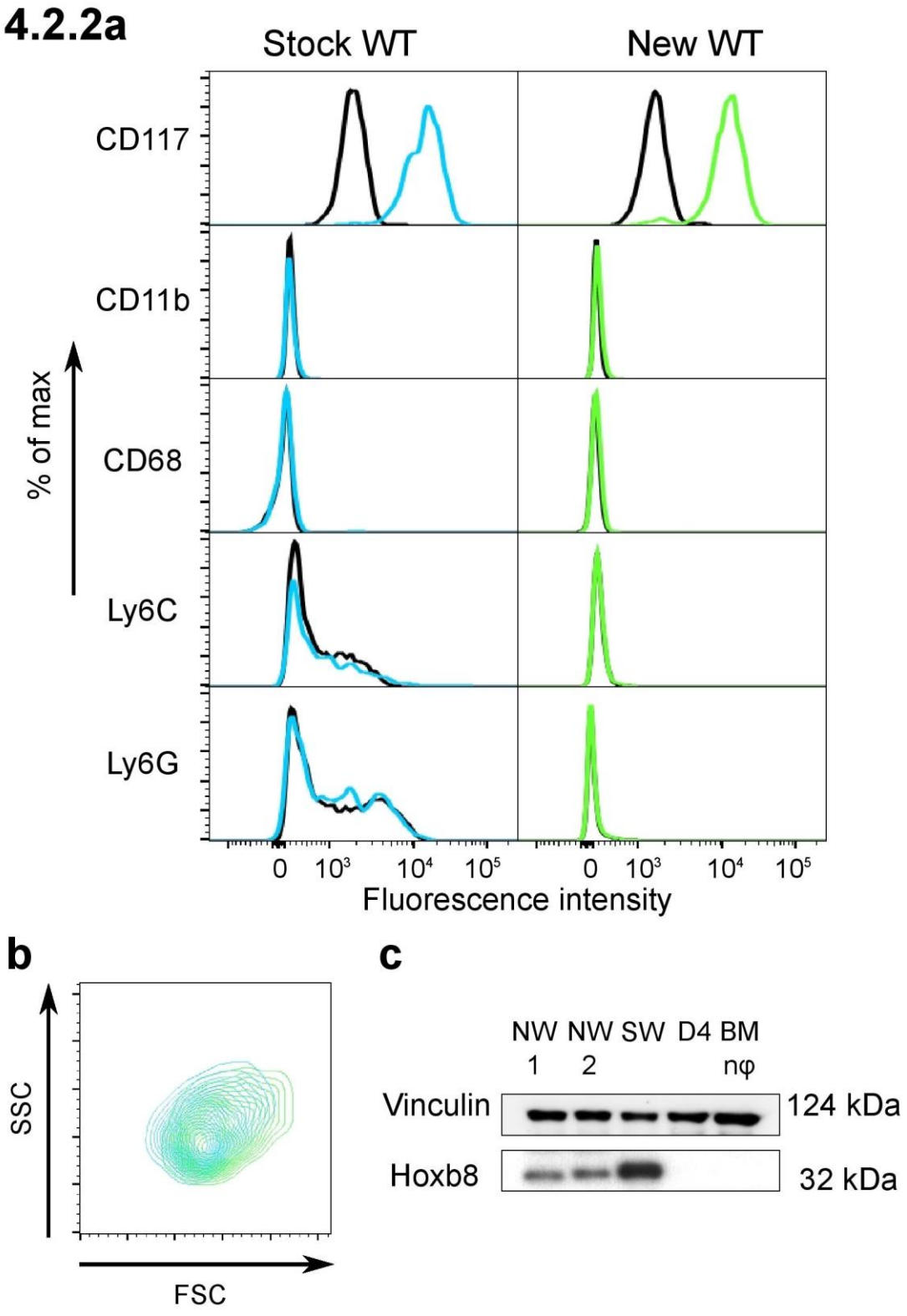

Figure 4.2.2 | Confirmation of new conditionally immortalised Hoxb8 progenitor cells compared to stock Hoxb8 cells (a-b). (**a**) *Representative analysis of cell marker expression presented as fluorescence intensity (x-axis), normalised to the mode (y-axis). Unstained controls are in black; stained cells are in blue for stock*

Hoxb8 progenitors and green for newly synthesised Hoxb8 progenitors. (**b**) *Representative Western blots using antibodies for vinculin and Hoxb8. The samples loaded from left to right were: 2 replicates of newly immortalised progenitors (NW), one replicate of stock progenitors (SW), one replicate of stock 4 day differentiated neutrophils (D4), one replicate of primary neutrophils (BM nφ).*

4.3 Optimisation of Hoxb8 cell viability and proliferation after estradiol removal

To cause the Hoxb8 progenitors to differentiate into neutrophil-like cells, they are seeded at low numbers in a dish with medium supplemented with SCF and granulocyte-colony stimulating factor (G-CSF), but lacking estradiol. Cell proliferation and purity of differentiated cells have been published before with this cocktail of growth factors (Wang *et al.*, 2006; McDonald *et al.*, 2011b). The SCF is needed for expansion of cells and their viability, G-CSF is for granulocyte differentiation. Cell viability, as assessed by trypan blue exclusion, and cell numbers were recorded daily for 6 days for both WT and *Hvcn1*$^{-/-}$ genotypes (**Fig. 4.3**). There were no significant differences between either cell line. Cell viability was stable above 95% live cells for the first 3 days in culture. Viability started to drop by day 4, then fell steeply between day 5 and 6 to ~ 60%. Cell expansion was evident between days 0-4 and proliferation stopped after day 5 which coincided with a decrease in cell viability. At day 4 the cells had expanded ~20-fold from the original numbers. Even at day one they have approximately doubled in number. After the evaluation of the maximum cell number and viability, 4 days of differentiation appears to be optimal. These results are consistent with published studies of Hoxb8 progenitor differentiation into neutrophils who also demonstrated day 4 as optimal for neutrophil differentiation (Wiesmeier *et al.*, 2016; McDonald *et al.*, 2011a).

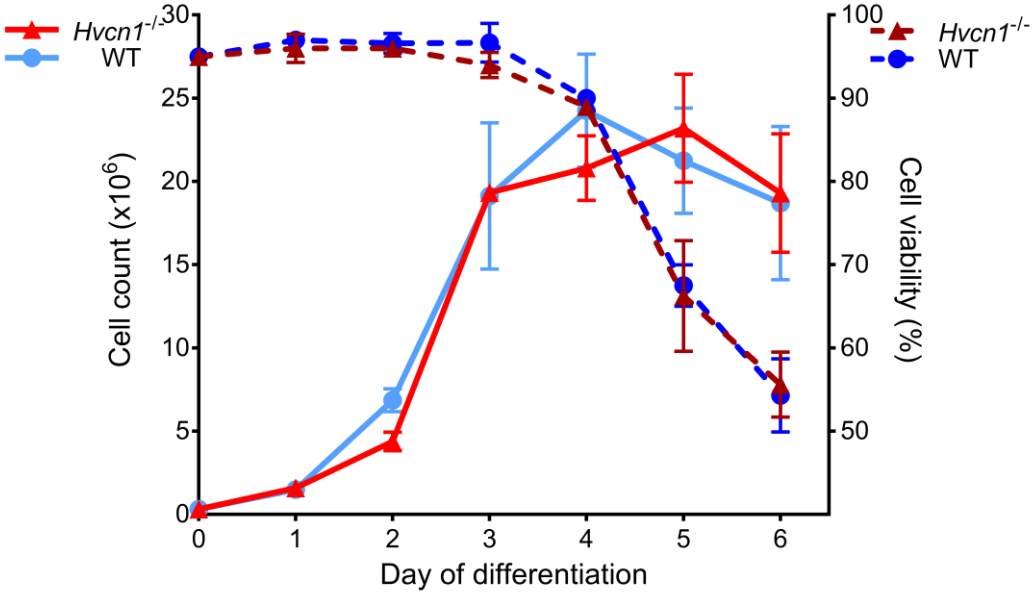

Figure 4.3 | Cell viability and expansion of Hoxb8 cells after removal of estrogen and addition of G-CSF. *Cell count on the left y-axis is presented by solid lines, while cell viability on the right y-axis is presented by dashed lines over 6 days of cell differentiation. Cells were seeded at 2.5 x 10^5 per plate. Measurements for WT (blue lines) and Hvcn1$^{-/-}$ cells (red lines) are shown as mean ± SEM, n = 5.*

4.4 Time course of cell surface differentiation markers

Next, I recorded the changes in cell surface markers between days 2 and 6 of differentiation from undifferentiated progenitors and compared then with primary bone marrow (BM) neutrophils. **Figure 4.4a** shows representative plots of cell surface expression in both models in stained versus unstained cells. **Figure 4.4b** shows quantification of cell surface marker expression by geometric mean fluorescence intensity (MFI) of averaged from three experiments. **Figure 4.4c** presents the forward scatter (FSC) by side scatter (SSC) for each cell type, to demonstrate the changes in cell size and granularity accompanying cell differentiation. CD117, also known as c-kit, is a marker for the haematopoietic cells (Ogawa *et al.*, 1991) and is a tyrosine kinase receptor for SCF (Williams *et al.*, 1990). Undifferentiated Hoxb8 cells express high levels of CD117 and by day 2 of differentiation it has reduced by ~75%, and completely gone by day 4. BM neutrophils do not express CD117. CD11b or Mac-1

is a beta-2 integrin that is abundantly expressed on myeloid cells such as neutrophils and monocytes (Fossati-Jimack *et al.*, 2013; Lim *et al.*, 2015). **Figure 4.4b** shows it is not expressed by undifferentiated Hoxb8 cells but is rapidly upregulated day 2 after initiation of differentiation. CD11b expression was maximal at day 2 and stable for at least 6 days. The expression level of CD11b on differentiated hoxb8 cells was comparable to that found on BM neutrophils.

The antigens Ly6C and Ly6G together make up the epitope Gr-1, however higher expression of Ly6C is used to distinguish early monocytes that have recently left the bone marrow (Sunderkötter *et al.*, 2004) and Ly6G is more highly expressed on neutrophils (Fleming, Fleming & Malek, 1993). From the second day of differentiation, the Hoxb8 cells express the same level of Ly6C as primary neutrophils. For Ly6G the expression was different to primary neutrophils; there was an increasing expression of Ly6G as the cell differentiated, but it was much lower than that expressed by primary neutrophils. This pattern has been observed before - it appears to be a quirk acquired from cells derived from C57BL/6 mice, as differentiated cells from Balb/C mice have normal expression of Gr-1 (Wang *et al.*, 2006), while intermediate expression of Gr-1 in day 4 differentiated cells was previously reported by other groups in C57BL/6 derived Hoxb8 cells (Wiesmeier *et al.*, 2016; Gautam *et al.*, 2013)(S3 and 4 figures in the first paper, figure 1 in the second).

There was very low expression of the macrophage marker CD68 on the differentiated Hoxb8 cells or BM neutrophils. This marker was included to distinguish any contaminating macrophage-like cells or abnormal differentiation pattern within the cell populations (Hume *et al.*, 2010). To confirm that the Hoxb8 cells did not express markers for other monocyte/macrophage lineages, antibodies

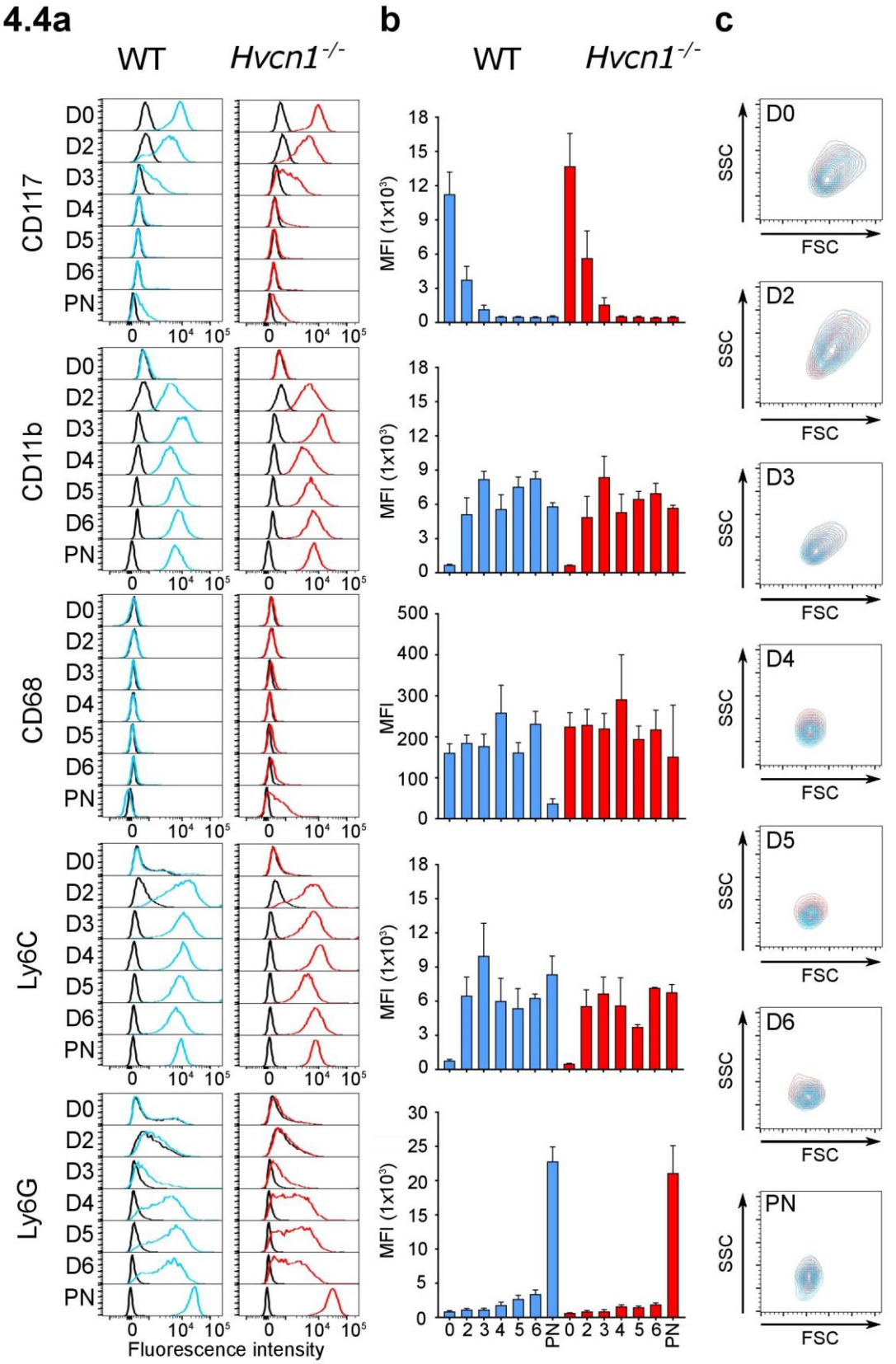
4.4a
WT
Hvcn1-/-
CD117
CD11b
CD68
Ly6C
Ly6G
D0
D2
D3
D4
D5
D6
PN
Fluorescence intensity
b
MFI (1x10³)
MFI
0 2 3 4 5 6 PN
c
SSC
FSC

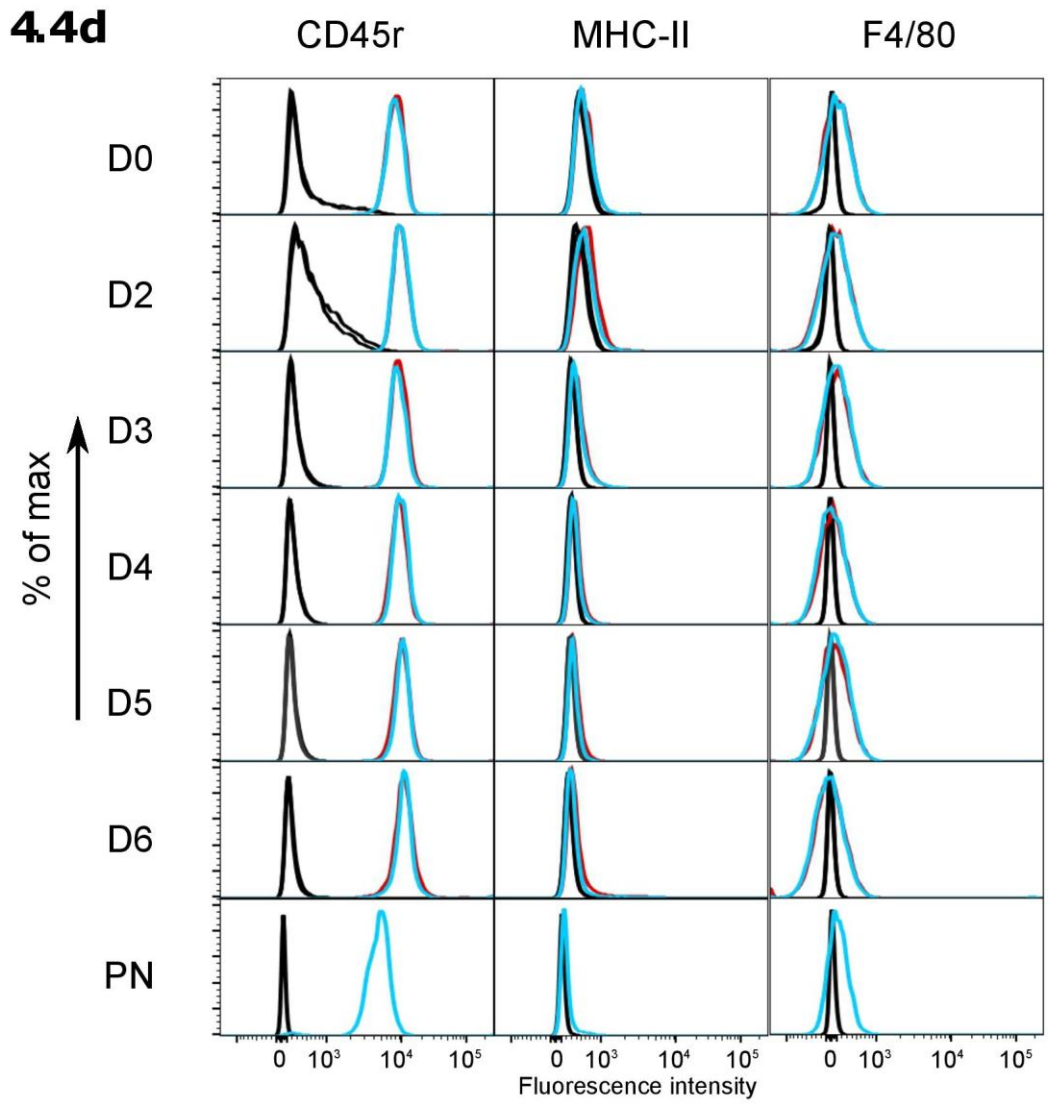

Figure 4.4 | Cell marker surface expression in Hoxb8 cells compared to primary neutrophils (a-d). (**a**) *Representative analyses of cell marker expression presented as fluorescence intensity on the x-axis, and percentage of expressing cells normalised to the mode (% of max). There is a compiled plot for each marker, with the identity of each cell-type annotated on the y-axis: D0 (undifferentiated progenitors), 2-6 of Hoxb8 differentiation, and primary neutrophils (PN). WT cells are shown in blue, Hvcn1$^{-/-}$ cells in red.* (**b**) *Quantitative analysis of each surface marker's expression in each cell-type. Mean fluorescence index (MFI) was calculated as the geometric mean fluorescence using FlowJo software, mean ± SEM, n=3.* (**c**) *Representative dot plots of WT cells (blue) and Hvcn1$^{-/-}$ cells (red) undergoing changes in forward scatter (FSC) and side scatter (SSC) with cell differentiation. Plots are annotated with each differentiation stage*. (**d**) *representative analyses presented in the same way as* (**a**)*, this time for mononuclear markers F4/80 and MHC-II, and CD45 receptor.*

for F4/80 and MHC-II (or I-A/I-E in mice) were also tested along with the pan-leukocyte marker CD45 receptor (CD45r) (**fig. 4.4d**). The progenitor and differentiated cells all had no detectable expression of F4/80 and MHC-II, but cells at all stages of differentiation highly expressed CD45r. These findings are consistent with the previous results: all the cells are of myeloid lineage, as they express the common leukocyte antigen CD45r, but they do not express classical mononuclear cell markers, MHC-II and F4/80.

4.5 Changes in Hoxb8 cell morphology following estradiol removal

Cells from each day of differentiation were cytospun onto glass slides and stained with Wright-Giemsa stain for cytoplasmic and nuclear observation. There were no observable differences in cell morphology between the two genotypes. The undifferentiated Hoxb8 cells had large nuclei which left little room for the blue cytoplasm. Already by day 2 in the differentiation medium, some of the cells were starting to contract and the nuclei were shrinking into a kidney shape with myelocytes and band cells present. There was some variety in cell size, visible in **figure 4.5**. The cytoplasm was also starting to turn pinker. By day 3, the cell membrane is blebbing, as small vesicles seem to be forming around the membrane. The cells have decreased further in size, as well as the nuclei into the characteristic lobules. The cytoplasm is much more transparent and pinker. Day 4 and 5 Hoxb8 neutrophils appear very much the same, apart from they have lost the ruffled membrane. Day 5 cells are a little smaller. Their size, nucleus, and cytoplasm look almost identical to the primary BM neutrophils. Day 6 cells, consistent with the viability data, are dying and degrading. This is apparent through the cytoplasm strewn across the slide, due to cell lysis, and contraction of some of the nuclei.

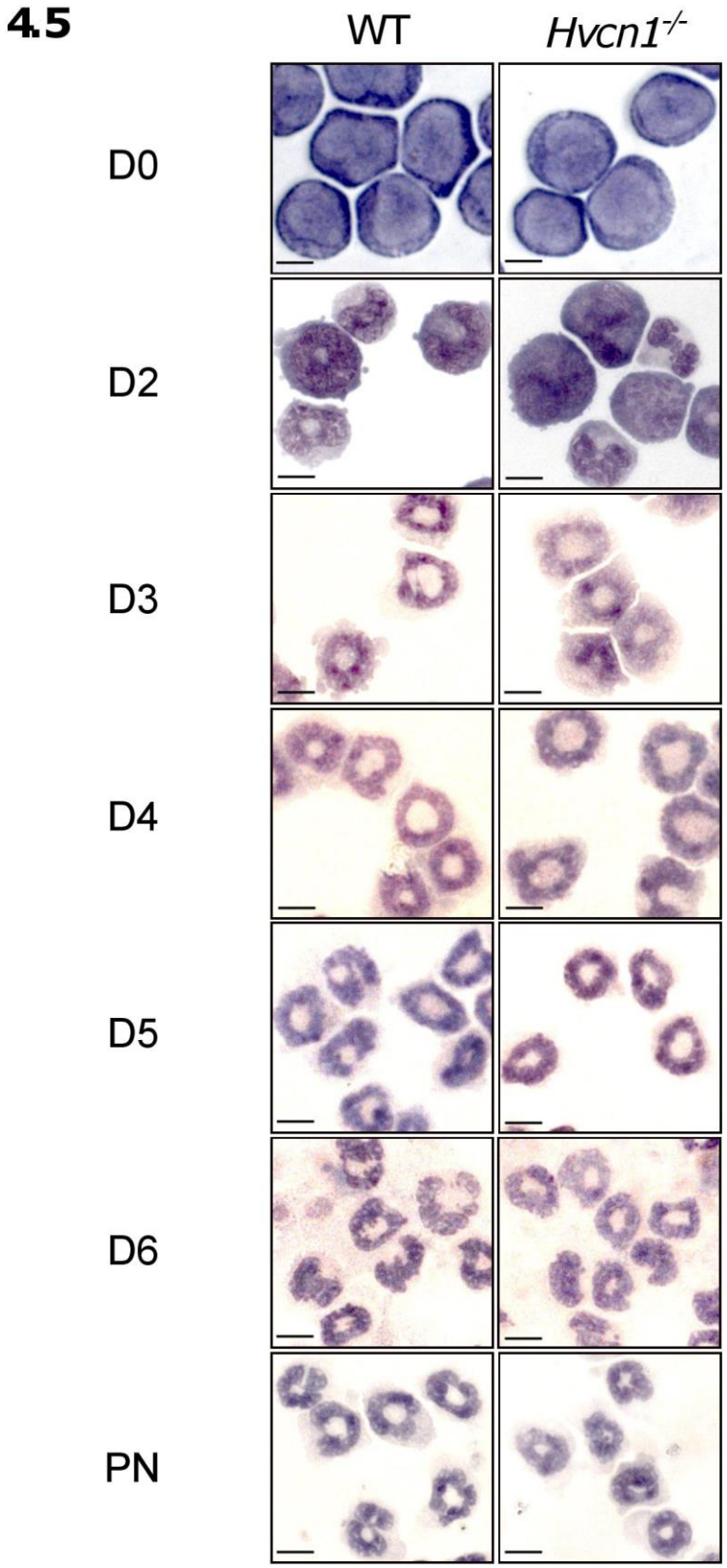

Figure 4.5 | Time course of changes in cell morphology of Hoxb8 neutrophils compared with primary neutrophils. *Cytospin cell preparations were fixed in methanol then treated with Wright-Giemsa stain. Cells for each stage of differentiation are placed from top to bottom: day 0 or undifferentiated progenitors, to primary BM*

neutrophils. Images were taken on a brightfield light microscope at x 63 magnification. Scale bar = 10 µm.

4.6 Western blotting of the Hoxb8 protein and NADPH oxidase subunits in Hoxb8 neutrophils and primary BM neutrophils

The findings in cell surface marker expression and morphology demonstrate that in as little as 2 days in the differentiation medium, significant changes are observed in the Hoxb8 cells that are leading them towards a neutrophil phenotype. Flow cytometry was used to measure external protein expression; I next used Western blotting to investigate intracellular protein content.

Cell lysates were prepared for each genotype in undifferentiated cells, day 2, 4, and 6 Hoxb8 neutrophils, and primary murine BM neutrophils. The lysates were normalised by viable cell number, as each cell type contained different levels of protein as determined by the bicinchoninic acid (BCA) assay. Vinculin, which has an approximate size of 120 kDa, was used as a housekeeping protein for all Western blots (**Fig 4.6**). Its expression was similar between all cell types and its high molecular weight allows smaller proteins of interest to be examined on the same membrane. The first protein investigated was Hoxb8, which is regulated via a estradiol sensitive promoter. I wanted to see how Hoxb8 expression changed when estradiol was removed from the supernatant during cell differentiation. Hoxb8 was strongly expressed in undifferentiated progenitor cells, and expression was still detected in day 2 cells although it was at about half the intensity. Four days into the differentiation Hoxb8 was no longer detectable. Primary BM neutrophils also did not express Hoxb8.

I next looked at some of the components of the neutrophil NADPH oxidase isoform. The main catalytic core of the oxidase is the flavocytochrome b_{558}, which is a heterodimer of one molecule of $p22^{phox}$ and one molecule of $gp91^{phox}$, otherwise known as NOX2 (Dinauer *et al.*, 1987). In mice, $gp91^{phox}$ is coded for by the *Cybb*

gene and shares 93% amino acid homology with the human version, although the protein band visible in Western blots is around 58 kDa (Pollock *et al.*, 1995) instead of the human 91 kDa (Parkos *et al.*, 1987). It is well known that the human NOX2 has many N-linked glycosylation sites which contribute to the broad smear present on the membrane (Harper, Chaplin & Segal, 1985). The murine NOX2 has fewer sites, leading to the more defined blot (Pollock *et al.*, 1995). NOX2 expression in Hoxb8 and primary neutrophils appeared to be the same compared to each genetic model. There was no detectable expression in undifferentiated Hoxb8 cells, but a faint band appeared in day 2 Hoxb8 cells around 65 kDa. In day 4 Hoxb8 cells the band was more intense as a large smear between 50 to 60 kDa. It was very similar to the band for primary neutrophils, if slightly less intense. Day 6 Hoxb8 cells had a band centred at the same size as day 4 and primary neutrophils, but the smear was less intense.

The faint band present in day 2 cells is situated further up the membrane than the conventional smear, meaning it is of greater molecular weight. It may be a precursor form of the protein, or perhaps contamination of some sort. The defined band suggests that the protein is not very glycosylated.

While the flavocytochrome carries out the electron transport, it is dependent on the binding of other subunits for its function. The gene *Ncf1* codes for the $p47^{phox}$ protein and *Ncf2* for $p67^{phox}$. Both are located in the cytosol, but upon phosphorylation, they translocate to the membrane to form a complex with the membrane-bound cytochrome b_{558}. They are also accompanied by $p40^{phox}$ and Rac2. The oxidase is only optimally activated once all subunits are correctly assembled.

In the representative Western blot in **figure 4.6**, neither p47phox nor $p67^{phox}$ proteins were detectable in undifferentiated and day 2 Hoxb8 cells. However, in day 4 and 6 Hoxb8 cells and primary neutrophils, there were relatively similar band intensities for both regulatory proteins. Based on the expression of these crucial components, day 4 neutrophils very much resemble primary neutrophils.

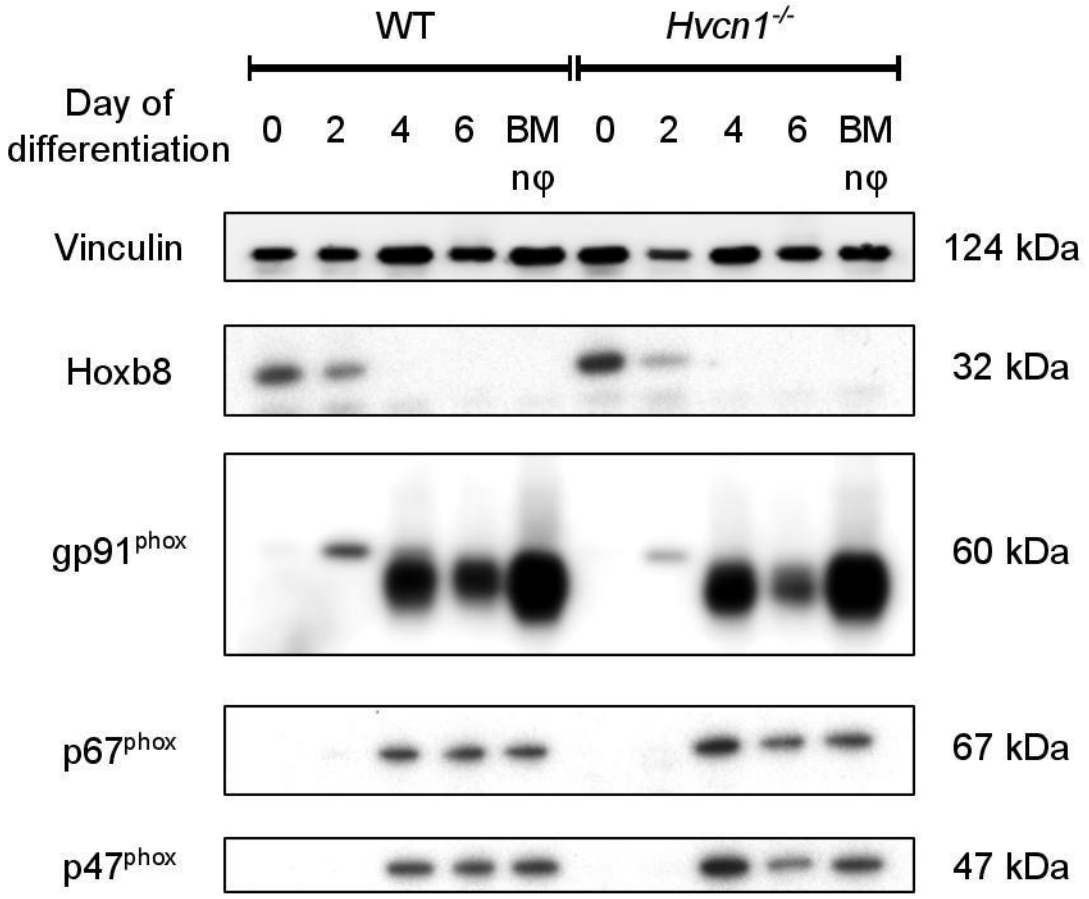

Figure 4.6 | Representative Western blot demonstrating Hoxb8 neutrophil development in WT and *Hvcn1*$^{-/-}$ cells. *All membranes shown contained the same samples but were split across two gels. From left to right, WT cells are positioned in increasing days of differentiation, then primary BM neutrophils for comparison, followed by Hvcn1*$^{-/-}$ *in the same order. The left side of the membranes specifies the targeted protein of the antibody, on the right side the observed band size. This blot is representative of n=3.*

4.7 The respiratory burst in Hoxb8 neutrophils

The respiratory burst was measured using the Amplex UltraRed assay. It works by recording the fluorescence of resorufin, the product of hydrogen peroxide (H_2O_2) reacting with the Amplex red reagent catalysed by horseradish peroxidase. H_2O_2 is a product of NADPH oxidase activity. Resorufin is cell-impermeable, so the oxidase is stimulated at the cell membrane by phorbol 12-myristate 13-acetate (PMA), a protein

kinase C agonist, which releases H_2O_2 into the extracellular medium where it can interact with the test reagents. This assay was carried out to test the function of the Hoxb8 neutrophils throughout their differentiation.

Figure 4.7 presents the respiratory burst measured from day 2 to 6 with undifferentiated progenitor cells in WT and *Hvcn1*$^{-/-}$ cells. Whereas in the previous experiments of cell viability, cell surface markers, and cell differentiation there were no differences between the two genetic models, here is shown a significant functional disparity. As has been seen before in the primary BM neutrophils, *Hvcn1*$^{-/-}$ Hoxb8 neutrophils had a lower respiratory burst than WT cells (Ramsey *et al.*, 2009; El Chemaly *et al.*, 2014). However, the NADPH oxidase activity between the two models followed the same pattern for each day of differentiation. Undifferentiated cells had no detectable H_2O_2, but by day 2 after 50 minutes of PMA stimulation, the relative fluorescent units (RFU) for WT cells was around 2000 (**Fig. 4.7a**). For *Hvcn1*$^{-/-}$ cells, it was a little under half of this (**Fig. 4.7b**). Day 3 neutrophils had a significant increase in activity, rising to approximately 8000 RFU for WT cells and 4500 for *Hvcn1*$^{-/-}$ cells. For day 5 cells, it was roughly the same levels, as the peak day for oxidase activity was day 4 hitting a maximum of 10,200 RFU for WT cells. The total H_2O_2 RFU of day 6 neutrophils fell to below half that of day 4 neutrophils for both models, despite there being the same number of viable cells present for each condition.

The relative oxidation rate shown in **figure 4.7c** was calculated from the steepest gradient of the curves from **4.7a and b**. It neatly shows the rise and fall of H_2O_2 production in both cell types, with day 4 again displaying the highest activity.

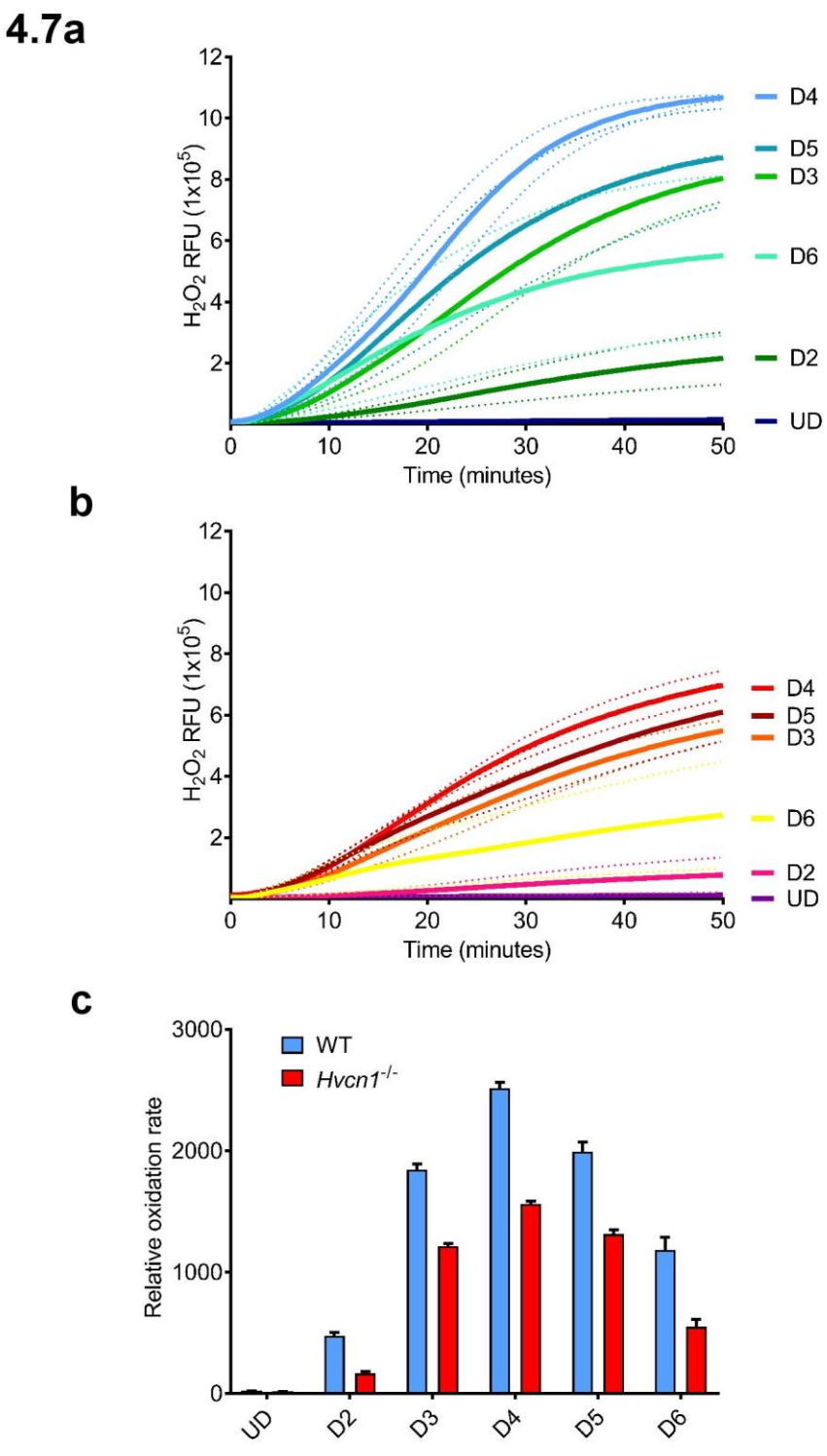

Figure 4.7 | Time course of respiratory burst activity in Hoxb8 neutrophils (a-c). (**a**) *WT and* (**b**) Hvcn1$^{-/-}$ *Hoxb8 cells at different days of differentiation that have been stimulated with PMA to induce the respiratory burst, measured every 30 seconds over 50 minutes. Mean ± SEM (shown as dashed lines), n=3.* (**c**) *The maximum rate of* H_2O_2 *induced fluorescence is plotted as mean ± SEM from the time course experiments. WT is blue, Hvcn1*$^{-/-}$ *is red, n=3 with 3 technical replicates.*

4.8 Comparison of respiratory burst activity in primary BM neutrophils with day 4 Hoxb8 neutrophils

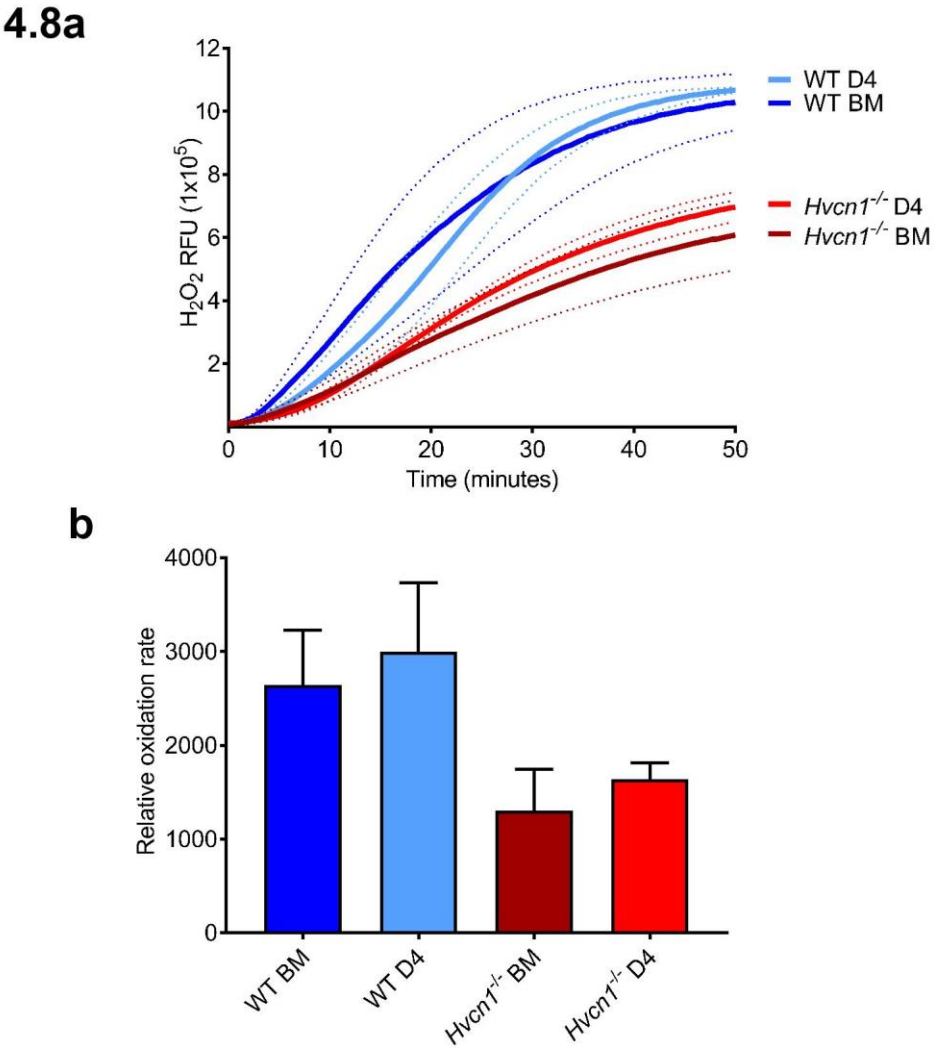

Figure 4.8 | Comparison of the respiratory burst in Hoxb8 neutrophils with primary neutrophils (a-b). (**a**) *Time course of the respiratory burst and* (**b**) *maximum rates of the respiratory burst are plotted in the same way as figure 4.7; mean ± SEM, n=3 and 3 technical replicates.*

Although days 5 and 6 Hoxb8 neutrophils had greater expression of the classical neutrophil marker Ly6G and had fully mature neutrophil morphology, day 4 neutrophils had greater cell viability and functional activity as measured by the Amplex UltraRed assay. These are more important parameters for assessment of a

relevant neutrophil model cell line as they demonstrate active functional aspects; therefore this day was chosen for comparison with primary BM murine neutrophils.

The time course of H_2O_2 induced fluorescence was compared between WT and *Hvcn1*$^{-/-}$ primary and Hoxb8 neutrophils (**Fig. 4.8a**), and the maximum gradient was also compared (F**ig. 4.8b**). There was no difference in H_2O_2 generation between the Hoxb8 and primary neutrophils. These data provide further evidence that the day 4 Hoxb8 neutrophils have developed into mature neutrophils.

4.9 Comparison of phagosomal pH in primary BM neutrophils with day 4 Hoxb8 neutrophils

In the previous chapter I have shown how NADPH oxidase activity is linked to phagosomal pH, here I wanted to find out if Hoxb8 neutrophils also had similar phagosomal pH to their primary neutrophil controls. Firstly, progenitor cells were not able to phagocytose the serum-opsonised *Candida* at all. However, day 4 neutrophils were able to phagocytose the particles almost as well as the primary cells. When phagosomal pH was measured approximately 30 minutes after addition of opsonised SNARF-labelled *Candida*, the pH and area of the phagosome were the same between Hoxb8 neutrophil and primary cell for each genotype (**Fig. 4.9a and b**). Consistent with the findings of the respiratory burst, WT Hoxb8 cells have a fully active NOX2 which creates a neutral to the slightly alkaline environment, whereas *Hvcn1*$^{-/-}$ cells have roughly 50-60% activity of the WT cells and have very alkaline (pH 10-11) and very swollen phagosomes. The swelling is thought to result from increased water moving into the phagosome with an osmotically active ion such as potassium. **Figure 4.9c-f** presents confocal images of the 4 different cell types about 15 minutes after the addition of *Candida*.

However, measuring phagosomal pH as a snapshot means that phagocytosis in unsynchronised, meaning that there will be a greater spread of data. Indeed, the whiskers on the boxplot in **figure 4.9a** range from pH 6 to 9 for WT cells, and from pH 8.5 to over 11 for *Hvcn1*$^{-/-}$ cells (**Fig. 4.9b**). Measuring pH kinetically over the first 30 minutes would allow any small variations to be noticed as each phagosome would be monitored individually. This experiment is displayed in **figure 4.9c and d**. For WT cells, consistent with the snapshot results, show that there is no statistical difference in the kinetic phagosomal pH profile between Hoxb8 and primary cells. There is an increase in pH within the first 5 to 10 minutes, where it tends to plateau for primary cells, and falls back a little for Hoxb8 cells. On the other hand, *Hvcn1*$^{-/-}$ neutrophils become very alkaline within the first 5 minutes after phagocytosis (**fig. 4.9c**). For the primary BM neutrophils, a pH between 10.5 and 11 is maintained for the next 25 minutes in most cells. *Hvcn1*$^{-/-}$ Hoxb8 neutrophils do not reach this, averaging around pH 10 for the remaining time course. Both cell types become very alkaline, but the difference in pH was found to be statistically significant ($p<0.0001$) when analysing the whole duration of the time course. In **figure 4.9d**, the phagosomal pH is shown at 15 minutes post phagocytosis to present a synchronised snapshot of the phagosomal environments. There was no obvious difference between WT cells, but it was again noticeable between the *Hvcn1*$^{-/-}$ cells ($p<0.05$).

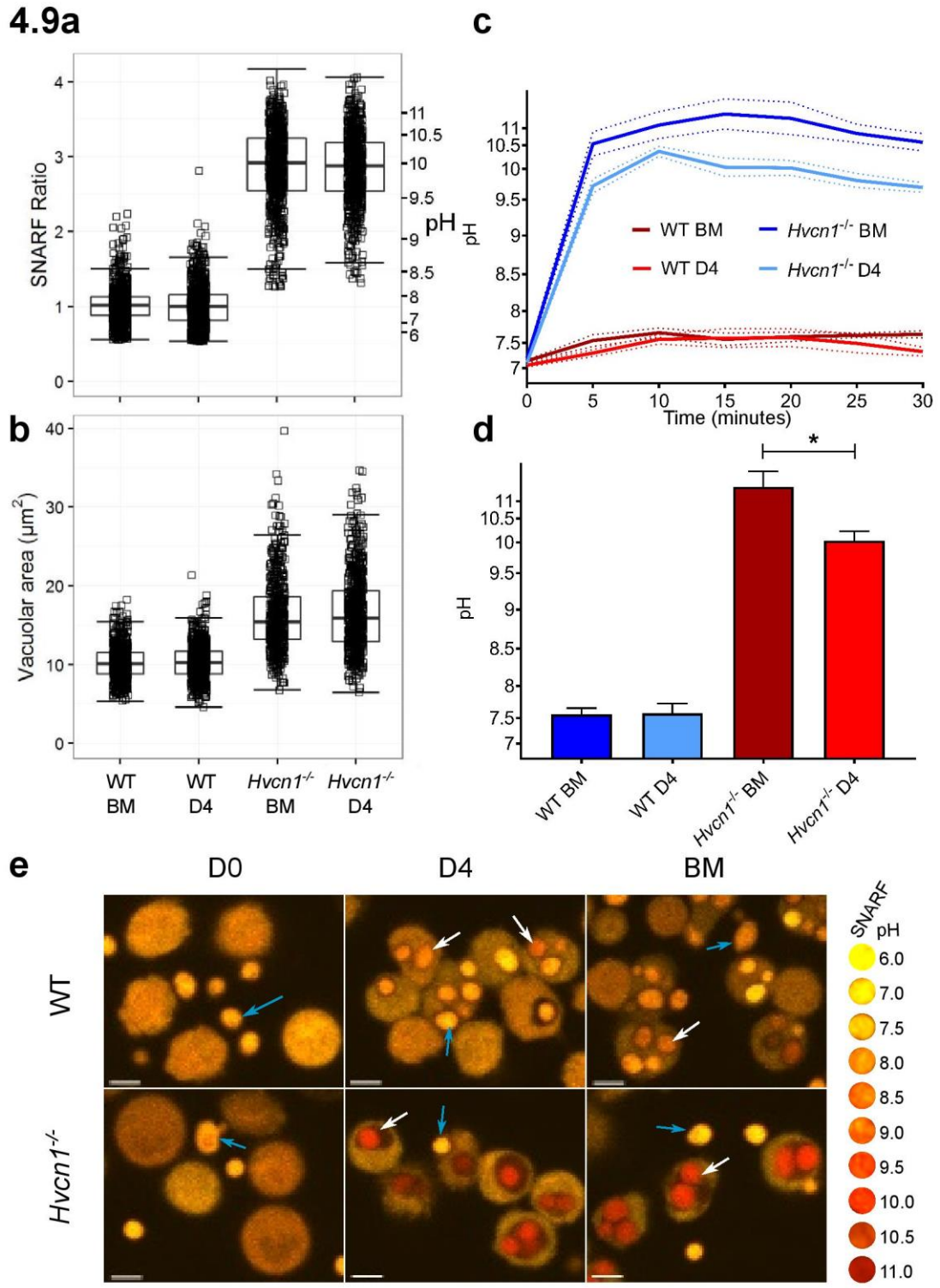

Figure 4.9 | Analysis of phagosomal ion fluxes in the Hoxb8 neutrophil model compared to primary neutrophils (a-h). *Quantitation of phagosomal pH* (**a**) *and area* (**b**) *in Hoxb8 day 4 differentiated cells and primary BM neutrophils in the WT and the Hvcn1*$^{-/-}$ *models. Each square represents an individual measurement; each condition has an overlaying boxplot showing the median and interquartile range, n=3, at least 100 measurements per condition were recorded in each experiment*. (**c**) *Time*

*course of changes in phagosomal pH in Hoxb8 day 4 neutrophils and primary neutrophils. Mean (solid line) ± SEM (dashed lines), n=3. Statistics were calculated by one-way ANOVA with Bonferroni post-test, ****=p<0.0001, ns=not significant.* (**d**) *Phagosomal pH at 15 minutes into the time course experiments. Mean ± SEM, n = 3. Statistics were calculated by one-way ANOVA with Bonferroni post-test, *=p<0.05, ns=not significant.* (**e**) *Representative confocal images of the phagocytosis snapshots, D0 (Hoxb8 progenitors), D4 (Hoxb8 D4 neutrophils), and BM (primary bone marrow neutrophils) with accompanying SNARF to pH colour key. White arrows point to engulfed Candida; blue arrows point to extracellular Candida. Scale bar = 10 µm.*

4.10 Preliminary localisation experiments of GFP-tagged LC3 in Hoxb8 neutrophils

The investigations described thus far in this chapter have focused on the characterisation of the Hoxb8 cell line to be used as a model of mouse neutrophils. Here, I demonstrate the possible subsequent applications of this cell model, particularly the use of viral plasmids to insert or remove genetic material in differentiated cells. A commonly used technique within cell biology is the targeting of fluorescent tags to a gene of interest so that the activity of the translated fusion protein can be tracked in the cell. This is especially useful for imaging in live cells of kinetic or transient processes.

I began a set of preliminary experiments in collaboration with Andrew Smith, a senior investigator at Microbial Diseases Department at UCL, and Tom Wileman from the University of East Anglia. The aim was to see if a type of non-canonical autophagy, microtubule-associated protein light-chain 3 (LC3)-associated phagocytosis (LAP), was functionally relevant in neutrophils. Autophagy is the process of “self-eating”, where cell components are internalised in double-membraned intracellular organelles called autophagosomes, in which the contents are degraded and recycled. The recruitment of LC3 to the membrane of these compartments is regarded as a defining

Figure 4.10.1 | Schematic of the link between phagocytosis and different classes of autophagy in neutrophils.

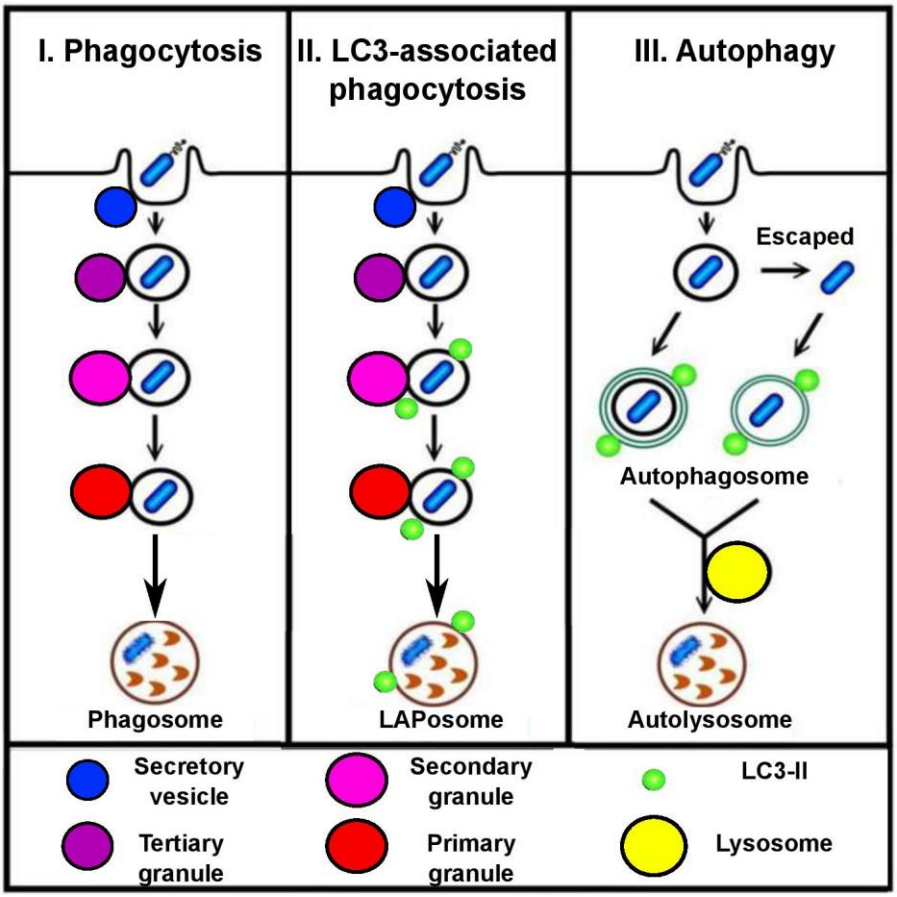

marker of autophagy. The cytosolic form of LC3 (LC3-I) is converted to LC3-II when conjugated to phosphatidylethanolamine (PE) in the membrane (Sou *et al.*, 2006). Although autophagy is a fundamental metabolic pathway, it also has essential roles in innate and adaptive immunity, such as the removal of intracellular pathogens. LAP is thought to bridge the gap between autophagy and conventional phagocytosis, as the LAPosome is made from a single membrane (like a phagosome), but it also recruits some autophagic machinery such as LC3 to its membrane after the engulfment of bacteria or fungal particles (**Fig. 4.10.1**). Similarly to phagocytosis, it has been reported that the recruitment and activity of NOX2 on the membrane is necessary for efficient LC3 recruitment (Huang *et al.*, 2009). Furthermore, there are increasing numbers of reports linking initiation of LAP in response to specific pathogens, such as *Listeria monocytogenes* (Gluschko *et al.*,

2018), *C. albicans* (Tam *et al.*, 2014) and *Burkholderia pseudomallei* (Gong *et al.*, 2011) amongst others.

While LAP has been shown to occur in the professional phagocytes - mouse bone marrow-derived neutrophils (Huang *et al.*, 2009), in primary macrophages (Gutierrez *et al.*, 2004; Gluschko *et al.*, 2018) and the RAW 264.7 macrophage cell line (Huang *et al.*, 2009; Gutierrez *et al.*, 2004) - it has not yet been shown in Hoxb8 neutrophils. If they prove to have LC3, they will make investigations into LAP and other autophagy pathways much more feasible in the neutrophil. The method used here for localisation of LC3 was an adenovirus kindly provided by Tom Wileman. Expansion of the adenovirus was generated through the infection of HEK293 cells, in the same way as making retroviral containing supernatant for infecting the bone marrow progenitors with the Hoxb8-expressing retrovirus. Day 3 or day 4 Hoxb8 neutrophils were generated as normal, then transferred into 6 wells and infected within a category 2 tissue culture suite with 1 ml of adenoviral supernatant per well. WT and *Hvcn1*$^{-/-}$ Hoxb8 neutrophils were both infected overnight for approximately 18 hours.

Both cell types had a successful infection of about 40-50% of cells, as evidenced by green puncta, which were not observed in uninfected control cells (**Fig. 4.10.2**). To explore the changes in LC3 localisation upon phagocytosis, cells were challenged with serum-opsonised SNARF-labelled heat killed *C. albicans*, in the same way as the previously described phagosomal pH assays (section **4.9**). The cells with *Candida* were incubated at 37 ˚C for 1 hour, then imaged on the confocal microscope. Z stacks of 1 µm were taken of cells of interest.

Bright green tracks of GFP-tagged LC3 protein were visibly forming around some of the engulfed particles in both genetic models **(Fig. 4.10.3 and 4**). In some cells, there were two bright circular foci at either end of the phagosome, perhaps as centres of origin of phagosomal scaffolding material. The LC3 labelling increased with time. Although there was GFP-LC3 present in the phagosomal membrane of some of the

Hvcn1$^{-/-}$ cells, it appeared to be denser in the WT cells, as the signal was much brighter in the cells analysed. However, the pattern of GFP-LC3 phagosomal localisation appeared to be consistent with the published work in bone marrow-derived neutrophils (Huang *et al.*, 2009).

These are preliminary experiments which need to be repeated with quantitative analyses, but these qualitative results provide a foundation for further investigation of LAP using Hoxb8 neutrophils. Furthermore, the use of *Candida* labelled with a pH indicator allows examination of whether it is NOX2 activity alone or the accompanying changes in pH which initiate and maintain LC3 phagosomal membrane formation.

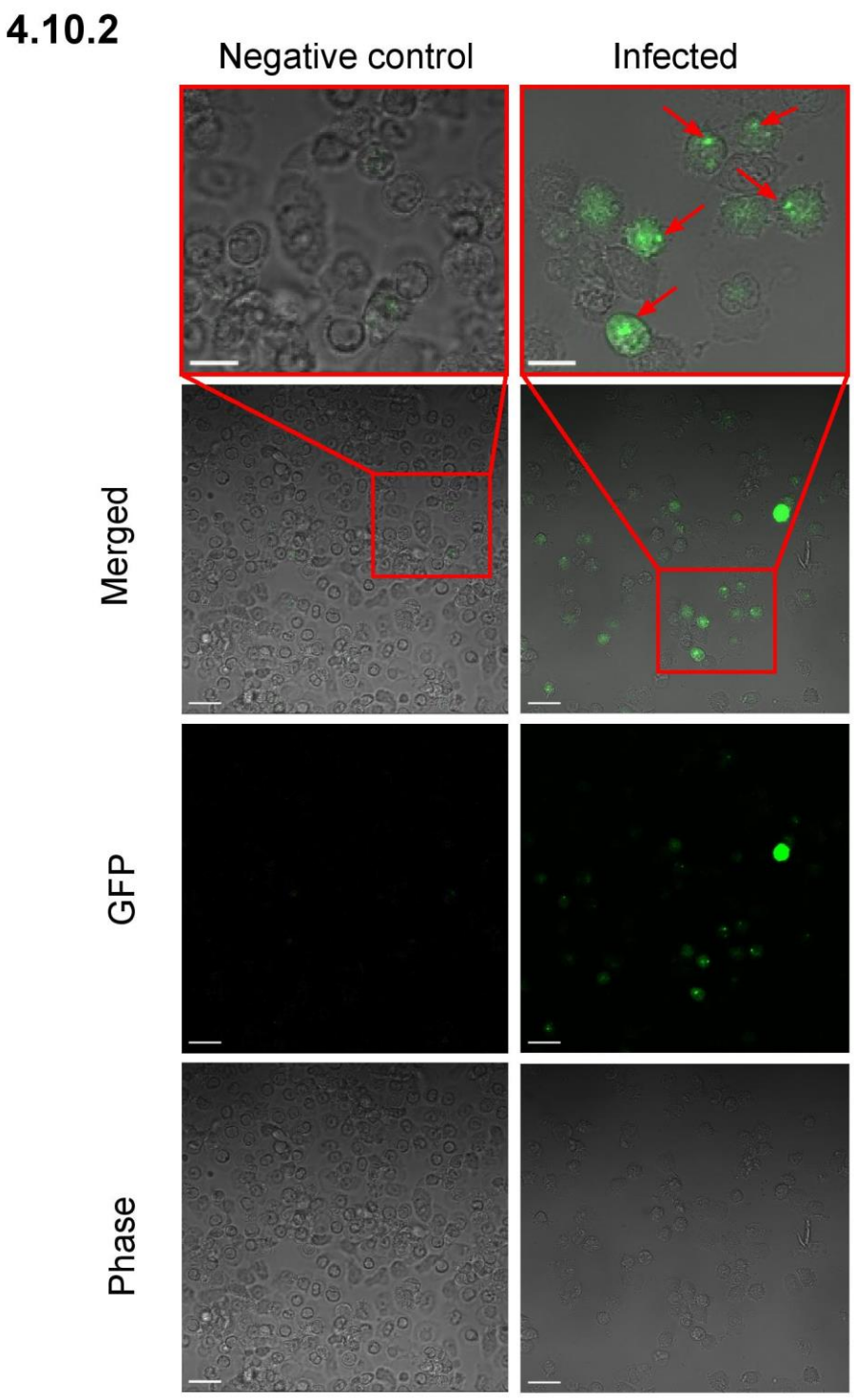

Figure 4.10.2 | Qualitative analysis of adenoviral GFP-tagged LC3 in WT day 4 Hoxb8 neutrophils. *Cells not infected are compared with infected cells, with brightfield phase and GFP laser settings. The red boxes show a magnified image from the two merged channels. The red arrows point to LC3 formation or autophagosomes in successfully transfected cells. Scale bars = 10 µm in red boxes, 20 µm in lower boxes.*

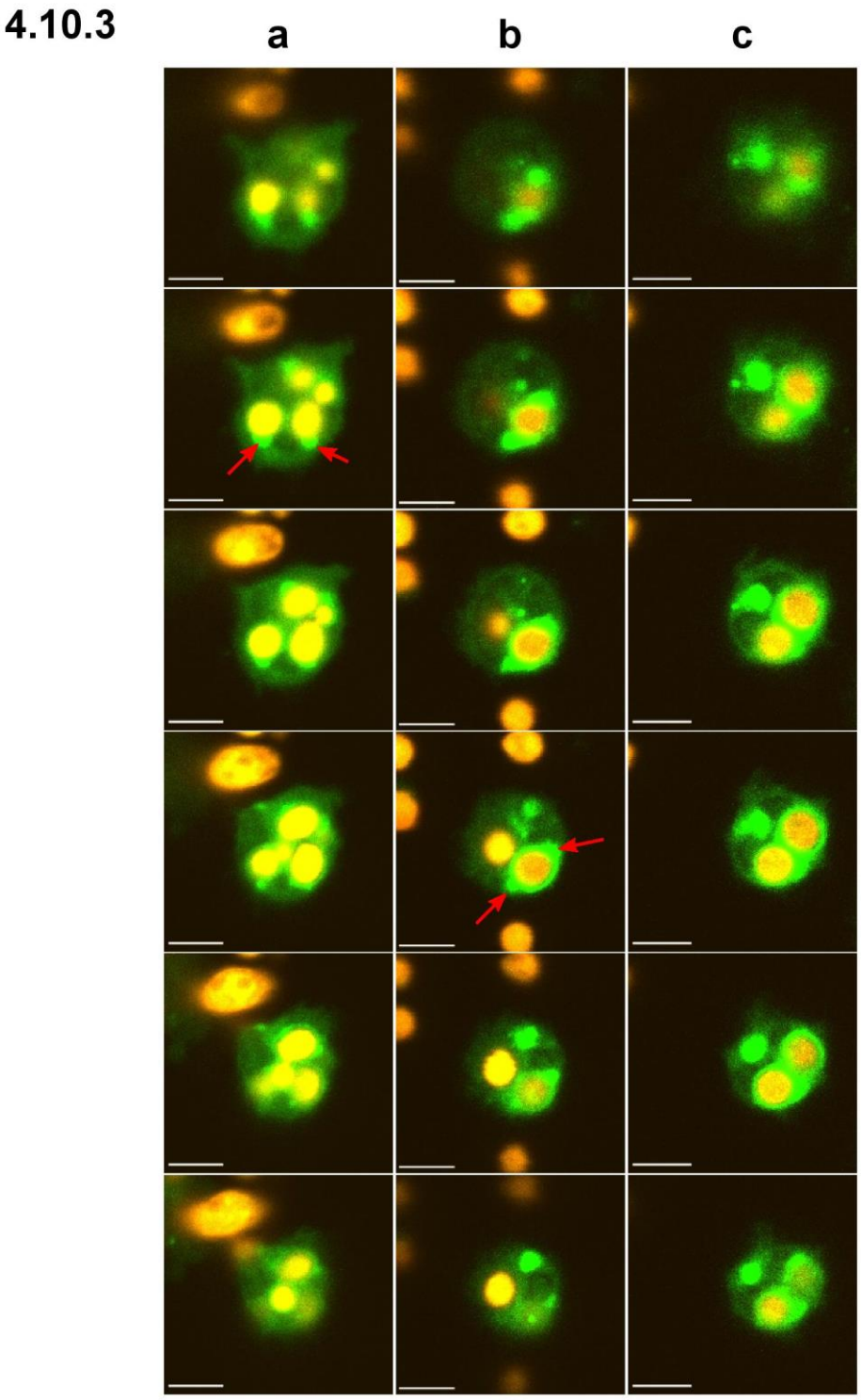

Figure 4.10.3 Qualitative analysis of GFP-LC3 formation in z stacks of phagocytosing WT day 4 neutrophils. (**a**) *An early phagosome with formative foci around engulfed Candida (red arrows).* (**b**) *A more advanced phagosome with a dense ring around one particle, foci at either pole (red arrows).* (**c**) *A cell containing 2 particles with bright GFP-LC3 labelled phagosomal membranes. Scale bars = 5 µm.*

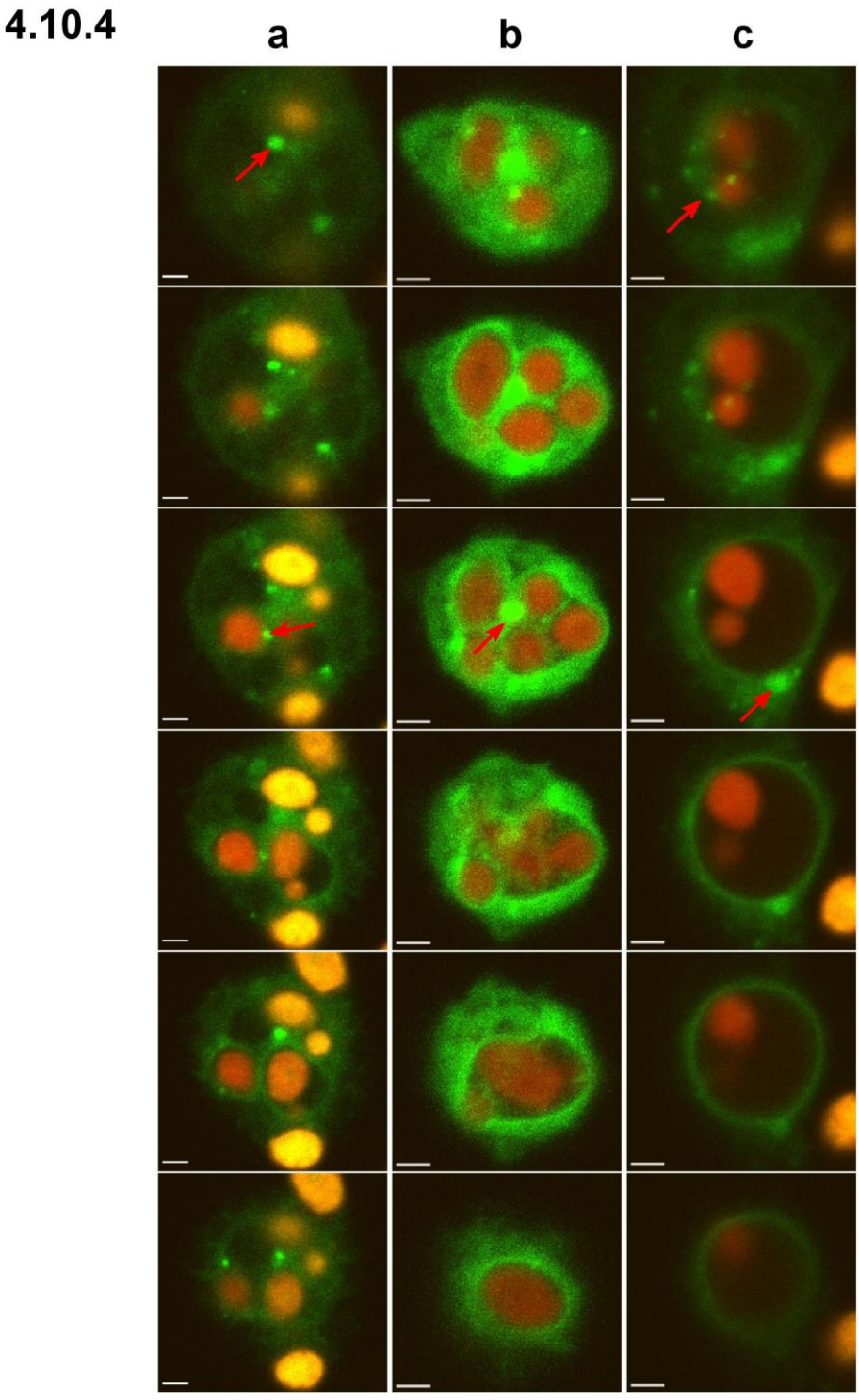

Figure 4.10.4 | Qualitative analysis of GFP-LC3 formation in z stacks of phagocytosing *Hvcn1*$^{-/-}$ day 4 neutrophils. (**a**) *A cell with scattered foci around some engulfed Candida (red arrows).* (**b**) *A cell containing several particles, some LC3 is located around the phagosomal membranes, with a bright central punctum (red arrow).* (**c**) *A cell containing a very swollen phagosome. One spot is present on the edge of the phagosome (bottom arrow), while there are scattered puncta on the top of the cell. Scalebar = 5 µm.*

4.11 Discussion

This chapter set out to assess the potential replacement of primary bone marrow neutrophils with a neutrophil cell line, in the context of investigating the phagosomal environment. The Hoxb8 cells used throughout my studies were generated out of the lab, but I was also able to generate a WT line myself through retroviral transduction of bone marrow cells with the *pMSCVneo-ER-Hoxb8* plasmid. The protocol is relatively straightforward, but a few variations exist in published methods that produce cells of different phenotypes. These variations should be noted with due care by researchers attempting to generate their cell lines, and when analysing and comparing the differentiated cells between published reports.

Probably the most significant impact on Hoxb8 cell generation are the contents in the extracellular medium in which the progenitors are transduced. As aforementioned, having SCF present in the medium with G-CSF creates cells of the granulocyte lineage (Wang *et al.*, 2006; McDonald *et al.*, 2011b), while SCF with GM-CSF generates cells that resemble macrophages (Wang *et al.*, 2006). Hoxb8 macrophages can also be produced when GM-CSF replaces SCF, and the resulting progenitors are differentiated with M-CSF after the removal of estradiol (Rosas *et al.*, 2011; Di Ceglie *et al.*, 2016). While the two macrophage differentiation methods appear to produce phenotypically similar cells, they have not yet been directly compared. One noticeable difference is that the undifferentiated GM-CSF Hoxb8 progenitors have high expression of CD11b (Rosas *et al.*, 2011), whereas the SCF-Hoxb8 cells have low (according to my own data and those published by (Wang *et al.*, 2006)).

The GM-CSF Hoxb8 cells do not only produce macrophages, according to Gran and colleagues monocytes can be acquired if the differentiation is stopped at 3 days using only GM-CSF as the growth factor (Gran *et al.*, 2018). However, if cell differentiation

time is increased, cells with dendritic cell characteristics are generated (Rosas *et al.*, 2011).

Moreover, a third haematopoietic growth factor, the ligand for the fms-like tyrosine kinase 3 receptor (Flt3L) (McKenna *et al.*, 2000), can be used in the expansion of Hoxb8 lineage cells. With Flt3L and M-CSF in the differentiation medium there were mostly macrophages, while Flt3L plus GM-CSF produced a mixed population of DCs and neutrophils (Redecke *et al.*, 2013). With other cytokine cocktail combinations, Redecke and co-workers also produced cells with similarities to B cells and T cells. These resulting permutations the cytokine cocktails have on the progenitors and their terminal cell progeny adds to our understanding of haematopoiesis and the bone marrow environment.

The Hoxb8 neutrophils used throughout this chapter correspond to those described by most published accounts (Wang *et al.*, 2006; McDonald *et al.*, 2011b; Zehrer *et al.*, 2018). Day 4 was found to be the optimum day for maturation by several parameters; the first was by cell viability and cell expansion. The medium was not changed or supplemented throughout differentiation to limit cell disruption, so it is possible the cells were running out of nutrients by day 6 which contributed to their degradation. Alternatively, it is well-known that neutrophils do not have lifespans of more than a few days, so if they appeared mature by day 4 and had entered cell cycle arrest (McDonald *et al.*, 2011b), they could not last for much longer based on primary neutrophil longevity. Four days of differentiation was also used by most groups (McDonald *et al.*, 2011b; Wiesmeier *et al.*, 2016; Weiss *et al.*, 2018; Zehrer *et al.*, 2018), but six days used by the original method (Wang *et al.*, 2006). Additionally, the number of cells seeded for differentiation has an impact on the cell maturation; the lower the number the quicker the maturation, but fewer cells in total. This expansion relationship may be altered for different research interests.

Researchers in the field have used Western blotting for investigation of protein expression in Hoxb8 differentiated cells, but as far as I am aware they have not yet studied in NADPH oxidase subunits. The protein expression is consistent with the functional respiratory burst experiments, in that there were almost identical levels of $gp91^{phox}$, $p47^{phox}$ and $p67^{phox}$ in primary cells compared with Hoxb8 day 4 neutrophils and no significant differences in the amount or rate of H_2O_2 detection. It is important to note that *Hvcn1*$^{-/-}$ neutrophils have the same amount of oxidase subunits as WT neutrophils, but different oxidase activity because of the missing charge compensating proton channel.

The similarity was not identical when measuring phagosomal pH. Although from snapshots of phagosomal pH and area the *Hvcn1*$^{-/-}$ Hoxb8 neutrophils appeared the same as the *Hvcn1*$^{-/-}$ primary neutrophils, in the time course experiments they were a little less alkaline. What consequences this may have on the cell functions can only be speculated without further research, but in the previous chapter, I showed that phagosomal pH fell before the respiratory burst in human neutrophils. Perhaps the *Hvcn1*$^{-/-}$ Hoxb8 neutrophils are lacking one or more ion channels that compensate a minor part of the NOX2-induced charge compensation. As such, they need to be used with caution in subsequent work, but this difference may be an advantage if the purpose is to elucidate which ion channels are involved in neutrophil phagosomal pH regulation.

Overall, the Hoxb8 neutrophil model provides a useful tool for investigations into neutrophil biology. As found with all cell lines, they exhibit differences to primary cells which warrant care when applying certain conclusions. Despite these, the advantages of their ease of cultivation and genetic alteration prove they have a place amongst the use of primary neutrophils and expansion of bone marrow progenitors *in vitro* without viral transduction.

Chapter Five: Variations in the phagosomal environments of human neutrophils and mononuclear phagocytes

Part of this work was carried out in collaboration with Simon Yona and Amit Patel at UCL. Their contributions are stated in relevant figure legends.

5.1 Background and aims

In my first results chapter, I investigated the ion conductances in the neutrophil phagocytic vacuole that contributed to NADPH oxidase-induced charge compensation. In the search for potential compensating channels, the literature of phagosomal pH regulation in other phagocytes was studied. The reasoning behind this was that other professional phagocytes – monocytes, macrophage subsets, and dendritic cell (DC) subsets – share similar functions with neutrophils and they share a common myeloid progenitor (or at least the haematopoietic stem cell for some DC subsets). Maybe they also share the same ion channels? But if they share similar mechanisms to regulate phagosomal pH, would that mean they also have similar phagosomal environments?

From previous reports, we know that different phagocytes exhibit different phagosomal pH, both in humans and mice. Macrophages have been most extensively studied, and the current dogma is that they have acidic vacuoles. This was found in mouse bone-marrow derived macrophages (Yates & Russell, 2005; El Chemaly *et al.*, 2014), rabbit alveolar macrophages (Nyberg *et al.*, 1992), mouse alveolar (Di *et al.*, 2006) and peritoneal macrophages (Geisow, D'Arcy Hart & Young, 1981). In human, in monocyte-derived (Bruns *et al.*, 2012) and alveolar (Di *et al.*, 2006; Bruns *et al.*, 2012) macrophages and macrophage-like cells from the THP-1 cell line (Bastiat-Sempe *et al.*, 2014). The only contrary report was by Canton from the

Grinstein lab, who found that macrophages polarised with IFN-γ and LPS maintained phagosomes of pH 7.5-8.5 for 30 minutes after phagocytosis of opsonised zymosan (Canton *et al.*, 2014).

It is known that monocytes, which constitute about 10% of all circulating white blood cells, are made up of three subsets in human peripheral blood (classified based on their CD14 and CD16 surface expression), classical $CD14^{+}$ $CD16^{-}$, intermediate $CD14^{+}$ $CD16^{+}$, and non-classical $CD14^{lo}$ $CD16^{+}$ (Passlick, Flieger & Ziegler-Heitbrock, 1989; Ziegler-Heitbrock *et al.*, 2010). Their phagosomal pHs have not been well characterised: in the reports that exist, they state that the whole monocyte population has acidic phagosomes (Wieland, Goetz & Neumeister, 2004; Narni-Mancinelli *et al.*, 2011). Classical monocytes make up approximately 85% of all monocytes, while intermediate and non-classical monocytes make up the difference in roughly equal numbers (Patel *et al.*, 2017; Boyette *et al.*, 2017).

Apart from neutrophils, it is only dendritic cells that have reportedly alkaline phagosomes. The pH between 7 and 8 is thought to disable the acidic lysosomal enzymes which would otherwise degrade antigens that DCs engulf and present on their cell surface membrane (Mantegazza *et al.*, 2008). Antigen presentation and subsequent activation of innate and adaptive cells are a crucial role of DCs.

Although there are studies comparing neutrophils with monocytes, or cultured macrophages to monocyte-derived DCs (MoDCs), there is no general report directly comparing all professional phagocytes together. Therefore, the investigations carried out in this chapter aimed to:

- Isolate peripheral cells or culture into differentiated cells using standard protocols
- Determine cell subsets by phenotypic analyses

- Measure phagosomal pH using the pH indicator SNARF-1 in monocytes, dendritic cells and monocyte-derived macrophages compared with neutrophils
- Measure the respiratory burst of suspension cells using the Amplex UltraRed assay
- Carry out a preliminary investigation into the pH of efferosomes in polarised monocyte-derived macrophages

5.2 Phagosomal pH and NADPH oxidase activity in neutrophils and monocytes

While neutrophils outnumber monocytes in the circulation, they are both able to travel quickly to sites of infection where they phagocytose pathogens (Rydstrom & Wick, 2007). Here I tested whether they share similar intracellular environments necessary to carry out this function. First, cells were isolated and analysed by flow cytometry and cytospin morphology. Neutrophils were isolated via dextran sedimentation, density gradient separation, and hypotonic lysis (**Fig. 5.2a**). The average purity was 94%, confirmed by the characteristic lobulated nuclei and pink, granulated cytoplasm. Monocytes were enriched from isolated peripheral blood mononuclear cells using a negative selection kit, which resulted in 91.8% purity (**Fig. 5.2b**). Most of the cells had kidney-shaped nuclei.

Phagosomal pH was then assessed kinetically over the first 30 minutes after ingestion of SNARF-labelled *Candida* (**Fig. 5.2c**). Neutrophil phagosomes alkalinised to a pH of approximately 8.5 within the first 5 minutes and were maintained for the remaining duration, as has been reported previously (Levine *et al.*, 2015). Monocytes also became alkaline, although to a lesser extent and more slowly. They reached a peak of about pH 7.7 after 10 minutes, which was maintained for the next 20 minutes. The

difference in pH calculated across the time course between neutrophils and monocytes was very significant: $p<0.0001$.

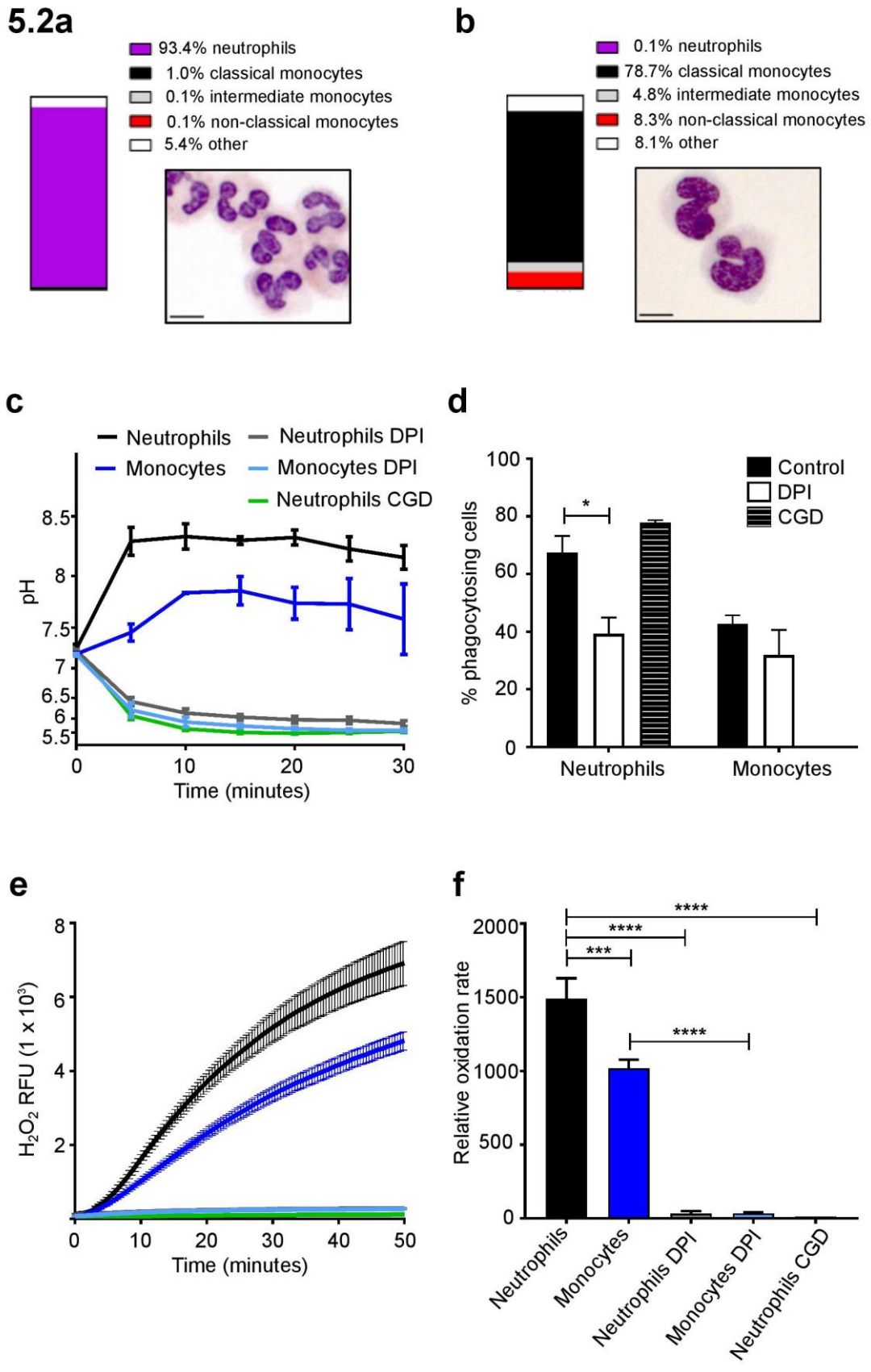

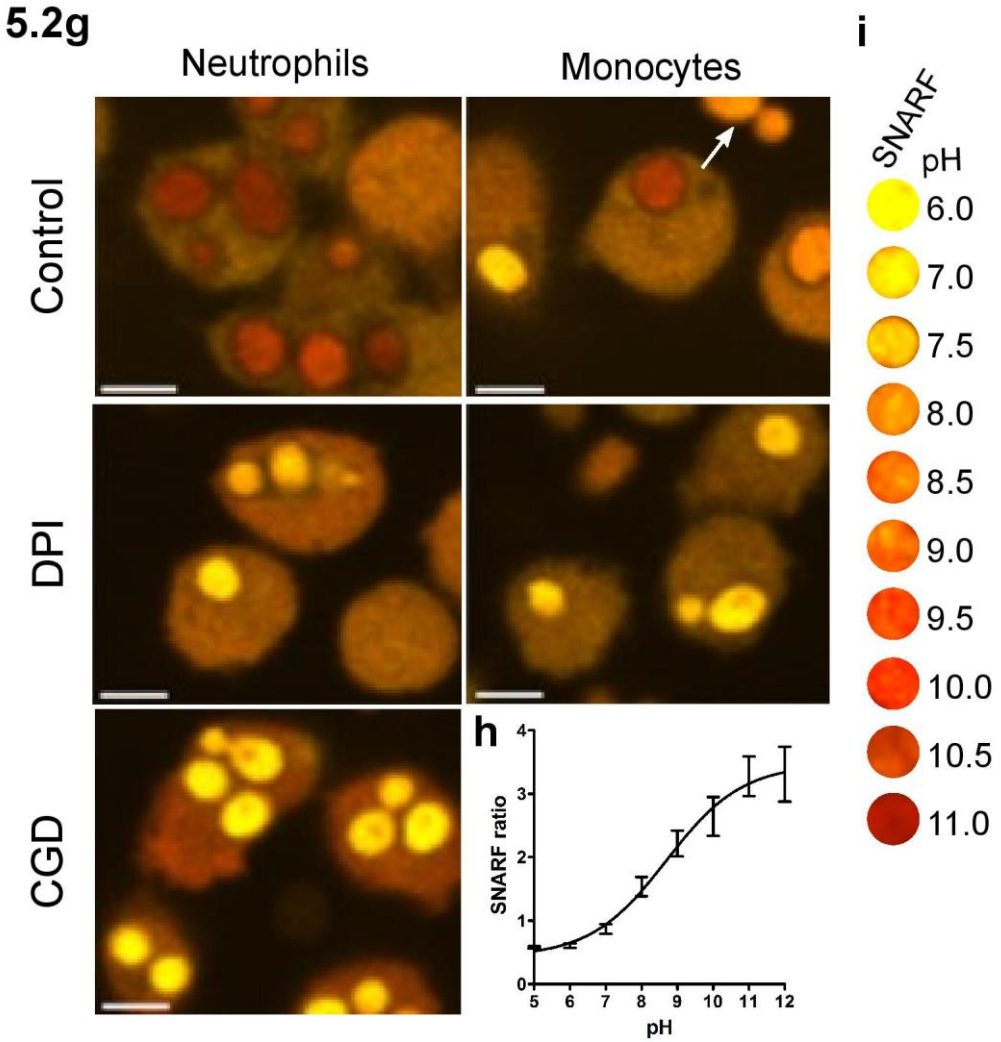

Figure 5.2 | Comparison of phagosomal pH and NOX2 activity between neutrophils and monocytes (a-h). *Isolation purity (carried out by A. A. Patel) and Wright-Giemsa stained preparations of* (**a**) *neutrophils and* (**b**) *monocytes.* (**c**) *Time course of changes in phagosomal pH when cells were challenged with SNARF-labelled Candida, with* (**d**) *quantitation of phagocytosis (mean ± SEM) from the pH time course experiments.* (**e**) *NADPH oxidase activity over 50 minutes after stimulation with PMA, mean (solid line) ± SEM (dashed lines) and* (**f**) *maximal respiratory rate*. *Calculated p values from one-way ANOVA with Bonferroni post-test analysis: *=p<0.05, ***=p<0.001, ****=p<0.0001, n = 3.* (**g**) *Illustrative confocal images taken from the time courses at about 15 minutes after particle phagocytosis, a white arrow points to an extracellular particle.* (**h**) *A graph showing the relationship of SNARF to pH and* (**i**) *a representative colour key. Scale bars = 10 µm.*

To determine the involvement of the NADPH oxidase on phagosomal pH, the cells were treated with 5 µM of diphenyleneiodonium (DPI), an inhibitor of the oxidase. It is a commonly used pharmacological inhibitor, but it has reported non-specific side effects. To account for these effects, cells were taken from a chronic granulomatous disease (CGD) patient who has a mutation in the CYBB gene which codes for gp91phox, specifically c.517delC, predicting p.Leu173CysfsX16 (information kindly supplied by Dirk Roos), which causes a complete loss of oxidase function (X-linked). Cells treated with DPI and those from the CGD patient for both neutrophils and monocytes rapidly acidified to pH 6-6.5 at 5 minutes, then to below pH 6 for the remaining test duration. The CGD results, therefore, confirm the findings with DPI, as there was no significant difference between their effects on pH (p>0.05). The difference between each control with DPI and with CGD conditions was statistically significant (p<0.0001). Representative confocal images of these conditions are shown in **figure 5.2g**, taken about 15 minutes after addition of *Candida*. The redder the engulfed *Candida*, the more alkaline the environment, while yellow is more acidic, demonstrated by the SNARF fluorescence to pH colour key (**Fig 5.2i**). Neutrophils had red, alkaline phagosomes, while there is more variety among the monocyte phagocytic vacuoles. Both neutrophils and monocytes treated with DPI, and both cell types from a CGD patient, had very yellow acidic phagosomes.

At the end of the time course assays, Trypan blue was added to the medium to quench extracellular fluorescence, and z-stacks were taken of the experimental field and another random location in the well. Phagocytosis was assessed by counting the number of cells which had phagocytosed at least one particle divided by the number of total cells. Neutrophils had a mean of 67.5% (SEM ± 5.7%), with monocytes slightly less (42.7% ± 2.9%), but the difference was not significant (**Fig. 5.2d**). However, treatment with DPI slightly reduced phagocytosis in neutrophils to 39.3% (SEM ± 9.8%, p<0.05). Neutrophils from the CGD patient phagocytosed efficiently; as it was

only possible to take a sample from one patient for one experiment, statistical analysis could not be performed, but this result suggests that CGD neutrophils could phagocytose better than healthy neutrophils treated with DPI. Monocytes treated with DPI phagocytosed normally.

Next, NADPH oxidase activity was measured using the same conditions. Similar to the phagosomal pH time courses, monocytes could mount an effective respiratory burst, but it was less than that of neutrophils, which has been observed before (de Rossi *et al.*, 2002; Chu *et al.*, 2013). As expected, the cells treated with DPI and cells from a CGD patient had almost no detectable NOX2 activity. The findings were the same in the kinetic measurement of total H_2O_2 induced fluorescence (**Fig. 5.2e**) and the maximum rate of fluorescence (**Fig. 5.2f**), meaning that the difference in the respiratory burst was significant between control conditions for neutrophils and monocytes, and between control and DPI or CGD conditions. There was no difference between the activity of cells treated with DPI and from CGD cells.

5.3 Phagosomal pH and NADPH oxidase activity in monocyte subsets

The previous data show that there are similarities between neutrophils and monocytes, but it remains to be answered if monocytes of different subsets also have similar phagosomal environments. There are increasing numbers of reported genetic differences between the subsets through whole genome and transcriptomic studies (Ingersoll *et al.*, 2010; Villani *et al.*, 2017; Cros *et al.*, 2010a; Wong *et al.*, 2011) which are confirmed in functional studies. So far, they have reported that the subsets have differences in cell size (Passlick, Flieger & Ziegler-Heitbrock, 1989), other surface markers than CD14 and CD16 expression (Ingersoll *et al.*, 2010), cytokine production (Almeida *et al.*, 2001), antigen presentation (Wong *et al.*, 2011; Zawada *et al.*, 2011), and migration (Cros *et al.*, 2010a), amongst others.

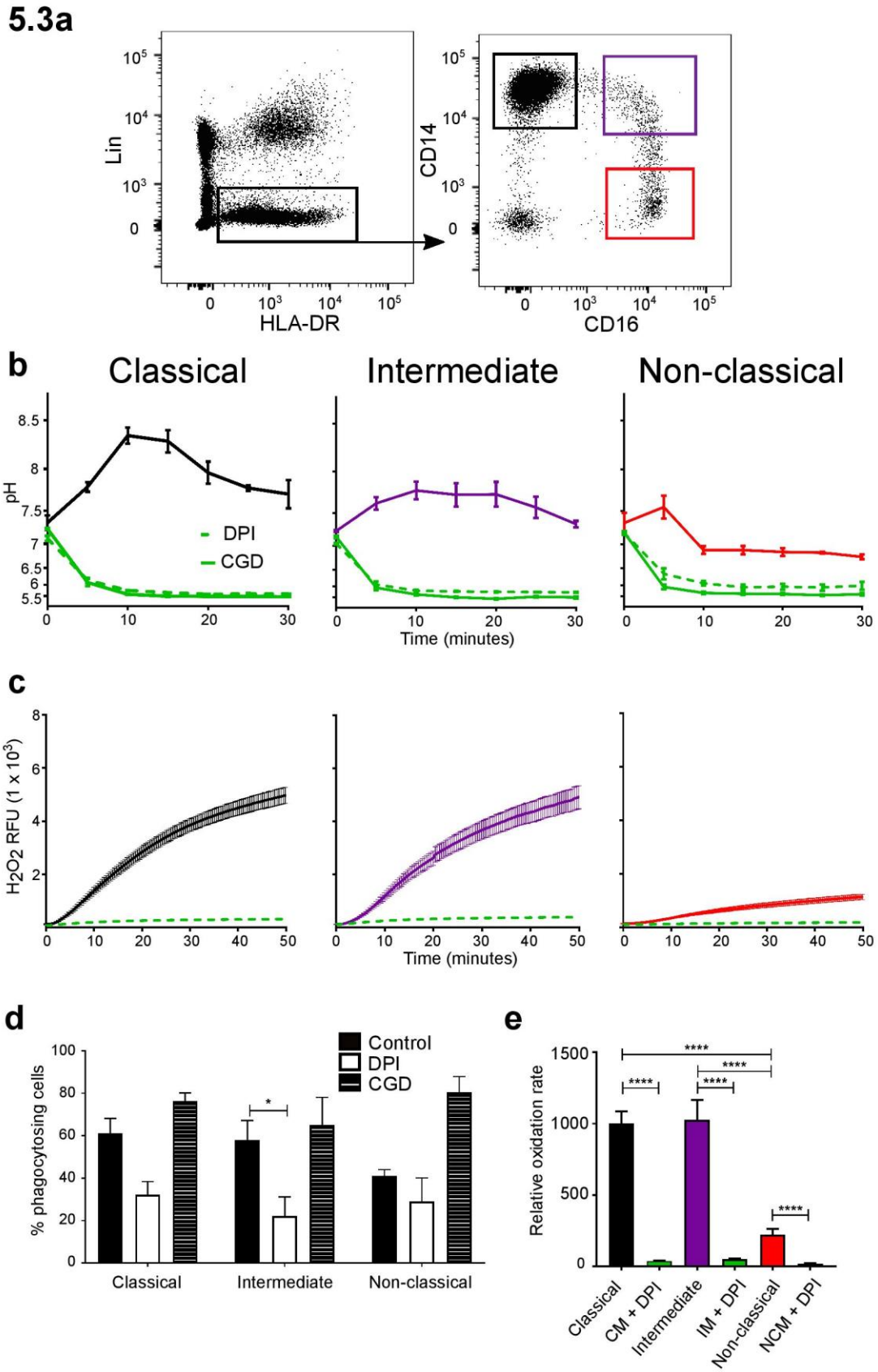

Figure 5.3 | The phagosomal environments of monocytes differ between subsets (a-h). *FACS gating strategy for monocyte subset isolation (by A. A. Patel)* (**a**) *lineage cells which expressed CD1c, CD3, CD11c, CD19, CD20, CD56, CD66b*

or CD123 were excluded, while the cells in the group gated on the HLA-DR axis were then separated by CD14 and CD16 expression into the monocyte subsets (shown in coloured boxes). (**b)** *Time course of changes in phagosomal pH in cells with and without 5 µM DPI, and in cells from a CGD patient. (**c**) NADPH oxidase activity over 50 minutes after stimulation with PMA, mean (solid line) ± SEM (dashed lines).* (**d**) *Quantitation of phagocytosis from the time course experiments, mean ± SEM,* (**e**) *maximal respiratory rate, mean ± SEM. Calculated p values from one-way ANOVA with Bonferroni post-test analysis: ****=p<0.0001, *=p<0.05, n = 3.* (**f**) *Representative confocal images from time course experiments with calibration of SNARF fluorescence to pH colour key. White arrows point to extracellular Candida. Scale bars = 10 µm.*

5.3f

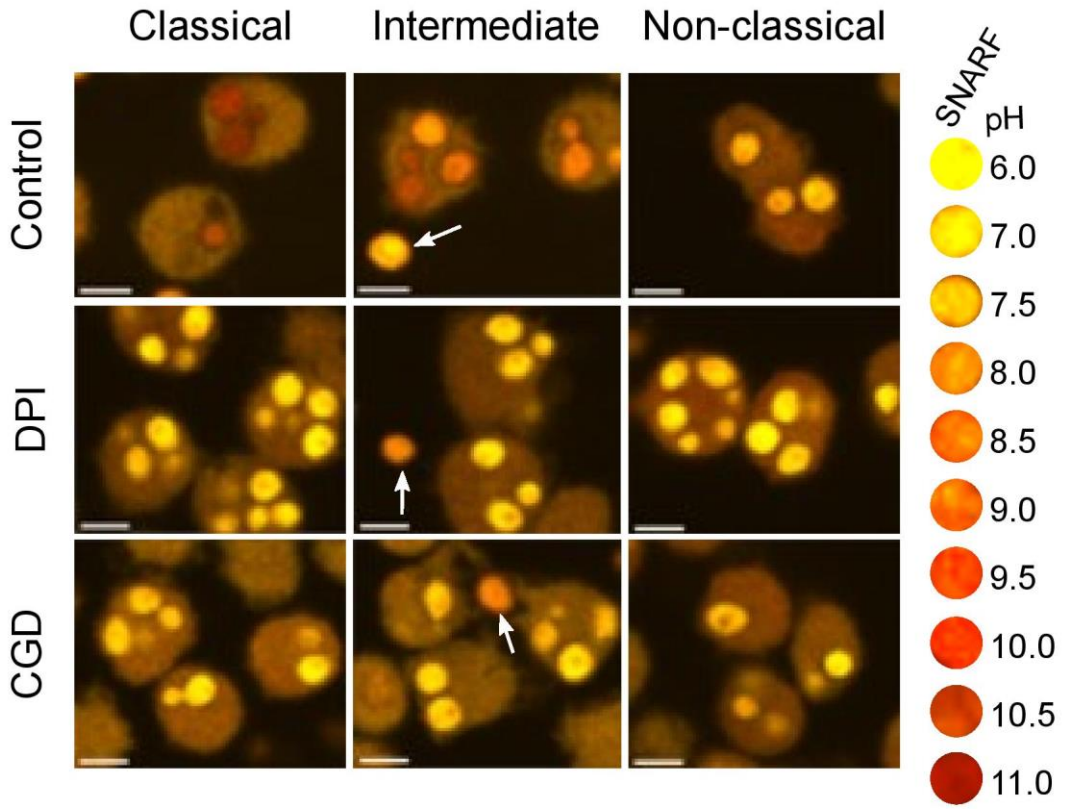

As there are currently no isolation kits available to separate the three subsets, they were divided by fluorescence assisted cell sorting (FACS) based on their CD14 and CD16 expression (**Fig. 5.3a**). The protocol was carried out by A. A. Patel using the panel described in his paper (Patel *et al.*, 2017).

It was found that the phagosomal pH profiles were distinct between the subsets (**Fig. 5.3b**). Classical monocytes were most like neutrophils; their phagosomes alkalinised

to around pH 8.5 by 10 minutes, but it was not maintained as it gradually fell to about pH 7.7. On the other hand, non-classical monocytes had a brief alkalinisation in the first 5 minutes, then the pH dropped to below 7.0 and remained slightly acidic for the remaining time course. Intermediate monocytes, true to their name, had phagosomal pH between the other two subsets. However, the phagosomes of all monocyte subsets became acidified when treated with DPI, which was further confirmed in cells from a CGD patient. Differences between each monocyte control condition were highly significant (p<0.0001) and between each control condition and DPI or CGD (p<0.0001). These findings are also represented by confocal image snapshots (**Fig. 5.3f**). Even though the phagosomal environments were different between subsets, the phagocytosis appeared equal between them (**Fig. 5.3**). However, again it was found that DPI caused a decrease in phagocytosis that was only statistically significant in intermediate monocytes (p<0.05). CGD monocytes from all subsets had good phagocytosis equivalent to healthy cells if not better.

Respiratory burst activity was assessed in the three subsets (**Fig. 5.3c and e**). Surprisingly, the total and rate of activity were very similar between classical and intermediate monocytes, despite there being differences in phagosomal pH. But non-classical monocytes exhibited a much smaller respiratory burst, where the rate was about 25% of classical and intermediate monocytes. These findings are consistent with the seminal report by Passlick and colleagues (Passlick, Flieger & Ziegler-Heitbrock, 1989), but differ from the report by Cros (Cros *et al.*, 2010a), who found that classical monocytes have the greatest respiratory burst while intermediate and non-classical monocytes both had very low bursts that were similar to each other. Here I found that all the monocytes have different phagosomal pH profiles, but classical and intermediate subsets share similar oxidase activity while non-classical monocytes have much lower activity.

5.4 Comparison of phagosomal environments between two dendritic cell subsets

DCs act as a crucial interface between the innate and adaptive arms of the immune system through their sensing of microbial components and subsequent activation of naïve T cells (Ridge, Di Rosa & Matzinger, 1998). They originate from the bone marrow by a unique pathway of lymphoid-myeloid haematopoiesis and differentiate into specialised subsets based on regulation of lineage-specific transcription factors (Lee *et al.*, 2015; McKenna *et al.*, 2000; Villani *et al.*, 2017). In blood, the main subtypes are plasmacytoid DCs (pDCs), class one conventional DCs (cDC1s), and class two conventional DCs (cDC2s) (Guilliams *et al.*, 2014). cDCs are mononuclear cells, but their formation is separate from that of monocytes. However, some monocytes *in vivo* can differentiate under inflammatory conditions into monocyte-derived DCs (MoDCs) (Segura *et al.*, 2013). MoDCs can also be generated *in vitro* only from classical monocytes (Boyette *et al.*, 2017; Sánchez-Torres *et al.*, 2001) and have been used as a surrogate model by many researchers as DCs are in scarce quantities in the blood, although their genetic profiles are divergent (Lee *et al.*, 2015; Breton *et al.*, 2015; Robbins *et al.*, 2008).

DCs were isolated from peripheral blood by the same FACS gating strategy employed for the monocyte subsets (**Fig. 5.4a**). No phagocytosis of SNARF-labelled *Candida* was detected by pDCs ($CD123^+$), cDC1s ($CD141^+$) were in too few numbers to accurately assess using these experimental parameters, leaving only cDC2s ($CD1c^+$) for examination with *in vitro* MoDCs. The differentiation of MoDCs from their parent classical monocytes was analysed using flow cytometry (**Fig. 5.4b**). They upregulated CD1a, CD1c and CD11c - all classical DC markers.

When challenged with SNARF-labelled *Candida*, the phagosomes of both subsets of DCs became acidic within the first 5 minutes and started to plateau around 10 minutes (**Fig. 5.4c**). MoDCs were less acidic than cDC2s, arriving at pH 6.5 at 30 minutes

after ingestion, compared to pH 6.0 for cDC2s. However, the phagosomal pH was affected by the addition of DPI with further acidification in both cell types, which was replicated in the cDC2s from a CGD patient. Interestingly, phagocytosis was not the same between DC subtypes; the MoDCs were much more phagocytic than the cDC2s by a mean of 60.7% ± SEM 2.7% to 26.0% ± 6.5% (p<0.05, **Fig. 5.4d**). This finding corresponds with a report that found MoDCs to have increased receptor-mediated endocytosis of immune complexes compared with cDC2 cells (Andersson *et al.*, 2012). Again, DPI treatment created a reduction in phagocytosis in MoDCs. Phagocytosis was already quite low in cDC2s, so the difference was not significant, but CGD cDC2s had comparatively much better phagocytosis than healthy cells.

Representative snapshot images of the pH time courses are shown in **figure 5.4g:** all the phagosomes appeared very yellow (acidic), apart from a few red phagosomes in MoDCs, an example is shown by the white arrow. Red phagosomes were scattered across the MoDC population in this manner, although most of their phagosomes were yellow. The white arrows in the other images point to extracellular *Candida* or unclosed phagosomes, while red arrows point to intracellular particles. It is also obvious how much larger the MoDCs are compared to cDC2s; they are not small and round like monocytes or conventional DCs but have changed into an almost macrophage-like morphology when they adhered to the microscopy plate.

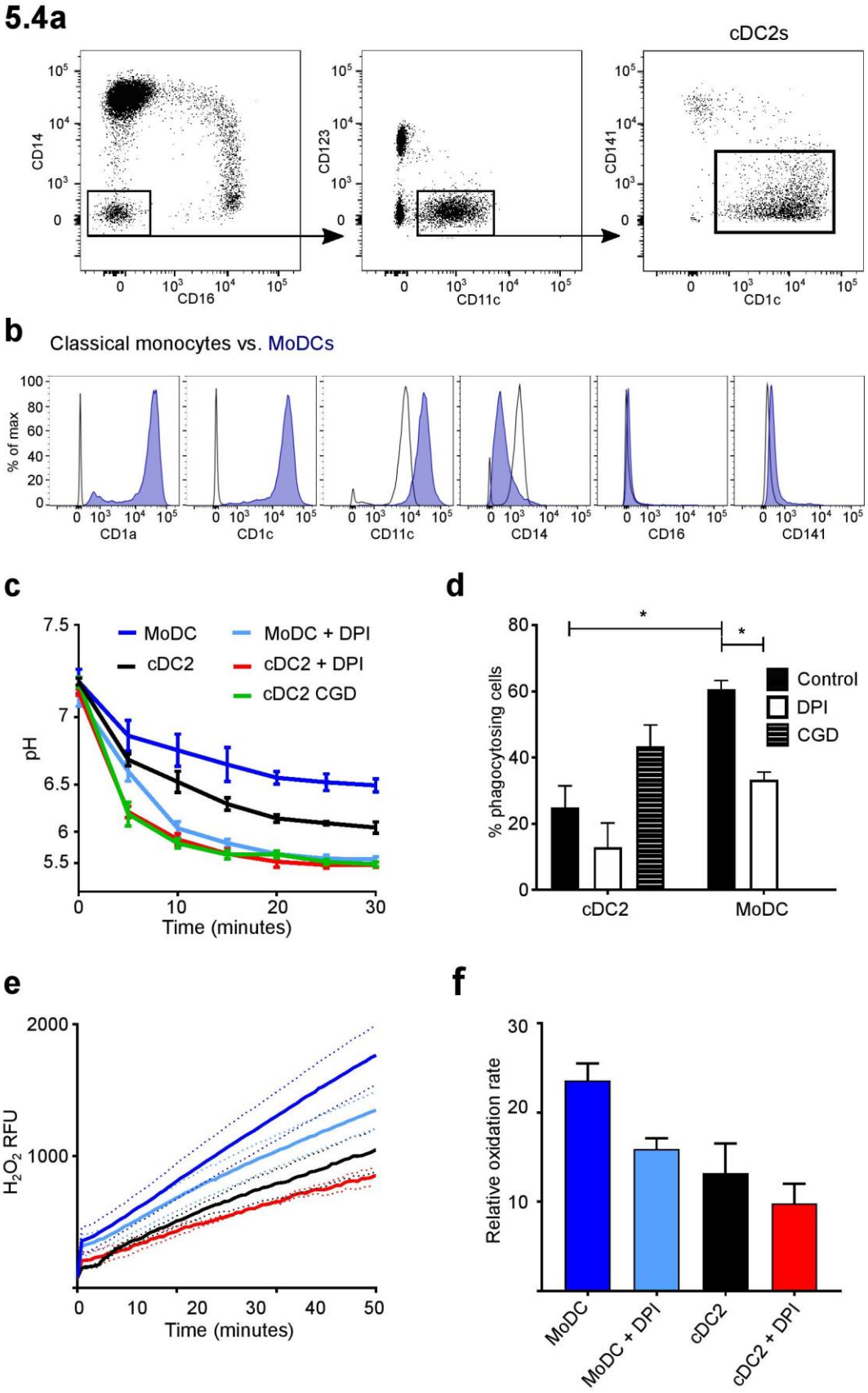
5.4a
cDC2s
CD14
CD16
CD123
CD11c
CD141
CD1c
b
Classical monocytes vs. MoDCs
% of max
CD1a
CD1c
CD11c
CD14
CD16
CD141
c
MoDC
cDC2
MoDC + DPI
cDC2 + DPI
cDC2 CGD
pH
Time (minutes)
d
% phagocytosing cells
Control
DPI
CGD
cDC2
MoDC
e
H2O2 RFU
Time (minutes)
f
Relative oxidation rate
MoDC
MoDC + DPI
cDC2
cDC2 + DPI

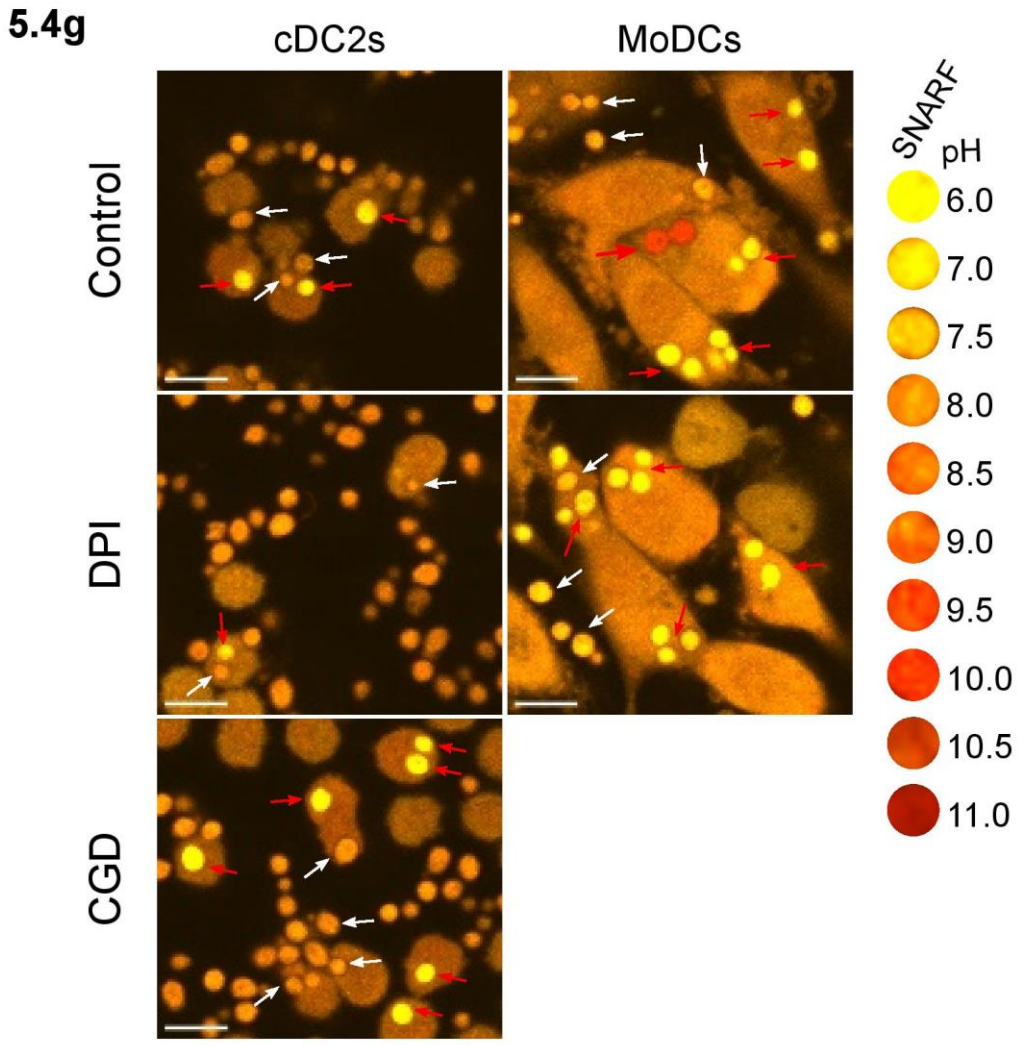

Figure 5.4 | cDC2s and MoDCs have acidic phagosomes with low oxidase activity (a-g). (**a**) *FACS gating strategy for isolating cDC2s based on their CD1c expression (by A. A. Patel); the CD14 and CD16 negative population was gated on CD11c and CD123; the CD11c*$^{+}$ *population was then gated on CD141 and CD1c.* (**b**) *Phenotypic analysis of MoDCs (blue) cell membrane surface expression compared with classical monocytes (grey).* (**c**) *Time course of changes in phagosomal pH in cDC2s and MoDCs, with treatment with DPI, and in cDC2s from a CGD patient.* (**d**) *Measurement of phagocytosis from time course experiments*. (**e**) *Time course of* H_2O_2 *induced fluorescence when stimulated with PMA,* (**f**) *maximal rate of* H_2O_2 *production from* (**e**). *Calculated p values from one-way ANOVA with Bonferroni post-test analysis: *=p<0.05, n = 3.* (**g**) *Representative images of phagocytosing cells. White arrows point to external Candida, and red arrows point to engulfed Candida. Scale bars = 10 µm.*

Respiratory burst activity was also different between the two cell types (**Fig. 5.4e and f**). MoDCs produced more H_2O_2 than cDC2s over the 50-minute time course (p<0.0001). Oxidase activity was reduced in both cell types with treatment with DPI but was only statistically significant in MoDCs. The relative oxidation rate was calculated between the last ten minutes of the time course, but there were no significant differences between cell conditions. To put these results into context, both subsets of DCs produced about 100-fold less H_2O_2 induced fluorescence than neutrophils.

5.5 The effect of LPS stimulation on MoDC phagosomal environment

There is some controversy in the field about the pH of DC phagosomes; it is either slightly alkaline between pH 7-8 (Mantegazza *et al.*, 2008; Dingjan *et al.*, 2016), or acidic under pH 6 (Rybicka *et al.*, 2011; Salao *et al.*, 2016). Unfortunately, the experimental protocols differ between these reports, particularly in how the cells are stimulated to activate the respiratory burst. Some research groups use pro-inflammatory ligands to activate DCs, such as the gram-negative bacterial wall component lipopolysaccharide (LPS) (Dinter *et al.*, 2014; Nastasi *et al.*, 2015; Ohradanova-Repic *et al.*, 2016), and formyl peptide receptor agonists such as *N*-formyl-Met-Leu-Phe (fMLP) have also been found to be effective (Karlsson *et al.*, 2007) in addition to PMA, while other labs used only PMA and did not record the use of any other priming agents (Andersson *et al.*, 2012; Mantegazza *et al.*, 2008). Both subsets of DCs were first tested without LPS, to remain consistent with the previous experiments with neutrophils and monocytes. As the phagosomal pH was found to be acidic and the respiratory burst activity was very small in these experiments, the effect of LPS was then tested on MoDCs with untreated MoDCs to see if the parameters could be augmented or were altered. MoDCs were treated with LPS overnight for 18 hours, and LPS was maintained in the experimental buffer.

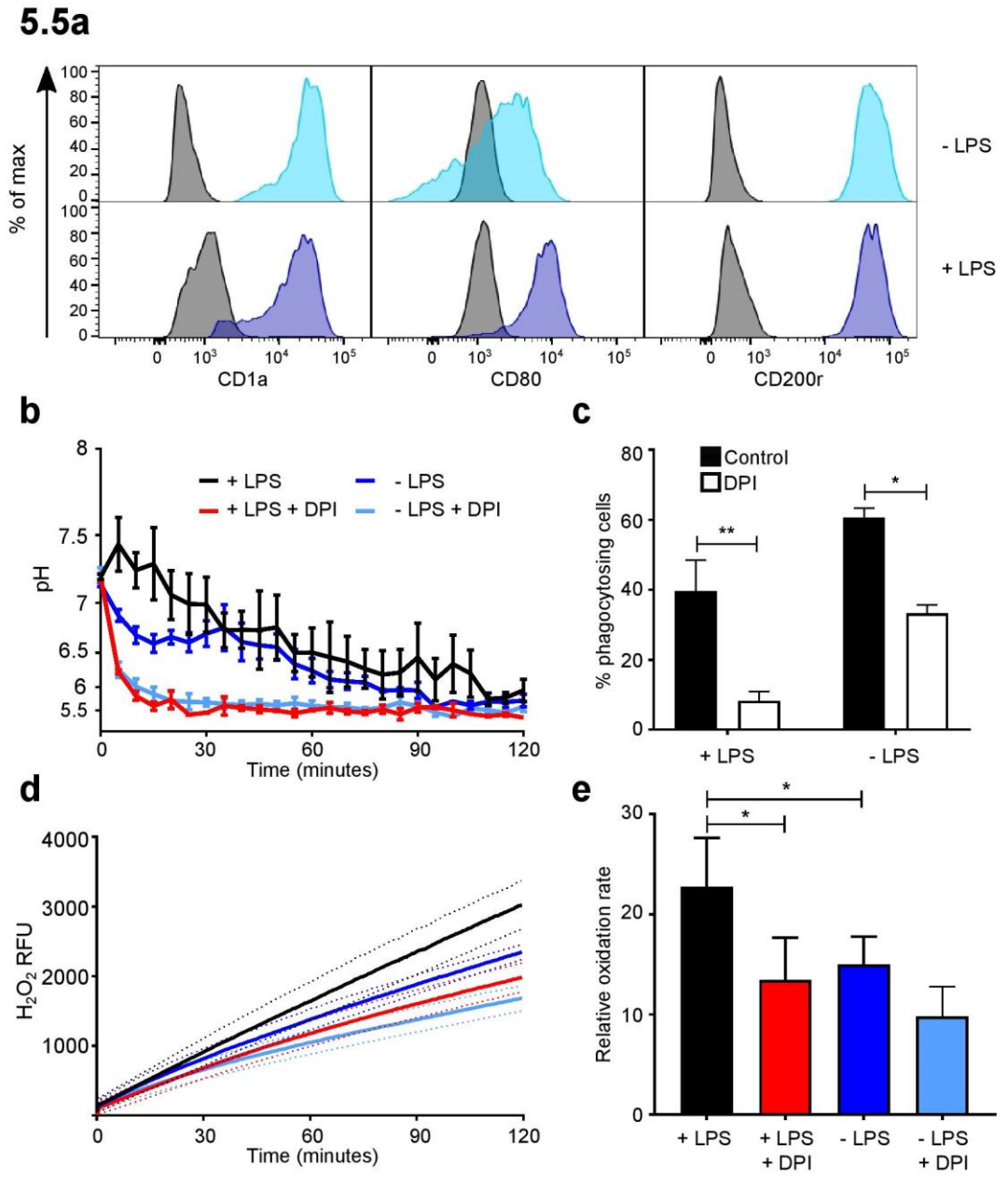

Figure 5.5 | LPS treatment increased the respiratory burst activity and phagosomal pH of MoDCs (a-f). (**a**) *Flow cytometry phenotypic analysis of differentiation in untreated and LPS treated MoDCs. Grey lines = unstained controls, light blue line = untreated MoDCs, dark blue line = LPS-treated MoDCs*. (**b**) *Time course of changes in phagosomal pH after phagocytosis of SNARF-labelled Candida, plotted as mean ± SEM in cells with and without treatment of 5 μM DPI.* (**c**) *Quantitation of phagocytosis from the time course experiments.* (**d**) *NADPH oxidase activity measured as H_2O_2 induced relative fluorescence units (RFU) after PMA stimulation, (**e**) relative oxidation rate calculated from the final 30 minutes of* (**d**). *Calculated p values from one-way ANOVA with Bonferroni post-test analysis: **=p<0.01, *=p<0.05, n = 3.* (**f**) *Representative confocal image snapshots of cells from*

the phagosomal pH experiments, with a SNARF-pH colour key. White arrows point to external or partially engulfed particles; red arrows point fully internalised particles. Scale bars = 10 µm.

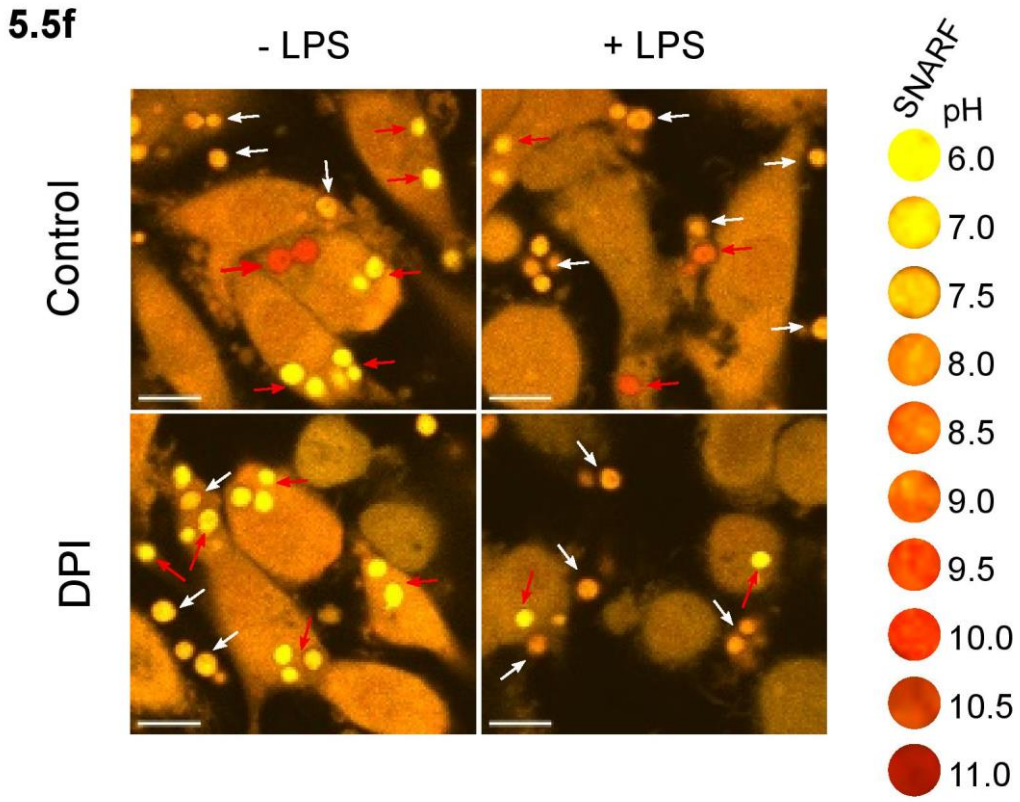

LPS is known to differentiate monocytes into a polarised "M1" macrophage phenotype, therefore, I studied the effect of LPS on some cell surface markers. They were CD80, used for classifying "M1" cells, CD200r for "M2" macrophages, and CD1a as a classical DC marker (Canton *et al.*, 2014). Both untreated and LPS treated MoDCs showed high expression of CD1a (**Fig. 5.5a**), repeating the findings from **figure 5.4b**. Interestingly they both showed high expression of CD200r, but CD80 was only upregulated in the treated MoDCs.

The changes in phagosomal pH were then compared between treated and untreated MoDCs (**Fig. 5.5b**). The experiment duration was increased to 2 hours to match the respiratory burst experiments, as suggested by other articles (Dingjan *et al.*, 2016; Mantegazza *et al.*, 2008; Kourjian *et al.*, 2016). While the phagosomes of untreated MoDCs acidified to pH 6.5 for the first 50 minutes, LPS-treated cells became more

alkaline to pH 7.4 within 5 minutes. After that, the phagosomal pH gradually fell until it reached the same pH as untreated cells at 50 minutes. They both reached pH 5.5 at 2 hours. In both cell types, the phagosomes were immediately acidified by treatment with DPI. The difference in phagosomal pH between treated and untreated MoDCs was highly significant (p<0.0001), and between each control condition with DPI (p<0.0001). DPI also decreased phagocytosis in both untreated and treated MoDCs (**Fig. 5.5c**). Fewer LPS-treated MoDCs phagocytosed opsonised *Candida* than non-treated MoDCs, but not by a significant margin.

The respiratory burst activity is shown in **figures 5.5d and e**. At 50 minutes into the assay, there was no marked difference between treated and untreated cells, but at 2 hours treated MoDCs produced more H_2O_2-induced fluorescence than untreated MoDCs. The calculated p value from one-way ANOVA with Bonferroni multiple comparison post-test between control conditions for the full-time course of oxidase activity was p<0.0001, and the same between each cell condition with DPI treatment. LPS-treated cells maintained a linear rate for the recorded 2 hours, while for untreated cells the rate started to slow down at 30 minutes. The relative oxidation rate (**Fig. 5.5e**) was calculated from the last 30 minutes of the time course experiment to highlight this difference, as the rates appear equal in the first 50 minutes of the experiment. The measured increase at the endpoint between untreated and LPS-treated MoDCs was about 22% (mean of 2344 to 3023 RFU), but still much lower than the burst of even non-classical monocytes tested at 50 minutes (mean of 1.15 x 10^4 RFU).

The representative snapshots of the phagosomal pH assays (**Fig 5.5f**) point to two red phagosomes in the LPS-treated MoDCs; although there were very red phagosomes observed in untreated-MoDCs (highlighted by the red arrow), there were also more very acidic yellow phagosomes. There were more red phagosomes in

treated cells, but they still had several acidic phagosomes (top left red arrow): there was heterogeneity in both cell types.

5.6 The effect of macrophage polarisation on phagosomal pH

The formation of the macrophage killing compartment undergoes different steps from that of neutrophils. It begins life as an early phagosome after engulfment of the pathogenic material. With increasing fusion of endosomes over time it becomes a late phagosome, then with fusion of lysosomes, it finally graduates into a phagolysosome (Yates, Hermetter & Russell, 2005). The reported pH of the macrophage phagolysosome has always been acidic under pH 6, in normal conditions, which is thought to be essential for the killing of bacteria. This is evidenced through studies with certain bacteria that fall prey to the acidic environment (Ip *et al.*, 2010), and those that can manipulate the host phagolysosome to make it more accommodating for their proliferation (Sturgill-Koszycki *et al.*, 1994; Podinovskaia *et al.*, 2013; Kasper *et al.*, 2014; Bewley *et al.*, 2011).

One of the few studies that report a different macrophage phagosomal pH was carried out in the Grinstein lab (Canton *et al.*, 2014). They found that by polarising human monocytes with GM-CSF, interferon (IFN)-γ and LPS, the resulting “M1” macrophages had alkaline phagosomes for at least for 30 minutes after phagocytosis. In contrast, monocytes polarised with M-CSF and IL-4 had the typical acidic phagosomal compartments (under pH 6).

The group first used fluorescein isothiocyanate (FITC) labelled zymosan to measure phagosomal pH in “M1” and “M2” subsets, then confirmed the “M1” alkaline phagosomes using SNARF-1. FITC has a lower pKa value, 6.3 (Lavis, Rutkoski & Raines, 2007), than SNARF-1, 7.5 (Tsien, 1989), meaning that SNARF-1 is better suited for measuring more alkaline environments. I set out to repeat these findings

using only SNARF-1 as per the previous experiments, but also in comparison with monocytes cultured without the differentiating cytokines (“M0” macrophages).

Using the same differentiation markers as Canton, I optimised the differentiation protocol to generate the different subsets by culturing the monocytes in the microscopy plates then lifting them off for flow cytometry analysis (**Fig. 5.6a**). The “M1” subset showed increased expression of CD80, the M1 marker, from M0 cells. While the “M2” subsets showed increased CD200r expression from “M0” macrophages. None of the macrophage subsets expressed the classical dendritic cell marker, CD1a.

The phagosomal pH time course experiments were consistent with the Canton paper (**Fig. 5.6b**). “M1” macrophages were alkaline at 5 minutes after phagocytosis, and like neutrophils, maintained phagosomal pH at around pH 8.5 for at least 25 minutes. “M2” macrophages acidified their phagosomes in a similar fashion to non-classical monocytes, by maintaining their phagosomes around pH 6 for the experiment duration. There were a few scattered alkaline phagosomes in “M0” macrophages over the first 15 minutes, but the mean phagosomal pH was closer to that of “M2” cells by remaining under pH 7.5.

Cells were also treated with DPI to study the effect of the oxidase on phagosomal pH. “M1” macrophages exhibited robust acidification, as did “M0” cells, to fall to about pH 6 and pH 5.5 at 30 minutes for each respectively. The phagosomes of “M2” macrophages also further acidified, but the decrease was not significantly different. It may mean that NOX2 does not play an integral role in phagosomal pH regulation of “M2” cells compared to “M1” and “M0” macrophages.

Representative snapshots of each cell subset are displayed in **figure 5.6c**, approximately 15 minutes after addition of yeast particles. There was heterogeneity in all control cell conditions; some “M1” macrophages had yellow, acidic phagosomes,

while some “M2” macrophages had very red, alkaline phagosomes, but all cells had very yellow, acidic phagosomes when treated with DPI.

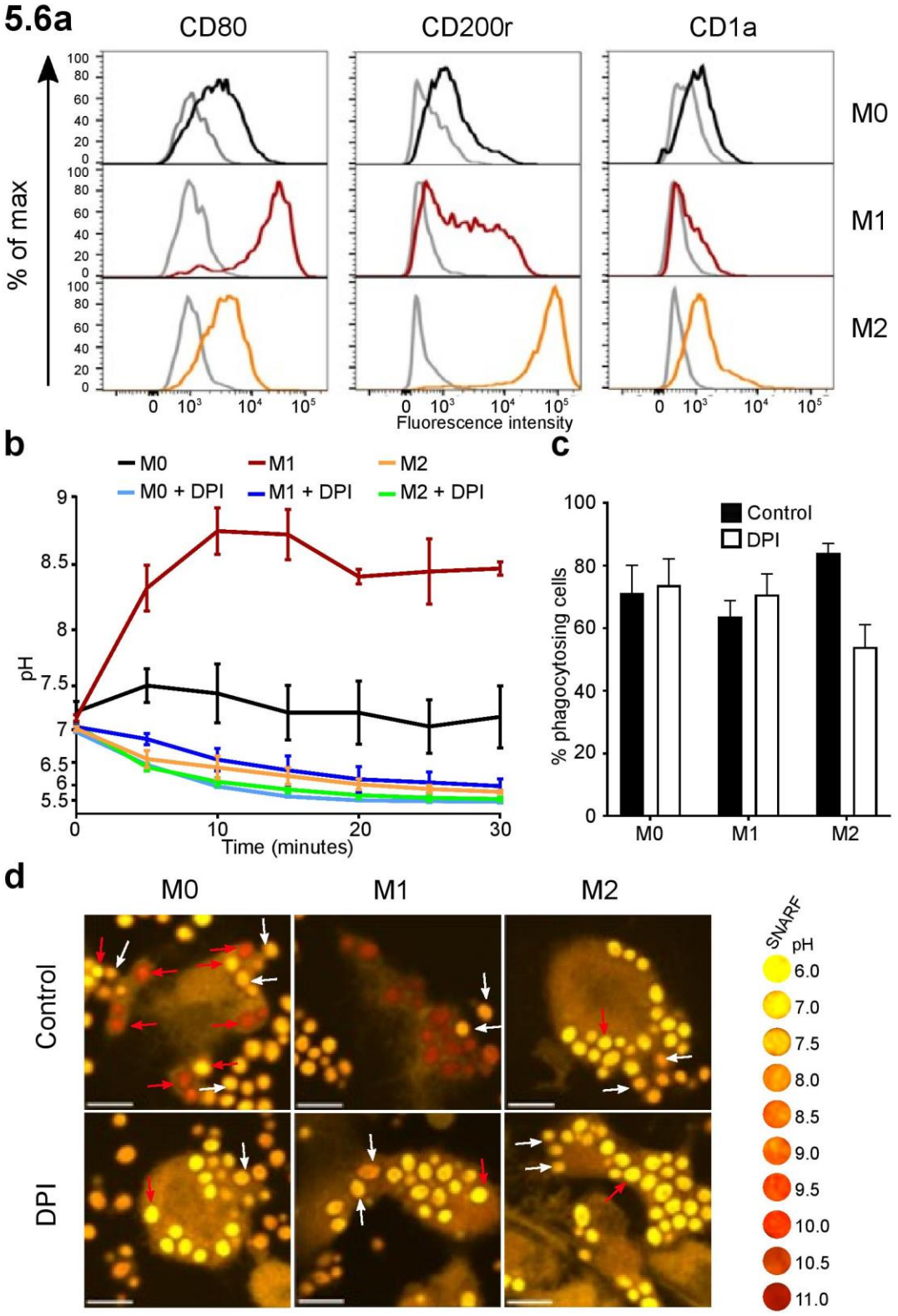

Figure 5.6 | Phagosomal pH varies between different monocyte-derived macrophage subsets (a-d). (**a**) *Phenotypic validation by flow cytometry of monocyte-derived macrophage differentiation from undifferentiated macrophages "M0" into classically activated "M1" and alternatively activated "M2" macrophages. CD80 was used as a marker for "M1" differentiation, CD200r for "M2", and CD1a to exclude dendritic cell differentiation. Isotype controls are shown in grey for each cell and marker.* (**b**) *Time course of changes in phagosomal pH in the three subsets with and without 5 μM DPI.* (**c**) *Measurement of phagocytosis from the time course experiments, mean is plotted ± SEM, n = 3.* (**d**) *Confocal image snapshots of cells approximately 15 minutes after Candida challenge, red arrows show internal particles; white arrows point to external. Scale bars = 10 μm.*

5.7 Preliminary investigations of pH within the efferosomes of polarised monocyte-derived macrophages

Efferocytosis is an essential process in multicellular organisms with constant cell turnover, but it is also very important in the context of inflammation. Macrophages (Hart *et al.*, 1997) and dendritic cells (Tzelepis *et al.*, 2015) are the main players in the removal of apoptosing cells, the majority of which are neutrophils, in the resolution of inflammation (Martin *et al.*, 2012).

One study of efferocytosis in human polarised macrophages (Yin *et al.*, 2016) found that human "M0" and "M2" macrophages were much more phagocytic in their apoptotic neutrophil uptake than "M1" macrophages, which has been shown elsewhere (McPhillips *et al.*, 2007; Michlewska *et al.*, 2009; Feng *et al.*, 2011). However, to the best of my knowledge, "efferosomal" pH has not yet been studied in human "M1" or "M2" macrophages, but found to be acidic in mouse bone-marrow derived macrophages (Bagaitkar *et al.*, 2018). As I had a method set up for measuring phagosomal pH in macrophages, I wanted to attempt to measure pH inside macrophage efferosomes.

To generate human apoptotic neutrophils, neutrophils were isolated from fresh blood and resuspended in RPMI with human serum albumin and antibiotics, and left to spontaneously apoptose in the cell culture incubator (Maderna *et al.*, 2005). Apoptosis was assessed by the annexin V-propidium iodide flow cytometry assay (Vermes *et al.*, 1995)(**Fig. 5.7.1**). When cells begin to undergo apoptosis, phosphatidylserine (PS) translocates from the inner side of the plasma membrane to the outer surface. Annexin V, here conjugated to the fluorescent probe FITC, binds to PS with high affinity. Propidium iodide (PI) allows detection of necrotic cells through their damaged cell membrane, which can also express PS, but intact cells will not stain well with PI (Wallberg, Tenev & Meier, 2016).

Freshly isolated neutrophils had mostly viable cells that were negative for annexin V and for PI. After 24 hours incubation, there was an increase in early apoptotic (annexin V^+/PI^-) and late apoptotic (annexin V^+/PI^+) cells, which was further increased at 48 hours. The forward by the side scatter plot also shows the decline from the neat population of healthy cells at 0 hours, to increased debris and smaller cells at 24 and 48 hours. At 24 hours, about 60% of cells were in early or late apoptosis, while for 48 hours is was about 71%.

The staining of apoptotic neutrophils with the succinimidyl ester form of SNARF-1 was then optimised. 24 hr neutrophils labelled more efficiently and degraded less quickly than the 48 hr cells; their number was severally reduced in the washing steps. Polarised macrophages were generated by the same method as used for the previous experiments. In contrast to the phagosomal pH experiments, macrophages were stained with calcein. This is also a cell-permeable cytosolic dye that emits on the green end of the spectrum, so that engulfed neutrophils could be delineated from macrophages.

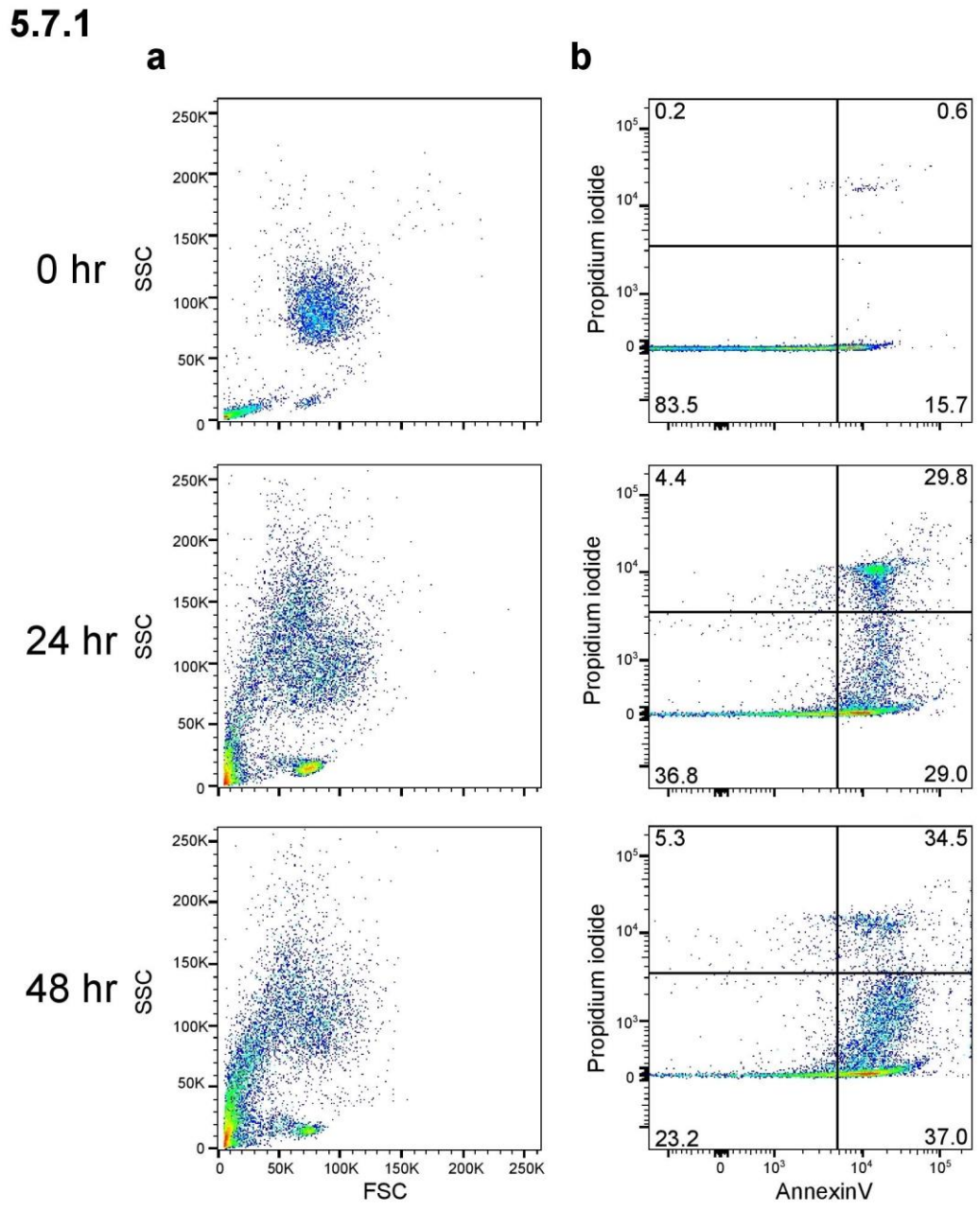

Figure 5.7.1 | AnnexinV-Propidium iodide assay for apoptotic neutrophils (a-b). *Forward by side scatter dot plots on panel* (**a**) *show degradation and shrinkage of cells with spontaneous apoptosis in neutrophils: freshly isolated, 24 hr and 48 hr after isolation. Panel* (**b**) *presents plots of measured fluorescence intensity of FITC conjugated to annexin V versus propidium iodide. Inside the plots, the bottom left panel show viable cells, bottom right early apoptotic cells, top right late apoptotic/necrotic cells. Numbers are percentages of total cell population in that quadrant.*

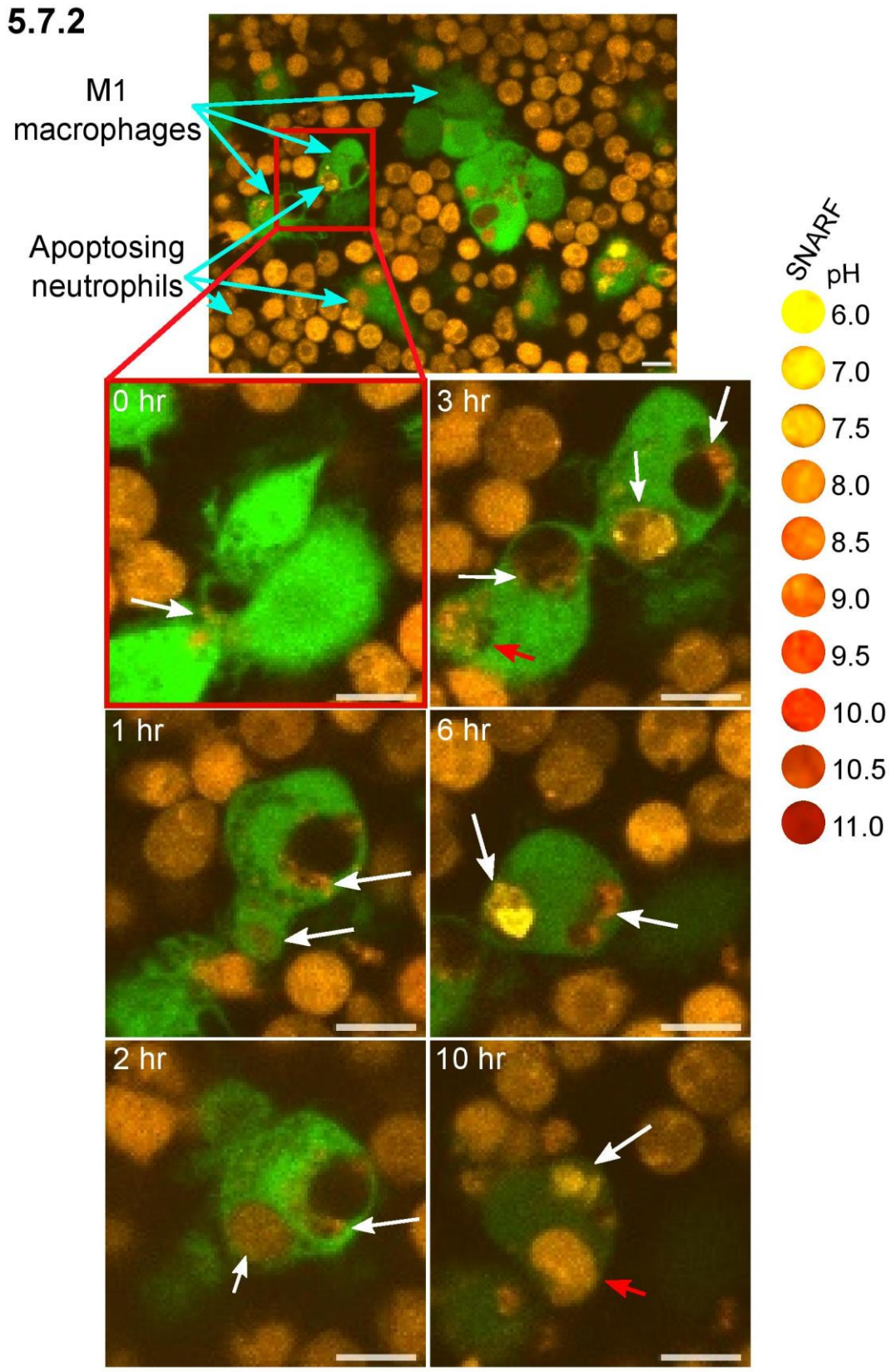

Figures 5.7.2 and 5.7.3 | Confocal images of live polarised macrophages efferocytosing apoptotic neutrophils. *The top image is a widefield shot of macrophages approximately 2 hours after addition of neutrophils, scale bars = 20 µm.*

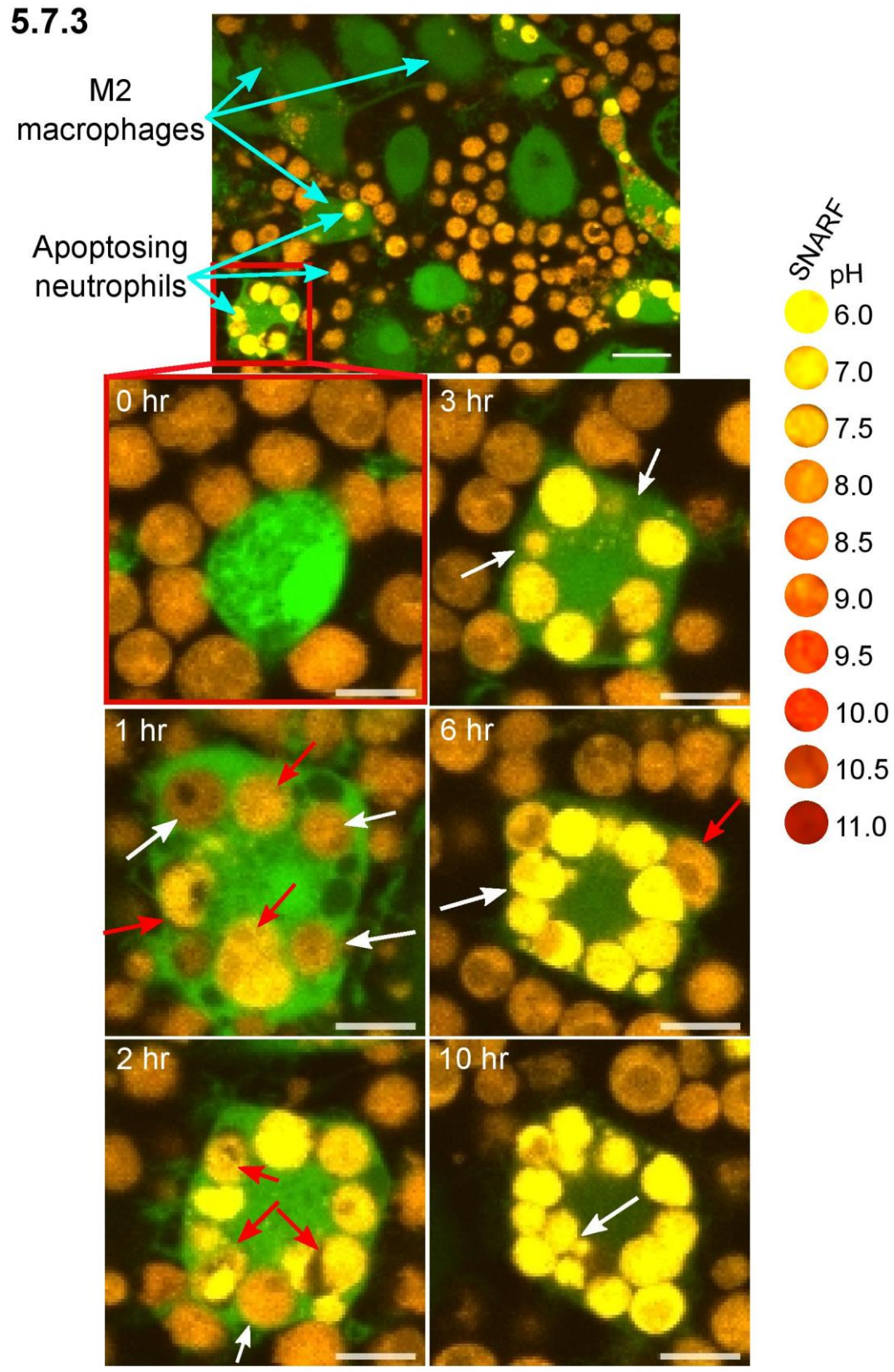

The smaller boxes show a magnified area detailing the progression of efferocytosis from 0 to 10 hours in "M1" (5.7.2) and "M2" (5.7.3) polarised macrophages. Scale bars = 10 µm.

Labelled neutrophils were added to macrophages; then an image was taken every 5 minutes for 12-15 hours. Efferocytosis is known to be a slower process than phagocytosis (Yin *et al.*, 2016). The preliminary results are shown qualitatively in **figures 5.7.2** (for “M1” macrophages) and **5.7.3** (for “M2” macrophages).

Figure 5.7.2 details efferocytosis in classically activated “M1” macrophages. Based on a qualitative assessment of two full experiments, they were poorly phagocytic as few cells took up apoptosing neutrophils (AN), and those that did took up a small number. However, the smaller images show a time course of a “M1” macrophages taking up some AN. At 0 hr, the white arrow points to a cell being taken up within a small dark efferosome at one end of the macrophage. At 1 hr, the void within the efferosome has become larger, and fragments of the AN are visible around the corner of the compartment as small orange fragments. This is maintained to 2 hr, when the macrophage takes up another AN (bottom arrow). But at 3 hr, the new bottom efferosome has changed in colour from orange (neutral) to yellow (more acidic), while the original efferosome has remained orange if becoming more red. A cell in the bottom left corner also has efferosomes containing orange AN; the white arrow points to another efferosome with empty space, the red arrow points to a slightly earlier engulfment. At 6 hr the more alkaline efferosome is maintained, while the other efferosome becomes even more acidic (<pH 7). Both have decreased in size. Four hours later, the acidic compartment is still acidic and has further shrunk (white arrow). The alkaline efferosome is not visible, but the red arrow points to a newly phagocytosed AN.

The wide-field view of “M2” macrophages, shown in the top image of **figure 5.7.3**, shows cells that appear more phagocytic than the “M1” macrophages, even though at 2 hours after addition of AN there are some macrophages which have not engulfed any particles. The lower panels magnify one highly active macrophage. By 1 hour after challenge with AN, the cell has engulfed at least 8 particles. The red arrows point

to later efferosomes with yellower, more acidic (~ pH 7) engulfed particles, and the white arrows indicate slightly earlier engulfed AN. An hour later, the macrophage has taken up more particles, such as one depicted by the white arrow. The red arrows show some engulfed AN starting to contract and break down with more acidic pH. The 3-hr image shows further degradation of dispersed particles with compartments below pH 6. Three hours later, the macrophage has engulfed more AN, such as one highlighted by a red arrow. The white arrow demonstrates engulfed AN from an earlier time point that are still very acidic, in contrast to the neutral extracellular AN. Four hours later, the engulfed AN are still very acidic and smaller in size, but not totally degraded.

5.8 Discussion

This chapter set out to directly compare the phagosomal environments of several phagocytic immune cells using the same pH indicator, SNARF-1, and with the same NADPH oxidase activity assay. There appeared to be differences between all subsets of cells examined, but they mostly fell into two groups. Those with more alkaline phagosomes; neutrophils, classical monocytes, LPS-treated monocyte-derived DCs and “M1” macrophages, and those with more acidic phagosomes; non-classical monocytes, cDC2 dendritic cells, untreated MoDCs, and “M2” macrophages. A summary **figure 5.8** compares all cell subsets together by (a) phagosomal pH at 15 minutes after ingestion, and (b) maximum rate of NOX2 activity. The macrophages were not tested by Amplex UltraRed assay as it was only optimised for suspension cells.

It is of importance to know the specific pH of each cell’s phagosome, as it will have a consequential effect on the enzymology of proteins within these compartments and in turn on the cell’s function. Generally speaking, the functions of the phagosomal

compartments in innate phagocytes can be split into two categories: killing and digestion of pathogenic and host material, or antigen processing and presentation.

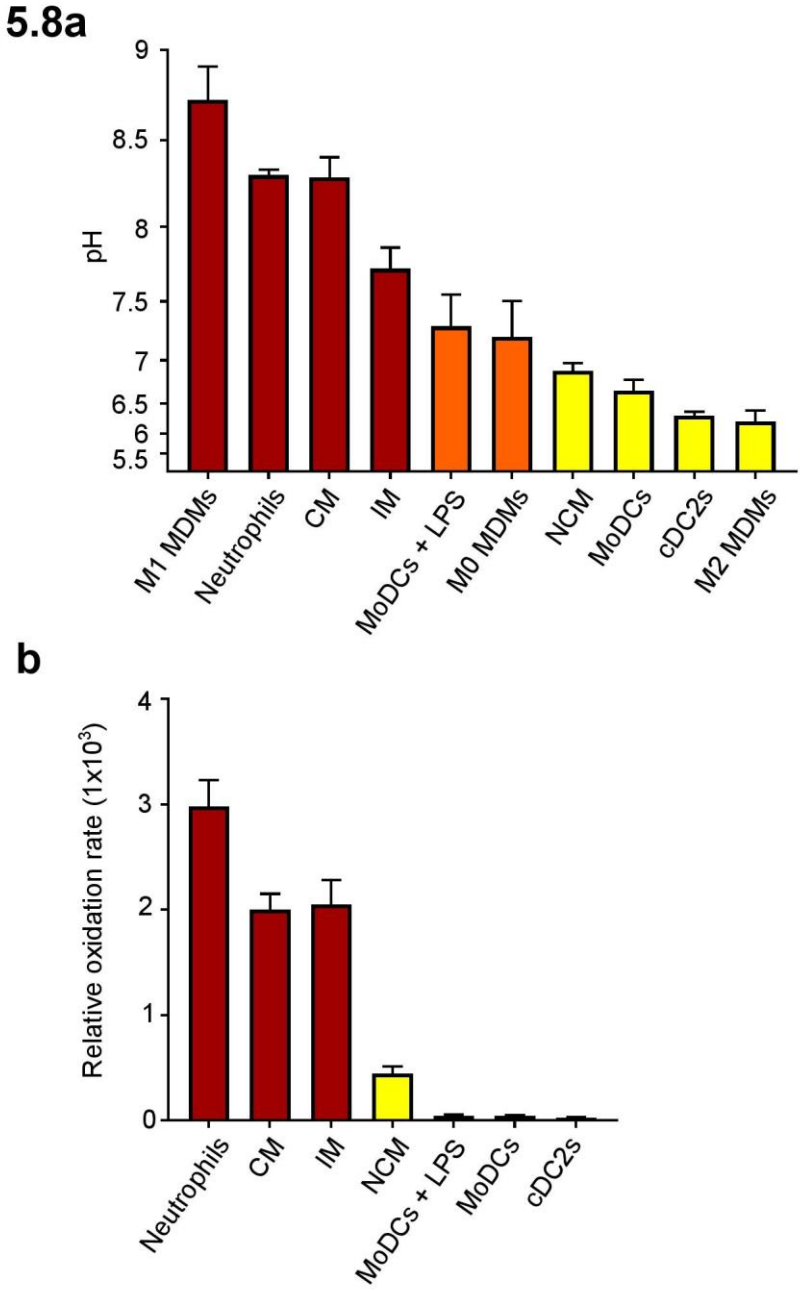

Figure 5.8 | A summary of chapter five's main results (a-b). (**a**) *Phagosomal pH at 15 minutes post phagocytosis from the time course experiments.* (**b**) *The maximum rate of H_2O_2-induced fluorescence calculated from the respiratory burst experiments. Data are plotted as mean ± SEM. MDMs = monocyte-derived macrophages, CM = classical monocytes, IM = intermediate monocytes, MoDCs = monocyte-derived dendritic cells, NCM = non-classical monocytes, cDC2s = classical dendritic cells class 2.*

The primary function of neutrophils is the efficient containment and killing of pathogens. The modes of killing fall into oxidative and non-oxidative pathways. Two closely related serine proteases present in the azurophil granules have been shown to be essential for killing of certain bacteria - neutrophil elastase and cathepsin G. In a genetic mice model, mice lacking elastase succumbed to Gram-negative *Klebsiella pneumoniae* and *Escherichia coli* infection, but were resistant to Gram-positive *Staphylococcus aureus* bacteria (Belaaouaj, 2002). A model of cathepsin G deficiency found that the mice were vulnerable to *S. aureus* and *Candida albicans* challenge (Reeves *et al.*, 2002), but cathepsin G and elastase deficient mice were resistant to *Aspergillus fumigatus* and *Burkholderia cepacia* infections (Vethanayagam *et al.*, 2011). In accordance with the alkaline phagosomal pH, both these enzymes have optimal activity between pH 7.5-8.5 (Korkmaz, Moreau & Gauthier, 2008; Reeves *et al.*, 2002; Levine *et al.*, 2015).

Elastase and cathepsin G are also present in monocytes, but in lower quantities (Campbell, Silverman & Campbell, 1989) and the study did not differentiate between monocyte subsets. This is the first time that phagosomal pH was studied between the human monocyte subsets and shown to be different, which supports the studies that they have various functions. In steady-state human conditions, work from the lab of Simon Yona showed for the first time that classical monocytes can differentiate into intermediate monocytes, which then, in turn, can differentiate into non-classical monocytes (Patel *et al.*, 2017). Specifically, approximately 1% of circulating classical monocytes differentiate into intermediate monocytes, but all the intermediate monocytes become non-classical monocytes.

However, in certain disease states this equilibrium is altered. For example, in many bacterial, viral, and parasital infections, observed numbers of intermediate and non-classical (Tolouei Semnani *et al.*, 2014) subsets were augmented, which contrasted with autoimmune conditions where the only altered subset was the intermediate

population (Ren *et al.*, 2017). If classical monocytes are the primary microbicidal monocyte, why are the other two subsets elevated in specific disease conditions?

One possible reason may be that the intermediate subset is involved in activating the adaptive immune system, as intermediate monocytes have reported superior antigen presenting ability compared with classical and non-classical monocytes. This is defined by increased expression of MHC I and II and HLA-DR (Wong *et al.*, 2011; Zawada *et al.*, 2011; Lee *et al.*, 2017), and activation of naïve T cells. I found that the intermediate monocytes had mildly alkaline phagosomes with a robust respiratory burst, which is purported by other researchers to be essential for antigen preservation before its presentation in dendritic cells (Mantegazza *et al.*, 2008).

Non-classical monocytes have been implicated in the control of viral infections through the production of pro-inflammatory cytokines (Cros *et al.*, 2010b) and in tissue-repair functions, as they are biased precursors of “M2” macrophages (Olingy *et al.*, 2017; Auffray *et al.*, 2007). The phagosomal pH data here would support this link, as both are acidic thus suggesting that they have similar phagosomal pH regulation machinery. “M2” macrophages also have reported low NADPH oxidase activity in comparison to “M1” macrophages (Canton *et al.*, 2014), which correlates with the observations made here in classical versus non-classical monocytes.

The phagosomal pH results of cDC2s and MoDCs give weight to concerns that MoDCs are not an accurate model of cDC2s. Their increased pH and NOX2 activity compared to cDC2s could be due to residual components from their monocyte origins. TLR stimulation via LPS pre-treatment of MoDCs caused an increase in phagosomal pH and NADPH oxidase activity compared with untreated MoDCs. This suggests that the microbial wall component might be directing the cells to perform pathogen killing of any subsequent internalised particle. Is the alkaline environment necessary for killing or antigen presentation, or both?

Conversely, in macrophages there are many cases where acidification is necessary for bacterial killing, as aforementioned in the results section 5.6. Although the *in vitro* macrophage polarisation model is not perfect and probably not representative of the physiological situation, it is useful in this area of research as a tool to push the cell into different phenotypic extremes. For example, Yates and colleagues examined phagosomal activities in mouse bone marrow-derived classically activated macrophages, differentiated with IFN-γ and LPS (Yates *et al.*, 2007). They found that the phagosomes had reduced lysosomal fusion, reduced proteolysis, lipolysis and β-galactosidase activity. When this is taken together with reports that classically activated macrophages have increased ROS production and microbial killing (Nathan *et al.*, 1983; Murray, Rubin & Rothermel, 1983; Canton *et al.*, 2014), and inhibition of acid hydrolases such as cathepsin L (Honey & Rudensky, 2003), it appears to fit with the neutrophil relationship between NADPH oxidase activity, increased pH, and intracellular pathogen killing. While alternatively activated macrophages thought to be a general model of homeostatic and wound healing cells, with functions such as complete degradation of pathogenic material via efferocytosis, suppress the inflammatory response. My preliminary investigations into efferocytosis by polarised macrophages suggest “M2” cells are better at this task then “M1” cells.

While this chapter’s investigation adds to our understanding of the NADPH oxidase’s involvement in different phagocytic immune cells, the next crucial step is to relate these differences to mechanistic cell function. It is known that the same enzymes are present in different cells, but they have different phagosomal pH kinetic profiles. Resolving the holes in the story of intracellular pH to cell function will provide greater insight into health and disease and assist in new immunological therapies.

Chapter Six: General discussion

6.1 Summary of findings

Chapter Three: Investigating ion channels in the neutrophil phagosome

- The NADPH oxidase inhibitor DPI reduced human neutrophil phagosomal pH and NOX2 activity in a dose-dependent manner, but phagosomal pH began to acidify before oxidase activity was significantly affected.
- The broad-spectrum chloride ion channel inhibitors DCPIB and FFA with the proton channel inhibitor zinc chloride decreased phagosomal pH, increased phagosomal area, and decreased NOX2 activity.
- The broad-spectrum potassium ion channel inhibitors anandamide and quinidine increased phagosomal pH, decreased phagosomal area with zinc treatment, and decreased NOX2 activity.
- Knockout mouse models for *Clic1*, *Clc3*, *Kcc3*, *Lrrc8a* did not exhibit convincing differences in phagosomal pH and area or NOX2 activity compared to wild-type controls.

Chapter Four: Characterising the Hoxb8 immortalised myeloid cell line

- With increasing days of differentiating, Hoxb8 cells massively proliferated but cell viability began to drop after four days. Day 4 was the optimal differentiation duration regarding cell number and viability, and respiratory burst subunit expression and activity.
- As Hoxb8 cells differentiated they upregulated expression of Mac-1, Ly6C and Ly6G and down-regulated expression of c-kit.

- While day 4 Hoxb8 neutrophils showed comparable expression of c-kit, Mac-1, and Ly6C to primary neutrophils, they showed lower expression of Ly6G.
- Hoxb8 neutrophils showed no expression of macrophage markers CD68, F4/80 or MHC-II at any stage of their differentiation.
- There was no difference in expression of any tested markers between the wildtype or *Hvcn1*$^{-/-}$ models.
- There was no difference between the respiratory burst activity of Hoxb8 day 4 neutrophils or primary neutrophils, which was consistent with western blotting of NADPH oxidase subunit expression.
- Hoxb8 neutrophils appeared to have similar phagosomal pH and area to primary neutrophils, although the phagosomal pH profile of *Hvcn1*$^{-/-}$ Hoxb8 day 4 neutrophils was less alkaline than *Hvcn1*$^{-/-}$ primary neutrophils.
- Both WT and *Hvcn1*$^{-/-}$ Hoxb8 neutrophils can be transfected with an adenovirus and displayed LC3 localisation.

Chapter Five: Variations in the phagosomal environments of human neutrophils and mononuclear phagocytes

- Neutrophils have more alkaline phagosomal pH and greater respiratory burst profiles when directly compared to the whole monocyte population.
- Classical monocytes have more alkaline phagosomes, those of intermediate monocytes are more neutral, while those of non-classical monocytes are more acidic. Phagocytosis is the same between subsets.
- Classical and intermediate monocytes have similar oxidase activity, while it is lower in non-classical monocytes.
- cDC2s have more acidic phagosomes than MoDCs and have lower oxidase activity and phagocytosis.
- Phagosomal pH and oxidase activity were increased in MoDCs after LPS stimulation.

- “M1” monocyte-derived macrophages have very alkaline phagosomes in comparison to “M0” and “M2” macrophages. Phagocytosis was not different between the subsets.
- DPI generally caused a decrease in phagocytosis in most cells tested, but particularly intermediate monocytes and MoDCs with and without treatment of LPS. Phagocytosis was unaffected in CGD cells.

6.2 Overall discussion of findings and future directions

Confocal microscopy of cells and *Candida* stained with the pH indicator SNARF-1 has been the main experimental technique used throughout this thesis. In chapter three, the method was used to screen various ion channels for their role in neutrophil phagosomal regulation through charge compensation of the NADPH oxidase. However, no individual channel was identified, only broad effects of potential chloride and potassium ion conductances. The experiments were conducted as snapshots of phagocytosis, which has certain limitations. One is that phagocytosis was unsynchronised, and it has been established in the other results chapters that pH can vary considerably within the first 30 minutes after ingestion. Any small change in phagosomal pH or area effected by a deficiency in an ion channel may be overlooked as general population variation. Also, as the snapshots are taken at one focal plane the snapshot may not be capturing the largest diameter of the phagosome. Measuring the pH and area kinetically may reveal differences caused by specific channel inhibitors.

To progress this investigation, instead of using live mouse models, the Hoxb8 myeloid cell model can be used. As it was demonstrated in chapter four, they had very similar phenotypes to primary neutrophils when their phagosomal environments were compared. The genetic engineering system CRISPR/Cas9 can be employed to make

targeted gene alterations without the time and expense of housing live animals. It has already been tested and found to be successful in Hoxb8 progenitors by other researchers (Di Ceglie *et al.*, 2016; Gran *et al.*, 2018; Hammerschmidt *et al.*, 2018; Leithner *et al.*, 2018). A CRISPR genetic screen has been carried out in a different cell line to investigate macrophage phagosomal pH regulation. Sedlyarov and colleagues used a CRISPR knockout library of solute carrier (SLC) proteins in the human myeloid U937 cell line (Sedlyarov *et al.*, 2018). They ran the in-house generated library against 391 different SLC genes and found only one to influence the U937 macrophages – SLC4A7. It is an electroneutral sodium bicarbonate co-transporter that regulates cytosolic pH, which indirectly regulates phagosomal pH. The group make the point that not all researchers use a bicarbonate-based experimental buffer, which is more physiologically relevant than phosphate or HEPES based buffers. Therefore, bicarbonate ion transporters may have been overlooked in other studies. This is true, and a limitation of the studies conducted within this thesis. However, there was still evidence of chloride and potassium ion involvement in phagosomal pH regulation, suggesting that charge compensation is not entirely performed by bicarbonate buffering. These data together further point towards the theory that multiple channels are involved in NADPH oxidase-induced charge compensation and phagosomal pH regulation.

Another limitation of this study is the pH range of SNARF-1, as the lowest pH it can accurately detect is pH 5 to 5.5. It was originally chosen by our laboratory because it is more suited for detection of alkaline environments, such as neutrophil phagosomes. Consequently, the acidic environments measured within this report may, in reality, be more acidic when tested with other reagents. However, SNARF-1 was sufficient to detect significant variability between different cell types and conditions.

SNARF-1 has been used by other researchers to measure intracellular pH. Chapter five successfully repeated the findings from the Grinstein lab (Canton *et al.*, 2014)

that polarised macrophages have differing phagosomal pH. SNARF-1 was also used in LPS treated monocyte-derived DCs by another group where they found the mean phagosomal pH to be around 7.5 30-60 minutes after ingestion of SNARF-1-labelled dextran (Dingjan *et al.*, 2016). SNARF-1 can also be used to quantify cytosolic pH, and the group led by DeCoursey (Morgan *et al.*, 2009) found similar results in human neutrophils to those published by this laboratory (Levine *et al.*, 2015). It is reassuring when results can be corroborated by other groups using the same reagents. Confusing differences arise in the literature when different experimental methods are used without knowledge of their inherent limitations.

For example, the use of FITC as a neutrophil phagosomal pH indicator. It was found in as early as 1984 that myeloperoxidase (MPO), an enzyme present in massive quantities and almost exclusive to neutrophils (Amanzada *et al.*, 2011), can react with FITC to cause a partial quenching of fluorescence and a decrease in pKa (Hurst *et al.*, 1984). This means that the dye is no longer sensitive in the neutral to mildly acidic phagosomal regions, and the neutrophil is observed as more acidic than it might be. To get around this, researchers have used the MPO inhibitor sodium azide during neutrophil phagocytosis (Nunes, Guido & Demaurex, 2015). But treatment with sodium azide has different complications. It was also found to lower observed neutrophil pH, but in a mechanism that was independent of MPO and action on the dye itself, as the other MPO inhibitors 4-aminobenzoic acid hydrazide and potassium cyanide had no effect, and FITC ratio was not altered in extracellular SNARF-labelled Candida in different pH buffers and sodium azide (Levine *et al.*, 2015). Therefore, its use should be avoided in the measurement of intracellular pH in neutrophils but permitted for phagocytes which contain much lower levels of MPO such as monocytes and macrophages (Arnhold & Flemmig, 2010).

Having said this, to confirm and extend my observations on the phagosomal pH of the different phagocytes, ideally the experiments should be repeated using a different

pH indicator that has a more acidic range. There are suitable variants of SNARF such as SNARF-4F and SNARF-5F which have lower pKas of 6.4 and 7.2 respectively (Liu, Diwu & Leung, 2001), but still have dual emission spectra. SNARF-4F has been used to measure biofilm pH (Hunter & Beveridge, 2005) and macrophage cytosolic pH (Bewley *et al.*, 2011), while SNARF-5F has been used to measure pH within hippocampal neurons (Cheng, Kelly & Church, 2008) and also macrophage cytosolic pH (Canton *et al.*, 2014). Although pHrodo is commonly used for measuring acidic environments (Bernardo, Long & Simons, 2010; Fabbrini *et al.*, 2012), for neutrophil phagosomal pH measurement it should be used with caution as its fluorescence was found to be perturbed by NOX2 related oxidation (Rybicka *et al.*, 2012a).

The other principal parameter investigated throughout this thesis was measurement of NADPH oxidase activity. In the first results chapter, the main technique was measuring oxygen tension during phagocytosis of opsonised *Candida*. I gathered consistent results when using human neutrophils, as enough cells can be isolated relatively easily from 80-100 ml of blood for each experiment – for the Seahorse 24 well plates, there needs to be a robust cell monolayer. This method does not use any fluorescent probes or chemical intermediates; it only uses a laser sensor to detect oxygen molecules. But for some reason, the results were less consistent when using mouse neutrophils. They did not adhere very well to the plate bottom even with the adherent Cell-Tak. For this reason, the Amplex UltraRed assay was employed for measuring NOX2 activity in mouse neutrophils in the next results chapter. Although recording of changes in extracellular oxygen concentration incurred by phagocytosis is more physiologically relevant than changes in hydrogen peroxide extracellular concentration incurred by PMA plasma membrane stimulation, it produced consistent results in both chapters five and six. It also required much fewer cells than the Seahorse assay, which was a necessity for chapter five when testing other

mononuclear phagocytes: from 80 ml of human blood, only 1-3 x 10^5 cDCs and intermediate and non-classical monocytes were usually recovered.

However, there are other possible methods for measuring phagocytosis-associated oxygen consumption. There is a Seahorse apparatus commercially available that uses a 96 well plate, which could potentially be optimised for the low mononuclear cell numbers. Other population-based assays require the use of fluorescent probes, such as measuring intracellular ROS production using flow cytometry. One commonly used assay utilises the OxyBURST green probe, which fluoresces when it undergoes oxidation. There are two commercially available forms: the H_2DCFDA or the H_2FFDA form. They are both fluorescein derivatives but have different properties. Oxidation of H_2DCFDA is sensitive to pH like fluorescein – the fluorescence intensity increases with increasing pH above pH 8 and is lower in pH under 6 (Van Acker *et al.*, 2016), while the oxidised product of H_2FFDA appears more resistant to pH (Chen, 2002). Currently, only the H_2DCFDA form is available linked to silica beads or human IgG complexes, which makes it suitable for flow cytometry as well as microscopy, while the H_2FFDA form is only available coupled to the carrier protein bovine serum albumin (BSA). It, therefore, requires more technical processing for phagosomal ROS detection: a technique developed by Yates and Russell involves linking the BSA part to silica beads via a cyanide crosslinker (VanderVen, Yates & Russell, 2009). As the dye is easily oxidised even by exposure to air, they also labelled the beads with the pH-insensitive Alexa Fluor-594 succinimidyl ester to allow ratiometric calibration. For confirmation of the chapter five results, ideally this protocol would be carried out in neutrophils and the other mononuclear cells, this time optimising macrophage intracellular ROS detection. However, there may be difficulty optimising the protocol for OxyBURST labelling of *Candida* particles, as they have autofluorescence with emission in the green area of the spectrum (peaking at 520-580 nm) (Graus, Neumann & Timlin, 2017), the same as the dye emission (Chen, 2002).

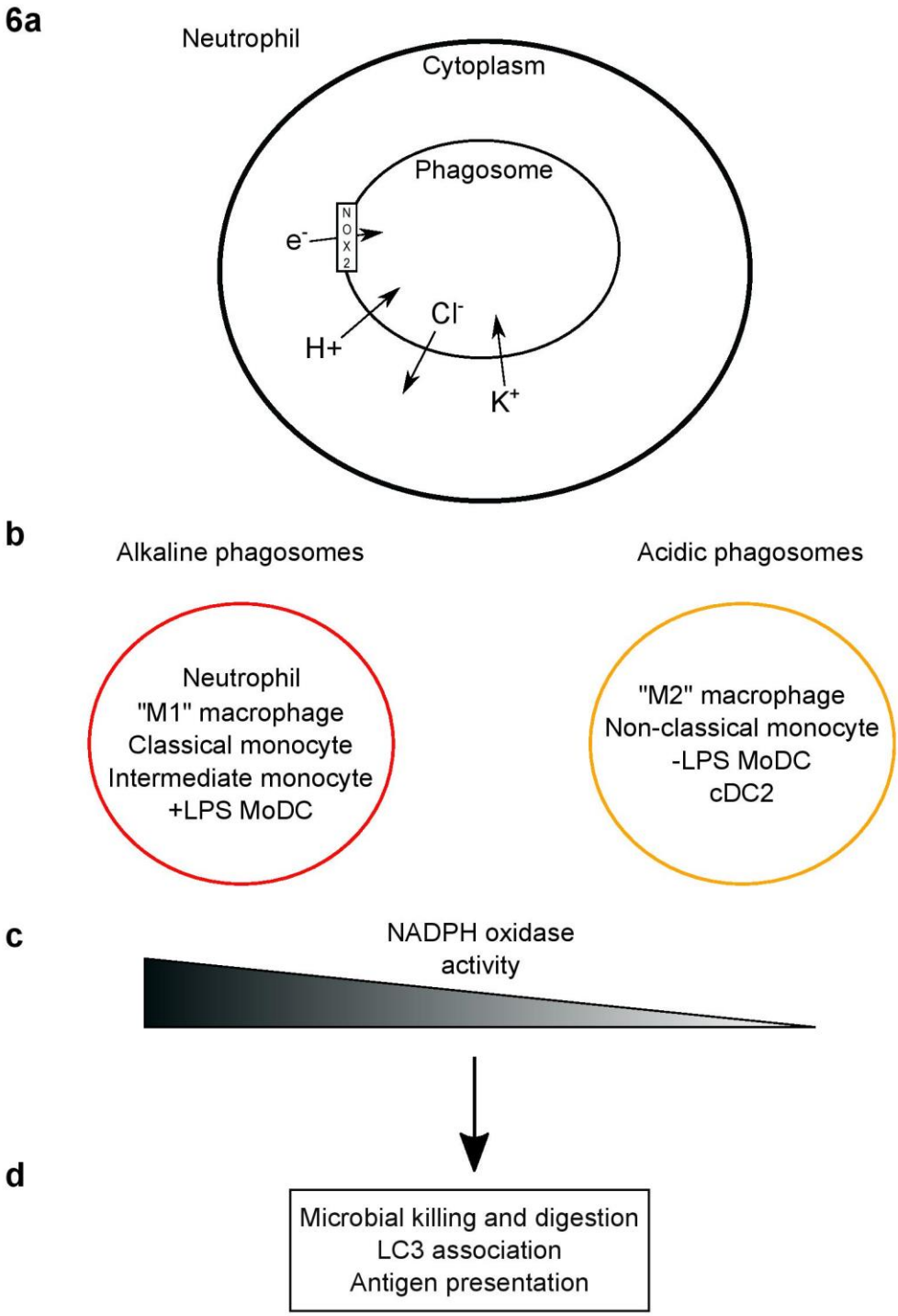

Figure 6 | A schematic summary (a-d). *(**a**) NOX2-induced charge compensation across the neutrophil phagosome. Protons enter the phagosome via HVCN1. Chapter 3 demonstrated potential potassium and chloride conductances but could not identify specific channels. (**b**) Innate immune cells were broadly categorised into more alkaline or more acidic phagosomes. (**c**) Generally, cells with more alkaline phagosomes had higher NADPH oxidase activity. (**d**) The observations of different phagosomal environments in different cell types will help to elucidate different phagosomal functions.*

This thesis has investigated NADPH oxidase activity, which in turn influences phagosomal pH, but the consequential effect of these processes yet to be studied is the regulation of phagosomal enzyme activity. There are a number of extracellular enzyme activities for proteases such as elastase and different cathepsins, but it is necessary to measure intracellular activity in the phagosome with the correct physiological conditions. The combined efforts of the Yates and Russell groups have not only been limited to intracellular ROS detection, but also to intracellular enzyme detection and activity. They developed an assay to measure intracellular Cathepsin B and L activity by coating beads with protein substrates. The substrates have an attached rhodamine group so that when the substrates are cleaved by the specific enzymes, a fluorescent product is formed (Podinovskaia *et al.*, 2013). Other enzyme-specific substrates with conjugated rhodamine are available, such as for elastase, or could be custom-ordered. But to be sure that the substrate is specific, it is necessary to run control experiments with enzyme specific inhibitors. Once these conditions are satisfied, it would be very interesting to follow specific enzyme activity temporally to see how it correlates with the pH and ROS kinetic profiles.

These ideas naturally lead to the fundamental effects of the interrelationships between NADPH oxidase activity, pH, and phagosome enzyme activity; how they work together to kill and digest engulfed pathogens or to process and present engulfed antigens to activate other immune cells. Through bacterial killing experiments already published, there are cases of redundancy of the antimicrobial systems. For instance, certain bacteria are susceptible to non-oxidative, i.e. granule protease-induced, killing such as *Streptococcus pneumoniae* (Standish & Weiser, 2009) while others are resistant to proteases but not the direct effect of the NADPH oxidase (*S. aureus* (Buvelot *et al.*, 2016)). Patients with genetic defects in the phagosomal defences, such as CGD, Chediak-Higashi syndrome and Papillon-

Lefèvre disease help to increase our understanding of the nuanced balance of oxidative and non-oxidative antimicrobial mechanisms.

Finally, the other side of phagosomal enzyme function is its involvement in antigen presentation. It is currently thought that DCs initially have NADPH oxidase-induced alkaline phagosomes to inhibit lysosomal cathepsins with low pH optima from degrading antigen before it is presented on the cell surface membrane (Mantegazza *et al.*, 2008; Dingjan *et al.*, 2016). There is conflicting evidence that the oxidase is not causing alkalinisation but instead acidification, and it is the reductive environment alone that inhibits degradative enzymes (Rybicka *et al.*, 2012b; Salao *et al.*, 2016).

An emerging complementary process that links NOX2 activity with antigen presentation and intracellular microbial containment is mechanisms related to autophagy. To present antigen via MHC-I or -II and to cross-present these to T cells requires autophagy-related proteins (Ghislat & Lawrence, 2018), and some bacteria are thought to be internalised into specific intracellular compartments in macrophages by LAP, such *as Listeria monocytogenes* (Gluschko *et al.*, 2018) or *C. albicans* (Tam *et al.*, 2014) until the microbial antigens are processed. Both these processes are thought to occur by NOX2 activity. The autophagy linked to microbial clearance is present in all the professional phagocytes, while its link to antigen presentation is predominantly in DCs and macrophages. The preliminary data gathered in chapter four demonstrated the expression of GFP-LC3 in Hoxb8 neutrophils that had phagocytosed SNARF-labelled *Candida*. It would be very interesting to use the same method to view LC3 localisation in the other professional phagocytes after phagocytosis of different microbes and in efferocytosis, and to relate this to pH as well as NOX2 activity.

Appendix

List of publications

Foote, J.R., Behe, P., Frampton, M., Levine, A.P., Segal, A.W., 2017. An Exploration of Charge Compensating Ion Channels across the Phagocytic Vacuole of Neutrophils. Front. Pharmacol. 8, 94. https://doi.org/10.3389/fphar.2017.00094

Foote, J.R., Levine, A.P., Behe, P., Duchen, M.R., Segal, A.W., 2017. Imaging the neutrophil phagosome and cytoplasm using a ratiometric pH indicator. J. Vis. Exp. 2017. https://doi.org/10.3791/55107

Behe, P., Foote, J.R., Levine, A.P., Platt, C.D., Chou, J., Benavides, F., Geha, R.S., Segal, A.W., 2017. The LRRC8A mediated "swell activated" chloride conductance is dispensable for vacuolar homeostasis in neutrophils. Front. Pharmacol. 8. https://doi.org/10.3389/fphar.2017.00262

Maini, A., Foote, J.R., Hayhoe, R., Patel, A.A., O'Brien, A., Avraham-Davidi, I., Yona, S., 2018. Monocyte and Neutrophil Isolation, Migration, and Phagocytosis Assays. Curr. Protoc. Immunol. 122, e53. https://doi.org/10.1002/cpim.53

Foote, J.R., Patel, A.A., Yona, S., Segal, A.W., 2018. Variations in the phagosomal environment of human neutrophils and mononuclear phagocyte subsets. bioRxiv 394619. https://doi.org/10.1101/394619

References

Abo, A., Boyhan, A., West, I., Thrasher, A. J., and Segal, A. W. (1992). Reconstitution of neutriphil NADPH oxidase activity in the cell free system by four components: p67-phox, p47-phox, p21rac1, and cytochrome b-245. *J. Biol. Chem.* 267, 16767–16770.

Abramovich, C., and Humphries, R. K. (2005). Hox regulation of normal and leukemic hematopoietic stem cells. *Curr. Opin. Hematol.* 12, 210–216. doi:10.1097/01.moh.0000160737.52349.aa.

Adolfsson, J., Borge, O. J., Bryder, D., Theilgaard-Mönch, K., Åstrand-Grundström, I., Sitnicka, E., et al. (2001). Upregulation of Flt3 expression within the bone marrow Lin-Sca1+c-kit+stem cell compartment is accompanied by loss of self-renewal capacity. *Immunity* 15, 659–669. doi:10.1016/S1074-7613(01)00220-5.

Adragna, N. C., Ravilla, N. B., Lauf, P. K., Begum, G., Khanna, A. R., Sun, D., et al. (2015a). Regulated phosphorylation of the K-Cl cotransporter KCC3 is a molecular switch of intracellular potassium content and cell volume homeostasis. *Front. Cell. Neurosci.* 9, 255. doi:10.3389/fncel.2015.00255.

Adragna, N. C., Ravilla, N. B., Lauf, P. K., Begum, G., Khanna, A. R., Sun, D., et al. (2015b). Regulated phosphorylation of the K-Cl cotransporter KCC3 is a molecular switch of intracellular potassium content and cell volume homeostasis. *Front. Cell. Neurosci.* 9, 255. doi:10.3389/fncel.2015.00255.

Alloatti, A. S., Kotsias, F., Pauwels, A.-M., Beyaert, R., Hoffmann, E., and Correspondence, S. A. (2015). Toll-like Receptor 4 Engagement on Dendritic Cells Restrains Phago-Lysosome Fusion and Promotes Cross-Presentation of Antigens. *Immunity* 43, 1087–1100. doi:10.1016/j.immuni.2015.11.006.

Almeida, J., Bueno, C., Algueró, M. C., Sanchez, M. L., de Santiago, M., Escribano, L., et al. (2001). Comparative Analysis of the Morphological, Cytochemical, Immunophenotypical, and Functional Characteristics of Normal Human Peripheral Blood Lineage−/CD16+/HLA-DR+/CD14−/lo Cells, CD14+ Monocytes, and CD16− Dendritic Cells. *Clin. Immunol.* 100, 325–338. doi:10.1006/CLIM.2001.5072.

Amanzada, A., Malik, I. A., Nischwitz, M., Sultan, S., Naz, N., and Ramadori, G. (2011). Myeloperoxidase and elastase are only expressed by neutrophils in normal and in inflamed liver. *Histochem. Cell Biol.* 135, 305–15. doi:10.1007/s00418-011-0787-1.

Ambruso, D. R., Knall, C., Abell, A. N., Panepinto, J., Kurkchubasche, A., Thurman, G., et al. (2000). Human neutrophil immunodeficiency syndrome is associated with an inhibitory Rac2 mutation. *Proc. Natl. Acad. Sci.* 97, 4654–4659. doi:10.1073/pnas.080074897.

Andersson, L. I. M., Cirkic, E., Hellman, P., and Eriksson, H. (2012). Myeloid blood dendritic cells and monocyte-derived dendritic cells differ in their endocytosing capability. *Hum. Immunol.* 73, 1073–1081. doi:10.1016/J.HUMIMM.2012.08.002.

Andronic, J., Bobak, N., Bittner, S., Ehling, P., Kleinschnitz, C., Herrmann, A. M., et al. (2013). Identification of two-pore domain potassium channels as potent modulators of osmotic volume regulation in human T lymphocytes. *Biochim. Biophys. Acta* 1828, 699–707. doi:10.1016/j.bbamem.2012.09.028.

Aratani, Y., Kura, F., Watanabe, H., Akagawa, H., Takano, Y., Suzuki, K., et al. (2002). Relative contributions of myeloperoxidase and NADPH-oxidase to the early host defense against pulmonary infections with Candida albicans and Aspergillus fumigatus. *Med. Mycol.* 40, 557–63.

Argiropoulos, B., and Humphries, R. K. (2007). Hox genes in hematopoiesis and leukemogenesis. *Oncogene* 26, 6766–6776. doi:10.1038/sj.onc.1210760.

Arnhold, J., and Flemmig, J. (2010). Human myeloperoxidase in innate and acquired immunity. *Arch. Biochem. Biophys.* 500, 92–106. doi:10.1016/J.ABB.2010.04.008.

Attali, B., Wang, N., Kolot, A., Sobko, A., Cherepanov, V., and Soliven, B. (1997). Characterization of delayed rectifier Kv channels in oligodendrocytes and progenitor cells. *J. Neurosci.* 17, 8234–45.

Auffray, C., Fogg, D., Garfa, M., Elain, G., Join-Lambert, O., Kayal, S., et al. (2007). Monitoring of blood vessels and tissues by a population of monocytes with patrolling behavior. *Science* 317, 666–70. doi:10.1126/science.1142883.

Averaimo, S., Milton, R. H., Duchen, M. R., and Mazzanti, M. (2010). Chloride intracellular channel 1 (CLIC1): Sensor and effector during oxidative stress. *FEBS Lett.* 584, 2076–2084. doi:10.1016/j.febslet.2010.02.073.

Babior, B. M., Kipnes, R. S., and Curnutte, J. T. (1973). Biological defense mechanisms. The production by leukocytes of superoxide, a potential bactericidal agent. *J. Clin. Invest.* 52, 741–4. doi:10.1172/JCI107236.

Bach, G., Chen, C.-S., and Pagano, R. E. (1999). Elevated lysosomal pH in Mucolipidosis type IV cells. *Clin. Chim. Acta* 280, 173–179. doi:10.1016/S0009-8981(98)00183-1.

Bagaitkar, J., Huang, J., Zeng, M. Y., Pech, N. K., Monlish, D. A., Perez-Zapata, L. J., et al. (2018). NADPH oxidase activation regulates apoptotic neutrophil clearance by murine macrophages. *Blood* 131, 2367–2378. doi:10.1182/blood-2017-09-809004.

Baldridge, C. W., and Gerard, R. W. (1933). The Extra Respiration of Phagocytosis. *Am. J. Physiol.* 103, 235–236.

Barber, N., Belov, L., and Christopherson, R. I. (2008). All-trans retinoic acid induces different immunophenotypic changes on human HL60 and NB4 myeloid leukaemias. *Leuk. Res.* 32, 315–322. doi:10.1016/j.leukres.2007.04.013.

Barro-Soria, R., Perez, M. E., and Larsson, H. P. (2015). KCNE3 acts by promoting voltage sensor activation in KCNQ1. *Proc. Natl. Acad. Sci.* 112, E7286–E7292. doi:10.1073/pnas.1516238112.

Bastiat-Sempe, B., Love, J. F., Lomayesva, N., and Wessels, M. R. (2014). Streptolysin O and NAD-glycohydrolase prevent phagolysosome acidification and promote group A Streptococcus survival in macrophages. *MBio* 5, e01690-14. doi:10.1128/mBio.01690-14.

Bedard, K., and Krause, K.-H. (2007). The NOX family of ROS-generating NADPH

oxidases: physiology and pathophysiology. *Physiol. Rev.* 87, 245–313. doi:10.1152/physrev.00044.2005.

Belaaouaj, A. (2002). Neutrophil elastase-mediated killing of bacteria: lessons from targeted mutagenesis. *Microbes Infect.* 4, 1259–1264. doi:10.1016/S1286-4579(02)01654-4.

Belaaouaj, A., McCarthy, R., Baumann, M., Gao, Z., Ley, T. J., Abraham, S. N., et al. (1998). Mice lacking neutrophil elastase reveal impaired host defense against gram negative bacterial sepsis. *Nat. Med.* 4, 615–618. doi:10.1038/nm0598-615.

Belambri, S. A., Rolas, L., Raad, H., Hurtado-Nedelec, M., Dang, P. M.-C., and El-Benna, J. (2018). NADPH oxidase activation in neutrophils: Role of the phosphorylation of its subunits. *Eur. J. Clin. Invest.*, e12951. doi:10.1111/eci.12951.

Benna, J. E., Dang, P. M., Gaudry, M., Fay, M., Morel, F., Hakim, J., et al. (1997). Phosphorylation of the respiratory burst oxidase subunit p67(phox) during human neutrophil activation. Regulation by protein kinase C-dependent and independent pathways. *J. Biol. Chem.* 272, 17204–8.

Bernardo, J., Long, H. J., and Simons, E. R. (2010). Initial cytoplasmic and phagosomal consequences of human neutrophil exposure to Staphylococcus epidermidis. *Cytom. Part A* 77, 243–252. doi:10.1002/cyto.a.20827.

Bewley, M. A., Marriott, H. M., Tulone, C., Francis, S. E., Mitchell, T. J., Read, R. C., et al. (2011). A cardinal role for cathepsin D in co-ordinating the host-mediated apoptosis of macrophages and killing of pneumococci. *PLoS Pathog.* 7, e1001262. doi:10.1371/journal.ppat.1001262.

Birnie, G. D. (1988). The HL60 cell line: A model system for studying human myeloid cell differentiation. *Br. J. Cancer* 58, 41–45.

Bjerregaard, M. D., Jurlander, J., Klausen, P., Borregaard, N., and Cowland, J. B. (2003). The in vivo profile of transcription factors during neutrophil differentiation in human bone marrow. *Blood* 101, 4322–4332. doi:10.1182/blood-2002-03-0835.

Blow, A. M., and Barrett, A. J. (1977). Action of human cathepsin G on the oxidized B chain of insulin. *Biochem. J.* 161, 17–9.

Bond, J., and Varley, J. (2005). Use of flow cytometry and SNARF to calibrate and measure intracellular pH in NS0 cells. *Cytom. Part A* 64, 43–50. doi:10.1002/cyto.a.20066.

Bonvillain, R. W., Painter, R. G., Adams, D. E., Viswanathan, A., Lanson, N. A., and Wang, G. (2010). RNA interference against CFTR affects HL60-derived neutrophil microbicidal function. *Free Radic. Biol. Med.* 49, 1872–80. doi:10.1016/j.freeradbiomed.2010.09.012.

Borregaard, N., Kjeldsen, L., Lollike, K., and Sengeløv, H. (1992). Ca(2+)-dependent translocation of cytosolic proteins to isolated granule subpopulations and plasma membrane from human neutrophils. *FEBS Lett.* 304, 195–7.

Borregaard, N., Kjeldsen, L., Lollike, K., and Sengeløv, H. (1995). Granules and secretory vesicles of the human neutrophil. *Clin. Exp. Immunol.* 101, 6–9. doi:10.1111/j.1365-2249.1995.tb06152.x.

Borregaard, N., Kjeldsen, L., Sengeløv, H., Diamond, M. S., Springer, T. A., Anderson, H. C., et al. (1994). Changes in subcellular localization and surface expression of L-selectin, alkaline phosphatase, and Mac-1 in human neutrophils during stimulation with inflammatory mediators. *J. Leukoc. Biol.* 56, 80–7.

Bouin, A. P., Grandvaux, N., Vignais, P. V, and Fuchs, A. (1998). p40(phox) is phosphorylated on threonine 154 and serine 315 during activation of the phagocyte NADPH oxidase. Implication of a protein kinase c-type kinase in the phosphorylation process. *J. Biol. Chem.* 273, 30097–103.

Boyette, L. B., Macedo, C., Hadi, K., Elinoff, B. D., Walters, J. T., Ramaswami, B., et al. (2017). Phenotype, function, and differentiation potential of human monocyte subsets. *PLoS One* 12, e0176460. doi:10.1371/journal.pone.0176460.

Breton, G., Lee, J., Zhou, Y. J., Schreiber, J. J., Keler, T., Puhr, S., et al. (2015). Circulating precursors of human CD1c+ and CD141+ dendritic cells. *J. Exp. Med.* 212, 401–13. doi:10.1084/jem.20141441.

Bright, G. R., Fisher, G. W., Rogowska, J., and Taylor, D. L. (1989). Chapter 6 Fluorescence Ratio Imaging Microscopy. *Methods Cell Biol.* 30, 157–192. doi:10.1016/S0091-679X(08)60979-6.

Brockbank, S., Downey, D., Elborn, J. S., and Ennis, M. (2005). Effect of cystic fibrosis exacerbations on neutrophil function. *Int. Immunopharmacol.* 5, 601–608. doi:10.1016/j.intimp.2004.11.007.

Brunelli, L., Crow, J. P., and Beckman, J. S. (1995). The Comparative Toxicity of Nitric Oxide and Peroxynitrite to Escherichia coli. *Arch. Biochem. Biophys.* 316, 327–334. doi:10.1006/ABBI.1995.1044.

Bruns, H., Stegelmann, F., Fabri, M., Döhner, K., van Zandbergen, G., Wagner, M., et al. (2012). Abelson tyrosine kinase controls phagosomal acidification required for killing of Mycobacterium tuberculosis in human macrophages. *J. Immunol.* 189, 4069–78. doi:10.4049/jimmunol.1201538.

Buckler, K. J., and Vaughan-Jones, R. D. (1990). Application of a new pH-sensitive fluoroprobe (carboxy-SNARF-1) for intracellular pH measurement in small, isolated cells. *Pflügers Arch. Eur. J. Physiol.* 417, 234–239. doi:10.1007/BF00370705.

Bullen, J. J., Rogers, H. J., and Leigh, L. (1972). Iron-binding proteins in milk and resistance to escherichia coli infection in infants. *Br. Med. J.* 1, 69–75. doi:10.1136/bmj.1.5792.69.

Bülow, E., Bengtsson, N., Calafat, J., Gullberg, U., and Olsson, I. (2002). Sorting of neutrophil-specific granule protein human cathelicidin, hCAP-18, when constitutively expressed in myeloid cells. *J. Leukoc. Biol.* 72, 147–53.

Burgess, A. W., Camakaris, J., and Metcalf, D. (1977). Purification and properties of colony-stimulating factor from mouse lung-conditioned medium. *J. Biol. Chem.* 252, 1998–2003.

Burlak, C. (2005). Maturation of Human Neutrophil Phagosomes Includes Incorporation of Molecular Chaperones and Endoplasmic Reticulum Quality Control Machinery. *Mol. Cell. Proteomics* 5, 620–634. doi:10.1074/mcp.M500336-MCP200.

Busetto, S., Trevisan, E., Decleva, E., Dri, P., and Menegazzi, R. (2007). Chloride Movements in Human Neutrophils during Phagocytosis: Characterization and Relationship to Granule Release. *J. Immunol.* 179, 4110–4124. doi:10.4049/jimmunol.179.6.4110.

Buvelot, H., Posfay-Barbe, K. M., Linder, P., Schrenzel, J., and Krause, K.-H. (2016). *Staphylococcus aureus* , phagocyte NADPH oxidase and chronic granulomatous disease. *FEMS Microbiol. Rev.* 41, fuw042. doi:10.1093/femsre/fuw042.

Campanelli, D., Detmers, P. A., Nathan, C. F., and Gabay, J. E. (1990). Azurocidin and a homologous serine protease from neutrophils. Differential antimicrobial and proteolytic properties. *J. Clin. Invest.* 85, 904–915. doi:10.1172/JCI114518.

Campbell, E. J., Silverman, E. K., and Campbell, M. A. (1989a). Elastase and cathepsin G of human monocytes. Quantification of cellular content, release in response to stimuli, and heterogeneity in elastase-mediated proteolytic activity. *J. Immunol.* 143, 2961–8.

Campbell, E. J., Silverman, E. K., and Campbell, M. A. (1989b). Elastase and cathepsin G of human monocytes. Quantification of cellular content, release in response to stimuli, and heterogeneity in elastase-mediated proteolytic activity. *J. Immunol.* 143, 2961–8.

Canton, J., Khezri, R., Glogauer, M., and Grinstein, S. (2014). Contrasting phagosome pH regulation and maturation in human M1 and M2 macrophages. *Mol. Biol. Cell* 25, 3330–3341. doi:10.1091/mbc.E14-05-0967.

Capasso, M., Bhamrah, M. K., Henley, T., Boyd, R. S., Langlais, C., Cain, K., et al. (2010). HVCN1 modulates BCR signal strength via regulation of BCR-dependent generation of reactive oxygen species. *Nat. Immunol.* 11, 265–72. doi:10.1038/ni.1843.

Cech, P., and Lehrer, R. I. (1984). Phagolysosomal pH of human neutrophils. *Blood* 63, 88–95.

Chacko, B. K., Kramer, P. A., Ravi, S., Johnson, M. S., Hardy, R. W., Ballinger, S. W., et al. (2013). Methods for defining distinct bioenergetic profiles in platelets, lymphocytes, monocytes, and neutrophils, and the oxidative burst from human blood. *Lab. Investig.* 93, 690–700. doi:10.1038/labinvest.2013.53.

Chen, C.-S. (2002a). Phorbol ester induces elevated oxidative activity and alkalization in a subset of lysosomes. *BMC Cell Biol.* 3, 1. doi:10.1186/1471-2121-3-21.

Chen, C. S. (2002b). Phorbol ester induces elevated oxidative activity and alkalization in a subset of lysosomes. *BMC Cell Biol.* 3, 21. doi:10.1186/1471-2121-3-21.

Cheng, Y. M., Kelly, T., and Church, J. (2008). Potential contribution of a voltage-activated proton conductance to acid extrusion from rat hippocampal neurons. *Neuroscience* 151, 1084–1098. doi:10.1016/J.NEUROSCIENCE.2007.12.007.

Chiswick, E. L., Mella, J. R., Bernardo, J., and Remick, D. G. (2015). Acute-Phase Deaths from Murine Polymicrobial Sepsis Are Characterized by Innate Immune Suppression Rather Than Exhaustion. *J. Immunol.* 195, 3793–802. doi:10.4049/jimmunol.1500874.

Chris Fraley, Adrian E. Raftery, Thomas Brendan Murphy, and Luca Scrucca

(2012). mclust Version 4 for R: Normal Mixture Modeling for Model-Based Clustering, Classification, and Density Estimation.

Chu, J., Song, H. H., Zarember, K. A., Mills, T. A., and Gallin, J. I. (2013). Persistence of the bacterial pathogen Granulibacter bethesdensis in chronic granulomatous disease monocytes and macrophages lacking a functional NADPH oxidase. *J. Immunol.* 191, 3297–307. doi:10.4049/jimmunol.1300200.

Clark, L. C., Wolf, R., Granger, D., and Taylor, Z. (1953). Continuous Recording of Blood Oxygen Tensions by Polarography. *J. Appl. Physiol.* 6, 189–193. doi:10.1152/jappl.1953.6.3.189.

Collins, S. J., Gallo, R. C., and Gallagher, R. E. (1977). Continuous growth and differentiation of human myeloid leukaemic cells in suspension culture. *Nature* 270, 347–349. doi:10.1038/270347a0.

Cros, J., Cagnard, N., Woollard, K., Patey, N., Zhang, S.-Y., Senechal, B., et al. (2010a). Human CD14dim Monocytes Patrol and Sense Nucleic Acids and Viruses via TLR7 and TLR8 Receptors. *Immunity* 33, 375–386. doi:10.1016/j.immuni.2010.08.012.

Cros, J., Cagnard, N., Woollard, K., Patey, N., Zhang, S.-Y., Senechal, B., et al. (2010b). Human CD14dim Monocytes Patrol and Sense Nucleic Acids and Viruses via TLR7 and TLR8 Receptors. *Immunity* 33, 375–386. doi:10.1016/J.IMMUNI.2010.08.012.

Cross, A. R. (2000). p40(phox) Participates in the activation of NADPH oxidase by increasing the affinity of p47(phox) for flavocytochrome b(558). *Biochem. J.* 349, 113–7.

Cross, A. R., and Jones, O. T. G. (1986). The effect of the inhibitor diphenylene iodonium on the superoxide-generating system of neutrophils Specific labelling of a component polypeptide of the oxidase.

Cross, A. R., and Segal, A. W. (2004). The NADPH oxidase of professional phagocytes - Prototype of the NOX electron transport chain systems. *Biochim. Biophys. Acta - Bioenerg.* 1657, 1–22. doi:10.1016/j.bbabio.2004.03.008.

Crow, J. P. (1997). Dichlorodihydrofluorescein and dihydrorhodamine 123 are sensitive indicators of peroxynitrite in vitro: Implications for intracellular measurement of reactive nitrogen and oxygen species. *Nitric Oxide - Biol. Chem.* 1, 145–157. doi:10.1006/niox.1996.0113.

D'Alo', F., Johansen, L. M., Nelson, E. A., Radomska, H. S., Evans, E. K., Zhang, P., et al. (2003). The amino terminal and E2F interaction domains are critical for C/EBPα-mediated induction of granulopoietic development of hematopoietic cells. *Blood* 102, 3163–3171. doi:10.1182/blood-2003-02-0479.

Dakic, A., Metcalf, D., Di Rago, L., Mifsud, S., Wu, L., and Nutt, S. L. (2005). PU.1 regulates the commitment of adult hematopoietic progenitors and restricts granulopoiesis. *J. Exp. Med.* 201, 1487–1502. doi:10.1084/jem.20050075.

Dale, D. C., Boxer, L., Liles, W. C., Majno, G., Craddock, C., Rather, L., et al. (2008). The phagocytes: neutrophils and monocytes. *Blood* 112, 935–45. doi:10.1182/blood-2007-12-077917.

Dalton, W. T., Ahearn, M. J., McCredie, K. B., Freireich, E. J., Stass, S. A., and Trujillo, J. M. (1988). HL-60 cell line was derived from a patient with FAB-M2 and not FAB-M3. *Blood* 71, 242–7.

De Kouchkovsky, I., and Abdul-Hay, M. (2016). 'Acute myeloid leukemia: A comprehensive review and 2016 update.' *Blood Cancer J.* 6, e441–e441. doi:10.1038/bcj.2016.50.

de Rossi, L., Gott, K., Horn, N., Hecker, K., Hutschenreuter, G., and Rossaint, R. (2002). Xenon preserves neutrophil and monocyte function in human whole blood. *Can. J. Anesth.* 49, 942–945. doi:10.1007/BF03016879.

deCathelineau, A. M., and Henson, P. M. (2003). The final step in programmed cell death: phagocytes carry apoptotic cells to the grave. *Essays Biochem.* 39, 105–17. doi:10.1042/BSE0390105.

Decher, N., Lang, H. J., Nilius, B., Brüggemann, A., Busch, A. E., and Steinmeyer, K. (2001). DCPIB is a novel selective blocker of I(Cl,swell) and prevents swelling-induced shortening of guinea-pig atrial action potential duration. *Br. J. Pharmacol.* 134, 1467–79. doi:10.1038/sj.bjp.0704413.

DeCoursey, T. E., Morgan, D., and Cherny, V. V. (2003a). The voltage dependence of NADPH oxidase reveals why phagocytes need proton channels. *Nature* 422, 531–534. doi:10.1038/nature01523.

DeCoursey, T. E., Morgan, D., and Cherny, V. V. (2003b). The voltage dependence of NADPH oxidase reveals why phagocytes need proton channels. *Nature* 422, 531–534. doi:10.1038/nature01523.

Delamarre, L., Pack, M., Chang, H., Mellman, I., and Trombetta, E. S. (2005). Differential lysosomal proteolysis in antigen-presenting cells determines antigen fate. *Science (80-.).* 307, 1630–1634. doi:10.1126/science.1108003.

DeLeo, F. R., and Quinn, M. T. (1996). Assembly of the phagocyte NADPH oxidase: molecular interaction of oxidase proteins. *J. Leukoc. Biol.* 60, 677–91.

Demirkhanyan, L. H., Marin, M., Padilla-Parra, S., Zhan, C., Miyauchi, K., Jean-Baptiste, M., et al. (2012). Multifaceted mechanisms of HIV-1 entry inhibition by human α-defensin. *J. Biol. Chem.* 287, 28821–28838. doi:10.1074/jbc.M112.375949.

Deng, W., Mahajan, R., Baumgarten, C. M., and Logothetis, D. E. (2016). The ICl,swell inhibitor DCPIB blocks Kir channels that possess weak affinity for PIP2. *Pflugers Arch.* doi:10.1007/s00424-016-1794-9.

Desjardins, M., Huber, L. A., Parton, R. G., and Griffiths, G. (1994). Biogenesis of phagolysosomes proceeds through a sequential series of interactions with the endocytic apparatus. *J. Cell Biol.* 124, 677–88.

Di, A., Brown, M. E., Deriy, L. V, Li, C., Szeto, F. L., Chen, Y., et al. (2006). CFTR regulates phagosome acidification in macrophages and alters bactericidal activity. *Nat. Cell Biol.* 8, 933–44. doi:10.1038/ncb1456.

Di, A., Gao, X.-P., Qian, F., Kawamura, T., Han, J., Hecquet, C., et al. (2012). The redox-sensitive cation channel TRPM2 modulates phagocyte ROS production and inflammation. *Nat. Immunol.* 13, 29–34. doi:10.1038/ni.2171.

Di, A., Kiya, T., Gong, H., Gao, X., and Malik, A. B. (2017). Role of the phagosomal redox-sensitive TRP channel TRPM2 in regulating bactericidal activity of macrophages. *J. Cell Sci.* 130, 735–744. doi:10.1242/jcs.196014.

Di Ceglie, I., van den Akker, G. G. H., Ascone, G., ten Harkel, B., Ha cker, H., van de Loo, F. A. J., et al. (2016). Genetic modification of ER-Hoxb8 osteoclast precursors using CRISPR/Cas9 as a novel way to allow studies on osteoclast

biology. *J. Leukoc. Biol.* 101, 1–11. doi:10.1189/jlb.1AB0416-180RR.

Dinauer, M. C., Orkin, S. H., Brown, R., Jesaitis, A. J., and Parkos, C. A. (1987). The glycoprotein encoded by the X-linked chronic granulomatous disease locus is a component of the neutrophil cytochrome b complex. *Nature* 327, 717–720. doi:10.1038/327717a0.

Dingjan, I., Verboogen, D. R., Paardekooper, L. M., Revelo, N. H., Sittig, S. P., Visser, L. J., et al. (2016). Lipid peroxidation causes endosomal antigen release for cross-presentation. *Sci. Rep.* 6, 22064. doi:10.1038/srep22064.

Dinter, J., Gourdain, P., Lai, N. Y., Duong, E., Bracho-Sanchez, E., Rucevic, M., et al. (2014). Different antigen-processing activities in dendritic cells, macrophages, and monocytes lead to uneven production of HIV epitopes and affect CTL recognition. *J. Immunol.* 193, 4322–4334. doi:10.4049/jimmunol.1400491.

Dranka, B. P., Benavides, G. A., Diers, A. R., Giordano, S., Zelickson, B. R., Reily, C., et al. (2011). Assessing bioenergetic function in response to oxidative stress by metabolic profiling. *Free Radic. Biol. Med.* 51, 1621–1635. doi:10.1016/j.freeradbiomed.2011.08.005.

Dusi, S., Donini, M., and Rossi, F. (1996). Mechanisms of NADPH oxidase activation: translocation of p40phox, Rac1 and Rac2 from the cytosol to the membranes in human neutrophils lacking p47phox or p67phox. *Biochem. J.* 314 (Pt 2), 409–12.

Dustin, M. L. (2016). Complement Receptors in Myeloid Cell Adhesion and Phagocytosis. *Microbiol. Spectr.* 4. doi:10.1128/microbiolspec.MCHD-0034-2016.

Edgar, R., Domrachev, M., and Lash, A. E. (2002). Gene Expression Omnibus: NCBI gene expression and hybridization array data repository. *Nucleic Acids Res.* 30, 207–10. doi:10.1093/NAR/30.1.207.

Egesten, A., Breton-Gorius, J., Guichard, J., Gullberg, U., and Olsson, I. (1994). The heterogeneity of azurophil granules in neutrophil promyelocytes: immunogold localization of myeloperoxidase, cathepsin G, elastase, proteinase 3, and bactericidal/permeability increasing protein. *Blood* 83, 2985–94.

El Chemaly, A., Nunes, P., Jimaja, W., Castelbou, C., and Demaurex, N. (2014a). Hv1 proton channels differentially regulate the pH of neutrophil and macrophage phagosomes by sustaining the production of phagosomal ROS that inhibit the delivery of vacuolar ATPases. *J. Leukoc. Biol.* 95, 827–839. doi:10.1189/jlb.0513251.

El Chemaly, A., Nunes, P., Jimaja, W., Castelbou, C., and Demaurex, N. (2014b). Hv1 proton channels differentially regulate the pH of neutrophil and macrophage phagosomes by sustaining the production of phagosomal ROS that inhibit the delivery of vacuolar ATPases. *J. Leukoc. Biol.* 95, 827–839. doi:10.1189/jlb.0513251.

Ellson, C. D., Davidson, K., Ferguson, G. J., O'Connor, R., Stephens, L. R., and Hawkins, P. T. (2006). Neutrophils from p40phox-/- mice exhibit severe defects in NADPH oxidase regulation and oxidant-dependent bacterial killing. *J. Exp. Med.* 203, 1927–37. doi:10.1084/jem.20052069.

Elsen, S., Doussière, J., Villiers, C. L., Faure, M., Berthier, R., Papaioannou, A., et al. (2004). Cryptic O2- -generating NADPH oxidase in dendritic cells. *J. Cell*

Sci. 117, 2215–26. doi:10.1242/jcs.01085.

Embgenbroich, M., and Burgdorf, S. (2018). Current concepts of antigen cross-presentation. *Front. Immunol.* 9, 1643. doi:10.3389/fimmu.2018.01643.

Fabbrini, M., Sammicheli, C., Margarit, I., Maione, D., Grandi, G., Giuliani, M. M., et al. (2012). A new flow-cytometry-based opsonophagocytosis assay for the rapid measurement of functional antibody levels against Group B Streptococcus. *J. Immunol. Methods* 378, 11–19. doi:10.1016/j.jim.2012.01.011.

Faulkner, K., and Fridovich, I. (1993). Luminol and lucigenin as detectors for O2ṡ-. *Free Radic. Biol. Med.* 15, 447–451. doi:10.1016/0891-5849(93)90044-U.

Faurschou, M., and Borregaard, N. (2003). Neutrophil granules and secretory vesicles in inflammation. *Microbes Infect.* 5, 1317–1327. doi:10.1016/j.micinf.2003.09.008.

Feng, X., Deng, T., Zhang, Y., Su, S., Wei, C., and Han, D. (2011). Lipopolysaccharide inhibits macrophage phagocytosis of apoptotic neutrophils by regulating the production of tumour necrosis factor α and growth arrest-specific gene 6. *Immunology* 132, 287–95. doi:10.1111/j.1365-2567.2010.03364.x.

Fischmeister, R., and Hartzell, H. C. (2005). Volume sensitivity of the bestrophin family of chloride channels. *J. Physiol.* 562, 477–491. doi:10.1113/jphysiol.2004.075622.

Flannagan, R. S., Cosío, G., and Grinstein, S. (2009). Antimicrobial mechanisms of phagocytes and bacterial evasion strategies. *Nat. Rev. Microbiol.* 7, 355–366. doi:10.1038/nrmicro2128.

Flannagan, R. S., Heit, B., and Heinrichs, D. E. (2016). Intracellular replication of Staphylococcus aureus in mature phagolysosomes in macrophages precedes host cell death, and bacterial escape and dissemination. *Cell. Microbiol.* 18, 514–535. doi:10.1111/cmi.12527.

Flannagan, R. S., Jaumouillé, V., and Grinstein, S. (2011). The Cell Biology of Phagocytosis. doi:10.1146/annurev-pathol-011811-132445.

Fleming, T. J., Fleming, M. L., and Malek, T. R. (1993). Selective expression of Ly-6G on myeloid lineage cells in mouse bone marrow. RB6-8C5 mAb to granulocyte-differentiation antigen (Gr-1) detects members of the Ly-6 family. *J. Immunol.* 151, 2399–408.

Foote, J. R., Behe, P., Frampton, M., Levine, A. P., and Segal, A. W. (2017). An Exploration of Charge Compensating Ion Channels across the Phagocytic Vacuole of Neutrophils. *Front. Pharmacol.* 8, 94. doi:10.3389/fphar.2017.00094.

Forst, S., Weiss, J., Maraganore, J. M., Heinrikson, R. L., and Elsbach, P. (1987). Relation between binding and the action of phospholipases A2 on Escherichia coli exposed to the bactericidal/permeability-increasing protein of neutrophils. *Biochim. Biophys. Acta (BBA)/Lipids Lipid Metab.* 920, 221–225. doi:10.1016/0005-2760(87)90098-1.

Fossati-Jimack, L., Ling, G. S., Cortini, A., Szajna, M., Malik, T. H., McDonald, J. U., et al. (2013). Phagocytosis is the main CR3-mediated function affected by the lupus-associated variant of CD11b in human myeloid cells. *PLoS One* 8,

e57082. doi:10.1371/journal.pone.0057082.

Foxman, E. F., Campbell, J. J., and Butcher, E. C. (1997). Multistep navigation and the combinatorial control of leukocyte chemotaxis. *J. Cell Biol.* 139, 1349–60.

Gabay, J. E., and Almeida, R. P. (1993). Antibiotic peptides and serine protease homologs in human polymorphonuclear leukocytes: defensins and azurocidin. *Curr. Opin. Immunol.* 5, 97–102. doi:10.1016/0952-7915(93)90087-9.

Gabay, J. E., Scott, R. W., Campanelli, D., Griffith, J., Wilde, C., Marra, M. N., et al. (1989). Antibiotic proteins of human polymorphonuclear leukocytes. *Proc. Natl. Acad. Sci. U. S. A.* 86, 5610–4.

Ganly, P., Walker, L. C., and Morris, C. M. (2004). Familial mutations of the transcription factor RUNX1 (AML1, CBFA2) predispose to acute myeloid leukemia. *Leuk. Lymphoma* 45, 1–10. doi:10.1080/1042819031000139611.

Gaurav, R., Bewtra, A. K., and Agrawal, D. K. (2015). Chloride Channel 3 Channels in the Activation and Migration of Human Blood Eosinophils in Allergic Asthma. *Am. J. Respir. Cell Mol. Biol.* 53, 235–45. doi:10.1165/rcmb.2014-0300OC.

Gautam, S., Kirschnek, S., Gentle, I. E., Kopiniok, C., Henneke, P., Häcker, H., et al. (2013). Survival and differentiation defects contribute to neutropenia in glucose-6-phosphatase-β (G6PC3) deficiency in a model of mouse neutrophil granulocyte differentiation. *Cell Death Differ.* 20, 1068–1079. doi:10.1038/cdd.2013.39.

Gautier, L., Cope, L., Bolstad, B. M., and Irizarry, R. A. (2004). affy--analysis of Affymetrix GeneChip data at the probe level. *Bioinformatics* 20, 307–315. doi:10.1093/bioinformatics/btg405.

Gazendam, R. P., van de Geer, A., van Hamme, J. L., Tool, A. T. J., van Rees, D. J., Aarts, C. E. M., et al. (2016). Impaired killing of Candida albicans by granulocytes mobilized for transfusion purposes: a role for granule components. *Haematologica*, haematol.2015.136630-. doi:10.3324/haematol.2015.136630.

Gazzano-Santoro, H., Parent, J. B., Conlon, P. J., Kasler, H. G., Tsai, C. M., Lill-Elghanian, D. A., et al. (1995). Characterization of the structural elements in lipid A required for binding of a recombinant fragment of bactericidal/permeability-increasing protein rBPI23. *Infect. Immun.* 63, 2201–2205.

Gazzano-Santoro, H., Parent, J. B., Grinna, L., Horwitz, A., Parsons, T., Theofan, G., et al. (1992). High-affinity binding of the bactericidal/permeability-increasing protein and a recombinant amino-terminal fragment to the lipid A region of lipopolysaccharide. *Infect. Immun.* 60, 4754–4761.

Gees, M., Owsianik, G., Voets, T., and Voets, T. (2012). “TRP Channels,” in *Comprehensive Physiology* (Hoboken, NJ, USA: John Wiley & Sons, Inc.), 563–608. doi:10.1002/cphy.c110026.

Geisow, M. J., D’Arcy Hart, P., and Young, M. R. (1981). Temporal changes of lysosome and phagosome pH during phagolysosome formation in macrophages: Studies by fluorescence spectroscopy. *J. Cell Biol.* 89, 645–652. doi:10.1083/jcb.89.3.645.

George, A., Pushkaran, S., Li, L., An, X., Zheng, Y., Mohandas, N., et al. (2010). Altered phosphorylation of cytoskeleton proteins in sickle red blood cells: The

role of protein kinase C, Rac GTPases, and reactive oxygen species. *Blood Cells, Mol. Dis.* 45, 41–45. doi:10.1016/j.bcmd.2010.02.006.

Gerencser, A. A., Neilson, A., Choi, S. W., Edman, U., Yadava, N., Oh, R. J., et al. (2009). Quantitative microplate-based respirometry with correction for oxygen diffusion. *Anal. Chem.* 81, 6868–6878. doi:10.1021/ac900881z.

Ghislat, G., and Lawrence, T. (2018). Autophagy in dendritic cells. *Cell. Mol. Immunol.* doi:10.1038/cmi.2018.2.

Giambelluca, M. S., and Gende, O. A. (2011). Cl−/HCO3- exchange activity in fMLP-stimulated human neutrophils. doi:10.1016/j.bbrc.2011.05.046.

Gilman-Sachs, A., Tikoo, A., Akman-Anderson, L., Jaiswal, M., Ntrivalas, E., and Beaman, K. (2015). Expression and role of a2 vacuolar-ATPase (a2V) in trafficking of human neutrophil granules and exocytosis. *J. Leukoc. Biol.* 97, 1121–1131. doi:10.1189/jlb.3A1214-620RR.

Ginhoux, F., and Guilliams, M. (2016). Tissue-Resident Macrophage Ontogeny and Homeostasis. *Immunity* 44, 439–449. doi:10.1016/j.immuni.2016.02.024.

Gluschko, A., Herb, M., Wiegmann, K., Krut, O., Neiss, W. F., Utermöhlen, O., et al. (2018). The β2 Integrin Mac-1 Induces Protective LC3-Associated Phagocytosis of Listeria monocytogenes. *Cell Host Microbe* 23, 324–337.e5. doi:10.1016/j.chom.2018.01.018.

Gombart, A. F., Shiohara, M., Kwok, S. H., Agematsu, K., Komiyama, A., and Koeffler, H. P. (2001). Neutrophil-specific granule deficiency: homozygous recessive inheritance of a frameshift mutation in the gene encoding transcription factor CCAAT/enhancer binding protein--epsilon. *Blood* 97, 2561–7.

Gong, L., Cullinane, M., Treerat, P., Ramm, G., Prescott, M., Adler, B., et al. (2011). The Burkholderia pseudomallei Type III Secretion System and BopA Are Required for Evasion of LC3-Associated Phagocytosis. *PLoS One* 6, e17852. doi:10.1371/journal.pone.0017852.

Goodridge, H. S., Reyes, C. N., Becker, C. A., Katsumoto, T. R., Ma, J., Wolf, A. J., et al. (2011). Activation of the innate immune receptor Dectin-1 upon formation of a 'phagocytic synapse.' *Nature* 472, 471–475. doi:10.1038/nature10071.

Gordon, S., and Plüddemann, A. (2018). Macrophage Clearance of Apoptotic Cells: A Critical Assessment. *Front. Immunol.* 9, 127. doi:10.3389/fimmu.2018.00127.

Gran, S., Honold, L., Fehler, O., Zenker, S., Eligehausen, S., Kuhlmann, M. T., et al. (2018). Imaging, myeloid precursor immortalization, and genome editing for defining mechanisms of leukocyte recruitment in vivo. *Theranostics* 8, 2407–2423. doi:10.7150/thno.23632.

Graus, M. S., Neumann, A. K., and Timlin, J. A. (2017). Hyperspectral fluorescence microscopy detects autofluorescent factors that can be exploited as a diagnostic method for Candida species differentiation. *J. Biomed. Opt.* 22, 16002. doi:10.1117/1.JBO.22.1.016002.

Graves, A. R., Curran, P. K., Smith, C. L., and Mindell, J. A. (2008). The Cl-/H+ antiporter ClC-7 is the primary chloride permeation pathway in lysosomes. *Nature* 453, 788–792. doi:10.1038/nature06907.

Gray, K. A., Yates, B., Seal, R. L., Wright, M. W., and Bruford, E. A. (2015). Genenames.org: the HGNC resources in 2015. *Nucleic Acids Res.* 43, D1079-

85. doi:10.1093/nar/gku1071.

Green, J. N., Chapman, A. L. P., Bishop, C. J., Winterbourn, C. C., and Kettle, A. J. (2017). Neutrophil granule proteins generate bactericidal ammonia chloramine on reaction with hydrogen peroxide. *Free Radic. Biol. Med.* 113, 363–371. doi:10.1016/j.freeradbiomed.2017.10.343.

Grégoire, C., Welch, H., Astarie-dequeker, C., and Maridonneau-parini, I. (1998). Expression of azurophil and specific granule proteins during differentiation of NB4 cells in neutrophils. *J. Cell. Physiol.* 175, 203–210.

Grinstein, S., Furuya, W., and Biggar, W. D. (1986). Cytoplasmic pH regulation in normal and abnormal neutrophils. Role of superoxide generation and Na+/H+ exchange. *J. Biol. Chem.* 261, 512–4.

Growney, J. D., Shigematsu, H., Li, Z., Lee, B. H., Adelsperger, J., Rowan, R., et al. (2005). Loss of Runx1 perturbs adult hematopoiesis and is associated with a myeloproliferative phenotype. *Blood* 106, 494–504. doi:10.1182/blood-2004-08-3280.

Guilliams, M., Ginhoux, F., Jakubzick, C., Naik, S. H., Onai, N., Schraml, B. U., et al. (2014). Dendritic cells, monocytes and macrophages: a unified nomenclature based on ontogeny. *Nat. Rev. Immunol.* 14, 571–578. doi:10.1038/nri3712.

Guinamard, R., Simard, C., and Del Negro, C. (2013). Flufenamic acid as an ion channel modulator. *Pharmacol. Ther.* 138, 272–84. doi:10.1016/j.pharmthera.2013.01.012.

Guo, J., and Ikeda, S. R. (2004). Endocannabinoids Modulate N-Type Calcium Channels and G-Protein-Coupled Inwardly Rectifying Potassium Channels via CB1 Cannabinoid Receptors Heterologously Expressed in Mammalian Neurons. *Mol. Pharmacol.* 65, 665–674. doi:10.1124/mol.65.3.665.

Gupta, D., Shah, H. P., Malu, K., Berliner, N., and Gaines, P. (2014). Differentiation and characterization of myeloid cells. *Curr. Protoc. Immunol.* 104, Unit 22F.5. doi:10.1002/0471142735.im22f05s104.

Gutierrez, M. G., Master, S. S., Singh, S. B., Taylor, G. A., Colombo, M. I., and Deretic, V. (2004). Autophagy Is a Defense Mechanism Inhibiting BCG and Mycobacterium tuberculosis Survival in Infected Macrophages. *Cell* 119, 753–766. doi:10.1016/J.CELL.2004.11.038.

Hahn, I., Klaus, A., Janze, A.-K., Steinwede, K., Ding, N., Bohling, J., et al. (2011). Cathepsin G and Neutrophil Elastase Play Critical and Nonredundant Roles in Lung-Protective Immunity against Streptococcus pneumoniae in Mice. *Infect. Immun.* 79, 4893–4901. doi:10.1128/IAI.05593-11.

Hammerschmidt, S. I., Werth, K., Rothe, M., Galla, M., Permanyer, M., Patzer, G. E., et al. (2018). CRISPR/Cas9 Immunoengineering of Hoxb8-Immortalized Progenitor Cells for Revealing CCR7-Mediated Dendritic Cell Signaling and Migration Mechanisms in vivo. *Front. Immunol.* 9, 1949. doi:10.3389/fimmu.2018.01949.

Han, J., and Burgess, K. (2010). Fluorescent Indicators for Intracellular pH. *Chem. Rev.* 110, 2709–2728. doi:10.1021/cr900249z.

Harper, A. M., Chaplin, M. F., and Segal, A. W. (1985). Cytochrome b-245 from human neutrophils is a glycoprotein. *Biochem. J.* 227, 783–8.

Hart, S. P., Dougherty, G. J., Haslett, C., and Dransfield, I. (1997). CD44 regulates phagocytosis of apoptotic neutrophil granulocytes, but not apoptotic lymphocytes, by human macrophages. *J. Immunol.* 159, 919–25.

Heiner, I., Eisfeld, J., and Lückhoff, A. (2003). Role and regulation of TRP channels in neutrophil granulocytes. *Cell Calcium* 33, 533–540. doi:10.1016/S0143-4160(03)00058-7.

Heiner, I., Radukina, N., Eisfeld, J., Kühn, F., and Lückhoff, A. (2005). Regulation of TRPM2 channels in neutrophil granulocytes by ADP-ribose: a promising pharmacological target. *Naunyn. Schmiedebergs. Arch. Pharmacol.* 371, 325–33. doi:10.1007/s00210-005-1033-y.

Henderson, L. M., and Chappell, J. B. (1993). Dihydrorhodamine 123: a fluorescent probe for superoxide generation? *Eur. J. Biochem.* 217, 973–80.

Henderson, L. M., Chappell, J. B., and Jones, O. T. (1987). The superoxide-generating NADPH oxidase of human neutrophils is electrogenic and associated with an H+ channel. *Biochem. J.* 246, 325–9.

Henderson, L. M., and Meech, R. W. (1999). Evidence that the product of the human X-linked CGD gene, gp91-phox, is a voltage-gated H(+) pathway. *J. Gen. Physiol.* 114, 771–86.

Herrero-Turrión, M. J., Calafat, J., Janssen, H., Fukuda, M., and Mollinedo, F. (2008). Rab27a regulates exocytosis of tertiary and specific granules in human neutrophils. *J. Immunol.* 181, 3793–803. doi:10.4049/JIMMUNOL.181.6.3793.

Hill, C. P., Yee, J., Selsted, M. E., and Eisenberg, D. (1991). Crystal structure of defensin HNP-3, an amphiphilic dimer: Mechanisms of membrane permeabilization. *Science (80-.).* 251, 1481–1485. doi:10.1126/science.2006422.

Hirche, T. O., Gaut, J. P., Heinecke, J. W., and Belaaouaj, A. (2005). Myeloperoxidase plays critical roles in killing Klebsiella pneumoniae and inactivating neutrophil elastase: effects on host defense. *J. Immunol.* 174, 1557–65. doi:10.4049/jimmunol.174.3.1557.

Hodge, R. G., and Ridley, A. J. (2016). Regulating Rho GTPases and their regulators. *Nat. Rev. Mol. Cell Biol.* 17, 496–510. doi:10.1038/nrm.2016.67.

Holland, S. M. (2010). Chronic Granulomatous Disease. *Clin. Rev. Allergy Immunol.* 38, 3–10. doi:10.1007/s12016-009-8136-z.

Hondeghem, L. M., and Matsubara, T. (1988). Quinidine blocks cardiac sodium channels during opening and slow inactivation in guinea-pig papillary muscle. *Br. J. Pharmacol.* 93, 311–8.

Honey, K., and Rudensky, A. Y. (2003). Lysosomal cysteine proteases regulate antigen presentation. *Nat. Rev. Immunol.* 3, 472–482. doi:10.1038/nri1110.

Huang, C., Sindic, A., Hill, C. E., Hujer, K. M., Chan, K. W., Sassen, M., et al. (2007). Interaction of the Ca^{2+} -sensing receptor with the inwardly rectifying potassium channels Kir4.1 and Kir4.2 results in inhibition of channel function. *Am. J. Physiol. Physiol.* 292, F1073–F1081. doi:10.1152/ajprenal.00269.2006.

Huang, J., Canadien, V., Lam, G. Y., Steinberg, B. E., Dinauer, M. C., Magalhaes, M. A. O., et al. (2009). Activation of antibacterial autophagy by NADPH oxidases. *Proc. Natl. Acad. Sci. U. S. A.* 106, 6226–31. doi:10.1073/pnas.0811045106.

Hume, D. A., Summers, K. M., Raza, S., Baillie, J. K., and Freeman, T. C. (2010). Functional clustering and lineage markers: Insights into cellular differentiation and gene function from large-scale microarray studies of purified primary cell populations. *Genomics* 95, 328–338. doi:10.1016/J.YGENO.2010.03.002.

Hunter, R. C., and Beveridge, T. J. (2005). Application of a pH-sensitive fluoroprobe (C-SNARF-4) for pH microenvironment analysis in Pseudomonas aeruginosa biofilms. *Appl. Environ. Microbiol.* 71, 2501–10. doi:10.1128/AEM.71.5.2501-2510.2005.

Hurst, J. K. (2012). What really happens in the neutrophil phagosome? *Free Radic. Biol. Med.* 53, 508–20. doi:10.1016/j.freeradbiomed.2012.05.008.

Hurst, J. K., Albrich, J. M., Green, T. R., Rosen, H., and Klebanoff, S. (1984). Myeloperoxidase-dependent fluorescein chlorination by stimulated neutrophils.

Ichikawa, M., Asai, T., Chiba, S., Kurokawa, M., and Ogawa, S. (2004). Runx1/AML-1 ranks as a master regulator of adult hematopoiesis. *Cell Cycle* 3, 722–724. doi:10.4161/cc.3.6.951.

Ichikawa, Y., Pluznik, D. H., and Sachs, L. (1966). In vitro control of the development of macrophage and granulocyte colonies. *Proc. Natl. Acad. Sci. U. S. A.* 56, 488–495. doi:10.1073/pnas.56.2.488.

Ihle, J. N., Keller, J., Henderson, L., Klein, F., and Palaszynski, E. (1982). Procedures for the purification of interleukin 3 to homogeneity. *J. Immunol.* 129, 2431–6.

Imlay, J. A. (2003). Pathways of Oxidative Damage. *Annu. Rev. Microbiol.* 57, 395–418. doi:10.1146/annurev.micro.57.030502.090938.

Ingersoll, M. A., Spanbroek, R., Lottaz, C., Gautier, E. L., Frankenberger, M., Hoffmann, R., et al. (2010). Comparison of gene expression profiles between human and mouse monocyte subsets. *Blood* 115, e10-9. doi:10.1182/blood-2009-07-235028.

Ip, W. K. E., Sokolovska, A., Charriere, G. M., Boyer, L., Dejardin, S., Cappillino, M. P., et al. (2010). Phagocytosis and phagosome acidification are required for pathogen processing and MyD88-dependent responses to Staphylococcus aureus. *J. Immunol.* 184, 7071–81. doi:10.4049/jimmunol.1000110.

Ishiguro, H., Namkung, W., Yamamoto, A., Wang, Z., Worrell, R. T., Xu, J., et al. (2006). Effect of Slc26a6 deletion on apical Cl-/HCO3- exchanger activity and cAMP-stimulated bicarbonate secretion in pancreatic duct. *AJP Gastrointest. Liver Physiol.* 292, G447–G455. doi:10.1152/ajpgi.00286.2006.

Iversen, M. B., Gottfredsen, R. H., Larsen, U. G., Enghild, J. J., Praetorius, J., Borregaard, N., et al. (2016). Extracellular superoxide dismutase is present in secretory vesicles of human neutrophils and released upon stimulation. *Free Radic. Biol. Med.* 97, 478–488. doi:10.1016/j.freeradbiomed.2016.07.004.

Iwatsuki, N., and Petersen, O. H. (1985). Inhibition of Ca2+-activated K+ channels in pig pancreatic acinar cells by Ba2+, Ca2+, quinine and quinidine. *Biochim. Biophys. Acta* 819, 249–57.

Iyer, G. Y. N., Islam, M. F., and Quastel, J. H. (1961). Biochemical aspects of phagocytosis. *Nature* 192, 535–541. doi:10.1038/192535a0.

Jacob, C., Leport, M., Szilagyi, C., Allen, J. ., Bertrand, C., and Lagente, V. (2002). DMSO-treated HL60 cells: a model of neutrophil-like cells mainly expressing

PDE4B subtype. *Int. Immunopharmacol.* 2, 1647–1656. doi:10.1016/S1567-5769(02)00141-8.

Jagannathan-Bogdan, M., and Zon, L. I. (2013). Hematopoiesis. *Development* 140, 2463–2467. doi:10.1242/dev.083147.

Jang, S., and Imlay, J. A. (2007). Micromolar Intracellular Hydrogen Peroxide Disrupts Metabolism by Damaging Iron-Sulfur Enzymes. *J. Biol. Chem.* 282, 929–937. doi:10.1074/jbc.M607646200.

Jankowski, A., and Grinstein, S. (1999). A noninvasive fluorimetric procedure for measurement of membrane potential. Quantification of the NADPH oxidase-induced depolarization in activated neutrophils. *J. Biol. Chem.* 274, 26098–104.

Jankowski, A., Scott, C. C., and Grinstein, S. (2002). Determinants of the phagosomal pH in neutrophils. *J. Biol. Chem.* 277, 6059–66. doi:10.1074/jbc.M110059200.

Jefferis, R., and Lund, J. (2002). Interaction sites on human IgG-Fc for FcγR: current models. *Immunol. Lett.* 82, 57–65. doi:10.1016/S0165-2478(02)00019-6.

Jenssen, H., and Hancock, R. E. W. (2009). Antimicrobial properties of lactoferrin. *Biochimie* 91, 19–29. doi:10.1016/j.biochi.2008.05.015.

Jentsch, T. J. (2016). VRACs and other ion channels and transporters in the regulation of cell volume and beyond. *Nat. Rev. Mol. Cell Biol.* 17, 293–307. doi:10.1038/nrm.2016.29.

Jethwaney, D., Islam, M. R., Leidal, K. G., de Bernabe, D. B.-V., Campbell, K. P., Nauseef, W. M., et al. (2007). Proteomic analysis of plasma membrane and secretory vesicles from human neutrophils. *Proteome Sci.* 5, 12. doi:10.1186/1477-5956-5-12.

Jiang, L., Salao, K., Li, H., Rybicka, J. M., Yates, R. M., Luo, X. W., et al. (2012). Intracellular chloride channel protein CLIC1 regulates macrophage function through modulation of phagosomal acidification. *J. Cell Sci.* 125, 5479–88. doi:10.1242/jcs.110072.

Jin, N. G., Kim, J. K., Yang, D. K., Cho, S. J., Kim, J. M., Koh, E. J., et al. (2003). Fundamental role of ClC-3 in volume-sensitive Cl- channel function and cell volume regulation in AGS cells. *Am. J. Physiol. Gastrointest. Liver Physiol.* 285, G938-48. doi:10.1152/ajpgi.00470.2002.

Johnson, J. L., Brzezinska, A. A., Tolmachova, T., Munafo, D. B., Ellis, B. A., Seabra, M. C., et al. (2010). Rab27a and Rab27b regulate neutrophil azurophilic granule exocytosis and NADPH oxidase activity by independent mechanisms. *Traffic* 11, 533–47. doi:10.1111/j.1600-0854.2009.01029.x.

Jyoti, A., Singh, A. K., Dubey, M., Kumar, S., Saluja, R., Keshari, R. S., et al. (2014). Interaction of Inducible Nitric Oxide Synthase with Rac2 Regulates Reactive Oxygen and Nitrogen Species Generation in the Human Neutrophil Phagosomes: Implication in Microbial Killing. *Antioxid. Redox Signal.* 20, 417–431. doi:10.1089/ars.2012.4970.

Kapur, R., Einarsdottir, H. K., and Vidarsson, G. (2014). IgG-effector functions: “The Good, The Bad and The Ugly.” *Immunol. Lett.* 160, 139–144. doi:10.1016/J.IMLET.2014.01.015.

Karlsson, A., Nixon, J. B., and McPhail, L. C. (2000). Phorbol myristate acetate

induces neutrophil NADPH-oxidase activity by two separate signal transduction pathways: dependent or independent of phosphatidylinositol 3-kinase. *J. Leukoc. Biol.* 67, 396–404.

Karlsson, A., Nygren, E., Karlsson, J., Nordström, I., Dahlgren, C., and Eriksson, K. (2007). Ability of monocyte-derived dendritic cells to secrete oxygen radicals in response to formyl peptide receptor family agonists compared to that of myeloid and plasmacytoid dendritic cells. *Clin. Vaccine Immunol.* 14, 328–30. doi:10.1128/CVI.00349-06.

Kasper, L., Seider, K., Gerwien, F., Allert, S., Brunke, S., Schwarzmüller, T., et al. (2014). Identification of Candida glabrata Genes Involved in pH Modulation and Modification of the Phagosomal Environment in Macrophages. *PLoS One* 9, e96015. doi:10.1371/journal.pone.0096015.

Kenmoku, S., Urano, Y., Kojima, H., and Nagano, T. (2007). Development of a Highly Specific Rhodamine-Based Fluorescence Probe for Hypochlorous Acid and Its Application to Real-Time Imaging of Phagocytosis. *J. Amer. Chem. Soc*. 129, 7313-7318. doi:10.1021/ja068740g.

Keyer, K., and Imlay, J. A. (1996). Superoxide accelerates DNA damage by elevating free-iron levels. *Proc. Natl. Acad. Sci. U. S. A.* 93, 13635–40.

Khanna-Gupta, a, Kolibaba, K., Zibello, T. a, and Berliner, N. (1994). NB4 cells show bilineage potential and an aberrant pattern of neutrophil secondary granule protein gene expression. *Blood*. 84, 294-302

Kim, C., and Dinauer, M. C. (2001). Rac2 is an essential regulator of neutrophil nicotinamide adenine dinucleotide phosphate oxidase activation in response to specific signaling pathways. *J. Immunol.* 166, 1223–32.

Kjeldsen, L., Sengeløv, H., Lollike, K., Nielsen, M. H., and Borregaard, N. (1994). Isolation and characterization of gelatinase granules from human neutrophils. *Blood*. 83, 1640-1649-302 doi:8123855.

Klebanoff, S. J. (2005). Myeloperoxidase: friend and foe. *J. Leukoc. Biol.* doi:10.1189/jlb.1204697.

Klebanoff, S. J., Kettle, A. J., Rosen, H., Winterbourn, C. C., and Nauseef, W. M. (2013). Myeloperoxidase: a front-line defender against phagocytosed microorganisms. *J. Leukoc. Biol.* 93, 185–198. doi:10.1189/jlb.0712349.

Kondo, M., Wagers, A. J., Manz, M. G., Prohaska, S. S., Scherer, D. C., Beilhack, G. F., et al. (2003). Biology of hematopoietic stem cells and progenitors: implications for clinical application. *Annu. Rev. Immunol.* 21, 759–806. doi:10.1146/annurev.immunol.21.120601.141007.

Kooy, N. W., Royall, J. A., Ischiropoulos, H., and Beckman, J. S. (1994). Peroxynitrite-mediated oxidation of dihydrorhodamine 123. *Free Radic. Biol. Med.* 16, 149–156. doi:10.1016/0891-5849(94)90138-4.

Korchak, H. M., Rossi, M. W., and Kilpatrick, L. E. (1998). Selective role for beta-protein kinase C in signaling for O-2 generation but not degranulation or adherence in differentiated HL60 cells. *J. Biol. Chem.* 273, 27292–9..

Korkmaz, B., Moreau, T., and Gauthier, F. (2008). Neutrophil elastase, proteinase 3 and cathepsin G: Physicochemical properties, activity and physiopathological functions. *Biochimie* 90, 227–242. doi:10.1016/J.BIOCHI.2007.10.009.

Kourjian, G., Rucevic, M., Berberich, M. J., Dinter, J., Wambua, D., Boucau, J., et

al. (2016). HIV Protease Inhibitor-Induced Cathepsin Modulation Alters Antigen Processing and Cross-Presentation. *J. Immunol.* 196, 3595–607. doi:10.4049/jimmunol.1600055.

Krause, K. H., and Welsh, M. J. (1990). Voltage-dependent and Ca2+-activated ion channels in human neutrophils. *J. Clin. Invest.* 85, 491–498. doi:10.1172/JCI114464.

Krautwurst, D., Seifert, R., Hescheler, J., and Schultz, G. (1992). Formyl peptides and ATP stimulate Ca2+ and Na+ inward currents through non-selective cation channels via G-proteins in dibutyryl cyclic AMP-differentiated HL-60 cells. Involvement of Ca2+ and Na+ in the activation of beta-glucuronidase release and superox. *Biochem. J.* 288, 1025–1035.

Kumar, H., Kawai, T., and Akira, S. (2011). Pathogen Recognition by the Innate Immune System. *Int. Rev. Immunol.* 30, 16–34. doi:10.3109/08830185.2010.529976.

Kumar, L., Chou, J., Yee, C. S. K., Borzutzky, A., Vollmann, E. H., von Andrian, U. H., et al. (2014). Leucine-rich repeat containing 8A (LRRC8A) is essential for T lymphocyte development and function. *J. Exp. Med.* 211, 929–942. doi:10.1084/jem.20131379.

Kurotaki, D., Yamamoto, M., Nishiyama, A., Uno, K., Ban, T., Ichino, M., et al. (2014). IRF8 inhibits C/EBPα activity to restrain mononuclear phagocyte progenitors from differentiating into neutrophils. *Nat. Commun.* 5, 4978. doi:10.1038/ncomms5978.

Lanotte, M., Martin-Thouvenin, V., Najman, S., Balerini, P., Valensi, F., and Berger, R. (1991). NB4, a maturation inducible cell line with t(15;17) marker isolated from a human acute promyelocytic leukemia (M3).

Lauber, K., Bohn, E., Kröber, S. M., Xiao, Y., Blumenthal, S. G., Lindemann, R. K., et al. (2003). Apoptotic cells induce migration of phagocytes via caspase-3-mediated release of a lipid attraction signal. *Cell* 113, 717–30.

Lavis, L. D., Rutkoski, T. J., and Raines, R. T. (2007). Tuning the pK a of Fluorescein to Optimize Binding Assays. *Anal. Chem.* 79, 6775–6782. doi:10.1021/ac070907g.

Lawrence, S. M., Corriden, R., and Nizet, V. (2018). The Ontogeny of a Neutrophil: Mechanisms of Granulopoiesis and Homeostasis. *Microbiol. Mol. Biol. Rev.* 82, e00057-17. doi:10.1128/MMBR.00057-17.

Lawson, N. D., and Berliner, N. (1999). Neutrophil maturation and the role of retinoic acid. *Exp. Hematol.* 27, 1355–67. doi:10.1016/S0301-472X(99)00085-5.

Lawson, N. D., Krause, D. S., and Berliner, N. (1998). Normal neutrophil differentiation and secondary granule gene expression in the EML and MPRO cell lines. *Exp Hematol* 26, 1178–1185.

Le Cabec, V., Calafat, J., and Borregaard, N. (1997). Sorting of the specific granule protein, NGAL, during granulocytic maturation of HL-60 cells. *Blood* 89, 2113–21.

Lebargy, R. E., Hancock, A. B., Gangloff, S., Achilefu, M., Guenounou, F., Tim, O., et al. (2017). Neutrophil Elastase Mediates Innate Host Protection against Pseudomonas aeruginosa. *J Immunol Ref. J. Immunol.* 181, 4945–4954. doi:10.4049/jimmunol.181.7.4945.

Lee, C.-Y., Herant, M., and Heinrich, V. (2011). Target-specific mechanics of phagocytosis: protrusive neutrophil response to zymosan differs from the uptake of antibody-tagged pathogens. *J. Cell Sci.* 124, 1106–14. doi:10.1242/jcs.078592.

Lee, J., Breton, G., Oliveira, T. Y. K., Zhou, Y. J., Aljoufi, A., Puhr, S., et al. (2015). Restricted dendritic cell and monocyte progenitors in human cord blood and bone marrow. *J. Exp. Med.* 212, 385–99. doi:10.1084/jem.20141442.

Lee, J., Tam, H., Adler, L., Ilstad-Minnihan, A., Macaubas, C., and Mellins, E. D. (2017). The MHC class II antigen presentation pathway in human monocytes differs by subset and is regulated by cytokines. *PLoS One* 12, e0183594. doi:10.1371/journal.pone.0183594.

Lee, Y.-M., Kim, B.-J., Chun, Y.-S., So, I., Choi, H., Kim, M.-S., et al. (2006). NOX4 as an oxygen sensor to regulate TASK-1 activity. *Cell. Signal.* 18, 499–507. doi:10.1016/j.cellsig.2005.05.025.

Lehrer, R. I., Ladra, K. M., and Hake, R. B. (1975). Nonoxidative Fungicidal Mechanisms of Mammalian Granulocytes: Demonstration of Components with Candidacidal Activity in Human, Rabbit, and Guinea Pig Leukocytes. 11, 1226–1234.

Lehrer, R. I., and Lu, W. (2012). α-Defensins in human innate immunity. *Immunol. Rev.* 245, 84–112. doi:10.1111/j.1600-065X.2011.01082.x.

Leithner, A., Renkawitz, J., De Vries, I., Hauschild, R., Häcker, H., and Sixt, M. (2018). Fast and efficient genetic engineering of hematopoietic precursor cells for the study of dendritic cell migration. *Eur. J. Immunol.* 48, 1074–1077. doi:10.1002/eji.201747358.

Lestienne, P., and Bieth, J. G. (1980). Activation of human leukocyte elastase activity by excess substrate, hydrophobic solvents, and ionic strength. *J. Biol. Chem.* 255, 9289–94.

Levine, A. P., Duchen, M. R., de Villiers, S., Rich, P. R., and Segal, A. W. (2015). Alkalinity of neutrophil phagocytic vacuoles is modulated by HVCN1 and has consequences for myeloperoxidase activity. *PLoS One* 10, e0125906. doi:10.1371/journal.pone.0125906.

Levine, A. P., and Segal, A. W. (2016). The NADPH Oxidase and Microbial Killing by Neutrophils, With a Particular Emphasis on the Proposed Antimicrobial Role of Myeloperoxidase within the Phagocytic Vacuole. *Microbiol. Spectr.* 4. doi:10.1128/microbiolspec.MCHD-0018-2015.

Levy, J., Kolski, G. B., and Douglas, S. D. (1989). Cathepsin D-Like Activity in Neutrophils and Monocytes. *Infect. Immun.*, 1632–1634.

Lian, Z., Kluger, Y., Greenbaum, D. S., Tuck, D., Gerstein, M., Berliner, N., et al. (2002). Genomic and proteomic analysis of the myeloid differentiation program: Global analysis of gene expression during induced differentiation in the MPRO cell line. *Blood* 100, 3209–3220. doi:10.1182/blood-2002-03-0850.

Lian, Z., Wang, L., Yamaga, S., Bonds, W., Beazer-Barclay, Y., Kluger, Y., et al. (2001). Genomic and proteomic analysis of the myeloid differentiation program. *Blood* 98, 513–524.

Liang, W., Huang, L., Zhao, D., He, J. Z., Sharma, P., Liu, J., et al. (2014). Swelling-activated Cl− currents and intracellular CLC-3 are involved in proliferation of

human pulmonary artery smooth muscle cells. *J. Hypertens.* 32, 318–330. doi:10.1097/HJH.0000000000000013.

Liantonio, A., Giannuzzi, V., Picollo, A., Babini, E., Pusch, M., and Conte Camerino, D. (2007). Niflumic acid inhibits chloride conductance of rat skeletal muscle by directly inhibiting the CLC-1 channel and by increasing intracellular calcium. *Br. J. Pharmacol.* 150, 235–47. doi:10.1038/sj.bjp.0706954.

Lim, C. Y., Owens, N. A., Wampler, R. D., Ying, Y., Granger, J. H., Porter, M. D., et al. (2014). Succinimidyl ester surface chemistry: Implications of the competition between aminolysis and hydrolysis on covalent protein immobilization. *Langmuir* 30, 12868–12878. doi:10.1021/la503439g.

Lim, K., Hyun, Y.-M., Lambert-Emo, K., Topham, D. J., and Kim, M. (2015). Visualization of integrin Mac-1 in vivo. *J. Immunol. Methods* 426, 120–7. doi:10.1016/j.jim.2015.08.012.

Lindemann, O., Strodthoff, C., Horstmann, M., Nielsen, N., Jung, F., Schimmelpfennig, S., et al. (2015). TRPC1 regulates fMLP-stimulated migration and chemotaxis of neutrophil granulocytes. *Biochim. Biophys. Acta* 1853, 2122–30. doi:10.1016/j.bbamcr.2014.12.037.

Link, T. M., Park, U., Vonakis, B. M., Raben, D. M., Soloski, M. J., and Caterina, M. J. (2010). TRPV2 has a pivotal role in macrophage particle binding and phagocytosis. *Nat. Immunol.* 11, 232–9. doi:10.1038/ni.1842.

Liu, J., Diwu, Z., and Leung, W.-Y. (2001). Synthesis and photophysical properties of new fluorinated benzo[c]xanthene dyes as intracellular pH indicators. *Bioorg. Med. Chem. Lett.* 11, 2903–2905. doi:10.1016/S0960-894X(01)00595-9.

Loike, J. D., Plitt, A., Kothari, K., Zumeris, J., Budhu, S., Kavalus, K., et al. (2013). Surface Acoustic Waves Enhance Neutrophil Killing of Bacteria. *PLoS One* 8, e68334. doi:10.1371/journal.pone.0068334.

Lominadze, G., Powell, D. W., Luerman, G. C., Link, A. J., Ward, R. A., and McLeish, K. R. (2005). Proteomic analysis of human neutrophil granules. *Mol. Cell. Proteomics* 4, 1503–21. doi:10.1074/mcp.M500143-MCP200.

Lord, B. I., Molineux, G., Pojda, Z., Souza, L. M., Mermod, J. J., and Dexter, T. M. (1991). Myeloid cell kinetics in mice treated with recombinant interleukin-3, granulocyte colony-stimulating factor (CSF), or granulocyte-macrophage CSF in vivo. *Blood* 77, 2154–2159.

Lucas, O., Hilaire, C., Delpire, E., and Scamps, F. (2012). KCC3-dependent chloride extrusion in adult sensory neurons. *Mol. Cell. Neurosci.* 50, 211–20. doi:10.1016/j.mcn.2012.05.005.

Lukacs, G. L., Nanda, A., Rotstein, O. D., and Grinstein, S. (1991). The chloride channel blocker 5-nitro-2-(3-phenylpropyl-amino) benzoic acid (NPPB) uncouples mitochondria and increases the proton permeability of the plasma membrane in phagocytic cells. *FEBS Lett.* 288, 17–20.

Lundqvist-Gustafsson, H., Gustafsson, M., and Dahlgren, C. (2000). Dynamic Ca2+changes in neutrophil phagosomes A source for intracellular Ca2+during phagolysosome formation? *Cell Calcium* 27, 353–362. doi:10.1054/CECA.2000.0130.

Maderna, P., Yona, S., Perretti, M., and Godson, C. (2005). Modulation of phagocytosis of apoptotic neutrophils by supernatant from dexamethasone-

treated macrophages and annexin-derived peptide Ac(2-26). *J. Immunol.* 174, 3727–33. doi:10.4049/JIMMUNOL.174.6.3727.

Mahankali, M., Peng, H.-J., Henkels, K. M., Dinauer, M. C., and Gomez-Cambronero, J. (2011). Phospholipase D2 (PLD2) is a guanine nucleotide exchange factor (GEF) for the GTPase Rac2. *Proc. Natl. Acad. Sci.* 108, 19617–19622. doi:10.1073/pnas.1114692108.

Maingret, F., Patel, A. J., Lazdunski, M., and Honoré, E. (2001). The endocannabinoid anandamide is a direct and selective blocker of the background K(+) channel TASK-1. *EMBO J.* 20, 47–54. doi:10.1093/emboj/20.1.47.

Mantegazza, A. R., Savina, A., Vermeulen, M., Pérez, L., Geffner, J., Hermine, O., et al. (2008). NADPH oxidase controls phagosomal pH and antigen cross-presentation in human dendritic cells. *Blood* 112, 4712–4722. doi:10.1182/blood-2008-01-134791.

Martin, C. J., Booty, M. G., Rosebrock, T. R., Nunes-Alves, C., Desjardins, D. M., Keren, I., et al. (2012). Efferocytosis is an innate antibacterial mechanism. *Cell Host Microbe* 12, 289–300. doi:10.1016/j.chom.2012.06.010.

Masia, R., Krause, D. S., and Yellen, G. (2015). The inward rectifier potassium channel Kir2.1 is expressed in mouse neutrophils from bone marrow and liver. *Am. J. Physiol. Cell Physiol.* 308, C264-76. doi:10.1152/ajpcell.00176.2014.

Maturana, A., Arnaudeau, S., Ryser, S., Banfi, B., Hossle, J. P., Schlegel, W., et al. (2001). Heme Histidine Ligands within gp91 ^{phox} Modulate Proton Conduction by the Phagocyte NADPH Oxidase. *J. Biol. Chem.* 276, 30277–30284. doi:10.1074/jbc.M010438200.

Matute, J. D., Arias, A. A., Wright, N. A. M., Wrobel, I., Waterhouse, C. C. M., Li, X. J., et al. (2009). A new genetic subgroup of chronic granulomatous disease with autosomal recessive mutations in p40 phox and selective defects in neutrophil NADPH oxidase activity. *Blood* 114, 3309–15. doi:10.1182/blood-2009-07-231498.

McCarty, N. A., McDonough, S., Cohen, B. N., Riordan, J. R., Davidson, N., and Lester, H. A. (1993). Voltage-dependent block of the cystic fibrosis transmembrane conductance regulator Cl- channel by two closely related arylaminobenzoates. *J. Gen. Physiol.* 102, 1–23.

McCracken, J. M., and Allen, L.-A. H. (2014). Regulation of human neutrophil apoptosis and lifespan in health and disease. *J. Cell Death* 7, 15–23. doi:10.4137/JCD.S11038.

McDonald, J. U., Cortini, A., Rosas, M., Fossati-Jimack, L., Ling, G. S., Lewis, K. J., et al. (2011a). In vivo functional analysis and genetic modification of in vitro-derived mouse neutrophils. *FASEB J.* 25, 1972–82. doi:10.1096/fj.10-178517.

McDonald, J. U., Cortini, A., Rosas, M., Fossati-Jimack, L., Ling, G. S., Lewis, K. J., et al. (2011b). In vivo functional analysis and genetic modification of in vitro-derived mouse neutrophils. *FASEB J.* 25, 1972–1982. doi:10.1096/fj.10-178517.

McKenna, H. J., Stocking, K. L., Miller, R. E., Brasel, K., De Smedt, T., Maraskovsky, E., et al. (2000). Mice lacking flt3 ligand have deficient hematopoiesis affecting hematopoietic progenitor cells, dendritic cells, and natural killer cells. *Blood* 95, 3489–97.

McLaughlin, N. J. D., Banerjee, A., Khan, S. Y., Lieber, J. L., Kelher, M. R., Gamboni-Robertson, F., et al. (2008). Platelet-activating factor-mediated endosome formation causes membrane translocation of p67phox and p40phox that requires recruitment and activation of p38 MAPK, Rab5a, and phosphatidylinositol 3-kinase in human neutrophils. *J. Immunol.* 180, 8192–203.

McPhillips, K., Janssen, W. J., Ghosh, M., Byrne, A., Gardai, S., Remigio, L., et al. (2007). TNF-alpha inhibits macrophage clearance of apoptotic cells via cytosolic phospholipase A2 and oxidant-dependent mechanisms. *J. Immunol.* 178, 8117–26.

Menegazzi, R., Busetto, S., Decleva, E., Cramer, R., Dri, P., and Patriarca, P. (1999). Triggering of chloride ion efflux from human neutrophils as a novel function of leukocyte beta 2 integrins: relationship with spreading and activation of the respiratory burst. *J. Immunol.* 162, 423–34.

Merle, N. S., Church, S. E., Fremeaux-Bacchi, V., and Roumenina, L. T. (2015). Complement system part I - molecular mechanisms of activation and regulation. *Front. Immunol.* 6, 262. doi:10.3389/fimmu.2015.00262.

Metcalf, D. (2013). The Colony-Stimulating Factors and Cancer. *Cancer Immunol. Res.* 1, 351–356. doi:10.1158/2326-6066.CIR-13-0151.

Michl, J., Pieczonka, M. M., Unkeless, J. C., and Silverstein, S. C. (1979). Effects of immobilized immune complexes on Fc- and complement-receptor function in resident and thioglycollate-elicited mouse peritoneal macrophages. *J. Exp. Med.* 150, 607–21. doi:10.1084/JEM.150.3.607.

Michlewska, S., Dransfield, I., Megson, I. L., and Rossi, A. G. (2009). Macrophage phagocytosis of apoptotic neutrophils is critically regulated by the opposing actions of pro-inflammatory and anti-inflammatory agents: key role for TNF-α. *FASEB J.* 23, 844–854. doi:10.1096/fj.08-121228.

Minieri, L., Pivonkova, H., Caprini, M., Harantova, L., Anderova, M., and Ferroni, S. (2013). The inhibitor of volume-regulated anion channels DCPIB activates TREK potassium channels in cultured astrocytes. *Br. J. Pharmacol.* 168, 1240–54. doi:10.1111/bph.12011.

Miyasaki, K. T., and Bodeau, A. L. (1991). In vitro killing of oral Capnocytophaga by granule fractions of human neutrophils is associated with cathepsin G activity. *J. Clin. Invest.* 87, 1585–93. doi:10.1172/JCI115172.

Miyasaki, K. T., and Bodeau, A. L. (1992). Human neutrophil azurocidin synergizes with leukocyte elastase and cathepsin G in the killing of Capnocytophaga sputigena. *Infect. Immun.* 60, 4973–5.

Moreland, J. G., Davis, a P., Bailey, G., Nauseef, W. M., and Lamb, F. S. (2006). Anion channels, including ClC-3, are required for normal neutrophil oxidative function, phagocytosis, and transendothelial migration. *J. Biol. Chem.* 281, 12277–88. doi:10.1074/jbc.M511030200.

Moreno-Galindo, E. G., Barrio-Echavarría, G. F., Vásquez, J. C., Decher, N., Sachse, F. B., Tristani-Firouzi, M., et al. (2010). Molecular basis for a high-potency open-channel block of Kv1.5 channel by the endocannabinoid anandamide. *Mol. Pharmacol.* 77, 751–8. doi:10.1124/mol.109.063008.

Morgan, B. P., and McGeer, P. L. (1995). Physiology and Pathophysiology of Complement: Progress and Trends. *Crit. Rev. Clin. Lab. Sci.* 32, 265–298.

doi:10.3109/10408369509084686.

Morgan, D., Capasso, M., Musset, B., Cherny, V. V, Ríos, E., Dyer, M. J. S., et al. (2009). Voltage-gated proton channels maintain pH in human neutrophils during phagocytosis. *Proc. Natl. Acad. Sci. U. S. A.* 106, 18022–18027. doi:10.1073/pnas.0905565106.

Morris, M. R., Doull, I. J. M., Dewitt, S., and Hallett, M. B. (2005). Reduced iC3b-mediated phagocytotic capacity of pulmonary neutrophils in cystic fibrosis. *Clin. Exp. Immunol.* 142, 68–75. doi:10.1111/j.1365-2249.2005.02893.x.

Murphy, R., and DeCoursey, T. E. (2006). Charge compensation during the phagocyte respiratory burst. *Biochim. Biophys. Acta* 1757, 996–1011. doi:10.1016/j.bbabio.2006.01.005.

Murray, H. W., Rubin, B. Y., and Rothermel, C. D. (1983). Killing of intracellular Leishmania donovani by lymphokine-stimulated human mononuclear phagocytes. Evidence that interferon-gamma is the activating lymphokine. *J. Clin. Invest.* 72, 1506–1510. doi:10.1172/JCI111107.

N'Diaye, E. N., Vaissiere, C., Gonzalez-Christen, J., Gregoire, C., Le Cabec, V., and Maridonneau-Parini, I. (1997). Expression of NADPH oxidase is induced by all-trans retinoic acid but not by phorbol myristate acetate and 1,25 dihydroxyvitamin D3 in the human promyelocytic cell line NB4. *Leukemia* 11, 2131–2136. doi:10.1038/sj.leu.2400855.

Nagasawa, K., Nakamura, M., Jimi, S., Hayashida, I., Ota, A., Kameda, S., et al. (1982). Phagocytosis-connected oxygen consumption by peripheral leukocytes from patients with systemic lupus erythematosus. *Acta Haematol.* 68, 84–8. doi:10.1159/000206957.

Nagl, M., Kacani, L., Müllauer, B., Lemberger, E.-M., Stoiber, H., Sprinzl, G. M., et al. (2002). Phagocytosis and killing of bacteria by professional phagocytes and dendritic cells. *Clin. Diagn. Lab. Immunol.* 9, 1165–8. doi:10.1128/CDLI.9.6.1165-1168.2002.

Nair-Gupta, P., Baccarini, A., Tung, N., Seyffer, F., Florey, O., Huang, Y., et al. (2014). TLR signals induce phagosomal MHC-I delivery from the endosomal recycling compartment to allow cross-presentation. *Cell* 158, 506–521. doi:10.1016/j.cell.2014.04.054.

Nanda, A., Brumell, J. H., Nordström, T., Kjeldsen, L., Sengelov, H., Borregaard, N., et al. (1996). Activation of proton pumping in human neutrophils occurs by exocytosis of vesicles bearing vacuolar-type H+-ATPases. *J. Biol. Chem.* 271, 15963–70.

Nandurkar, H. H., Robb, L., Tarlinton, D., Barnett, L., Köntgen, F., and Begley, C. G. (1997). Adult mice with targeted mutation of the interleukin-11 receptor (IL11Ra) display normal hematopoiesis. *Blood* 90, 2148–59.

Narni-Mancinelli, E., Soudja, S. M., Crozat, K., Dalod, M., Gounon, P., Geissmann, F., et al. (2011). Inflammatory Monocytes and Neutrophils Are Licensed to Kill during Memory Responses In Vivo. *PLoS Pathog.* 7, e1002457. doi:10.1371/journal.ppat.1002457.

Nastasi, C., Candela, M., Bonefeld, C. M., Geisler, C., Hansen, M., Krejsgaard, T., et al. (2015). The effect of short-chain fatty acids on human monocyte-derived dendritic cells. *Sci. Rep.* 5, 16148. doi:10.1038/srep16148.

Nathan, C. (2006). Neutrophils and immunity: challenges and opportunities. *Nat. Rev. Immunol.* 6, 173–182. doi:10.1038/nri1785.

Nathan, C. F. (1987). Neutrophil activation on biological surfaces. Massive secretion of hydrogen peroxide in response to products of macrophages and lymphocytes. *J. Clin. Invest.* 80, 1550–60. doi:10.1172/JCI113241.

Nathan, C. F., Murray, H. W., Wiebe, M. E., and Rubin, B. Y. (1983). Identification of interferon-gamma as the lymphokine that activates human macrophage oxidative metabolism and antimicrobial activity. *J. Exp. Med.* 158, 670–89.

Nathan, C., and Shiloh, M. U. (2000). Reactive oxygen and nitrogen intermediates in the relationship between mammalian hosts and microbial pathogens. *Proc. Natl. Acad. Sci. U. S. A.* 97, 8841–8.

Nguyen, G. T., Green, E. R., and Mecsas, J. (2017). Neutrophils to the ROScue: Mechanisms of NADPH Oxidase Activation and Bacterial Resistance. *Front. Cell. Infect. Microbiol.* 7, 373. doi:10.3389/fcimb.2017.00373.

Ni, H.-M., Bockus, A., Wozniak, A. L., Jones, K., Weinman, S., Yin, X.-M., et al. (2011). Dissecting the dynamic turnover of GFP-LC3 in the autolysosome. *Autophagy* 7, 188–204. doi:10.4161/AUTO.7.2.14181.

Nicola, N. A., Metcalf, D., Matsumoto, M., and Johnson, G. R. (1983). Purification of a factor inducing differentiation in murine myelomonocytic leukemia cells. Identification as granulocyte colony-stimulating factor. *J. Biol. Chem.* 258, 9017–23.

Nimmerjahn, F., and Ravetch, J. V. (2008). Fcγ receptors as regulators of immune responses. *Nat. Rev. Immunol.* 8, 34–47. doi:10.1038/nri2206.

Norling, L. V, and Perretti, M. (2013). Control of myeloid cell trafficking in resolution. *J. Innate Immun.* 5, 367–76. doi:10.1159/000350612.

Nunes-Hasler, P., Maschalidi, S., Lippens, C., Castelbou, C., Bouvet, S., Guido, D., et al. (2017). STIM1 promotes migration, phagosomal maturation and antigen cross-presentation in dendritic cells. *Nat. Commun.* 8, 1852. doi:10.1038/s41467-017-01600-6.

Nunes, P., Cornut, D., Bochet, V., Hasler, U., Oh-Hora, M., Waldburger, J.-M., et al. (2012). STIM1 Juxtaposes ER to Phagosomes, Generating Ca2+ Hotspots that Boost Phagocytosis. *Curr. Biol.* 22, 1990–1997. doi:10.1016/j.cub.2012.08.049.

Nunes, P., Demaurex, N., and Dinauer, M. C. (2013). Regulation of the NADPH oxidase and associated ion fluxes during phagocytosis. *Traffic* 14, 1118–31. doi:10.1111/tra.12115.

Nunes, P., Guido, D., and Demaurex, N. (2015). Measuring Phagosome pH by Ratiometric Fluorescence Microscopy. *J. Vis. Exp.*, e53402–e53402. doi:10.3791/53402.

Nutt, S. L., Metcalf, D., D'Amico, A., Polli, M., and Wu, L. (2005). Dynamic regulation of PU.1 expression in multipotent hematopoietic progenitors. *J. Exp. Med.* 201, 221–231. doi:10.1084/jem.20041535.

Nyberg, K., Johansson, U., Johansson, A., and Camner, P. (1992). Phagolysosomal pH in alveolar macrophages. *Environ. Health Perspect.* 97, 149–52. doi:10.1289/ehp.9297149.

O'Donnell, B. V, Tew, D. G., Jones, O. T., and England, P. J. (1993). Studies on the

inhibitory mechanism of iodonium compounds with special reference to neutrophil NADPH oxidase. *Biochem. J.* 290 (Pt 1, 41–49.

Odeberg, H., and Olsson, I. (1976). Microbicidal mechanisms of human granulocytes: synergistic effects of granulocyte elastase and myeloperoxidase or chymotrypsin-like cationic protein. *Infect. Immun.* 14, 1276–83.

Odell, E. W., and Segal, A. W. (1991). Killing of pathogens associated with chronic granulomatous disease by the non-oxidative microbicidal mechanisms of human neutrophils. *J. Med. Microbiol.* 34, 129–135. doi:10.1099/00222615-34-3-129.

Ogawa, M., Matsuzaki, Y., Nishikawa, S., Hayashi, S., Kunisada, T., Sudo, T., et al. (1991). Expression and function of c-kit in hemopoietic progenitor cells. *J. Exp. Med.* 174, 63–71.

Oh, S.-J., Park, J. H., Han, S., Lee, J. K., Roh, E. J., and Lee, C. J. (2008). Development of selective blockers for Ca^2(+)-activated Cl channel using Xenopus laevis oocytes with an improved drug screening strategy. *Mol. Brain* 1, 14. doi:10.1186/1756-6606-1-14.

Ohkuma, S., and Poole, B. (1978). Fluorescence probe measurement of the intralysosomal pH in living cells and the perturbation of pH by various agents. *Proc. Natl. Acad. Sci.* 75, 3327–3331. doi:10.1073/pnas.75.7.3327.

Ohradanova-Repic, A., Machacek, C., Fischer, M. B., and Stockinger, H. (2016). Differentiation of human monocytes and derived subsets of macrophages and dendritic cells by the HLDA10 monoclonal antibody panel. *Clin. Transl. Immunol.* 5, e55. doi:10.1038/cti.2015.39.

Okamoto, K., Iwasaki, N., Doi, K., Noiri, E., Iwamoto, Y., Uchigata, Y., et al. (2012). Inhibition of glucose-stimulated insulin secretion by KCNJ15, a newly identified susceptibility gene for type 2 diabetes. *Diabetes* 61, 1734–1741. doi:10.2337/db11-1201.

Okochi, Y., Sasaki, M., Iwasaki, H., and Okamura, Y. (2009). Voltage-gated proton channel is expressed on phagosomes. *Biochem. Biophys. Res. Commun.* 382, 274–9. doi:10.1016/j.bbrc.2009.03.036.

Olingy, C. E., San Emeterio, C. L., Ogle, M. E., Krieger, J. R., Bruce, A. C., Pfau, D. D., et al. (2017). Non-classical monocytes are biased progenitors of wound healing macrophages during soft tissue injury. *Sci. Rep.* 7, 447. doi:10.1038/s41598-017-00477-1.

Oliver, D., Lien, C.-C., Soom, M., Baukrowitz, T., Jonas, P., and Fakler, B. (2004). Functional conversion between A-type and delayed rectifier K+ channels by membrane lipids. *Science* 304, 265–70. doi:10.1126/science.1094113.

Ooi, C. E., Weiss, J., Doerfler, M. E., and Elsbach, P. (1991). Endotoxin-neutralizing properties of the 25 kD N-terminal fragment and a newly isolated 30 kD C-terminal fragment of the 55-60 kD bactericidal/permeability-increasing protein of human neutrophils. *J. Exp. Med.* 174, 649–55. doi:10.1084/jem.174.3.649.

Painter, R. G., Bonvillain, R. W., Valentine, V. G., Lombard, G. A., LaPlace, S. G., Nauseef, W. M., et al. (2008). The role of chloride anion and CFTR in killing of Pseudomonas aeruginosa by normal and CF neutrophils. *J. Leukoc. Biol.* 83, 1345–53. doi:10.1189/jlb.0907658.

Painter, R. G., Marrero, L., Lombard, G. A., Valentine, V. G., Nauseef, W. M., and

Wang, G. (2010). CFTR-mediated halide transport in phagosomes of human neutrophils. *J. Leukoc. Biol.* 87, 933–42. doi:10.1189/jlb.1009655.

Palazzolo, A. M., Suquet, C., Konkel, M. E., and Hurst, J. K. (2005). Green Fluorescent Protein-Expressing Escherichia coli as a Selective Probe for HOCl Generation within Neutrophils †. doi:10.1021/bi047342s.

Park, S., You, X., and Imlay, J. A. (2005). Substantial DNA damage from submicromolar intracellular hydrogen peroxide detected in Hpx- mutants of Escherichia coli. *Proc. Natl. Acad. Sci.* 102, 9317–9322. doi:10.1073/pnas.0502051102.

Parker, A., Cuddihy, S. L., Son, T. G., Vissers, M. C. M., and Winterbourn, C. C. (2011). Roles of superoxide and myeloperoxidase in ascorbate oxidation in stimulated neutrophils and H2O2-treated HL60 cells. *Free Radic. Biol. Med.* 51, 1399–405. doi:10.1016/j.freeradbiomed.2011.06.029.

Parker, L. C., Whyte, M. K. B., Dower, S. K., and Sabroe, I. (2005). The expression and roles of Toll-like receptors in the biology of the human neutrophil. *J. Leukoc. Biol.* 77, 886–892. doi:10.1189/jlb.1104636.

Parkos, C. A., Allen, R. A., Cochrane, C. G., and Jesaitis, A. J. (1987). Purified cytochrome b from human granulocyte plasma membrane is comprised of two polypeptides with relative molecular weights of 91,000 and 22,000. *J. Clin. Invest.* 80, 732–42. doi:10.1172/JCI113128.

Passlick, B., Flieger, D., and Ziegler-Heitbrock, H. (1989). Identification and characterization of a novel monocyte subpopulation in human peripheral blood. *Blood* 74.

Patel, A. A., Zhang, Y., Fullerton, J. N., Boelen, L., Rongvaux, A., Maini, A. A., et al. (2017). The fate and lifespan of human monocyte subsets in steady state and systemic inflammation. *J. Exp. Med.* 214.

Patel, A. J., Maingret, F., Magnone, V., Fosset, M., Lazdunski, M., and Honoré, E. (2000). TWIK-2, an inactivating 2P domain K+ channel. *J. Biol. Chem.* 275, 28722–30. doi:10.1074/jbc.M003755200.

Pereira-Leal, J. B., and Seabra, M. C. (2000). The mammalian Rab family of small GTPases: definition of family and subfamily sequence motifs suggests a mechanism for functional specificity in the Ras superfamily. *J. Mol. Biol.* 301, 1077–1087. doi:10.1006/JMBI.2000.4010.

Perkins, A. C., and Cory, S. (1993). Conditional immortalization of mouse myelomonocytic, megakaryocytic and mast cell progenitors by the Hox-2.4 homeobox gene. *EMBO J.* 12, 3835–46.

Perkins, A., Kongsuwan, K., Visvader, J., and Adams, J. M. (1990). Homeobox gene expression plus autocrine growth factor production elicits myeloid leukemia. *Proc. Natl. Acad. Sci.* 87, 8398–8402.

Perskvist, N., Roberg, K., Kulyté, A., and Stendahl, O. (2002). Rab5a GTPase regulates fusion between pathogen-containing phagosomes and cytoplasmic organelles in human neutrophils. *J. Cell Sci.* 115, 1321–30.

Peters, W., Scott, H. M., Chambers, H. F., Flynn, J. L., Charo, I. F., and Ernst, J. D. (2001). Chemokine receptor 2 serves an early and essential role in resistance to Mycobacterium tuberculosis. *Proc. Natl. Acad. Sci.* 98, 7958–7963. doi:10.1073/pnas.131207398.

Petheo, G. L., Orient, A., Baráth, M., Kovács, I., Réthi, B., Lányi, A., et al. (2010). Molecular and functional characterization of Hv1 proton channel in human granulocytes. *PLoS One* 5, e14081. doi:10.1371/journal.pone.0014081.

Pillay, J., den Braber, I., Vrisekoop, N., Kwast, L. M., de Boer, R. J., Borghans, J. A. M., et al. (2010). In vivo labeling with 2H2O reveals a human neutrophil lifespan of 5.4 days. *Blood* 116, 625–7. doi:10.1182/blood-2010-01-259028.

Platt, C. D., Chou, J., Houlihan, P., Badran, Y. R., Kumar, L., Bainter, W., et al. (2017). Leucine-rich repeat containing 8A (LRRC8A)–dependent volume-regulated anion channel activity is dispensable for T-cell development and function. *J. Allergy Clin. Immunol.* 140, 1651–1659.e1. doi:10.1016/J.JACI.2016.12.974.

Ploppa, A., George, T. C., Unertl, K. E., Nohe, B., and Durieux, M. E. (2011). ImageStream cytometry extends the analysis of phagocytosis and oxidative burst. *Scand. J. Clin. Lab. Invest.* 71, 362–369. doi:10.3109/00365513.2011.572182.

Podinovskaia, M., Lee, W., Caldwell, S., and Russell, D. G. (2013a). Infection of macrophages with Mycobacterium tuberculosis induces global modifications to phagosomal function. *Cell. Microbiol.* 15, 843–59. doi:10.1111/cmi.12092.

Podinovskaia, M., Lee, W., Caldwell, S., and Russell, D. G. (2013b). Infection of macrophages with *Mycobacterium tuberculosis* induces global modifications to phagosomal function. *Cell. Microbiol.* 15, 843–859. doi:10.1111/cmi.12092.

Poirier, V., and Av-Gay, Y. (2012). Mycobacterium tuberculosis modulators of the macrophage's cellular events. *Microbes Infect.* 14, 1211–1219. doi:10.1016/j.micinf.2012.07.001.

Poling, J. S., Rogawski, M. A., Salem, N., and Vicini, S. (1996). Anandamide, an endogenous cannabinoid, inhibits Shaker-related voltage-gated K+ channels. *Neuropharmacology* 35, 983–91.

Pollock, J. D., Williams, D. A., Gifford, M. A. C., Li, L. L., Du, X., Fisherman, J., et al. (1995). Mouse model of X–linked chronic granulomatous disease, an inherited defect in phagocyte superoxide production. *Nat. Genet.* 9, 202–209. doi:10.1038/ng0295-202.

Pullen, G. R., and Hosking, C. S. (1985). Differentiated HL60 promyelocytic leukaemia cells have a deficient myeloperoxidase/halide killing system. *Clin. exp. Immunol* 62, 304–309.

Qiu, M. R., Jiang, L., Matthaei, K. I., Schoenwaelder, S. M., Kuffner, T., Mangin, P., et al. (2010). Generation and characterization of mice with null mutation of the chloride intracellular channel 1 gene. *Genesis* 48, 127–36. doi:10.1002/dvg.20590.

Qiu, Z., Dubin, A. E., Mathur, J., Tu, B., Reddy, K., Miraglia, L. J., et al. (2014). SWELL1, a plasma membrane protein, is an essential component of volume-regulated anion channel. *Cell* 157. doi:10.1016/j.cell.2014.03.024.

R Core Team (2013). R: A Language and Environment for Statistical Computing. Available at: https://www.r-project.org/.

Raad, H., Paclet, M.-H., Boussetta, T., Kroviarski, Y., Morel, F., Quinn, M. T., et al. (2009). Regulation of the phagocyte NADPH oxidase activity: phosphorylation of gp91 ^{phox} /NOX2 by protein kinase C enhances its diaphorase activity and

binding to Rac2, p67 ^{phox} , and p47 ^{phox}. *FASEB J.* 23, 1011–1022. doi:10.1096/fj.08-114553.

Rada, B. K., Geiszt, M., Káldi, K., Timár, C., and Ligeti, E. (2004). Dual role of phagocytic NADPH oxidase in bacterial killing. *Blood* 104, 2947–2953. doi:10.1182/blood-2004-03-1005.

Ramsey, I. S., Moran, M. M., Chong, J. A., and Clapham, D. E. (2006). A voltage-gated proton-selective channel lacking the pore domain. *Nature* 440, 1213–6. doi:10.1038/nature04700.

Ramsey, I. S., Ruchti, E., Kaczmarek, J. S., and Clapham, D. E. (2009). Hv1 proton channels are required for high-level NADPH oxidase-dependent superoxide production during the phagocyte respiratory burst. *Proc. Natl. Acad. Sci. U. S. A.* 106, 7642–7. doi:10.1073/pnas.0902761106.

Rao, N. V, Wehner, N. G., Marshall, B. C., Gray, W. R., Gray, B. H., and Hoidal, J. R. (1991). Characterization of proteinase-3 (PR-3), a neutrophil serine proteinase. Structural and functional properties. *J. Biol. Chem.* 266, 9540–8.

Rapoport, A. P., Abboud, C. N., and DiPersio, J. F. (1992). Granulocyte-macrophage colony-stimulating factor (GM-CSF) and granulocyte colony-stimulating factor (G-CSF): Receptor biology, signal transduction, and neutrophil activation. *Blood Rev.* 6, 43–57. doi:10.1016/0268-960X(92)90007-D.

Redecke, V., Wu, R., Zhou, J., Finkelstein, D., Chaturvedi, V., High, A. A., et al. (2013). Hematopoietic progenitor cell lines with myeloid and lymphoid potential. *Nat. Methods* 10, 795–803. doi:10.1038/nmeth.2510.

Reeves, E. P., Lu, H., Jacobs, H. L., Messina, C. G. M., Bolsover, S., Gabella, G., et al. (2002). Killing activity of neutrophils is mediated through activation of proteases by K+ flux. *Nature* 416, 291–7. doi:10.1038/416291a.

Reeves, E. P., Nagl, M., Godovac-Zimmermann, J., and Segal, A. W. (2003). Reassessment of the microbicidal activity of reactive oxygen species and hypochlorous acid with reference to the phagocytic vacuole of the neutrophil granulocyte. *J. Med. Microbiol.* 52, 643–51. doi:10.1099/jmm.0.05181-0.

Regier, D. S., Greene, D. G., Sergeant, S., Jesaitis, A. J., and McPhail, L. C. (2000). Phosphorylation of p22phox is mediated by phospholipase D-dependent and -independent mechanisms. Correlation of NADPH oxidase activity and p22phox phosphorylation. *J. Biol. Chem.* 275, 28406–12. doi:10.1074/jbc.M004703200.

Ren, X., Mou, W., Su, C., Chen, X., Zhang, H., Cao, B., et al. (2017). Increase in Peripheral Blood Intermediate Monocytes is Associated with the Development of Recent-Onset Type 1 Diabetes Mellitus in Children. *Int. J. Biol. Sci.* 13, 209–218. doi:10.7150/ijbs.15659.

Rice, K. L., and Licht, J. D. (2007). HOX deregulation in acute myeloid leukemia. *J. Clin. Invest.* 117, 865–868. doi:10.1172/JCI31861.

Rice, W., Ganz, T., Kinkade, J., Selsted, M., Lehrer, R., and Parmley, R. (1987). Defensin-rich dense granules of human neutrophils. *Blood* 70, 757–765. doi:10.1182/blood-2014-12-567834.

Richards, D. M., and Endres, R. G. (2014). The Mechanism of Phagocytosis: Two Stages of Engulfment. *Biophys. J.* 107, 1542–1553. doi:10.1016/J.BPJ.2014.07.070.

Ridge, J. P., Di Rosa, F., and Matzinger, P. (1998). A conditioned dendritic cell can be a temporal bridge between a CD4+ T-helper and a T-killer cell. *Nature* 393, 474–478. doi:10.1038/30989.

Rieger, M. A., Hoppe, P. S., Smejkal, B. M., Eitelhuber, A. C., and Schroeder, T. (2009). Hematopoietic cytokines can instruct lineage choice. *Science (80-.).* 325, 217–218. doi:10.1126/science.1171461.

Robben, P. M., LaRegina, M., Kuziel, W. A., and Sibley, L. D. (2005). Recruitment of Gr-1 + monocytes is essential for control of acute toxoplasmosis. *J. Exp. Med.* 201, 1761–1769. doi:10.1084/jem.20050054.

Robbins, S. H., Walzer, T., Dembélé, D., Thibault, C., Defays, A., Bessou, G., et al. (2008). Novel insights into the relationships between dendritic cell subsets in human and mouse revealed by genome-wide expression profiling. *Genome Biol.* 9, R17. doi:10.1186/gb-2008-9-1-r17.

Roberts, A. W., Kim, C., Zhen, L., Lowe, J. B., Kapur, R., Petryniak, B., et al. (1999). Deficiency of the hematopoietic cell-specific Rho family GTPase Rac2 is characterized by abnormalities in neutrophil function and host defense. *Immunity* 10, 183–96. 2018].

Roche, J., Zeng, C., Barón, A., Gadgil, S., Gemmill, R. M., Tigaud, I., et al. (2004). Hox expression in AML identifies a distinct subset of patients with intermediate cytogenetics. *Leukemia* 18, 1059–1063. doi:10.1038/sj.leu.2403366.

Rorvig, S., Ostergaard, O., Heegaard, N. H., Borregaard, N., Rørvig, S., Ostergaard, O., et al. (2013). Proteome profiling of human neutrophil granule subsets, secretory vesicles, and cell membrane: correlation with transcriptome profiling of neutrophil precursors. *J Leukoc Biol* 94, 711–721. doi:10.1189/jlb.1212619.

Rosas, M., Osorio, F., Robinson, M. J., Davies, L. C., Dierkes, N., Jones, S. A., et al. (2011). Hoxb8 conditionally immortalised macrophage lines model inflammatory monocytic cells with important similarity to dendritic cells. *Eur. J. Immunol.* 41, 356–365. doi:10.1002/eji.201040962.

Rosen, H., Gordon, S., and North, R. J. (1989). Exacerbation of murine listeriosis by a monoclonal antibody specific for the type 3 complement receptor of myelomonocytic cells. Absence of monocytes at infective foci allows Listeria to multiply in nonphagocytic cells. *J. Exp. Med.* 170, 27–37. doi:10.1084/jem.170.1.27.

Rothe, G., and Valet, G. (1990). Flow cytometric analysis of respiratory burst activity in phagocytes with hydroethidine and 2',7'-dichlorofluorescin. *J. Leukoc. Biol.* 47, 440–448. doi:10.1002/jlb.47.5.440.

Rybicka, J. M., Balce, D. R., Chaudhuri, S., Allan, E. R. O., and Yates, R. M. (2012a). Phagosomal proteolysis in dendritic cells is modulated by NADPH oxidase in a pH-independent manner. *EMBO J.* 31, 932–44. doi:10.1038/emboj.2011.440.

Rybicka, J. M., Balce, D. R., Chaudhuri, S., Allan, E. R. O., and Yates, R. M. (2012b). Phagosomal proteolysis in dendritic cells is modulated by NADPH oxidase in a pH-independent manner. *EMBO J.* 31, 932–944. doi:10.1038/emboj.2011.440.

Rybicka, J. M., Balce, D. R., Chaudhuri, S., Allan, E. R., and Yates, R. M. (2011). Phagosomal proteolysis in dendritic cells is modulated by NADPH oxidase in a

pH-independent manner. *EMBO J.* 31440, 932–944. doi:10.1038/emboj.2011.440.

Rydstrom, A., and Wick, M. J. (2007). Monocyte Recruitment, Activation, and Function in the Gut-Associated Lymphoid Tissue during Oral Salmonella Infection. *J. Immunol.* 178, 5789–5801. doi:10.4049/jimmunol.178.9.5789.

Saito, M., Sato, R., Muñoz, N. M., Herrnreiter, A., Oyaizu, M., Kasugai, H., et al. (1997). Association of granular exocytosis with Ca(2+)-activated K+ channels in human eosinophils. *Am. J. Physiol.* 273, L16-21. Available at: http://www.ncbi.nlm.nih.gov/pubmed/9252535 [Accessed March 18, 2016].

Sakurai, C., Hashimoto, H., Nakanishi, H., Arai, S., Wada, Y., Sun-Wada, G.-H., et al. (2012). SNAP-23 regulates phagosome formation and maturation in macrophages. *Mol. Biol. Cell* 23, 4849–4863. doi:10.1091/mbc.E12-01-0069.

Salao, K., Jiang, L., Li, H., Tsai, V. W.-W., Husaini, Y., Curmi, P. M. G., et al. (2016a). CLIC1 regulates dendritic cell antigen processing and presentation by modulating phagosome acidification and proteolysis. *Biol. Open* 5, 620–30. doi:10.1242/bio.018119.

Salao, K., Jiang, L., Li, H., Tsai, V. W.-W., Husaini, Y., Curmi, P. M. G., et al. (2016b). CLIC1 regulates dendritic cell antigen processing and presentation by modulating phagosome acidification and proteolysis. *Biol. Open* 5.

Sánchez-Torres, C., García-Romo, G. S., Cornejo-Cortés, M. A., Rivas-Carvalho, A., and Sánchez-Schmitz, G. (2001). CD16+ and CD16- human blood monocyte subsets differentiate in vitro to dendritic cells with different abilities to stimulate CD4+ T cells. *Int. Immunol.* 13, 1571–81. Available at: http://www.ncbi.nlm.nih.gov/pubmed/11717198 [Accessed September 9, 2018].

Sasaki, M., Takagi, M., and Okamura, Y. (2006). A voltage sensor-domain protein is a voltage-gated proton channel. *Science* 312, 589–92. doi:10.1126/science.1122352.

Savina, A., and Amigorena, S. (2007). Phagocytosis and antigen presentation in dendritic cells. *Immunol. Rev.* 219, 143–156. doi:10.1111/j.1600-065X.2007.00552.x.

Savina, A., Jancic, C., Hugues, S., Guermonprez, P., Vargas, P., Moura, I. C., et al. (2006). NOX2 Controls Phagosomal pH to Regulate Antigen Processing during Crosspresentation by Dendritic Cells. *Cell* 126, 205–218. doi:10.1016/J.CELL.2006.05.035.

Sawyer, D. T., and Valentine, J. S. (1981). How Super Is Superoxide? Available at: https://pubs.acs.org/sharingguidelines [Accessed September 29, 2018].

Sbarra, A. J., and Karnovsky, M. L. (1959). The biochemical basis of phagocytosis. I. Metabolic changes during the ingestion of particles by polymorphonuclear leukocytes. *J. Biol. Chem.* 234, 1355–62.

Scherer, W. F., Syverton, J. T., and Gey, G. O. (1953). Studies on the propagation in vitro of poliomyelitis viruses. IV. Viral multiplication in a stable strain of human malignant epithelial cells (strain HeLa) derived from an epidermoid carcinoma of the cervix. *J. Exp. Med.* 97, 695–710.

Schiller, J., Benard, S., Reichl, S., Arnhold, J., and Arnold, K. (2000). Cartilage degradation by stimulated human neutrophils: Reactive oxygen species decrease markedly the activity of proteolytic enzymes. *Chem. Biol.* 7, 557–568.

doi:10.1016/S1074-5521(00)00013-2.

Schrader, J. W. (1998). Colony-Stimulating Factors. *Encycl. Immunol.*, 596–599. doi:10.1006/RWEI.1999.0158.

Schrenzel, J., Serrander, L., Bánfi, B., Nüße, O., Fouyouzi, R., Lew, D. P., et al. (1998). Electron currents generated by the human phagocyte NADPH oxidase. *Nature* 392, 734–737. doi:10.1038/33725.

Schumann, M. A., and Raffins, T. A. (1994). Activation of a Voltage-dependent Chloride Current in Human Neutrophils by Phorbol 12-Myristate 13-Acetate and Formyl-methionyl-leucyl-phenylalanine. *J. Biol. Chem.* 269, 2389–2398.

Schwartz, J., Leidal, K. G., Femling, J. K., Weiss, J. P., and Nauseef, W. M. (2009). Neutrophil Bleaching of GFP-Expressing Staphylococci: Probing the Intraphagosomal Fate of Individual Bacteria 1. *J Immunol* 183, 2632–2641. doi:10.4049/jimmunol.0804110.

Schwingshackl, A., Moqbel, R., and Duszyk, M. (2000). Involvement of ion channels in human eosinophil respiratory burst. *J. Allergy Clin. Immunol.* 106, 272–279. doi:10.1067/mai.2000.107752.

Sedlyarov, V., Eichner, R., Girardi, E., Essletzbichler, P., Goldmann, U., Nunes-Hasler, P., et al. (2018). The Bicarbonate Transporter SLC4A7 Plays a Key Role in Macrophage Phagosome Acidification. *Cell Host Microbe* 23, 766–774.e5. doi:10.1016/j.chom.2018.04.013.

Segal, A. W. (2005). How Neutrophils Kill Microbes. *Annu. Rev. Immunol.* 23, 197–223. doi:10.1146/annurev.immunol.23.021704.115653.How.

Segal, A. W., and Allison, A. C. (1979). “Oxygen Consumption by Stimulated Human Neutrophils,” in *Ciba.Found.Symp.* (John Wiley & Sons, Ltd.), 205–223. doi:10.1002/9780470715413.ch13.

Segal, A. W., and Coade, S. B. (1978). Kinetics of oxygen consumption by phagocytosing human neutrophils. Available at: http://www.ncbi.nlm.nih.gov/pubmed/718704 [Accessed September 26, 2018].

Segal, A. W., Dorling, J., and Coade, S. (1980). Kinetics of fusion of the cytoplasmic granules with phagocytic vacuoles in human polymorphonuclear leukocytes. Biochemical and morphological studies. *J. Cell Biol.* 85, 42–59. doi:10.1083/jcb.85.1.42.

Segal, A. W., Geisow, M., Garcia, R., Harper, A., and Miller, Robert (1981). The respiratory burst of phagocytic cells is associated with a rise in vacuolar pH. *Nature* 290, 406–409. doi:10.1038/290406a0.

Segal, A. W., and Jones, O. T. G. (1978). Novel cytochrome b system in phagocytic vacuoles of human granulocytes [25]. *Nature* 276, 515–517. doi:10.1038/276515a0.

Segura, E., Touzot, M., Bohineust, A., Cappuccio, A., Chiocchia, G., Hosmalin, A., et al. (2013). Human Inflammatory Dendritic Cells Induce Th17 Cell Differentiation. *Immunity* 38, 336–348. doi:10.1016/J.IMMUNI.2012.10.018.

Seita and Weissman (2010). Hematopoietic Stem Cell: Self-renewal versus Differentiation. *Wiley Interdiscip Rev Syst Biol Med* 2, 640–653. doi:10.1002/wsbm.86.Hematopoietic.

Semerad, C. L., Liu, F., Gregory, A. D., Stumpf, K., and Link, D. C. (2002). G-CSF is

an essential regulator of neutrophil trafficking from the bone marrow to the blood. *Immunity* 17, 413–423. doi:10.1016/S1074-7613(02)00424-7.

Sengelov, H., Follin, P., Kjeldsen, L., Lollike, K., Dahlgren, C., and Borregaard, N. (1995). Mobilization of granules and secretory vesicles during in vivo exudation of human neutrophils. *J Immunol* 154, 4157–4165. doi:10.4049/jimmunol.172.12.7684.

Serbina, N. V, and Pamer, E. G. (2006). Monocyte emigration from bone marrow during bacterial infection requires signals mediated by chemokine receptor CCR2. *Nat. Immunol.* 7, 311–317. doi:10.1038/ni1309.

Shafer, W. M., Katzif, S., Bowers, S., Fallon, M., Hubalek, M., Reed, M. S., et al. (2002). Tailoring an antibacterial peptide of human lysosomal cathepsin G to enhance its broad-spectrum action against antibiotic-resistant bacterial pathogens. *Curr. Pharm. Des.* 8, 695–702. doi:10.2174/1381612023395376.

Shefcyk, J., Molski, T. F., Volpi, M., Naccache, P. H., and Sha'afi, R. I. (1983). Phloretin is a potent inhibitor of rabbit neutrophil activation by chemotactic factors. *Biochim. Biophys. Acta* 728, 97–102.

Sheridan, J. W., Metcalf, D., and Stanley, E. R. (1974). Further studies on the factor in lung-conditioned medium stimulating granulocyte and monocyte colony formation in vitro. *J. Cell. Physiol.* 84, 147–158. doi:10.1002/jcp.1040840117.

Simchowitz, L., and De Weer, P. (1986). Chloride movements in human neutrophils. Diffusion, exchange, and active transport. *J. Gen. Physiol.* 88, 167–94.

Simchowitz, L., Foy, M. A., and Cragoe, E. J. (1990). A role for Na+/Ca2+ exchange in the generation of superoxide radicals by human neutrophils. *J. Biol. Chem.* 265, 13449–56.

Simchowitz, L., Spilberg, I., and De Weer, P. (1982). Sodium and potassium fluxes and membrane potential of human neutrophils: evidence for an electrogenic sodium pump. *J. Gen. Physiol.* 79, 453–79. doi:10.1085/jgp.79.3.453.

Skloot, R. (2010). *The immortal life of Henrietta Lacks*. New York: Crown Publishers

Song, X., and Norman, A. W. (1998). 1α,25-dihydroxyvitamin D3 and phorbol ester mediate the expression of alkaline phosphatase in NB4 acute promyelocylic leukemia cells. *Leuk. Res.* 22, 69–76. doi:10.1016/S0145-2126(97)00054-4.

Sørensen, O. E., Follin, P., Johnsen, A. H., Calafat, J., Tjabringa, G. S., Hiemstra, P. S., et al. (2001). Human cathelicidin, hCAP-18, is processed to the antimicrobial peptide LL-37 by extracellular cleavage with proteinase 3. *Blood* 97, 3951–9.

Sou, Y. S., Tanida, I., Komatsu, M., Ueno, T., and Kominami, E. (2006). Phosphatidylserine in addition to phosphatidylethanolamine is an in vitro target of the mammalian Atg8 modifiers, LC3, GABARAP, and GATE-16. *J. Biol. Chem.* 281, 3017–3024. doi:10.1074/jbc.M505888200.

Springer, T. A., and Dustin, M. L. (2012). Integrin inside-out signaling and the immunological synapse. *Curr. Opin. Cell Biol.* 24, 107–115. doi:10.1016/J.CEB.2011.10.004.

Standish, A. J., and Weiser, J. N. (2009). Human neutrophils kill Streptococcus pneumoniae via serine proteases. *J. Immunol.* 183, 2602–9. doi:10.4049/jimmunol.0900688.

Stanley, E. R., Berg, K. L., Einstein, D. B., Lee, P. S. W., Pixley, F. J., Wang, Y., et al. (1997). Biology and action of colony-stimulating factor-1. *Mol. Reprod. Dev.* 46, 4–10. doi:10.1002/(SICI)1098-2795(199701)46:1<4::AID-MRD2>3.0.CO;2-V.

Stobrawa, S. M., Breiderhoff, T., Takamori, S., Engel, D., Schweizer, M., Zdebik, A. A., et al. (2001). Disruption of ClC-3, a chloride channel expressed on synaptic vesicles, leads to a loss of the hippocampus. *Neuron* 29, 185–96.

Stoddard, J. S., Steinbach, J. H., and Simchowitz, L. (1993). Whole cell Cl- currents in human neutrophils induced by cell swelling. *Am. J. Physiol.* 265, C156-65.

Stuart, L. M., and Ezekowitz, R. A. B. (2005). Phagocytosis: Elegant complexity. *Immunity* 22, 539–550. doi:10.1016/j.immuni.2005.05.002.

Sturgill-Koszycki, S., Schlesinger, P. H., Chakraborty, P., Haddix, P. L., Collins, H. L., Fok, A. K., et al. (1994). Lack of acidification in Mycobacterium phagosomes produced by exclusion of the vesicular proton-ATPase. *Science (80-.).* 263, 678–681. doi:10.1126/science.8303277.

Sumimoto, H., Sakamoto, N., Nozaki, M., Sakaki, Y., Takeshige, K., and Minakami, S. (1992). Cytochrome b558, a component of the phagocyte NADPH oxidase, is a flavoprotein. *Biochem. Biophys. Res. Commun.* 186, 1368–1375. doi:10.1016/S0006-291X(05)81557-8.

Summers, F. A., Zhao, B., Ganini, D., and Mason, R. P. (2013). Photooxidation of Amplex Red to Resorufin: Implications of Exposing the Amplex Red Assay to Light. *Methods Enzymol.* 526, 1–17. doi:10.1016/B978-0-12-405883-5.00001-6.

Sun, Y.-T., Shieh, C.-C., Delpire, E., and Shen, M.-R. (2012). K^+-Cl^- cotransport mediates the bactericidal activity of neutrophils by regulating NADPH oxidase activation. *J. Physiol.* 590, 3231–43. doi:10.1113/jphysiol.2011.225300.

Sunderkötter, C., Nikolic, T., Dillon, M. J., Van Rooijen, N., Stehling, M., Drevets, D. A., et al. (2004). Subpopulations of mouse blood monocytes differ in maturation stage and inflammatory response. *J. Immunol.* 172, 4410–7.

Swanson, J. A. (2008). Shaping cups into phagosomes and macropinosomes. *Nat. Rev. Mol. Cell Biol.* 9, 639–649. doi:10.1038/nrm2447.

Swanson, J. A., and Hoppe, A. D. (2004). The coordination of signaling during Fc receptor-mediated phagocytosis. *J. Leukoc. Biol.* 76, 1093–1103. doi:10.1189/jlb.0804439.

Takahira, M., Sakurai, M., Sakurada, N., and Sugiyama, K. (2005). Fenamates and diltiazem modulate lipid-sensitive mechano-gated 2P domain K(+) channels. *Pflügers Arch. Eur. J. Physiol.* 451, 474–8. doi:10.1007/s00424-005-1492-5.

Tam, J. M., Mansour, M. K., Khan, N. S., Seward, M., Puranam, S., Tanne, A., et al. (2014). Dectin-1-dependent LC3 recruitment to phagosomes enhances fungicidal activity in macrophages. *J. Infect. Dis.* 210, 1844–54. doi:10.1093/infdis/jiu290.

Tamura, T., Kurotaki, D., and Koizumi, S. ichi (2015). Regulation of myelopoiesis by the transcription factor IRF8. *Int. J. Hematol.* 101, 342–351. doi:10.1007/s12185-015-1761-9.

Tatsuta, H., Ueda, S., Morishima, S., and Okada, Y. (1994). Voltage- and time-dependent K+ channel currents in the basolateral membrane of villus

enterocytes isolated from guinea pig small intestine. *J. Gen. Physiol.* 103, 429–46.

Teufelhofer, O., Weiss, R.-M., Parzefall, W., Schulte-Hermann, R., Micksche, M., Berger, W., et al. (2003). Promyelocytic HL60 cells express NADPH oxidase and are excellent targets in a rapid spectrophotometric microplate assay for extracellular superoxide. *Toxicol. Sci.* 76, 376–83. doi:10.1093/toxsci/kfg234.

Tkalcevic, J., Novelli, M., Phylactides, M., Iredale, J. P., Segal, A. W., and Roes, J. (2000). Impaired Immunity and Enhanced Resistance to Endotoxin in the Absence of Neutrophil Elastase and Cathepsin G. *Immunity* 12, 201–210. doi:10.1016/S1074-7613(00)80173-9.

Tohyama, Y., and Yamamura, H. (2009). Protein Tyrosine Kinase, Syk: A Key Player in Phagocytic Cells. *J. Biochem.* 145, 267–273. doi:10.1093/jb/mvp001.

Tolouei Semnani, R., Moore, V., Bennuru, S., McDonald-Fleming, R., Ganesan, S., Cotton, R., et al. (2014). Human monocyte subsets at homeostasis and their perturbation in numbers and function in filarial infection. *Infect. Immun.* 82, 4438–46. doi:10.1128/IAI.01973-14.

Traynor, T. R., Kuziel, W. A., Toews, G. B., and Huffnagle, G. B. (2000). CCR2 expression determines T1 versus T2 polarization during pulmonary Cryptococcus neoformans infection. *J. Immunol.* 164, 2021–7. doi:10.4049/jimmunol.164.4.2021.

Tsai, S., Bartelmez, S., Sitnicka, E., and Collins, S. (1994). Lymphohematopoietic progenitors immortalized by a retroviral vector harboring a dominant-negative retinoic acid receptor can recapitulate lymphoid, myeloid, and erythroid development. *Genes Dev.* 8, 2831–2841. doi:10.1101/gad.8.23.2831.

Tsai, S., and Collins, S. J. (1993). A dominant negative retinoic acid receptor blocks neutrophil differentiation at the promyelocyte stage. *Proc. Natl. Acad. Sci. U. S. A.* 90, 7153–7..

Tsien, R. Y. (1989). Chapter 5 Fluorescent Indicators of Ion Concentrations. *Methods Cell Biol.* 30, 127–156. doi:10.1016/S0091-679X(08)60978-4.

Tsuji, S., Iharada, A., Taniuchi, S., Hasui, M., and Kaneko, K. (2012). Increased Production of Nitric Oxide by Phagocytic Stimulated Neutrophils in Patients With Chronic Granulomatous Disease. *J. Pediatr. Hematol. / Oncol.* 34, 500–502. doi:10.1097/MPH.0b013e3182668388.

Tsuji, S., Taniuchi, S., Hasui, M., Yamamoto, A., and Kobayashi, Y. (2002). Increased nitric oxide production by neutrophils from patients with chronic granulomatous disease on trimethoprim-sulfamethoxazole. *Nitric oxide Biol. Chem.* 7, 283–8.

Turk, V., Stoka, V., Vasiljeva, O., Renko, M., Sun, T., Turk, B., et al. (2012). Cysteine cathepsins: From structure, function and regulation to new frontiers. *Biochim. Biophys. Acta - Proteins Proteomics* 1824, 68–88. doi:10.1016/J.BBAPAP.2011.10.002.

Tzelepis, F., Verway, M., Daoud, J., Gillard, J., Hassani-Ardakani, K., Dunn, J., et al. (2015). Annexin1 regulates DC efferocytosis and cross-presentation during Mycobacterium tuberculosis infection. *J. Clin. Invest.* 125, 752–68. doi:10.1172/JCI77014.

Urbaczek, A. C., Toller-Kawahisa, J. E., Fonseca, L. M., Costa, P. I., Faria, C. M. Q.

G., Azzolini, A. E. C. S., et al. (2014). Influence of FcγRIIIb polymorphism on its ability to cooperate with FcγRIIa and CR3 in mediating the oxidative burst of human neutrophils. *Hum. Immunol.* 75, 785–790. doi:10.1016/j.humimm.2014.05.011.

Uriarte, S. M., Powell, D. W., Luerman, G. C., Merchant, M. L., Cummins, T. D., Jog, N. R., et al. (2008). Comparison of Proteins Expressed on Secretory Vesicle Membranes and Plasma Membranes of Human Neutrophils. *J. Immunol.* 180, 5575–5581. doi:10.4049/jimmunol.180.8.5575.

Van Acker, H., Gielis, J., Acke, M., Cools, F., Cos, P., and Coenye, T. (2016). The Role of Reactive Oxygen Species in Antibiotic-Induced Cell Death in Burkholderia cepacia Complex Bacteria. *PLoS One* 11, e0159837. doi:10.1371/journal.pone.0159837.

VanderVen, B. C., Yates, R. M., and Russell, D. G. (2009). Intraphagosomal Measurement of the Magnitude and Duration of the Oxidative Burst. *Traffic* 10, 372–378. doi:10.1111/j.1600-0854.2008.00877.x.

Vermes, I., Haanen, C., Steffens-Nakken, H., and Reutellingsperger, C. (1995). A novel assay for apoptosis Flow cytometric detection of phosphatidylserine expression on early apoptotic cells using fluorescein labelled Annexin V. *J. Immunol. Methods* 184, 39–51. doi:10.1016/0022-1759(95)00072-I.

Vethanayagam, R. R., Almyroudis, N. G., Grimm, M. J., Lewandowski, D. C., Pham, C. T. N., Blackwell, T. S., et al. (2011). Role of NADPH oxidase versus neutrophil proteases in antimicrobial host defense. *PLoS One* 6, e28149. doi:10.1371/journal.pone.0028149.

Vicente, R., Escalada, A., Coma, M., Fuster, G., Sanchez-Tillo, E., Lopez-Iglesias, C., et al. (2003). Differential Voltage-dependent K+ Channel Responses during Proliferation and Activation in Macrophages. *J. Biol. Chem.* 278, 46307–46320. doi:10.1074/jbc.M304388200.

Vidarsson, G., Dekkers, G., and Rispens, T. (2014). IgG Subclasses and Allotypes: From Structure to Effector Functions. *Front. Immunol.* 5, 520. doi:10.3389/fimmu.2014.00520.

Vilim, V., and Wilhelm, J. (1989). What do we measure by a luminol-dependent chemiluminescence of phagocytes? *Free Radic. Biol. Med.* 6, 623–629. doi:10.1016/0891-5849(89)90070-1.

Villani, A.-C., Satija, R., Reynolds, G., Sarkizova, S., Shekhar, K., Fletcher, J., et al. (2017). Single-cell RNA-seq reveals new types of human blood dendritic cells, monocytes, and progenitors. *Science* 356, eaah4573. doi:10.1126/science.aah4573.

Voets, T., Droogmans, G., and Nilius, B. (1996). Potent block of volume-activated chloride currents in endothelial cells by the uncharged form of quinine and quinidine. *Br. J. Pharmacol.* 118, 1869–71.

von Tscharner, V., Prod'hom, B., Baggiolini, M., and Reuter, H. (1986). Ion channels in human neutrophils activated by a rise in free cytosolic calcium concentration. *Nature* 324, 369–372. doi:10.1038/324369a0.

Voss, F. K., Ullrich, F., Münch, J., Lazarow, K., Lutter, D., Mah, N., et al. (2014). Identification of LRRC8 heteromers as an essential component of the volume-regulated anion channel VRAC. *Science* 344, 634–8. doi:10.1126/science.1252826.

Wallberg, F., Tenev, T., and Meier, P. (2016). Analysis of apoptosis and necroptosis by fluorescence-activated cell sorting. *Cold Spring Harb. Protoc.* 2016, 347–352. doi:10.1101/pdb.prot087387.

Walrand, S., Valeix, S., Rodriguez, C., Ligot, P., Chassagne, J., and Vasson, M. P. (2003). Flow cytometry study of polymorphonuclear neutrophil oxidative burst: A comparison of three fluorescent probes. *Clin. Chim. Acta* 331, 103–110. doi:10.1016/S0009-8981(03)00086-X.

Wang, G. G., Calvo, K. R., Pasillas, M. P., Sykes, D. B., Häcker, H., and Kamps, M. P. (2006). Quantitative production of macrophages or neutrophils ex vivo using conditional Hoxb8. *Nat. Methods* 3, 287–293. doi:10.1038/nmeth865.

Wang, G., and Nauseef, W. M. (2015). Salt, chloride, bleach, and innate host defense. *J. Leukoc. Biol.* 98, 1–10. doi:10.1189/jlb.4RU0315-109R.

Wang, H., Yan, M., Sun, J., Jain, S., Yoshimi, R., Abolfath, S. M., et al. (2014). A Reporter Mouse Reveals Lineage-Specific and Heterogeneous Expression of IRF8 during Lymphoid and Myeloid Cell Differentiation. *J. Immunol.* 193, 1766–1777. doi:10.4049/jimmunol.1301939.

Wardman, P. (2007). Fluorescent and luminescent probes for measurement of oxidative and nitrosative species in cells and tissues: Progress, pitfalls, and prospects. *Free Radic. Biol. Med.* 43, 995–1022. doi:10.1016/J.FREERADBIOMED.2007.06.026.

Warner, N. L., and Moore, M. A. S. (1969). A Transplantable Myelomonocytic Leukemia in BALB/c Mice: Cytology, Karyotype, and Muramidase Content 1,2,3. *J. Natl. Cancer Inst.* 43, 963–982. Available at: https://academic.oup.com/jnci/article-abstract/43/4/963/902515 [Accessed October 2, 2018].

Warren, P. (2016). panp: Presence-Absence Calls from Negative Strand Matching Probesets. Available at: https://www.bioconductor.org/packages/release/bioc/html/panp.html.

Wei, G., Pazgier, M., De Leeuw, E., Rajabi, M., Li, J., Zou, G., et al. (2010). Trp-26 imparts functional versatility to human α-defensin HNP. *J. Biol. Chem.* 285, 16275–16285. doi:10.1074/jbc.M110.102749.

Weiss, E., Hanzelmann, D., Fehlhaber, B., Klos, A., Von Loewenich, F. D., Liese, J., et al. (2018). Formyl-peptide receptor 2 governs leukocyte influx in local staphylococcus aureus infections. *FASEB J.* 32, 26–36. doi:10.1096/fj.201700441R.

Weiss, J., Elsbach, P., Olsson, I., and Odeberg, H. (1978). Purification and characterization of a potent bactericidal and membrane active protein from the granules of human polymorphonuclear leukocytes. *J. Biol. Chem.* 253, 2664–2672. Available at: http://www.ncbi.nlm.nih.gov/pubmed/344320 [Accessed September 30, 2018].

Wheeler, M. A., Smith, S. D., García-Cardeña, G., Nathan, C. F., Weiss, R. M., and Sessa, W. C. (1997). Bacterial infection induces nitric oxide synthase in human neutrophils. *J. Clin. Invest.* 99, 110–116. doi:10.1172/JCI119121.

Wieland, H., Goetz, F., and Neumeister, B. (2004). Phagosomal acidification is not a prerequisite for intracellular multiplication of Legionella pneumophila in human monocytes. *J Infect Dis* 189, 1610–1614. doi:10.1086/382894\nJID31154 [pii].

Wientjes, F. B., Panayotou, G., Reeves, E., and Segal, A. W. (1996). Interactions between cytosolic components of the NADPH oxidase: p40phox interacts with both p67phox and p47phox. *Biochem. J.* 317 (Pt 3), 919–24.

Wiesmeier, M., Gautam, S., Kirschnek, S., and Häcker, G. (2016). Characterisation of Neutropenia-Associated Neutrophil Elastase Mutations in a Murine Differentiation Model In Vitro and In Vivo. doi:10.1371/journal.pone.0168055.

Williams, D. E., Eisenman, J., Baird, A., Rauch, C., Van Ness, K., March, C. J., et al. (1990a). Identification of a ligand for the c-kit proto-oncogene. *Cell* 63, 167–74.

Williams, G. T., Smith, C. A., Spooncer, E., Dexter, T. M., and Taylor, D. R. (1990b). Haemopoietic colony stimulating factors promote cell survival by suppressing apoptosis. *Nature* 343, 76–79. doi:10.1038/343076a0.

Winterbourn, C. C., and Kettle, A. J. (2012). Redox Reactions and Microbial Killing in the Neutrophil Phagosome. *Antioxid. Redox Signal.* 18, 642–660. doi:10.1073/pnas.0905565106.

Wong, K. L., Tai, J. J.-Y., Wong, W.-C., Han, H., Sem, X., Yeap, W.-H., et al. (2011). Gene expression profiling reveals the defining features of the classical, intermediate, and nonclassical human monocyte subsets. *Blood* 118, e16-31. doi:10.1182/blood-2010-12-326355.

Wong, K. L., Yeap, W. H., Tai, J. J. Y., Ong, S. M., Dang, T. M., and Wong, S. C. (2012). The three human monocyte subsets: implications for health and disease. *Immunol. Res.* 53, 41–57. doi:10.1007/s12026-012-8297-3.

Wrighton, D. C., Muench, S. P., and Lippiat, J. D. (2015). Mechanism of inhibition of mouse Slo3 (KCa 5.1) potassium channels by quinine, quinidine and barium. *Br. J. Pharmacol.* 172, 4355–63. doi:10.1111/bph.13214.

Wulff, H., and Zhorov, B. S. (2008). K+ channel modulators for the treatment of neurological disorders and autoimmune diseases. *Chem. Rev.* 108, 1744–73. doi:10.1021/cr078234p.

Xu, Q., Lee, K.-A., Lee, S., Lee, K. M., Lee, W.-J., and Yoon, J. (2013). A Highly Specific Fluorescent Probe for Hypochlorous Acid and Its Application in Imaging Microbe-Induced HOCl Production. *J. Am. Chem. Soc.* 135, 9944–9949. doi:10.1021/ja404649m.

Xu, Y. Z., Thuraisingam, T., de Lima Morais, D. A., Rola-Pleszczynski, M., and Radzioch, D. (2010). Nuclear Translocation of -Actin Is Involved in Transcriptional Regulation during Macrophage Differentiation of HL-60 Cells. *Mol. Biol. Cell* 21, 811–820. doi:10.1091/mbc.E09-06-0534.

Yamaguchi, T., Yamaguchi, T., and Hayakawa, T. (1998). Granulocyte Colony-Stimulating Factor Promotes Functional Maturation of O−2Generating System during Differentiation of HL-60 Cells to Neutrophil-like Cells. *Arch. Biochem. Biophys.* 353, 93–100. doi:10.1006/abbi.1998.0622.

Yamamori, T., Inanami, O., Nagahata, H., Cui, Y., and Kuwabara, M. (2000). Roles of p38 MAPK, PKC and PI3-K in the signaling pathways of NADPH oxidase activation and phagocytosis in bovine polymorphonuclear leukocytes. *FEBS Lett.* 467, 253–8.

Yamamoto, S., Shimizu, S., Kiyonaka, S., Takahashi, N., Wajima, T., Hara, Y., et al. (2008). TRPM2-mediated Ca2+influx induces chemokine production in

monocytes that aggravates inflammatory neutrophil infiltration. *Nat. Med.* 14, 738–47. doi:10.1038/nm1758.

Yamashiro, S., Kamohara, H., Wang, J. M., Yang, D., Gong, W. H., and Yoshimura, T. (2001). Phenotypic and functional change of cytokine-activated neutrophils: inflammatory neutrophils are heterogeneous and enhance adaptive immune responses. *J. Leukoc. Biol.* 69, 698–704.

Yao, H., Arunachalam, G., Hwang, J.-W., Chung, S., Sundar, I. K., Kinnula, V. L., et al. (2010). Extracellular superoxide dismutase protects against pulmonary emphysema by attenuating oxidative fragmentation of ECM. *Proc. Natl. Acad. Sci. U. S. A.* 107, 15571–6. doi:10.1073/pnas.1007625107.

Yasuaki, S., Daniels, R. H., Elmore, M. A., Finnen, M. J., Hill, M. E., and Lackie, J. M. (1993). Agonist-stimulated Cl− efflux from human neutrophils: A common phenomenon during neutrophil activation. *Biochem. Pharmacol.* 45, 1743–1751. doi:10.1016/0006-2952(93)90429-Z.

Yatani, A., Wakamori, M., Mikala, G., and Bahinski, A. (1993). Block of transient outward-type cloned cardiac K+ channel currents by quinidine. *Circ. Res.* 73, 351–9.

Yates, R. M., Hermetter, A., and Russell, D. G. (2005). The Kinetics of Phagosome Maturation as a Function of Phagosome/Lysosome Fusion and Acquisition of Hydrolytic Activity. *Traffic* 6, 413–420. doi:10.1111/j.1600-0854.2005.00284.x.

Yates, R. M., Hermetter, A., Taylor, G. A., and Russell, D. G. (2007). Macrophage Activation Downregulates the Degradative Capacity of the Phagosome. *Traffic* 8, 241–250. doi:10.1111/j.1600-0854.2006.00528.x.

Yates, R. M., and Russell, D. G. (2005). Phagosome Maturation Proceeds Independently of Stimulation of Toll-like Receptors 2 and 4. *Immunity* 23, 409–417. doi:10.1016/J.IMMUNI.2005.09.007.

Yin, C., Kim, Y., Argintaru, D., and Heit, B. (2016). Rab17 mediates differential antigen sorting following efferocytosis and phagocytosis. *Cell Death Dis.* 7, e2529. doi:10.1038/cddis.2016.431.

Zarember, K., Elsbach, P., Shin-Kim, K., and Weiss, J. (1997). p15s (15-kD antimicrobial proteins) are stored in the secondary granules of Rabbit granulocytes: implications for antibacterial synergy with the bactericidal/permeability-increasing protein in inflammatory fluids. *Blood* 89, 672–679.

Zawada, A. M., Rogacev, K. S., Rotter, B., Winter, P., Marell, R.-R., Fliser, D., et al. (2011). SuperSAGE evidence for CD14++CD16+ monocytes as a third monocyte subset. *Blood* 118, e50-61. doi:10.1182/blood-2011-01-326827.

Zehrer, A., Pick, R., Salvermoser, M., Boda, A., Miller, M., Stark, K., et al. (2018). A Fundamental Role of Myh9 for Neutrophil Migration in Innate Immunity. *J. Immunol.*, ji1701400. doi:10.4049/jimmunol.1701400.

Zhang, P., Iwasaki-Arai, J., Iwasaki, H., Fenyus, M. L., Dayaram, T., Owens, B. M., et al. (2004). Enhancement of hematopoietic stem cell repopulating capacity and self-renewal in the absence of the transcription factor C/EBPα. *Immunity* 21, 853–863. doi:10.1016/j.immuni.2004.11.006.

Zhao, H., Kalivendi, S., Zhang, H., Joseph, J., Nithipatikom, K., Vásquez-Vivar, J., et al. (2003). Superoxide reacts with hydroethidine but forms a fluorescent

product that is distinctly different from ethidium: Potential implications in intracellular fluorescence detection of superoxide. *Free Radic. Biol. Med.* 34, 1359–1368. doi:10.1016/S0891-5849(03)00142-4.

Zhao, H., and Kinnunen, P. K. J. (2003). Modulation of the activity of secretory phospholipase A2 by antimicrobial peptides. *Antimicrob. Agents Chemother.* 47, 965–971. doi:10.1128/AAC.47.3.965.

Zhao, L., and Lu, W. (2014). Defensins in innate immunity. *Curr. Opin. Hematol.* 21, 37–42. doi:10.1097/MOH.0000000000000005.

Ziegler-Heitbrock, L., Ancuta, P., Crowe, S., Dalod, M., Grau, V., Hart, D. N., et al. (2010). Nomenclature of monocytes and dendritic cells in blood. *Blood* 116, e74-80. doi:10.1182/blood-2010-02-258558.

Zielonka, J., Vasquez-Vivar, J., and Kalyanaraman, B. (2008). Detection of 2-hydroxyethidium in cellular systems: a unique marker product of superoxide and hydroethidine. *Nat. Protoc.* 3, 8–21. doi:10.1038/nprot.2007.473.